2015

The Development of a Hydrodynamics-Based Storm Severity Index

Gabriel Francis Todaro
University of North Florida, g.todaro@unf.edu

THE DEVELOPMENT OF A HYDRODYNAMICS-BASED STORM SEVERITY INDEX

by

Gabriel Todaro

A thesis submitted to the
School of Engineering
in partial fulfillment of the requirements for the degree of

Master of Science in Civil Engineering

UNIVERSITY OF NORTH FLORIDA
SCHOOL OF ENGINEERING

November, 2015

The thesis "Development of a Hydrodynamics-Based Storm Severity Index" submitted by Gabriel Todaro in partial fulfillment of the requirements for the degree of Master of Science in Civil Engineering has been

Approved by the thesis committee: Date:

_____ _____
Dr. William R. Dally, Ph.D., P.E.

_____ _____
Dr. Don T. Resio, Ph.D.

_____ _____
Dr. Christopher J. Brown, Ph.D., P.E.

Accepted for the School of Engineering:

_____ _____
Dr. Murat Tiryakioglu, Ph.D., C.Q.E.
Director of the School of Engineering

Accepted for the College of Computing, Engineering, and Construction:

_____ _____
Dr. Mark Tumeo, Ph.D., P.E.
Dean of the College of Computing, Engineering, and Construction

Accepted for the University:

_____ _____
Dr. John Kantner, Ph.D.
Dean of the Graduate School

CONTENTS

LIST OF FIGURES

LIST OF TABLES

ABSTRACT

A hydrodynamic-based storm severity scale that ranks the damage potential of a storm at a given coastal area is developed. Seventeen tropical and extratropical storm events at 113 different locations on the Atlantic coast and the Gulf of Mexico are examined in order to create and verify a Storm Severity Index Model (SSIM). The results from the SSIM are then used to create a location-based storm severity scale titled the Twenty-Four Point Storm Severity Scale. The Twenty-Four Point Scale is based on three subsets of factors. The first is the energy flux above the normal mean high water line that the storm produces, the second is the amount of overwash due to wave-induced runup, and the third is the inundation due to surge-induced flooding that occurs during the event. The advantage of this methodology is that it enables the level of risk associated with a storm to be examined for a specific region, rather than having a single broad value define the entire event. Although, the index is intended for use on sandy beaches with or without dunes, the general methodology could be extended to armored beaches.

CHAPTER 1: INTRODUCTION

According to the National Oceanic and Atmospheric Administration, approximately 40% of America's population lives directly along the Coastal Shoreline Counties (NOAA, 2010). This proximity to the shoreline has many benefits including economic advantages and more opportunity for leisure activities. However, the close proximity that many people have to the shoreline also creates an opportunity for disaster. The shoreline is vulnerable to damage due to meteorological events including tropical systems and nor'easters (a large extratropical system that gets its name from the direction that its winds blow). One line of defense against these disasters is to prevent wave and flooding inundation by constructing sea walls, levees, and beaches. However, determining whether or not these defenses will work during a particular storm and in a specific location is often uncertain.

For most people, when the term storm classification is mentioned, they think of the Saffir-Simpson Scale for ranking hurricanes. The Saffir-Simpson Scale was developed by Saffir (1973) and Simpson (1974) and is widely recognized since it is used by most local and national weather services when describing a storm system. However, the Saffir-Simpson Scale is not always the best index to use to characterize damage that a hurricane or other storm system may cause because it does not accurately reflect the effects of the storm surge. One example of its limitations occurred in New Orleans during Hurricane Katrina. As it approached Louisiana, Katrina was classified as a Category 3 storm. This classification led to a false sense of security for many people in the area who had lived through Hurricane Camille (a Category 5 storm) in

1969 without much damage. As a result, many people chose not to evacuate while they still had the chance, and approximately 1,500 perished (CNN, 2014). Max Mayfield, the director of the National Hurricane Center, said that after coping with one storm, people have a tendency to take the next one lightly, pointing to those who survived Camille then let their guard down for Katrina (Kaye, 2006). This loss of life could have been mitigated by the application of a better Storm Severity Index that addressed flooding due to storm surge, and which would have given more relevant information to the people living in coastal communities.

There are many factors that determine the amount of damage that an area will sustain in the event of a storm. These factors include the storm surge elevation, the nearshore wave energy, the storm duration, and the condition of the beach prior to the storm. An effective storm severity 'index' would need to encompass all of these parameters. It is important to note that this thesis deals with a storm severity index and not to a storm destruction index. Unlike a storm destruction index, a storm severity index does not take into account the damage to infrastructure. In this case, the storm severity index focuses on the damage to sandy beaches in the form of erosion and the potential for damage caused by wave-induced overwash and flood-induced inundation. That is, a storm that hits an undeveloped beach will receive the same ranking as if that same storm hits a populated area. It will be at the discretion of the person using the index to determine the impact that the results will have in terms of damage to people and infrastructure.

Currently the most viable indices appear to be the Storm Erosion Index of Miller and Livermont (2008) and the Coastal Storm Impulse Parameter (COSI) of Basco and Walker (2010) and Basco and Mahmoudpour (2012). While both of these indices are better than previous options, there is still much room for improvement. The major shortcomings of past indices are twofold. The first is that they do not take into account all of the factors that are necessary for the

development of fully comprehensive storm severity index. Some indices focus on one factor but by doing so, they become very limited in their application.

The second shortcoming of currently used indices have is that they assign a numeric value to a particular storm. When predicting the impact that a storm will have on an area, the storm itself should not receive a value, but rather the area that is being affected by the storm should be given a classification based on an estimate of the amount of danger that exists. By ranking the danger that each area along a coastline will face, it will allow for individual communities to be aware of the level of danger to expect. The goal of this thesis is to develop a rigorous means of quantifying the severity of storms in terms of the potential damage that it will inflict due to beach erosion, wave runup and overtopping, and flooding due to inundation at a given coastal location.

This thesis will start by discussing the indices mentioned previously, along with others, in more detail below. Next, the methodology behind the development of a Storm Severity Index Model (SSIM) is highlighted. This methodology is then applied to 1) several specific communities in New Jersey during Hurricane Sandy, 2) during eleven storms that had an impact on Ocean City, MD, and 3) during five miscellaneous storms that occurred in the Gulf of Mexico. The SSIM is applied to 113 locations in total, and the results are discussed and analyzed in each section. Finally, after the results of the SSIM are analyzed, a Twenty-Four Point Storm Severity Scale is developed.

CHAPTER 2: LITERATURE REVIEW

Throughout the years there have been a variety of attempts to create an effective storm severity index, each with a different methodology and based on different assumptions. They range from the Saffir-Simpson Scale, which classifies hurricanes on a scale of 1-5 based upon wind speeds and central pressures, to the COSI parameter which is based on using conservation of momentum to combine storm surge, wave dynamics, and currents. While each of these scales has value, what is lacking is a danger index that is specific to a given coastal region based on either predicted or measured storm characteristics. This section first discusses wind-based storm severity indices including the Saffir-Simpson Scale, then it moves on to a discussion of vulnerability indices, which include social factors such as age and size of population, and finally this section discusses hydrodynamics-based indices.

The Saffir-Simpson Scale was developed by H. S. Saffir and R. H. Simpson (1974). It is the first wind-based scale that is mentioned. It ranges on a scale of 1 to 5 based on the wind speeds and central pressures produced by a hurricane. As seen in Figure 2.1, the scale is a simple and effective means of predicting the potential damage done by a hurricane's winds but it does not take into account the damage inflicted by waves and storm surge.

The case of Hurricane Katrina demonstrated these limitations as most of the damage done was by the storm surge. Another limitation of the Saffir-Simpson Scale is that it is limited to only classifying hurricanes and it is not capable of ranking extratropical storms such as nor'easters. Some of the most potentially devastating Atlantic storms are nor'easters due to their size and

their duration. They are capable of creating massive erosion as well as flood damage in coastal areas.

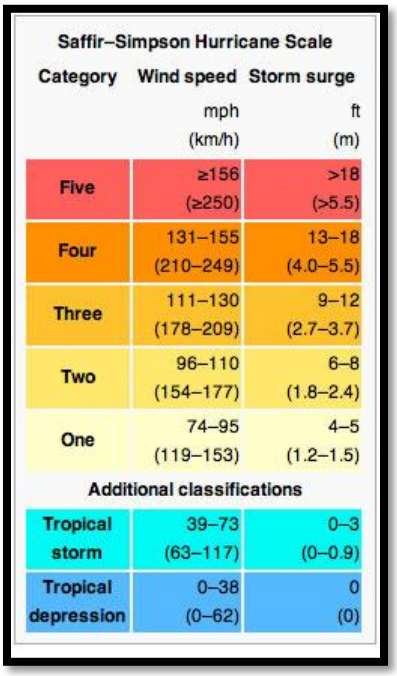

Saffir–Simpson Hurricane Scale		
Category	Wind speed	Storm surge
	mph (km/h)	ft (m)
Five	≥156 (≥250)	>18 (>5.5)
Four	131–155 (210–249)	13–18 (4.0–5.5)
Three	111–130 (178–209)	9–12 (2.7–3.7)
Two	96–110 (154–177)	6–8 (1.8–2.4)
One	74–95 (119–153)	4–5 (1.2–1.5)
Additional classifications		
Tropical storm	39–73 (63–117)	0–3 (0–0.9)
Tropical depression	0–38 (0–62)	0 (0)

Figure 2.1: The Saffir-Simpson Scale (National Science Foundation, 2007).

The Hurricane Severity Index (HSI) (Hebert & Weinzapfel, 2010) is an improvement on the Saffir-Simpson Scale because it takes into account the size of the hurricane instead of just the wind speeds. The scale gives equal weight to the storm's wind speed and radius to maximum winds in order to come up with a number on a 50-point scale that describes the destructive capability of hurricanes. The-50 point scale is split into two 25-point sections. The wind force is a quadratic function with 1 point for a 35 MPH tropical depression and up to 25 points for a hurricane with up to 175 MPH winds. The second section is the wind radii section shown in Figure 2.2. The point range for the wind radii section includes the maximum point value for the previous sections. Thus, for a storm with wind radii of 87, the point value would be 3+4+8+1 for

a total of 16 points (out of a maximum of 25). When the point values from the two sections are added together, it gives the potential for a storm to reach up to 50 points.

Wind Radii	Size Point Range
35 kts	1–3
50 kts	1–4
65 kts	1–8
87 kts	1–10

Figure 2.2: HSI Wind Radii Size Points (Impact Weather, 2008).

Although, the HSI is an improvement over the Saffir-Simpson Scale, it still neglects the damage inflicted by the waves and storm surge. Another limitation of the HSI is that, like the Saffir-Simpson Scale, it is only applicable to hurricanes and cannot be used to classify extratropical storms.

Another wind-based study was done by Haylock (2011). Haylock studied the uncertainty in the return levels of insured loss from European wind storms. The study was quantified using 70 storms. The storms were chosen based on the maximum 10 meter wind speeds over 72 hours taken from six-hourly instantaneous values and the wind gusts. This risk model is only applicable to extra-tropical storms and is limited in coastal applications based on its reliance on wind speeds as the primary source of data which has shown to be unreliable when predicting storm surges.

Wind-based scales are just one way in which people attempt to create storm severity indices. Another type of scale is related not just solely to physical factors, but also to social factors. These scales are generally classified as vulnerability scales. Much of the work of vulnerability scales are built off the work of Watts and Bohle (1993), who discuss the social aspect of vulnerability, focusing on hunger and famine.

One example of a vulnerability scale is a case study of Cape May County by Wu and Yarnal (2002) that demonstrates the increase in vulnerability of coastal communities to flooding from coastal storms. The case study applied a GIS-based methodology for flooding and storm surges. The study also takes into account sociological factors such as age, gender, race, income, and housing. The study combines the physical and social vulnerabilities to create an idea of the county's overall vulnerability. In terms of the physical factors, the main system used is the SLOSH (Sea, Lake and Overland Surges from Hurricanes) model run by the National Hurricane Center to estimate storm surges. The physical part of this case study focuses on vulnerability from flooding which means that it does not take into account other types of coastal damage such as erosion. Yarnal also worked on a paper by Rygel, O'Sullivan, and Yarnal (2006) that expands on this topic by focusing on a Social Vulnerability Index.

The Coastal City Flood Vulnerability Index (CCFVI) is based on the exposure, susceptibility, and resilience of a city to coastal flooding (Balica, Wright, & van der Meulen, 2012). The index gives a number from 0 to 1, indicating comparatively low or high coastal flood vulnerability. The CCFVI methodology uses a total of 19 indicators that are divided into 4 categories; hydro-geological, social, economic, and politico-administration. The hydro-geological indicators include sea level rise and storm surge while the main social indicator is the population close to the coastline. The CCFVI is designed to determine the vulnerability of a coastal city but cannot determine the damage that a storm will cause based on hydrodynamic factors. Due to its social, economic, and institutional components, the CCFVI is only practical to use on major cities. This limits its application to other coastal areas with smaller communities.

The advantage of a hydrodynamics-based storm severity index is that it allows for the incorporation of more storm factors. The first severity index to incorporate waves was an

Intensity Scale for Atlantic Coast Storms developed by Dolan and Davis (1992). They classified 1,347 storms that occurred from 1942 to 1984, in terms of significant wave height (H_S) and storm duration (t_d) using average linkage clustering. They used this information as an estimate of the relative "storm power" given by Equation 1:

$$\int H_s^2 \, dt_d \tag{1}$$

They computed the relative power of a given storm by keeping track of the number of hours during which deep water waves were above 5 ft. in height. Because the only factors taken into account are the significant wave height and storm duration, the Intensity Scale for Atlantic Coast Storms is capable of classifying extratropical systems which is an improvement over the Saffir-Simpson Scale and the Hurricane Severity Index. Although a useful tool for quantifying the damage potential of a storm, the intensity scale does not account for the storm surge or the pre-existing state and geometry of the beach and dune system.

A paper by You and Lord (2008) investigated the influence of the El Nino-Southern Oscillation (ENSO) on New South Wales (NSW) coastal storm severity. The Southern Oscillation Index (SOI) was compared with the yearly averaged storm severity. A simple linear relationship between extreme wave height and yearly SOI was derived. The storm severity, Ω, was defined as:

$$\Omega = f * H_{rms} \tag{2}$$

Where f is the relative frequency of storm occurrence and H_{rms} is the root-mean-square wave height. The paper found that at the NSW coast, coastal recession and increased coastal damage are expected in La Nina years, while beach recovery and less coastal threat are expected in El Nino years.

The Storm Erosion Index (SEI) by Miller and Livermont (2008) is rooted in the principle of the Brunn Rule (Brunn, 1962) for which it assumes that the beach profile will change solely due to an increase in water level. According to the Bruun Rule the beach response to a uniform increase in water level, S as shown in Figure 1.3. The $(h_* + B)$ term represents the vertical portion of the active profile, Δy is the horizontal recession of the beach, and W_* is the width of the surf zone:

$$\Delta y = -S\left(\frac{W_*}{h_* + B}\right) \tag{3}$$

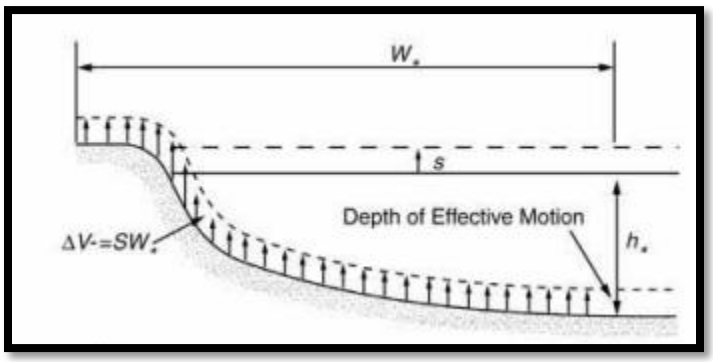

Figure 2.3: Illustration of Bruun Rule (Palma, 2015).

The Bruun Rule was later modified by Dean (1991) to include wave-induced setup in addition to storm surge. With H_b as the breaking wave height they find:

$$\Delta y = -W_*\left[\frac{0.068 * H_b + S}{B + 1.28 * H_b}\right] \tag{4}$$

With the exception of the berm height, B, each of the parameters in Equation 4 varies with time as the storm builds and wanes. The time varying shoreline change was used to define an index that represents the Instantaneous Erosion Intensity (IEI) expressed as Equation 5.

$$IEI(t_i) = -W_* (t_i)\left[\frac{0.068\, H_b (t_i) + S(t_i)}{B+1.28H_b (t_i)}\right] \quad (5)$$

Because Equation 5 represents the instantaneous intensity, the integration of the IEI over the duration of the storm is computed, and the result called the Storm Erosion Index (SEI). The SEI has potential value because it classifies storms due to their potential for beach erosion. This potential was demonstrated with its application to three storms; Tropical Storm Debby, Hurricane Isaac, and Hurricane Sandy (Wehof, Miller, & Engle, 2014). However, there are some concerns with the SEI. The SEI assumes a highly idealized beach and dune shape that does not contain any offshore bars that may be created during, or existed prior, to the storm. The beach shape plays a large role in determining the impact that the waves have on the beach face. Finally, the SEI also does not include the influence of the wave period, which plays a major role in beach behavior according to the Dean Number (Dean R. G., 1973). The Dean number (D), which is based on the process by which a breaking waves lifts particles from the bottom after which they settle back to the bed, is given by:

$$D = \frac{H_o}{\omega T} \quad (6)$$

In which H_o is the deep-water wave height, ω is the fall velocity of the sediment, and T is the wave period.

A subsequent coastal storm-strength parameter was introduced by Basco and Walker (2010). They named it the Coastal Storm Impulse Parameter (COSI) and it is based on computing and then integrating the momentum flux due to waves, surges, and overland currents over the duration of the storm. The COSI parameter is then used as an indicator of the amount of erosion that a beach might suffer. The horizontal momentum for free surface flow was found by

integrating the pressure distribution and the current speed over the water depth in the shore-normal direction:

$$\frac{1}{2}\rho g(s+h_o)^2+\rho(s+h_o)V^2 \tag{7}$$

where s is the storm surge (observed – predicted water level), h_0 is the mean water depth, and V is the depth-averaged cross-shore current. To find the storm surge parameter ($f_S(t)$), the current momentum is neglected, and the mean hydrostatic pressure term is subtracted which gives the following equation:

$$f_S(t)=\frac{1}{2}\rho g(s+h_o)^2+\frac{1}{2}\rho g h_o^2 \tag{8}$$

Assuming the wave crests to be parallel to the shoreline in shallow water, the maximum, depth-integrated, wave momentum flux ($M_F(t)$) was estimated as:

$$M_F(t)=\rho g h^2 A_o\left(\frac{h}{gT^2}\right)^{-A_1} \tag{9}$$

where:

$$A_0=0.6392\left(\frac{H}{h}\right)^{2.0256} \tag{10}$$

$$A_1=0.1804\left(\frac{H}{h}\right)^{-0.391} \tag{11}$$

H=local wave height, h= local water depth, and T=wave period.

The COSI parameter itself is simply the sum of the storm surge parameter ($f_s(t)$) and the maximum wave momentum parameter ($M_F(t)$) integrated over the duration of the storm.

$$I_S=\int\left[f_s(t)+M_F(t)\right]dt \tag{12}$$

This parameter was tested using 249 storms documented during a 10 year period using data collected at the Field Research Facility at Duck, North Carolina. The results of the test proved inconclusive because there was no clear correlation between COSI values and the volumetric change of the beach. The COSI parameter estimates the momentum flux of the incoming nonlinear waves and the increase of hydrostatic pressure due to the storm surge, but fails to incorporate any of the properties of the beach itself. Basco and Walker (2010) also note that the COSI parameter has difficulty predicting whether a beach will erode or accrete during a particular wave event. Because the geometry of the beach is not incorporated, any potential flooding cannot be assessed. Basco and Walker (2010) speculate that the type of beach profile prior to the storm could play a significant role in determining whether a storm will cause accretion or erosion. Investigations continue into the type of beach profile, the presence of nearshore bars, the swash zone slope, shoreline changes prior to the pre-storm profile, and adjacent profiles.

Another recent storm severity index is the hydrodynamics-based Surge Scale for hurricanes developed by Irish and Resio (2010). This scale is a simple hydrodynamics-based scale that accounts for the relative impact of hurricane intensity, size, speed, and the regional bathymetry. There were three major assumptions made during the development of this scale. The first assumption is that the surge is small with respect to the still-water depth so that the surge plus the depth is approximately equal to the depth. The second is that the only forces affecting the water column are the wind stresses at the water surface and the hydrostatic pressure gradient force in the water column. The third is that all forces are uniform in the horizontal spatial direction and that the winds are constant in the cross-shore direction. Ultimately, the surge height is dependent on the central pressure, along with the width and depth of the continental shelf.

The storm surge index (SSI) by Irish and Resio (2010) with improvements suggested by Kantha (2010) is defined in Equation 13. L_{30} is the characteristic shelf width, R_{33} is the measure of the storm size, and L_* is the reference shelf width which is chosen to be 40 km. ψ_X is a function that accounts for the size of the storm, ψ_t is a function that accounts for the speed of the storm (V_{sp}), and V_{max} is the maximum speed of the storm. V_{max}^{ref} is equal to 33 m/s.

$$SSI=\left(\frac{V_{max}}{V_{max}^{ref}}\right)^2\left(\frac{L_{30}}{L_*}\right)\psi_X\left(\frac{R_{33}}{L_{30}}\right)\psi_t\left(\frac{R_{33}}{L_{30}}\frac{V_{max}}{V_{sp}}\right) \quad (13)$$

The Surge Scale (SS) was evaluated using 29 historical storms. Figure 2.4 shows the surges from these storms plotted against the surge scale. These storms were shown to be uncorrelated when other scales are used, such as the Saffir-Simpson scale, but the SS was able to show a correlation between the storms at a regression value of R^2=0.72.

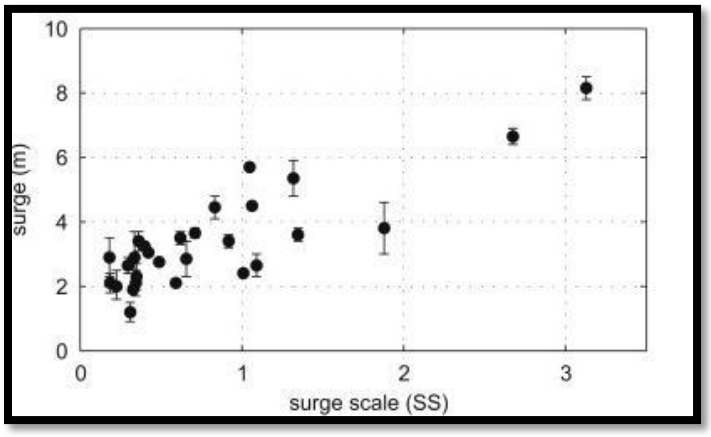

Figure 2.4: Surge Prediction of the Surge Scale from Irish and Resio (2010).

The inundation of a region due to the surge was not included in the scale, but the authors expect that the total inundated area can be generally expressed as a function of the width of the inland inundation, the alongshore distance, and the surge. This suggests that any inundation will heavily depend on the local conditions of the region. Unlike the destruction potential indices

proposed by Powell and Reinhold (2007) and Kantha (2008), the SS keeps the maximum surge separate from the expected flood damage. This is important because many local factors, including population density, affect the total damage potential of a hurricane. The SS also considers two spatial scales instead of just one. The hurricane size and the size scale related to the continental shelf geometry are both taken into account which allows for a regionally-dependent limit on surge generation to be incorporated.

As mentioned above, the factors that appear to be essential to consider in the development an effective storm severity index include:

1. The time history of storm surge elevation,
2. The nearshore wave conditions,
3. The duration of the storm, and
4. The condition of the beach prior to the storm.

For this thesis, all of these parameters are used in order to formulate a damage indicator that can be used to predict the amount of erosion, wave-induced overtopping, and inundation that will occur due to a storm event. The indicator will not take into account the population of an area or the amount of infrastructure present with which to estimate the amount of potential damage that might occur, but rather it will use an area's geological features to determine how much a storm event will impact a coastal area. While this thesis will not incorporate a location's population or infrastructure, the Twenty-Four Point Storm Severity Scale that is described below will have the potential to be expanded to in order to encompass those factors if desired. The geological features of a beach are important in all aspects of the potential damage caused by a storm at a coastal location. As discussed later in this thesis, the shape of the beach impacts the amount of energy flux that penetrates the mean high water line as well as the amount of

overwash and the amount of inundation that are produced during a storm event. Although the index developed here is intended for use on sandy beaches with or without dunes, the general methodology could be extended to armored shorelines.

During a coastal event there are three main ways in which damage is caused. These ways are beach erosion due to the storm, overtopping of the dunes from the waves, and flooding as the water level engulfs the height of the dune or sea wall. Each of these can occur in varying degrees of severity. The majority of the storm severity indices discussed above focus on either estimating the amount of erosion or the height of the storm surge. In order to create a comprehensive storm severity index all three modes of damage need to be included. The following section discusses the methodology behind the development of a Storm Severity Index Model (SSIM) that takes into account the four important storm factors in order to estimate the amount of damage a coastal area will suffer through erosion, runup-induced overwash, and flood-induced inundation.

CHAPTER 3: METHODOLOGY

There are two major assumptions that drive this thesis. The first is that the beach utilized in the model is in dynamic equilibrium and that the amount of energy flux produced below the normal mean high water level is part of this dynamic equilibrium. In essence, this means that the beach is acclimated to wave energy flux up to its normal average high tide line. When the beach receives a water level that rises above the normal mean high water line, there is a surge of wave energy flux to which the beach is not accustomed. The second assumption is that this additional energy flux can cause an impact to the beach shape. The main premise behind the Storm Severity Index Model developed during this thesis is that by explicitly including the 1) water level, 2) surf zone wave conditions, 3) pre-storm beach conditions, and 4) storm duration, a more rigorous, quantitative measure of 'severity' can be computed. As will be shown below, astronomic tides, wind-induced storm surge, and wave-induced setup are all included in the water level estimate. Surf zone wave conditions are to be provided by a computational wave transformation model (which also allows wave-induced setup to be computed), and a surveyed profile used to establish the pre-storm condition of the beach. If the time history of each of these parameters is available, then by integrating their effects the influence of storm duration can also be rigorously included.

The 'backbone' of the Storm Severity Index Model (SSIM) is the nearshore & surf zone wave transformation model of Dally (1987, 1992). The principal methodology behind this wave transformation model is based on the idea that much of the behavior of random waves in the surf zone can be portrayed by the collective behavior of a set of individual regular waves. This

indicates that waves measured outside of the surf zone can be transformed by calculating shoaling and breaking on a wave by wave basis. This means that random wave information from outside of the surf zone can be transformed by calculating shoaling, refraction, breaking, and reforming across an arbitrarily shaped beach profile on a wave-by-wave basis, and the results then combined. Part of the development of the SSIM herein was to introduce the computation of setup induced by wave breaking into the Dally random wave model, utilizing linear wave theory.

This basis is applied in this thesis to transform individual waves during a storm in order to calculate the amount of wave energy flux that penetrates the normal mean high water level due to the storm surge and the waves. The SSIM takes into account that the wave energy dissipates as the waves traverse across the surf zone. The dissipation of the energy reduces the energy flux across the surf zone. The model records the amount of energy that does not dissipate and penetrates the mean high water line. A more detailed description of how the SSIM functions is included in Appendix E. The original model of Dally (1987) was also modified to include the wave-induced setup in the water level, utilizing linear wave theory. In order to quantitatively characterize any erosion of the beach face and dune that occurred during the storm, the wave model was also used to compute the amount of wave energy flux (see Dean and Dalrymple, 2002, pg.92) that penetrates the normal mean high water level (MHW) due to the storm surge and the wave setup. The premise here is that a particular beach and dune system has already conformed to the normal mean high water level that is a result of the astronomical tides in the region – a premised originally adopted by Basco and Walker (2010). If wave energy flux penetrates above this normal high water level, then erosion of the beach face and dune is expected. It is important to note that this quantity depends rigorously on the incident wave conditions, the total water level (i.e. including surge, setup, and astronomical tide), and the shape

of the pre-storm beach profile. The integration of this quantity over the duration of the storm is called the 'Energy Flux Index' (EFI) is used to quantitatively infer the total amount of erosion that can be expected from the storm.

During a coastal event there are three main ways in which damage is caused. These ways include beach erosion due to the storm as discussed above, overtopping of the dunes by wave runup, and inundation flooding if the mean water level exceeds the height of the dune or sea wall. Each of these can occur to varying degrees. With erosion characterized by the EFI, the next step in developing the SSIM is to examine wave-induced runup, and to determine if it is sufficient to overwash the dune or coastal protection structure (e.g. revetment, seawall). The wave runup is a function of the Irribarren number and the wave height. The Irribarren number is a function of the beach slope, the height of the breaking waves, and the wave length and is given by (Dean & Dalrymple, 2002).

$$\xi = \frac{\tan\beta}{\sqrt{\frac{H_b}{L_o}}} \tag{14}$$

In which $\tan\beta$ is the slope of the beach face, H_b is the breaker height, and L_o is the wave length in deep water given by $gT^2/2\pi$. In order to determine whether overwash occurs, the elevation exceeded by 2% of runup events is calculated. This value is based on the Irribarren number and the beach slope, and many relationships are available in the literature. According to Mase (1989), if the beach slopes is less than 0.1 then the wave runup height exceeded by 2% of the runup events is calculated using Mase (1989) given by:

$$R = 1.86\zeta^{0.71}H \tag{15}$$

If the beach slope is greater than or equal to 0.1 and the Irribarren number is less than or equal to 2.0 then:

$$R=1.5\xi H \tag{16}$$

Finally, if the Irribarren number is greater than 2.0 then:

$$R=2.0\xi H \tag{17}$$

With the last two expressions based on irregular wave runup experiments conducted by the US Army Corps of Engineers (Ahrens, 1981).

If the elevation of the 2% runup is higher than the dune crest, then the volume of overwash is calculated. According to a U.S. Army Corps of Engineer report (Larson, Wise, & Kraus, 2004):

$$V_D \sim \frac{2\sqrt{2g}}{\alpha} T \frac{\left(R-Z_D\right)^2}{\sqrt{R}} \tag{18}$$

where alpha is equal to 2, R is the total runup level, and Z_D is the height of the dune.

If the total mean water level is higher than the dune crest, there will be inundation and the rate of flooding (QF), which has units of cubic feet per second per foot of shoreline, is computed using the formula for the rate of discharge for a broad-crested weir (Streeter & Wylie, 1979).

$$QF=3.03\left(FL-Z_D\right)^{1.5} \tag{19}$$

In which FL is the total mean water level. In order to find the volume per foot of shoreline, the rate of flooding is multiplied by the number of seconds that the inundation occurs. It is assumed that once inundation begins, overwash no longer occurs.

A major part of the effort for this thesis was in assembling historical data that were gathered from a variety of sources. These data, which include the beach profiles measured before and after each storm, were used as input to the model and when possible, used to determine the amount of erosion that each storm causes to the beach face. Offshore wave information was gathered from USACE hindcast information (U.S. Army Corps of Engineers, 2015) or NOAA

buoys (National Oceanic and Atmospheric Administration, 2015). Nearshore wave information was gathered from three separate sources. The first source used was an Advanced Circulation Model (ADCIRC) and Simulating Waves Nearshore Model (SWAN) run by Mike Salisbury at Atkins Engineering (personal communication, June 18, 2015) which provided the nearshore wave information during Hurricane Sandy. The second source is a hindcast done in 2005 by Offshore & Coastal Technologies (personal communication, June 3, 2015) that utilized NOAA offshore buoy 44009 as input. The final source of nearshore wave information was a version of the well-known wave transformation model STWAVE that was modified to include bottom friction in order to translate offshore wave conditions to nearshore ones. This source was used to provide the input for the model in the Gulf of Mexico region.

A flowchart is shown below in Figure 3.1 in order to visually represent the methodology involved in creating the SSIM. Once the SSIM was developed, it was then applied to three study areas. First, the SSIM was applied to the coast of New Jersey during Hurricane Sandy because of the large amount of qualitative and quantitative information that was available through the Richard Stockton College of New Jersey (2012). Next, the SSIM was applied to Ocean City, Maryland during eleven storms in order to compare the Energy Flux Index, overwash volume (V_D), and total inundation volume of multiple storms at one location. Finally, the SSIM was applied to five storms that struck several locations on the Gulf Coast of Florida. The results of this application are presented in the next chapters of this thesis.

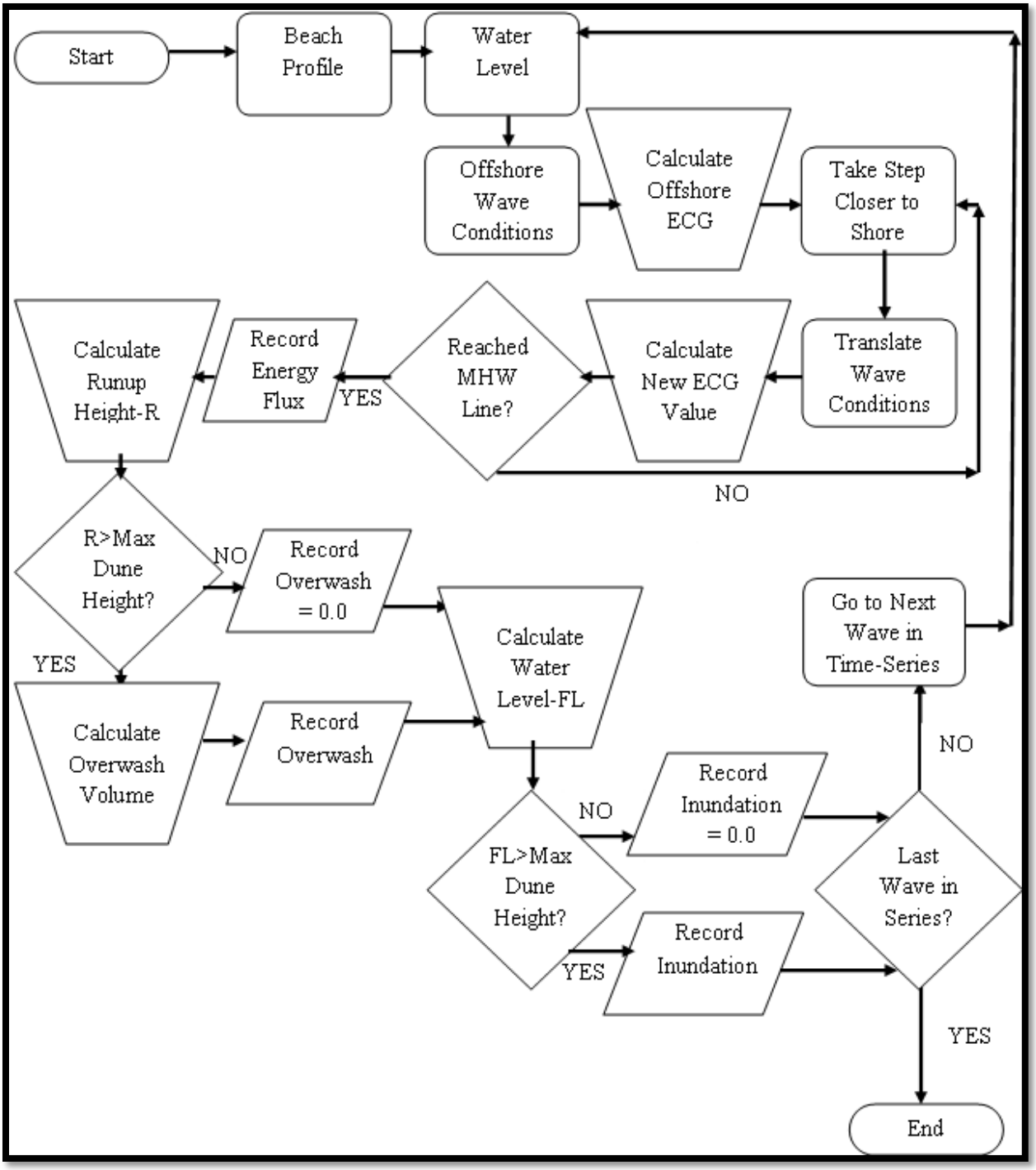

Figure 3.1: Flowchart of Storm Severity Index Model Methodology

CHAPTER 4: HURRICANE SANDY

The first storm severity index investigation of this thesis examines Hurricane Sandy. Sandy is ranked as the second costliest hurricane to strike the United States behind only Hurricane Katrina (Blake, et al., 2013). Hurricane Sandy formed in the Caribbean Sea in October of 2012. Sandy quickly strengthened and made landfall in Jamaica and then in Cuba. After emerging from Cuba, Sandy strengthened as it moved north along the Atlantic Coast of the United States. Sandy reached Category 2 intensity and made landfall near Brigantine, New Jersey. Sandy is best-known for the intensive damage that it caused in New York City, but the northern part of New Jersey also suffered large amounts of erosion and water damage.

Due to a large amount of available data, Sandy was used to assist in evaluating the Storm Severity Index Model (SSIM). The water levels were obtained from the National Oceanic and Atmospheric Administration (NOAA) gauge number 8519483 located at Bergen Point, NY, NOAA gauge 8534720 located at Atlantic City, NJ, and NOAA gauge 8536110 located at Cape May, NJ (National Oceanic and Atmospheric Administration, 2015). Water levels during the storm are found in Figure 4.1.A for Bergen Point, B for Atlantic City, and C for Cape May. The figures encapsulate the wide range of water levels that affected the coast of New Jersey. At Bergen Point, the water level reached eleven feet above the North American Vertical Datum of 1988 (NAVD88) while at Atlantic City the peak was five feet above NAVD88.

Wave information was generated using the wave model SWAN (Simulating Waves Nearshore Model) which was coupled to the storm surge model ADCIRC (Advanced Circulation

Model) by Mike Salisbury at Atkins Engineering (personal communication, June 18, 2015). The waves were produced offshore of the survey locations and include the significant wave height (H_{mo}), the peak wave period (in seconds), and the mean wave direction.

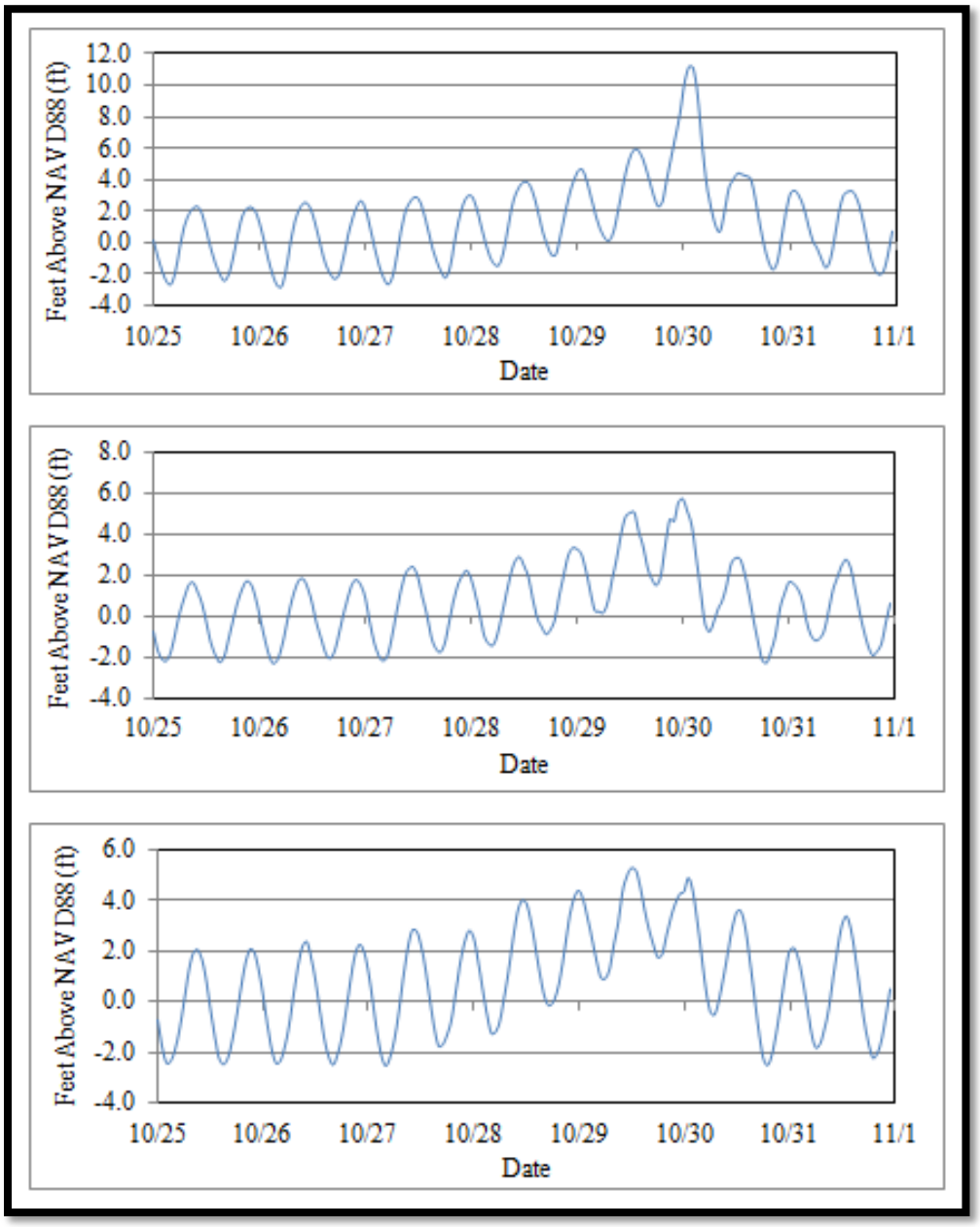

Figure 4.1: Water Levels during Hurricane Sandy at Bergen Point, Atlantic City, and Cape May.

Pre- and post-storm surveys of the beach at many locations are available from the Richard Stockton College of New Jersey Coastal Research Center (CRC) (The Richard Stockton College of New Jersey, 2012). These profiles were used as input for the SSIM. The CRC also has brief summaries of the condition of the beach at each survey location, including descriptions of damages. These descriptions were used to gauge the abilities of the SSIM. Due to the counterclockwise rotation of the hurricane winds, the areas north of the location where Sandy made landfall (Brigantine, New Jersey) received the worst of the storm, whereas the areas south of Brigantine were spared from significant flooding and wave damage.

In order to assess the capabilities of the SSIM, the amount of wave energy flux should, in general, be higher at profiles that are located farther north. There should also be more flooding in these areas due to the larger storm surges. The CRC divided its report into six sections: North and South Monmouth Counties, North and South Ocean Counties, Atlantic County, and Cape May County. Three or four locations that had good pre- and post-storm profiles were selected from each section with a total of twenty locations. The beach profiles that were selected for this investigation are presented in Figure 4.2, below. The following sections describe each of these locations individually, starting at Cape May in the south and ending with North Monmouth County. A summary of the CRC report from December of 2012 is included with results from the SSIM. Two of the profiles are examined in detail in the main body of this section while the remaining locations are available in Appendix A.

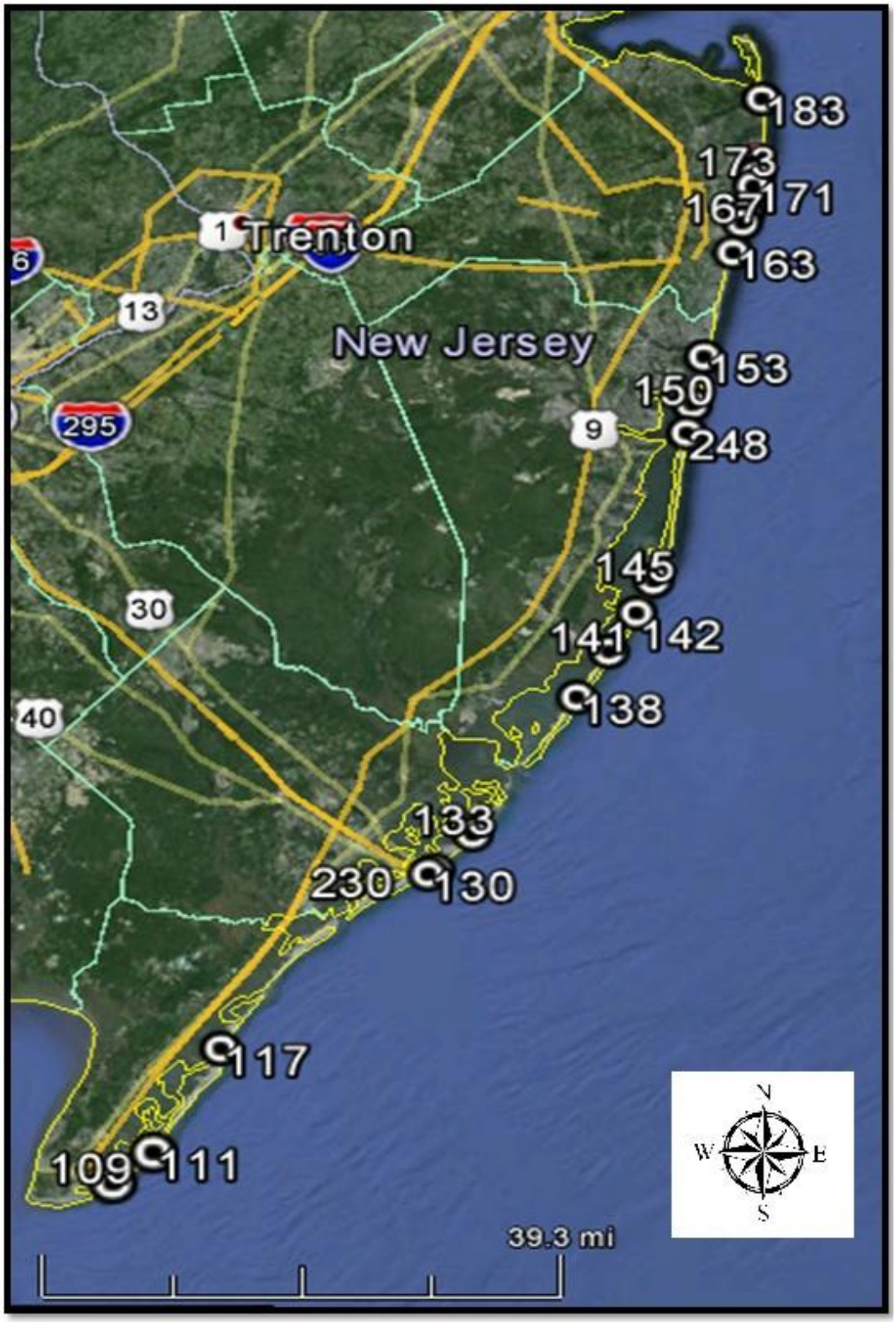

Figure 4.2: New Jersey Beach Profile Sites (Google.inc, 2015).

The pre-existing beach conditions are presented in Table 4.1. The offshore slope, the beachface slope, the maximum beach elevation, the normal mean high water elevation, and whether or not there is a boardwalk are provided in the table. The maximum heights of the beaches range from twelve to thirty feet of elevation above NAVD88. There are boardwalks present at three locations, NJBPN Site 248, Site 167, and Site 168. These boardwalks add complications to the analysis because of the way they interact with the beach profile surveys. The difficulties that they presented are discussed in detail in the following sections.

Table 4.1: Pre-existing Beach Conditions

Location	Beachface Slope	Offshore Slope	Maximum Beach Height (ft NAVD88)	Normal Mean High Water Elevation (ft NAVD88)	Boardwalk (Y/N)
109	0.040	0.05	23.09	1.99	NO
111	0.020	0.02	14.82	1.99	NO
117	0.020	0.02	17.95	1.99	NO
130	0.030	0.03	15.04	1.57	NO
230	0.050	0.03	16.29	1.57	NO
133	0.050	0.07	14.17	1.57	NO
138	0.092	0.02	21.77	1.57	NO
141	0.077	0.02	21.05	1.57	NO
142	0.040	0.02	20.08	1.57	NO
145	0.039	0.03	19.95	1.57	NO
248	0.040	0.03	15.00	1.09	YES at 10 ft.
150	0.097	0.05	28.38	1.09	NO
153	0.118	0.04	20.10	1.09	NO
163	0.026	0.02	12.56	1.78	NO
167	0.032	0.02	14.12	1.91	YES at 10 ft.
168	0.101	0.03	22.27	1.91	YES at 20 ft.
171	0.113	0.05	28.84	1.91	NO
173	0.140	0.05	30.32	1.91	NO
177	0.039	0.05	17.18	1.91	NO
183	0.056	0.02	18.46	1.91	NO

4.1 CAPE MAY COUNTY

There are three beach profiles that were selected from Cape May County. These locations are Raleigh Ave., Wildwood (New Jersey Beach Profile Network 109), 15th Ave., North Wildwood (NJBPN 111), and 80 St., Sea Isle City (NJBPN 117). Overall, Cape May County suffered relatively little compared to the northern part of the state. Ocean City itself (not included in profiles) suffered some inundation due to the lack of beach protection in some areas, but to the south there was little to no overwash or inundation.

Raleigh Avenue, Wildwood, NJBPN 109

The Raleigh Avenue site is the southernmost site observed in this report. The beach itself was flooded and sand was forced to the toe of the dune, but no overwash occurred at this location. Figure A.1.A (located in Appendix A) shows the pre- and post-storm profiles at the site. Figure A.1.B shows that the significant wave heights reached approximately 12 ft. above mean sea level. Using this wave height, along with the water levels, and pre-storm profile data, the SSIM was run. The results from the SSIM are shown in Figure A.1.D. Between October 25th and November 1st, the location absorbed an estimated 28.8 kW-hours per linear foot of shoreline above the mean high water line. The energy flux time series reached a peak of 1.74 kW per linear foot at 1:00 PM on October 29th, 2012. The normal mean high water level is 1.99 ft and the dune height comes up to 23 ft. At this location, the beach flattened out and there was a net loss of 10 cubic yards per foot above the zero elevation datum (NAVD88).

15th Avenue, North Wildwood, NJBPN 111

The second site surveyed was 15th Avenue which is located just south of the Hereford Inlet. The initial beach conditions can be seen in Figure A.2.A. Waves flowed across the dry beach area and deposited sand at the foot of the dune but no overtopping occurred at this location. This site was a part of FEMA-coordinated beach repair in late 2011 and consequently has a wide beach face. The dune at this location rose to about 14 ft high which was enough to prevent the water from overtopping. The normal mean high water line was at 1.99 ft NAVD88. The beach was flattened by Sandy with a loss of 18.17 cubic yards per foot above the zero elevation datum (NAVD88). The energy flux time series reached a peak power of 0.69 kW per linear foot at 1:00 PM on October 29th, with an EFI value of 9.8 kW-hours per linear foot. The results from the SSIM can be seen in Figure A.2.D in Appendix A.

80th Street, Sea Isle City, NJBPN 117

This was the final location from Cape May County to be run through the SSIM. Just prior to Sandy, a new foredune was installed as additional protection for the beach. This foredune was completely lost but the main dune, with an elevation of 18 ft, was able to prevent overtopping despite large amounts of erosion (32.71 cubic yards per ft) above the zero elevation datum (NAVD88). The normal mean high water line at this location was at 1.99 ft and the amount of energy flux that exceeds that line can be seen in Figure A.3.D, which contains the SSIM results. The peak power at this location was 0.99 kW per linear foot at 1:00 PM on October 29th. The index number at Site 117 was 14.65 kW-hours per linear foot.

4.2 ATLANTIC COUNTY

There are three profiles chosen from Atlantic County, New Jersey. These locations are North Carolina Avenue, Atlantic City (NJBPN 130), Rhode Island Avenue, Atlantic City (NJBPN 230), and 4th Street North, Brigantine (NJBPN 133). Sandy made landfall near Brigantine and as a result there was more damage in Atlantic County then in Cape May County. However, this damage was minor compared to the areas north of the landfall point. The undeveloped part of Brigantine was overwashed by ocean waves from the bay to the marshes. Where development begins, waves crashed over the promenade and flooded Brigantine Boulevard. At the southern end of the promenade, dunes and a dry beach exist and in this area there was very little overwash. Atlantic City, as a whole, performed much better than Brigantine due to Federal beach nourishment projects that raised the dunes to 14.5 ft (NAVD88). These dunes were just large enough to withstand the wave run-up. The areas south of Atlantic City, especially Margate City and Borough of Longport, suffered to a greater extent. These areas lacked proper dunes and as a result many properties received damage.

North Carolina Avenue, Atlantic City, NJBPN 130

North Carolina Avenue was the southernmost site used in Atlantic County. A 2011 federal beach maintenance fill added to the dune and berm which widened the beach enough to mitigate most of the damage. The beach profile is shown in Figure A.4.A. The dune extends to an elevation of 15 feet with a 200 foot berm in front of it. Sandy managed to wash away the berm and flatten the profile but did not manage to produce any overwash at this location. Site 130 lost 27.70 cubic yard per foot of beach above the zero datum during the storm. In Figure A.4.B, the offshore and nearshore wave heights are shown. At this site, the maximum nearshore

wave heights are approximately 9 feet. The mean high water line is at 1.57 (NAVD88). The SSIM estimated the EFI value at the site to be 20.5 kW-hours per linear foot with the peak power being 1.71 kW per linear foot at 12:00 PM on October 30th. The results from the SSIM can be seen in Figure A.4.D.

Rhode Island Avenue, Atlantic City, NJBPN 230

Rhode Island Avenue is located near the Absecon Inlet jetty. The berm was wide due to a Federal maintenance in 2012 but the volume of sand in the berm was greatly reduced post Sandy. Site 230 has a 14 foot dune that managed to resist the power of Sandy but the beach lost 28.75 cubic yards per foot of sand above the zero elevation datum (NAVD88). When the SSIM was applied to this location, the maximum power was 0.92 kW per linear foot on October 30th at 12:00 PM as seen in Figure A.5.D. The index number was estimated to be 9.1 kW-hours per linear foot. The normal mean high water line at site 230 is at 1.57 feet (NAVD88).

4th Street North, Brigantine, NJBPN 133

The 4th Street site is the northernmost point from Atlantic County that was run in the SSIM. The results of the SSIM run can be seen in Figure A.6.D in Appendix A. The peak power was at 12:00 PM on October 30th and its magnitude was 2.40 kW per linear foot. The Energy Flux Index value above the mean high water line of 1.57 ft (NAVD88) was estimated to be 29.43 kW-hours per linear foot. The beach at site 133 is not particularly wide but the dune height of 16 feet above the NAVD88 datum is larger than the surrounding sites. The site lost 30.71 cubic yards per linear foot above the zero elevation datum (NAVD88). According to the CRC, the site had some minor overwash but the SSIM estimated no overwash at this location.

4.3 SOUTH OCEAN COUNTY

There are four profiles taken from south Ocean County. From South to North, these sites are Old Whaling Road (124th Street), Long Beach Township (NJBPN 138), 8th Street, Ship Bottom (NJPBN 141), Tranquility Drive, Harvey Cedars (NJBPN 142), and 26th Street, Barnegat Light (NJBPN 145). One thing that Sandy demonstrated is that larger dunes and wide beaches play a large part in determining how susceptible a region is to wave damage and overwash. The damage was minimal in areas with large dunes, but in areas without enough protection, the damage was catastrophic. All four of the locations mentioned below have dunes that rise to at least 20 feet above NAVD88. This enabled these areas to have little or no overwash while areas nearby suffered much more water damage.

Old Whaling Road, Long Beach Township, NJBPN 138

Old Whaling Road was the first site observed in South Ocean County. This location experienced erosion of the foredune and berm but did not experience any overwash (although a similar dune a couple of blocks away failed and overwash occurred). The Old Whaling Road dune has a height of approximately 21 feet above NAVD88 (as seen in Figure A.7.A). The site experienced the loss of 23.20 cubic yards per foot of beach above the zero elevation datum. The SSIM supported the claim of no overwash occurring at this location despite the fact that this location experienced an EFI value of 66.9 kW-hours per linear foot above the mean high water line of 1.57 feet (NAVD88). The site also experienced a peak power of 5.57 kW per linear foot on October 30th at midnight. The SSIM results are located in Figure A.7.D. These energy levels were produced by the waves found in Figure A.7.B. When compared to the wave heights at previous locations, it is obvious that the storm has gotten stronger further north. One area where

there appears to be some error is between October 27th and 28th. The buoy heights during this time period are lower than the predicted SWAN heights. This may have resulted in an overestimation of energy flux during this time period. However, even if there is an overestimation, the main part of the storm did not impact the area until the 29th which means that this overestimation likely does not have a large impact on the results for Site 138.

8th Street, Ship Bottom, NJBPN 141

The location in Ship Bottom experienced erosion of the beach and dune but the dune was not breached and no overwash occurred. The initial beach conditions can be seen in Figure A.8.A. The dune had an elevation of approximately 21 feet above NAVD88. This site lost 40.35 cubic yards per linear foot above the zero elevation datum (NAVD88). The SSIM was used on this location and the results can be seen in Figure A.8.D. The peak power was 4.25 kW per linear foot and it occurred at midnight on October 30th. The index number at this site was calculated to be about 56.66 kW-hours per linear foot of beach above the normal mean high water level of 1.57 feet above NAVD88. The SSIM also estimated that there was no overwash at this location.

Tranquility Drive, Harvey Cedars, NJBPN 142

The third location in the southern part of Ocean County is Tranquility Drive in Harvey Cedars. At this location there was a significant loss of beach width and dune but no overwash. The shoreline retreated by 100 feet and the top of the 21 foot dune was almost entirely removed. The site lost 42.30 cubic yards per foot of shoreline above the zero elevation datum (NAVD88). The SSIM at this location produced less energy at this location than at other areas in Ocean County. Figure A.9.D shows that the peak power was only 1.98 kW per foot (At midnight on

October 30th). This is less than half of the peak power that occurred at Site 141, which is located just 4 miles south of Site 142. The Energy Flux Index value was estimated to be 19.51 kW-hours per linear foot and the SSIM estimated no overwash at this location.

26th Street, Barnegat Light, NJBPN 145

The final location in the southern part of Ocean County is 26th Street. This location has a wide beach, approximately 22 foot high dune elevations, and is covered in dense vegetation. The wide beach and tall dune were enough to survive moderate erosion (25.10 cubic yards per foot above the zero elevation datum which is referenced to NAVD88) and prevent most overwash. According to the CRC, there was overwash into the dune but not enough to make it beyond. This result is supported by the SSIM which indicated an estimate of 8.52 cubic feet of overwash per foot of shoreline. This result helps to support the validity of the SSIM's overwash component since it is concurrent with the description of the overwash estimated by the CRC. The rest of the SSIM results are found in Figure A.10.D. The peak power at this location was 4.10 kW per linear foot (midnight on October 30th) with an index number of 53.69 kW-hours per linear foot.

4.4 NORTH OCEAN COUNTY

There were three sites chosen in North Ocean County. They are Franklin Avenue, Seaside Heights (NJBPN 248), White Avenue, Lavallette (NJBPN 150), and 1117 Ocean Avenue, Mantoloking (NJBPN 153). The Franklin Avenue location is next to a boardwalk and amusement park. This area did not have a dune and as a result it sustained a lot of damage. Other than a few isolated areas, the northern part of Ocean County was hit very hard by Sandy. This includes overwash at Site 248 and the complete failure of the dune at NJBPN 153.

Franklin Avenue, Seaside Heights, NJBPN 248

The Franklin Avenue site is located next to an amusement park on a pier. It was one of the two locations that was highlighted in the main body of this thesis due to the difficulty it presented when attempting to use the SSIM. This location has no dune and the boardwalk only reaches up to 15 feet above NAVD88. According to the CRC, this area was subjected to catastrophic damage to infrastructure and property. This area was one where the SSIM had a problem. The SSIM indicated that only 221.75 cubic feet per foot of shoreline of overwash occurred at this site. This was less overwash than what was expected according to the CRC report. One possible explanation for the underestimation is that the SSIM was treating the shape of the profile as a solid sand dune rather than a manmade boardwalk. The difference being that a sand dune can be treated as impermeable but a boardwalk cannot. It is susceptible to water passing through it and there is a chance of the boardwalk breaking due to the power of the waves. To demonstrate this, the SSIM was run a second time without the boardwalk present in the beach profile. On this run, the highest point of the profile was only about 10 feet above NAVD88 and as a result the overwash became a more reasonable 9,134 cubic feet per foot of shoreline. This indicates that the SSIM may not be fully adaptable to structures other than dunes and sea walls. Modifying the SSIM to deal with different structures could be one area in which further studies are possible. The beach profiles at this location with and without the boardwalk can be found below in Figure 4.3.A. The beach above the zero elevation datum lost 51.70 cubic yards per foot of shoreline. The wave heights at this location can be observed in Figure 4.3.C. The SSIM results can be found below as well in Figure 4.3.D. The index number estimated by the SSIM was 49.65 kW-hours per linear foot while the peak power was 3.74 kW per linear foot at 1:00 AM on October 30th.

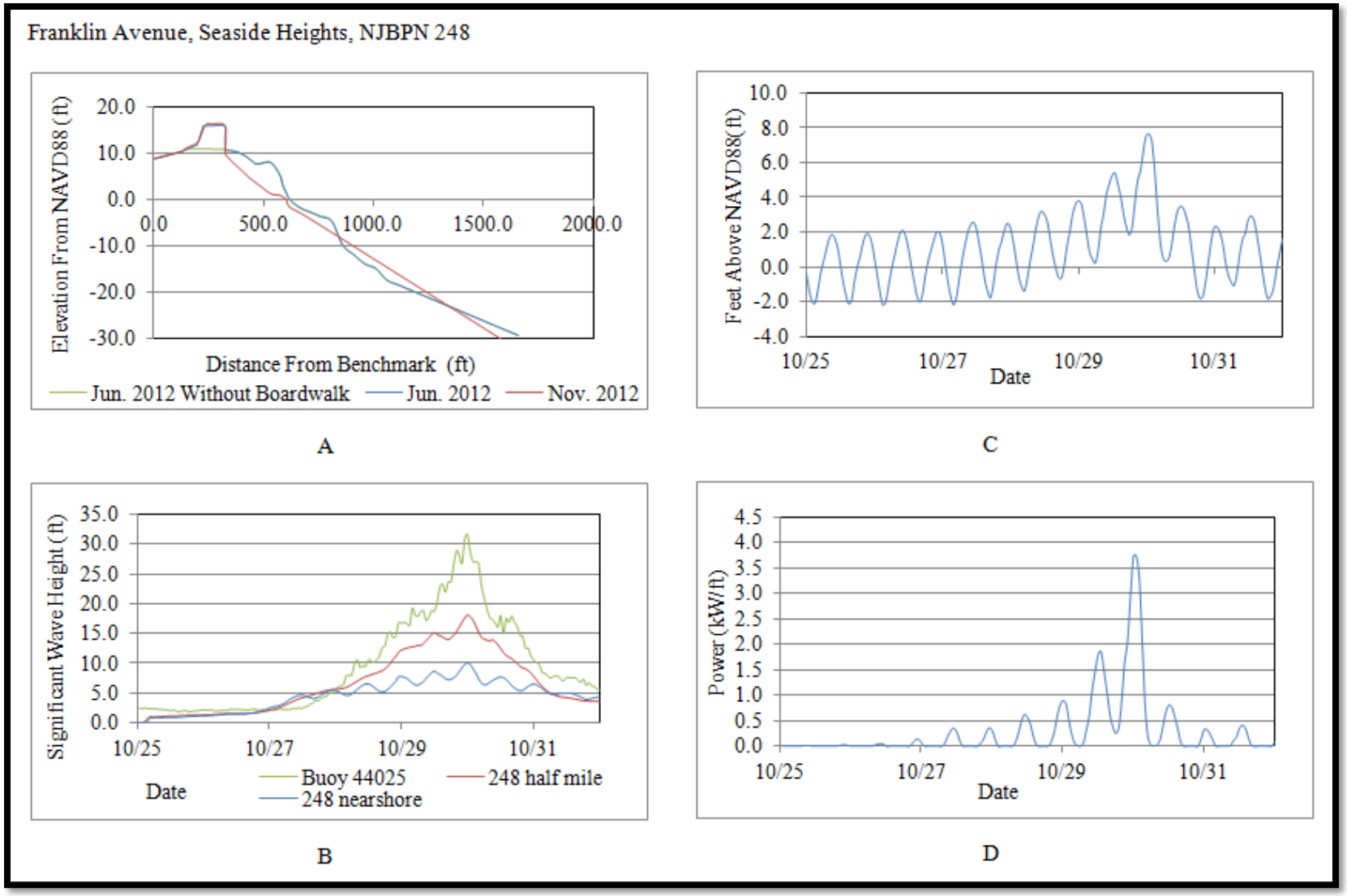

Figure 4.3: NJBPN Site 248 Conditions and Results.A) The pre- and post-Hurricane Sandy profiles. B) Hurricane Sandy wave heights. C) Water levels at NJBPN 248. D) SSIM Results at NJBPN Site 248 during Hurricane Sandy.

White Avenue, Lavallette, NJBPN 150

The White Avenue location has a high dune of approximately 25 feet above NAVD88. This location suffered a lot of erosion of the dune. In total, 39.30 cubic yards per foot of shoreline was eroded above the zero elevation datum (NAVD88). While other locations in this region suffered, at this survey point, the dune was tall enough to prevent any overwash. The SSIM also reports no overwash at this location. The SSIM results are presented in Figure A.12.D. This is the site that had the most energy estimated by the SSIM. The program estimated that the EFI number to be 147.60 kW-hours per linear foot with a maximum power of 9.34 kW per linear foot at 1:00 AM on the morning of October 30th.

1117 Ocean Avenue, Mantoloking, NJBPN 153

This is another area where the SSIM had trouble. Unlike Site 248, this location has a dune instead of a boardwalk. However, unlike the other locations that were surveyed, the dune at this location was completely beached. This site is located just above the main breach that occurred at Herbert Street. The breach occurred due to the lack of sand on the shoreline which created a thin beach that was not able to force waves to break early. There were three new tidal inlets that were carved into this region due to the lack of beach width and twelve homes were swept away. This breach means that the SSIM would be expected to produce inundation, however, because the pre-storm beach profile is used, the SSIM did not record any inundation or overwash at this location. Like with Site 248, the SSIM was run a second time at this location, this time the post-storm profile was used in order to determine what the predicted damage would be under the worst possible conditions for the dune. This second run yielded results of 1,336.29

cubic feet per foot of overwash and 491,760 cubic feet per foot of inundation. The inundation started on October 29th. The SSIM run produced a peak power of 5.59 kW per linear foot at 1:00 AM on October 30th. The index number at this site was estimated to be 60.45 kW-hours per linear foot. These results are shown in Figure A.13.D. The dune at this location was originally 22 feet tall. Because the dune was completely breached, the amount of sand lost was 109.6 cubic yards per foot above the zero elevation datum (NAVD88).

4.5 SOUTH MONMOUTH COUNTY

The selection of profiles from South Monmouth County includes three profiles. They are 5th Avenue, Belmar (NJBPN 163), 3rd Avenue, Asbury Park (NJBPN 167), and Corlies Avenue, Allenhurst (NJBPN 168). Monmouth County is where most of the energy from Sandy was calculated because it is the northern-most county that was observed. The three profiles in the southern part of the county had poor results when it came to overwash and many homes were damaged in this region due to a lack of dunes in many places.

5th Avenue, Belmar, NJBPN 163

The first site in South Monmouth County is 5th Avenue. According to the CRC, 5th Avenue has no dune; rather it is a wide, dry beach that was submerged by the storm. Sand was carried onto Ocean Avenue along with the flooding. The beach reached a peak of about 12 feet above NAVD88 and it lost 39.50 cubic yards per foot of sand above the zero elevation line (NAVD88). The SSIM was used at this location and the index number was found to be 39.66 kW-hours per linear foot with the peak power occurring at 1:00 AM on October 30th with a magnitude of 4.65 kW per linear foot. According to the SSIM, the overwash was estimated to be

2018.16 cubic feet per foot of shoreline. There was also inundation estimated to be at 74,160 cubic feet per foot which started early morning of October 30th. The SSIM graph can be seen in Figure A.14.D.

3rd Avenue, Asbury Park, NJBPN 167

The 3rd Avenue location was the second site that was highlighted in the body of this thesis. Like Site 248, there was a boardwalk that was present at this location. The sand from the beach was ramped up to the boardwalk that separates the beach from Ocean Avenue. This allowed the waves to pass over the boardwalk without damaging it. The natural beach itself only has about an 11 foot elevation above NAVD88. Water rushed over the boardwalk and flooded Ocean Avenue. The beach profile for this location can be seen in Figure A.15.A. This location lost 22.40 cubic yards per foot of sand above the zero elevation datum. The wave heights for this location are displayed in Figure A.15.C. The SSIM estimated a peak power of 6.56 kW per foot which occurred at 1:00 AM on October 30th. The energy flux levels are shown in Figure A.15.D. The index number at this site was calculated to be 63.59 kW-hours per linear foot. The SSIM was again run twice at this location. The first run was with the boardwalk, and the second without it. The overwash at Site 167 was estimated to be 14,160.11 cubic feet per foot of shoreline. The first run did not produce any estimate for inundation but the run without the boardwalk produced 133,560 cubic feet per foot of water. This location is another example of the possible modifications that can be made to the SSIM. Perhaps it is simply enough to remove the boardwalk shape from the beach profile in order to estimate the amount of flooding purely from the beach shape.

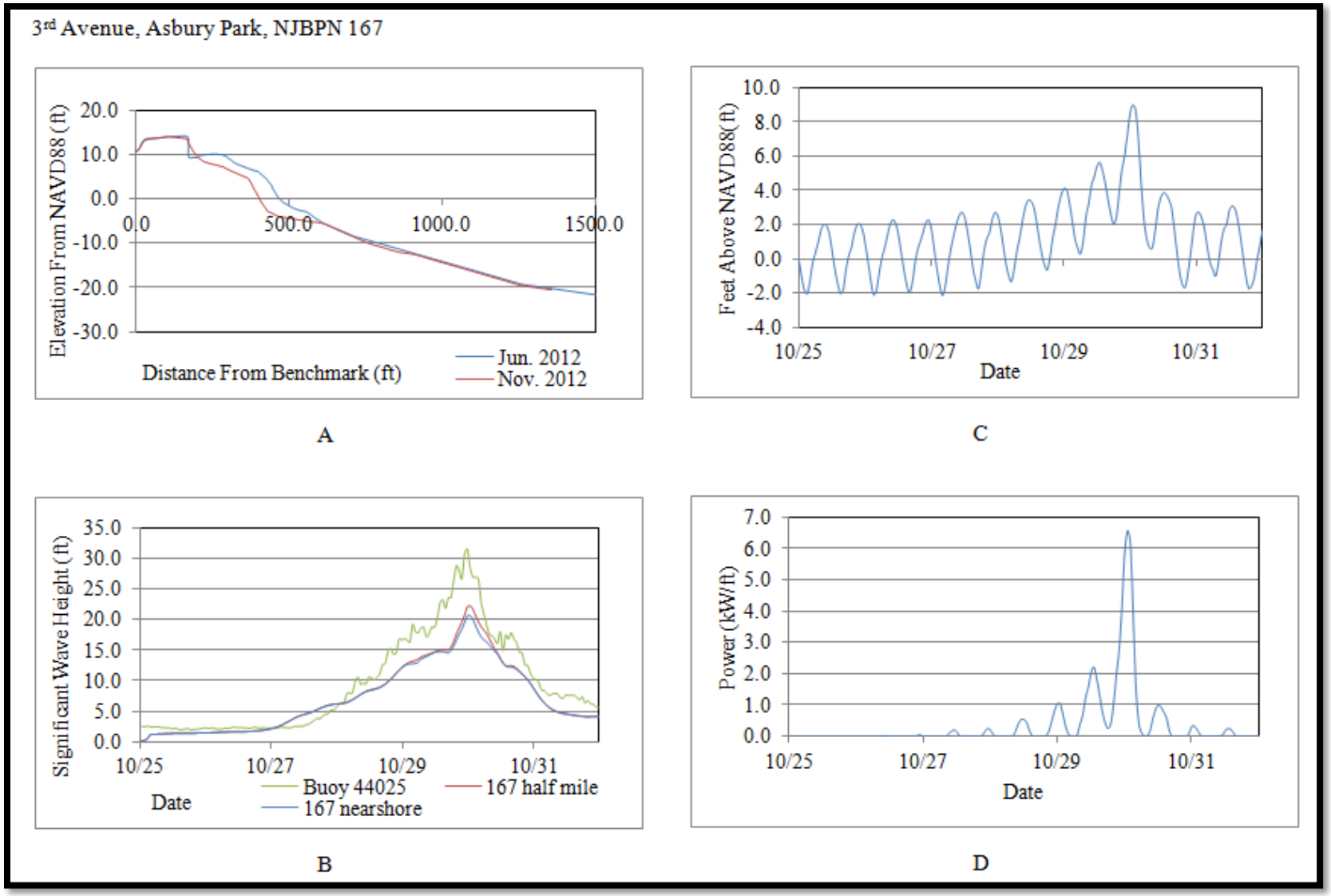

Figure 4.4: NJBPN Site 167 Conditions and Results. A) The pre- and post-Hurricane Sandy profiles. B) Hurricane Sandy wave heights. C) Water levels at NJBPN 167. D) SSIM Results at NJBPN Site 167 during Hurricane Sandy.

Corlies Avenue, Allenhurst, NJBPN 168

Site 168 sits on top of an old concrete wall that drops vertically onto the beach. There is a wooden boardwalk just landward of the wall at an elevation of 20 feet over NAVD88. About 50 feet of boardwalk was stripped from the supports according to the CRC report. Some sand and water ruined the landscaping across the street which indicates that there was some overwash at this location. A few blocks to the South, Loch Arbor was completely overwashed with 3-4 feet of sand in people's yards. The SSIM results can be viewed in Figure A.16.D. The index number was found to be 60.99 kW-hours per linear foot with a peak power of 6.74 kW per linear foot which occurred at 1:00 AM on October 30th. The SSIM also estimated an overwash of 290.83 cubic feet per foot which is consistent with the CRC report of some overwash in the area. At this location the beach experienced erosion of 32.30 cubic yards of sand per foot of shoreline (NAVD88).

4.6 NORTH MONMOUTH COUNTY

North Monmouth County is the final section of the New Jersey coastline that was covered in this thesis. This is the northernmost section and as a result, it averaged the highest amount of energy flux above the mean high water line. Also, each of the four profiles studied experienced overwash. The four profiles in this section are Pullman Avenue, Elberon (NJBPN 171), West End Avenue, Long Branch (NJBPN 173), 404 Ocean Avenue, Long Branch (NJBPN 177), and Via Ripa Street, Sea Bright (NJBPN 183). The power of Sandy was again demonstrated on this part of New Jersey as the beaches in this area have much better protection then the ones in the

middle part of the state. Yet despite the higher dunes, there was still significant damage in the area.

Pullman Avenue, Elberon, NJBPN 171

The site at Pullman Avenue has a high bluff with an elevation of 28 feet NAVD88. The waves broke on the revetment with heights of at least 35 feet and smashed the sides of homes located at the top of the bluff. The SSIM estimated that the index number at this site was 123.42 kW-hours per linear foot. The peak power can be seen Figure A.17.D. It occurred at 1:00 AM on October 30th with a value of 11.04 kW per linear foot. The SSIM estimated that the overwash would be equal to 464.26 cubic feet per foot at this location. The beach at this site sustained 13.60 cubic yards per foot of erosion above the zero elevation datum (NAVD88).

West End Avenue, Long Branch, NJBPN 173

The site at West End Avenue has a rock revetment protecting the base of the bluff with a boardwalk 15 feet above the revetment. There is no dune at this location which allowed Sandy to roll over the beach and strike the revetment, causing damage to it. There was overwash at this location, evidenced from the debris and sand deposits on landward properties. The revetment ultimately held but the boardwalk was destroyed in many places. The SSIM estimates that the index number was 120.12 kW-hours per linear foot with a peak of 11.00 kW-hours per linear foot which occurred at 1:00 AM on October 30th. The SSIM results can be seen in Figure A.18.D. The SSIM also estimated that the overwash would be approximately 631.34 cubic feet per foot. The beach lost 23.90 cubic yards per foot of sand above the zero elevation datum (NAVD88).

404 Ocean Avenue, Long Branch, NJBPN 177

This location did not have a dune and overwash flooded into the street beyond the beach. The beach at this location lost 45.87 yards per cubic foot of sand above the zero elevation datum (NAVD88). The SSIM estimated 2473.91 cubic feet per foot of overwash. It also estimated the index number from Sandy at this location to be 86.76 kW-hours per linear foot. The peak power at this site was 8.76 kW per foot and it occurred at 1:00 AM on October 30th. The SSIM matched the description of the overwash as no inundation occurred yet a lot of sand and water made it to the street above the beach. The results from the SSIM can be seen in Figure A.19.D.

Via Ripa Street, Sea Bright, NJBPN 183

The northernmost location that was used for the SSIM during Sandy was Via Ripa Street in Sea Bright, NJ. The beach profile is displayed in Figure A.20.A. At this location an engineered dune was not constructed due to the presence of seawall that rises to 18 feet above NAVD88. According to the CRC report, there was not as much overwash as expected at this location. The report speculated that this could be due to smaller wave heights at this location due to the proximity to the fetch limit produced by Long Island. The results from SWAN are shown below in Figure A.20.B. The significant wave heights rise to 18 feet which may result in an over-prediction of the overwash at this location. The SSIM estimated the overwash to total 2113.18 cubic feet per foot which is similar to the overwash produced at the previous site (NJBPN 177). The SSIM also estimated the EFI value to be 91.42 kW-hours per linear foot. These results can be seen in Figure A.20.D with a maximum power of 9.14 kW per linear foot. The site lost 34.10 cubic yards of sand per foot of shoreline during Sandy.

4.7 ANALYSIS OF STORM SEVERITY INDEX MODEL DURING HURRICANE SANDY

Hurricane Sandy was used as the main storm to test the SSIM due to the large amount of information that was available regarding pre- and post-storm beach profiles, wave heights, and water levels. There are three main components of the SSIM; the energy fluxes, the runup-induced overwash rates, and the inundation volumes. The correlation of the three to the damages inflicted by Sandy is to be examined. The SSIM appears to provide the proper trend when it comes to the energy fluxes above the normal mean high water line. Due to the way Sandy struck the coast of New Jersey the energy fluxes were expected to increase from south to north. The summary of the SSIM results in Figure 4.5 meets this expectation.

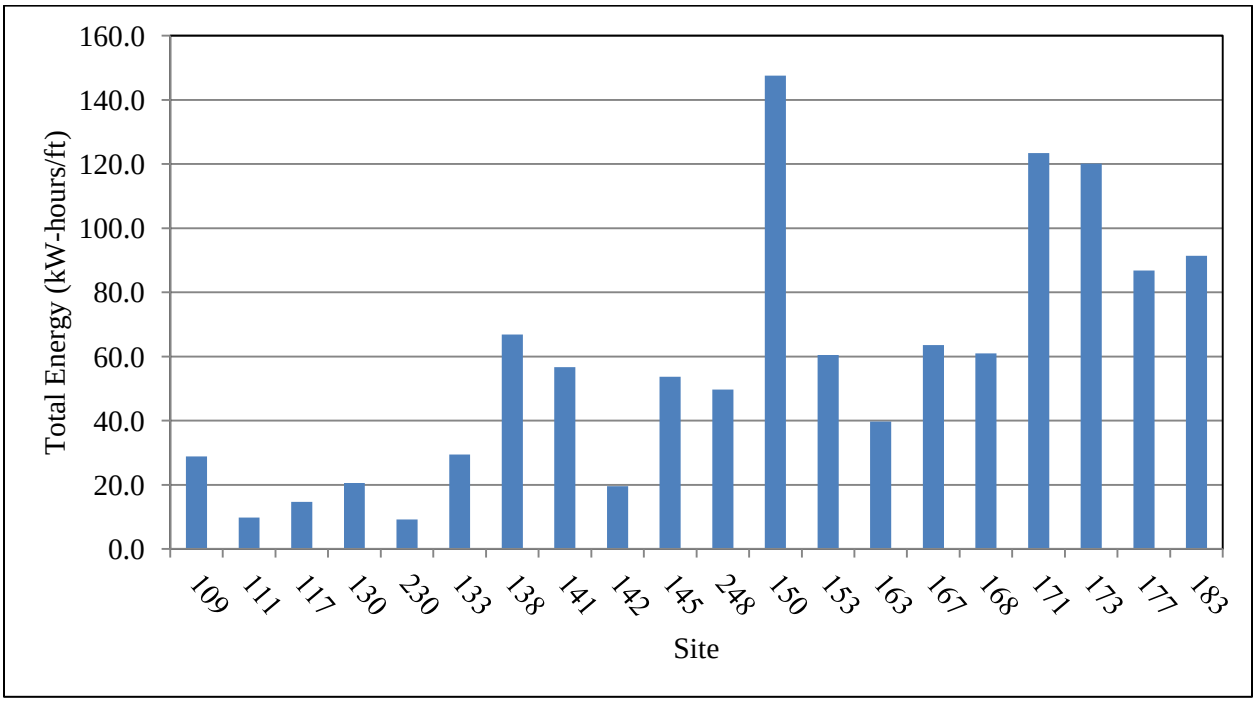

Figure 4.5: Energy Flux Index for each Location during Sandy.

While the energy fluxes do not uniformly increase from south to north, as a whole the average Energy Flux Index for each section of coastline that was observed does increase. The

lack of uniform increase is due to the fact that the energy flux above the mean high water line takes into account the beach profile shape rather than just the wave characteristics. Locations that experience similar wave properties could have very different levels of energy penetration due to factors such as the slope (height and width) of the beach as well as the elevation of the normal mean high water line.

One example of this is Site 138. Site 138 has a much steeper beach face then the other locations nearby (see Table 4.1). The site has a slope of about 0.09 while Site 141 and Site 142 have slopes of approximately 0.07 and 0.04, respectively. As a result, the Site 138 location received more energy flux penetration than the other two nearby sites. The presence of any offshore bars also plays a factor in where the waves will break, and as a result, how much energy reaches the shoreline.

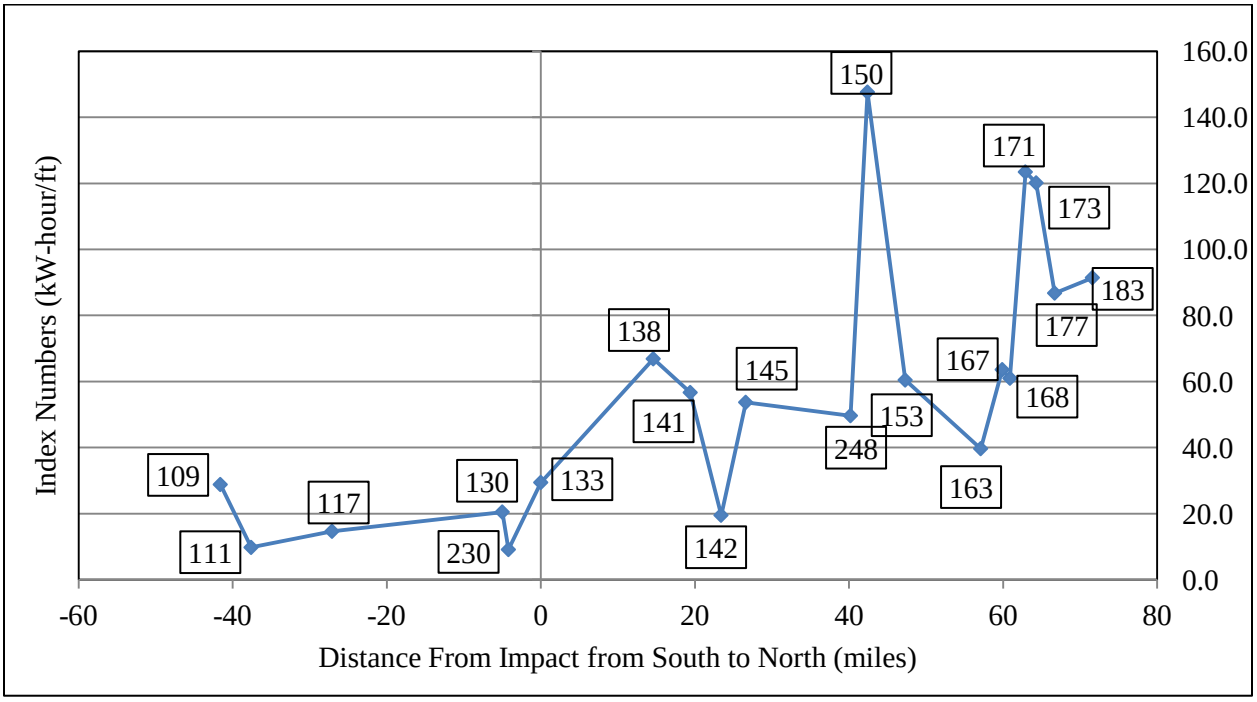

Figure 4.6: Energy Flux Index Numbers compared to the Distance from Landfall.

Figure 4.6 (above) shows the local index numbers in proximity to Sandy's landfall location (Atlantic City, NJ). The negative numbers on the x-axis are south of Atlantic City and the positive numbers indicate north. For the most part the trend is as expected with the higher index numbers located in the northern part of the state. However, there are a few outliers that can be seen in the figure. NJBPN Site 150, along with Site 171 and Site 173, has high values compared to the adjacent areas, while Site 142 and Site 163 have lower values. In order to determine why these sites are outliers, the investigation turned to the shape of those beaches. In all of the outliers, the beach is either relatively steep or relatively flatter compared to the other beaches in the vicinity. The steep beaches produce higher index numbers while shallow beaches produce smaller ones. This reinforces the importance of the beach shape when considering the effect of a storm on the coastline.

The second part of the SSIM addresses the amount of runup-induced overwash that occurs at a location. Overall, the SSIM did a good job in predicting the amount of overwash at the locations when compared to the CRC reports. The reports were not always numerically descriptive when it comes to the run-ups, water levels, and other damages but the qualitative descriptions were often enough to provide a good idea of how much overwash an area received. One concern that occurred when testing the model was how the model faired when boardwalks were included as part of the beach profile (as they were in some of the CRC reports). Because the boardwalks are elevated, when they are included in the beach profile, they add elevation to the highest point of the beach. Because the highest point of the beach factors into the amount of overwash and inundation an area receives, increasing the elevation of the beach causes the SSIM to under predict the overwash at some locations. Including a boardwalk in the beach profile can be subjective because there are some times where it is appropriate to include it. If the boardwalk

is part of a sea wall, for example, then it might be necessary to include it in the profile. However, there are other times when the boardwalk allows water to pass under or through it which does not prevent any overwash on the landward side. In these cases (as noted in some of the site descriptions above), it is necessary to remove the boardwalk from the profile to obtain a reasonable result.

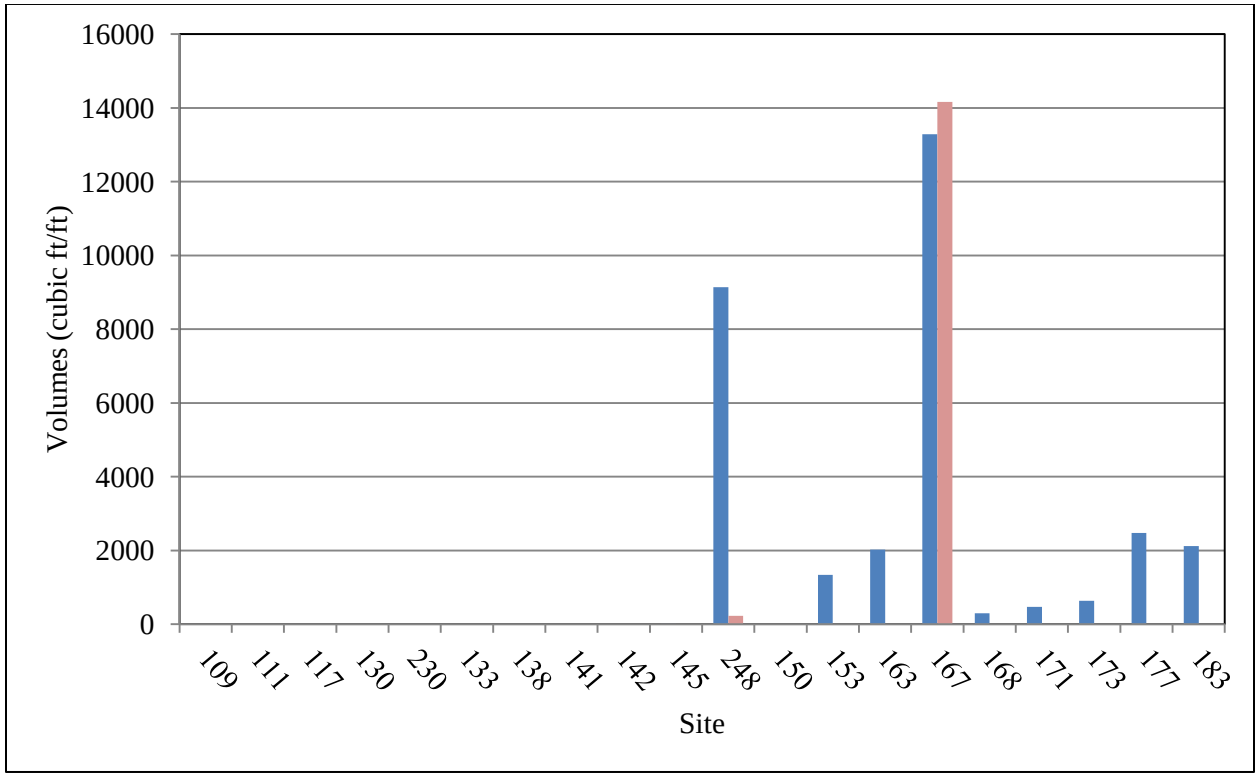

Figure 4.7: Overwash Volumes from Sandy. The blue lines represent the final Storm Severity Index Model runs while the red lines indicate any runs that included the boardwalk in the profile.

Figure 4.7 shows the overwash volumes per foot at each location. The locations with the red bars indicate sites where the boardwalk was included in the beach profile. There are three locations with red bars; Site 248, Site 153 (it is not visible because the value is small), and Site 167. Site 248 and Site 153 both experience increased overwash after the boardwalk is removed. Site 167 is the only site to lose overwash volume after removing the boardwalk. The reason for

this is due to the inundation that occurred at this site. When inundation commences, overwash is assumed to be included in the inundation volume. Because Site 167 experienced a large amount of inundation, the overwash only occurred for a small amount of time. The volumes of inundation at the New Jersey sites are presented below in Figure 4.8.

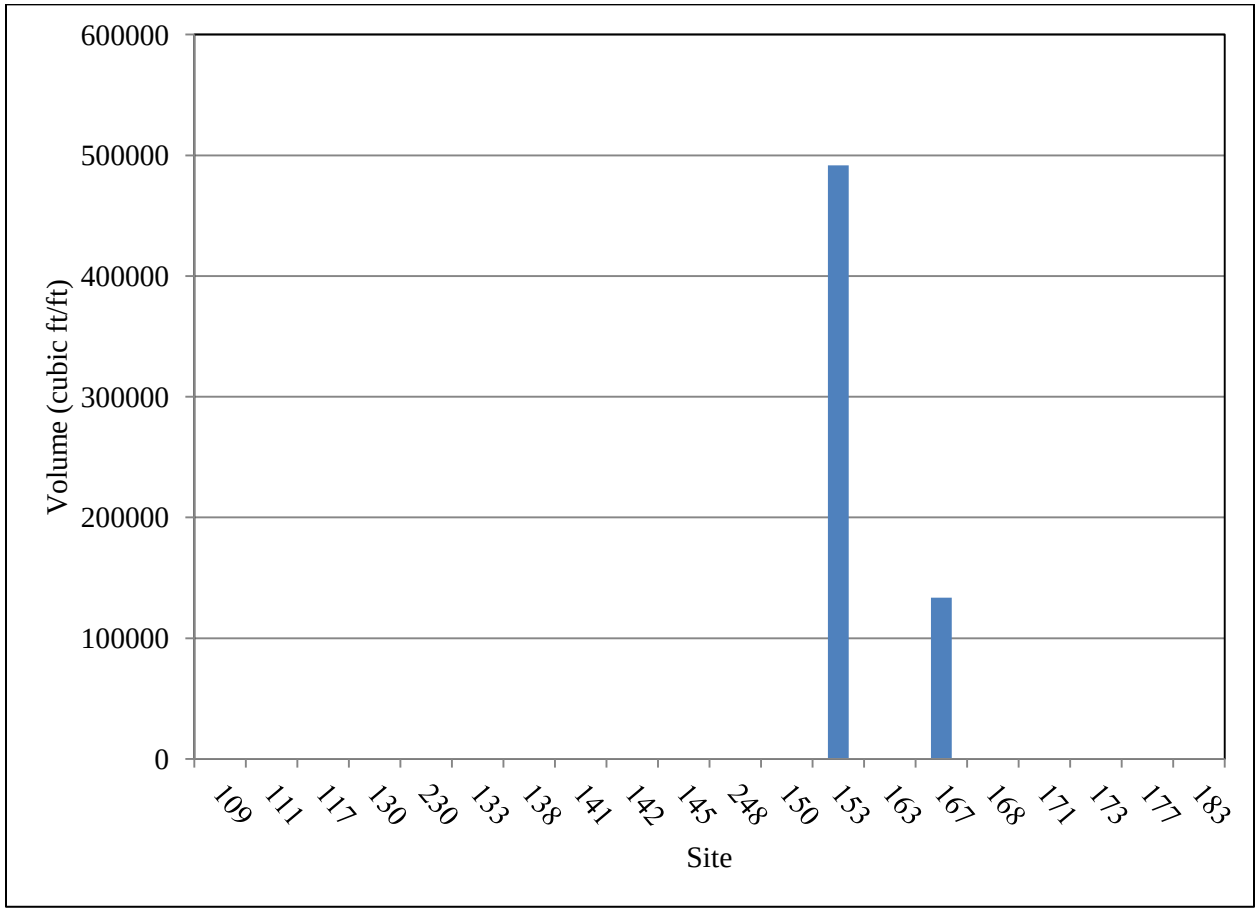

Figure 4.8: Volume of Inundation at each Site during Sandy.

While there were a significant number of sites that experienced overwash, only two of the sites studied suffered inundation. It is important to recall that the inundation at Site 153 was due to the failure of the dune and in order to estimate the results, the post-storm profile was used in the SSIM. This means that the inundation volume is likely overestimated because the dune was

breached in the middle of the storm instead of at the beginning. This result is simply included to give an idea of the maximum amount of flooding that the site could have experienced.

Overall, except for the dune breach at Site 153, the SSIM provided a reasonable estimate for the overwash and inundation at the given sites. Table 4.2 provides a compendium of the results that were displayed in the figures located in Appendix A. It includes the Energy Flux Index, the peak power, the volume of overwash, the volume of inundation and the volume of sand lost above the zero elevation datum at each location.

Table 4.2: Hurricane Sandy Storm Severity Index Results

Site	EFI Value (kW-hours/ft)	Peak Power (kW/ft)	Overwash (cubic ft/ft)	Inundation (cubic ft/ft)	Sand Lost Above Zero Datum (cubic yards per foot)
109	28.80	1.74	0.0	0.0	-10.00
111	9.80	0.69	0.0	0.0	-18.17
117	14.70	0.99	0.0	0.0	-32.71
130	20.50	1.71	0.0	0.0	-27.70
230	9.10	0.92	0.0	0.0	-30.27
133	29.40	2.40	0.0	0.0	-23.20
138	66.90	4.35	0.0	0.0	-40.35
141	56.70	4.25	0.0	0.0	-42.30
142	19.50	1.98	0.0	0.0	-25.10
145	53.70	4.11	8.5	0.0	-39.30
248	49.70	3.74	9134.1	0.0	-109.60
150	147.60	9.34	0.0	0.0	-39.50
153	60.40	5.59	1336.3	491760.0	-22.40
163	39.70	4.65	2018.2	0.0	-32.30
167	63.60	6.57	13285.7	133560.0	-13.60
168	61.00	6.74	290.8	0.0	-23.90
171	123.40	11.04	464.3	0.0	-45.87
173	120.10	11.00	631.3	0.0	-34.10
177	86.80	8.76	2473.9	0.0	-28.75
183	91.40	9.14	2113.2	0.0	-51.70
Avg	57.60	4.99	1587.8	31266.0	-34.50

CHAPTER 5: OCEAN CITY

The next section of this thesis focuses on the storms that impacted Ocean City, Maryland between 1990 and 2003. Instead of focusing on the impact that one storm had over a large area like in Chapter 4, Chapter 5 focuses on 11 storms hitting a 10 mile stretch of beach over the span of 13 years. A brief description of each storm is included below. The beach profiles were obtained from the archives of Offshore & Coastal Technologies, Inc. from William Grosskopf, P.E. (personal communication, June 6, 2015). The beach surveys were conducted using a sled, which is highly accurate, but because the beach surveys were taken to monitor the beach fill rather than study the effects of the storm, the pre- and post-storm surveys do not always occur

just before or just after the storm which makes determining the amount of sand lost during a storm event problematic.

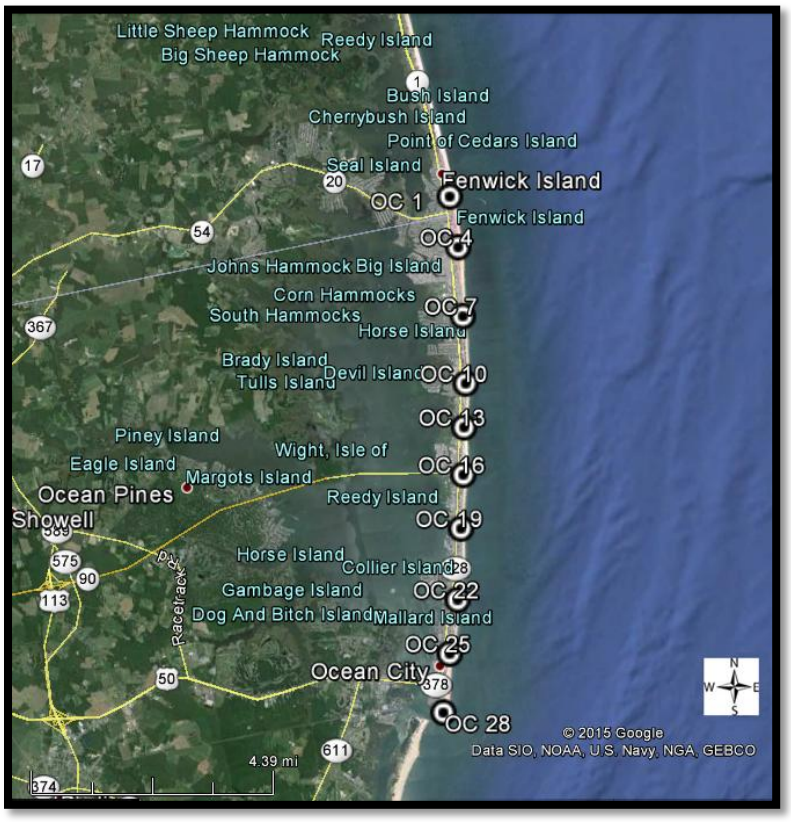

Figure 5.1 shows the locations of all the beach profile surveys. The beach profiles at each location remain the same general shape throughout the years but there are some changes to the beach face depending on when the survey was taken. Graphs of each individual profile can be found in Appendix C. Graphs of the beach profiles through time can be found below in Figure 5.2 through Figure 5.11 in order to show the change in the profiles over time. Table 5.1 below lists the 11 recorded storms along with the date of impact and the number of profiles that were available during each event.

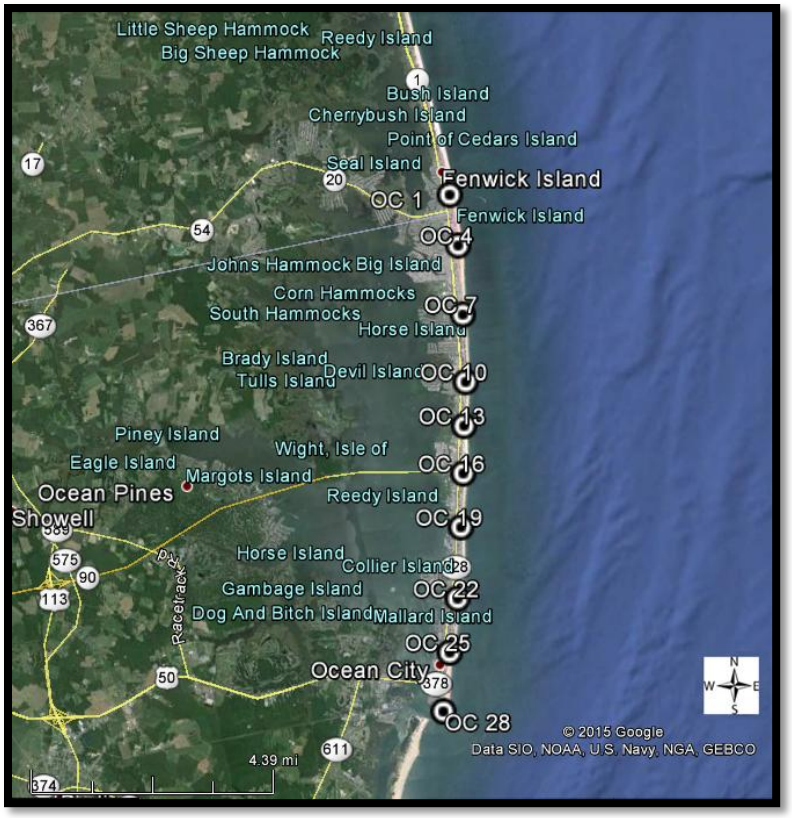

Figure 5.1: Locations of Ocean City Surveys (Google.inc, 2015).

Table 5.1: List of Storms that Impacted Ocean City, MD 1990-2003

Storm	Month	Day	Year	Number of Profiles	Peak Significant Wave Height from Hindcast (ft)	Peak Storm Surge (ft)
Unknown Storm	Aug	20	1990	8	9.2	3.80
Hurricane Bob	Aug	16	1991	4	11.2	2.52
January N.E.	Jan	1	1992	3	20.7	5.96
Maryland Ice Storm	Feb	28	1994	5	19.4	5.34
Christmas N.E.	Dec	21	1994	5	11.5	3.77
N. American Blizzard	Jan	5	1996	10	15.1	5.28
T.S. Josephine	Oct	5	1996	10	13.8	4.62
The El Nino Winter	Jan	28	1998	8	17.1	5.89
Hurricane Floyd	Sept	16	1999	10	12.5	3.87
T.S. Helene	Sept	22	2000	10	8.5	4.07
Hurricane Isabel	Sept	18	2003	10	14.4	2.66

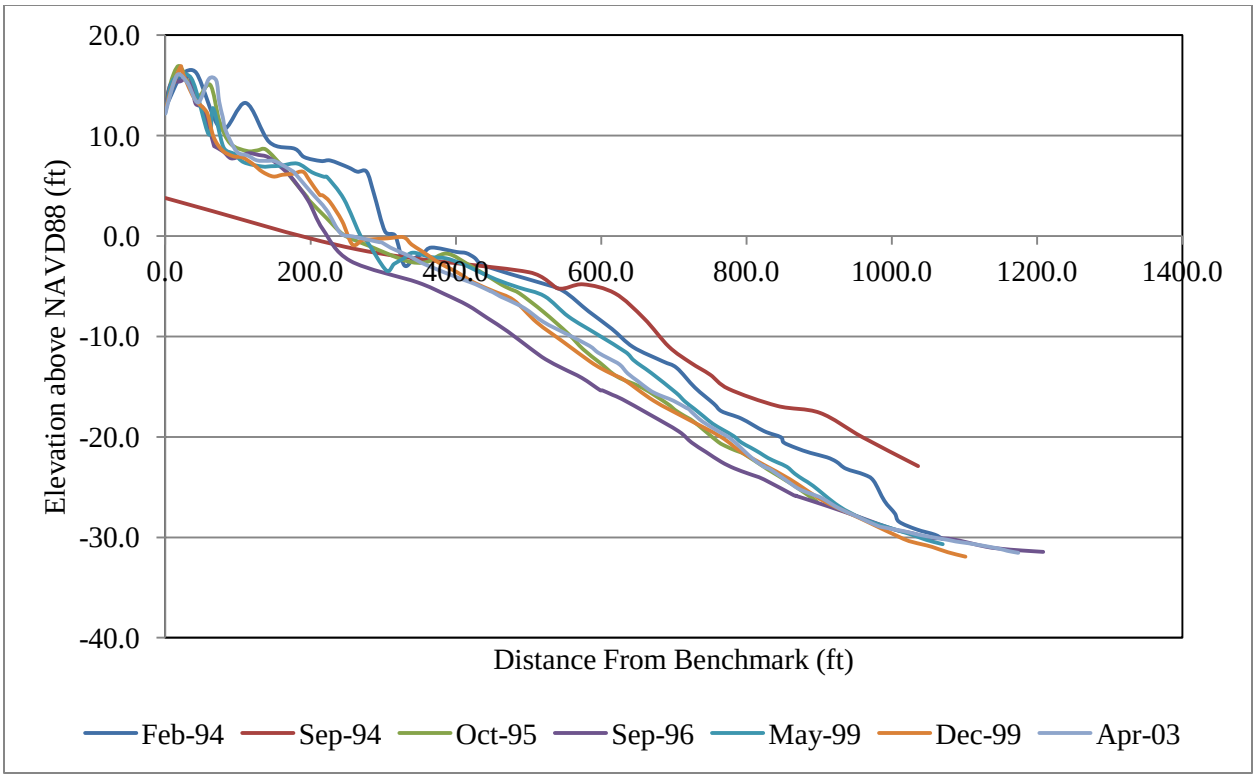

Figure 5.2: Progression of Beach Profiles surveyed at OC 1.

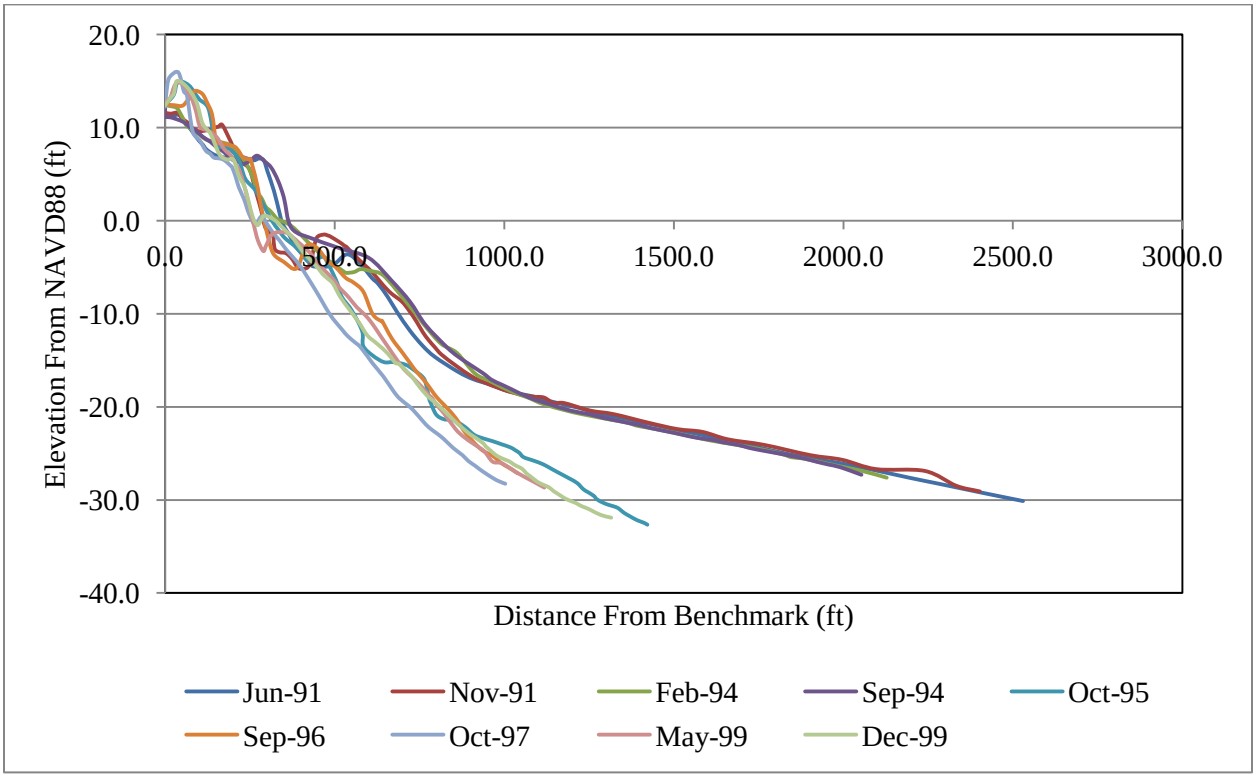

Figure 5.3: Progression of Beach Profiles surveyed at OC 4.

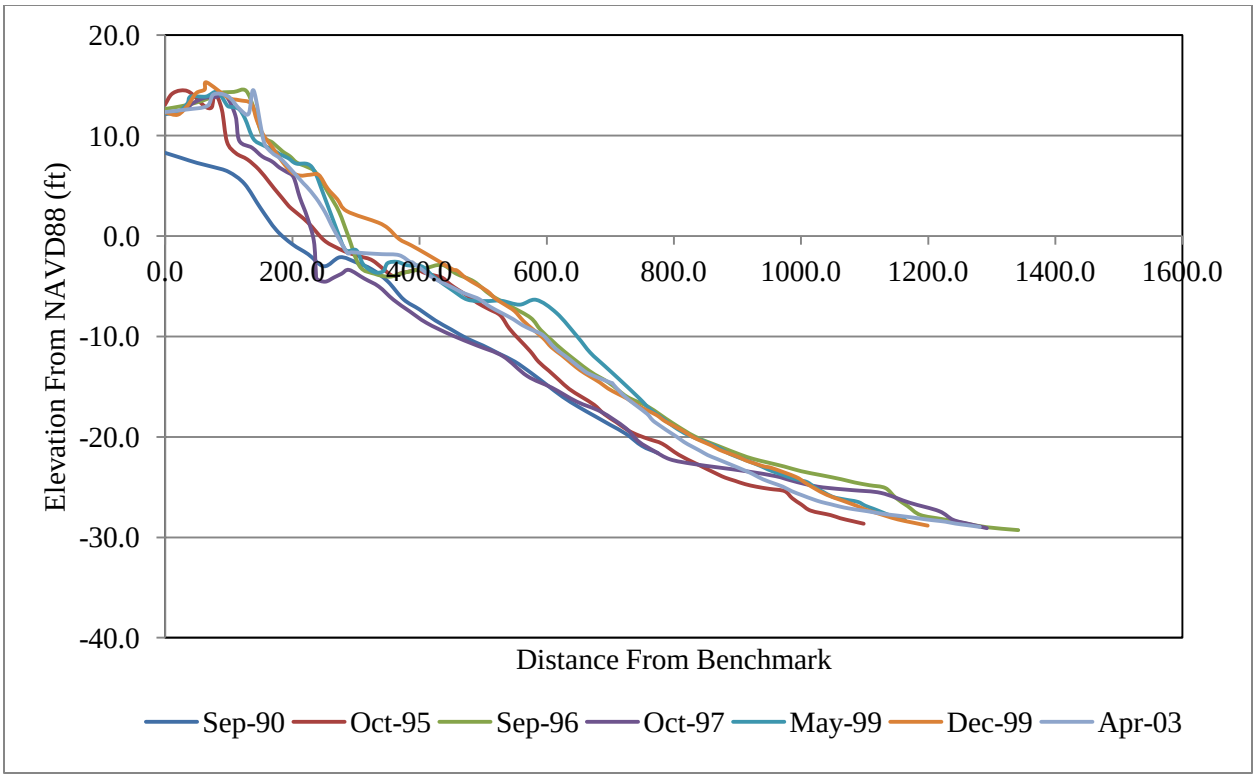

Figure 5.4: Progression of Beach Profiles surveyed at OC 7.

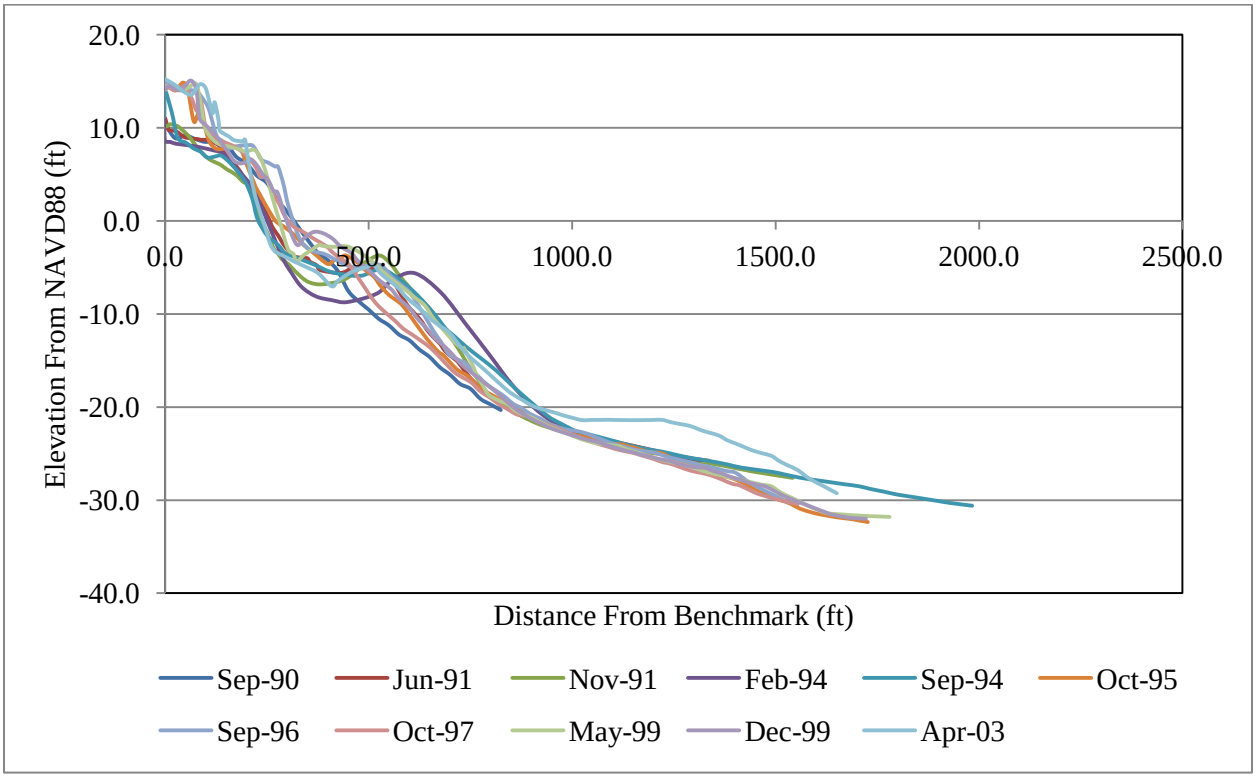

Figure 5.5: Progression of Beach Profiles surveyed at OC 10.

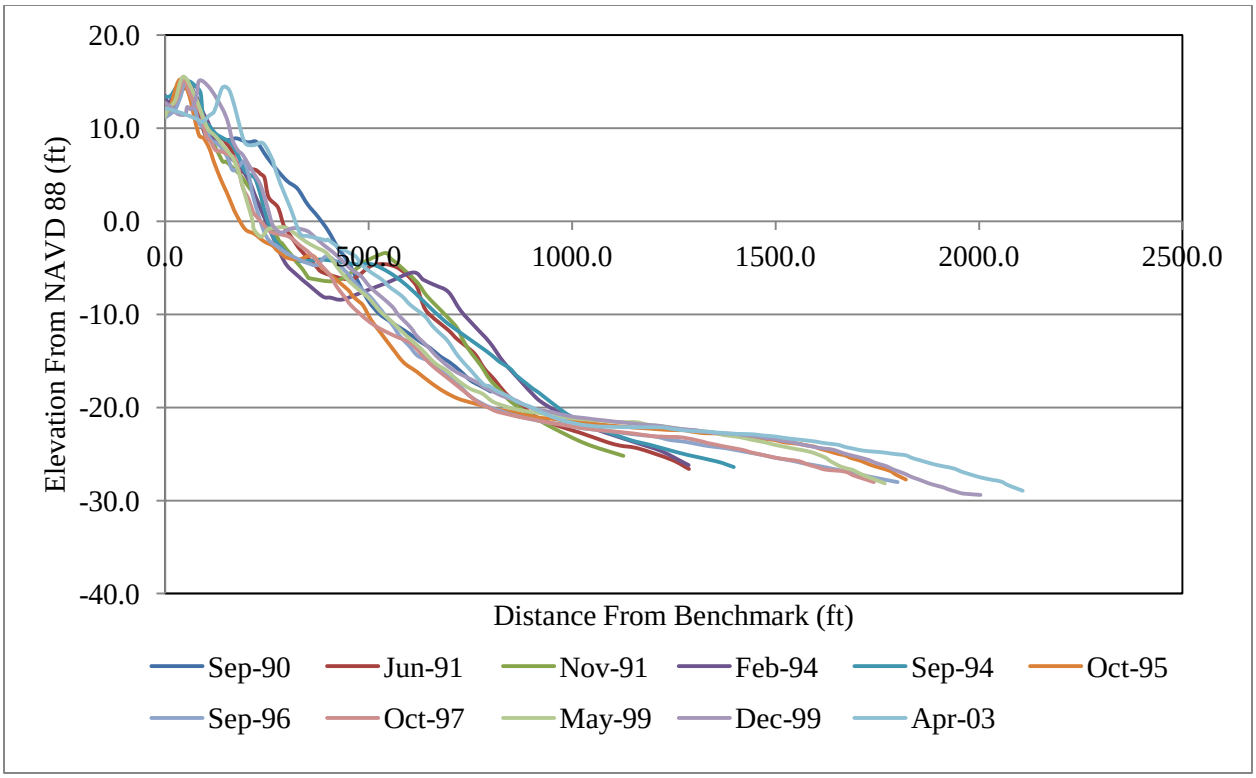

Figure 5.6: Progression of Beach Profiles surveyed at OC 13.

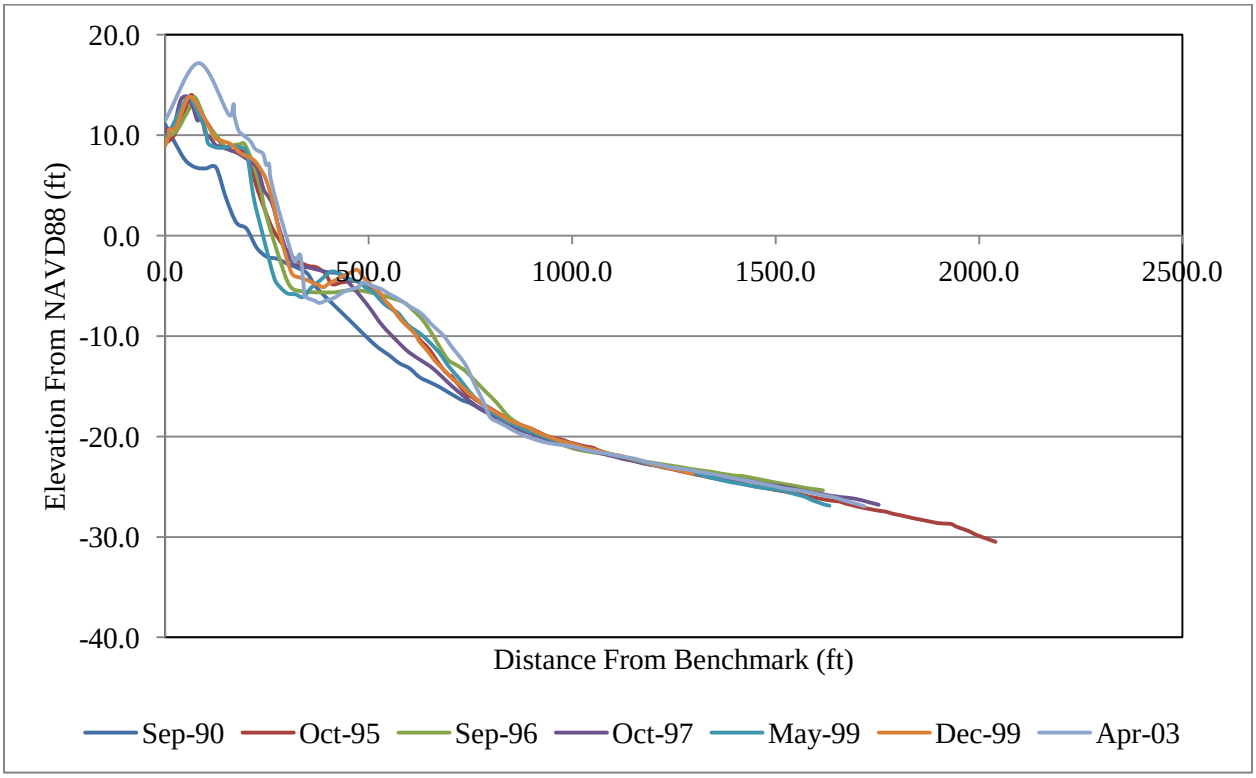

Figure 5.7: Progression of Beach Profiles surveyed at OC 16.

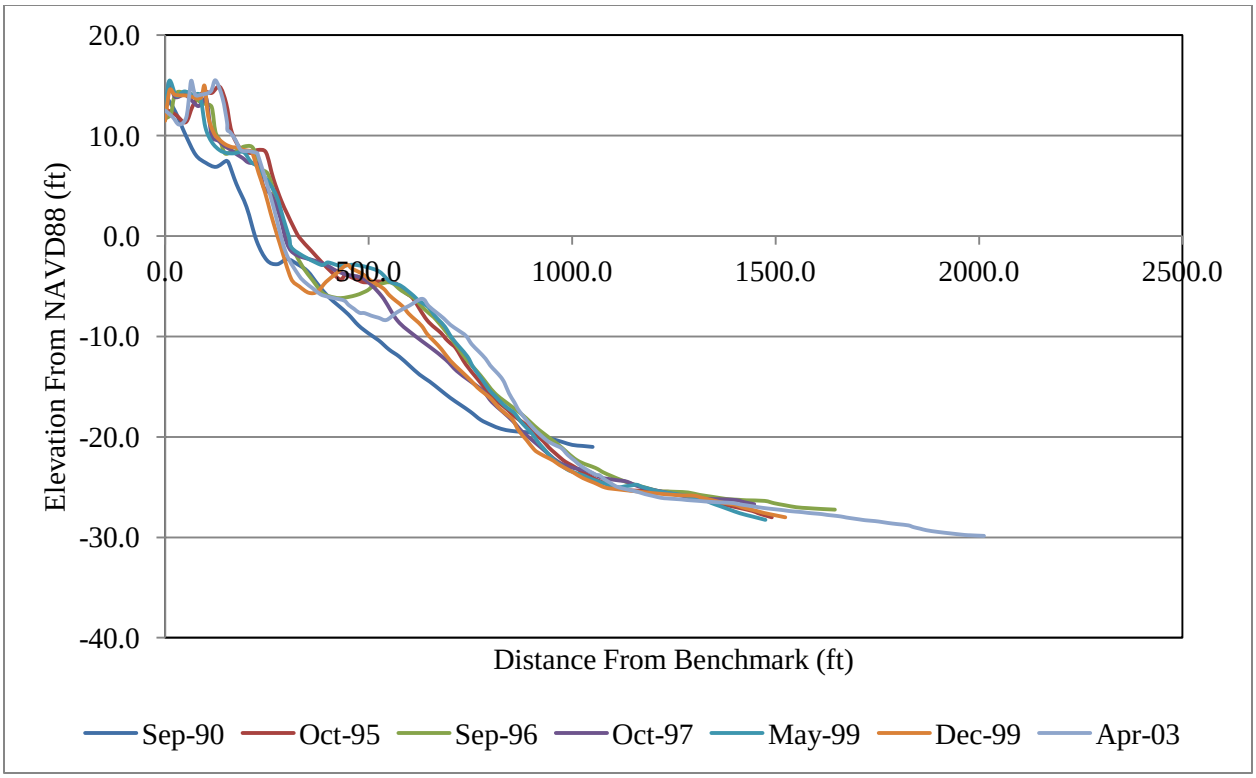

Figure 5.8: Progression of Beach Profiles surveyed at OC 19.

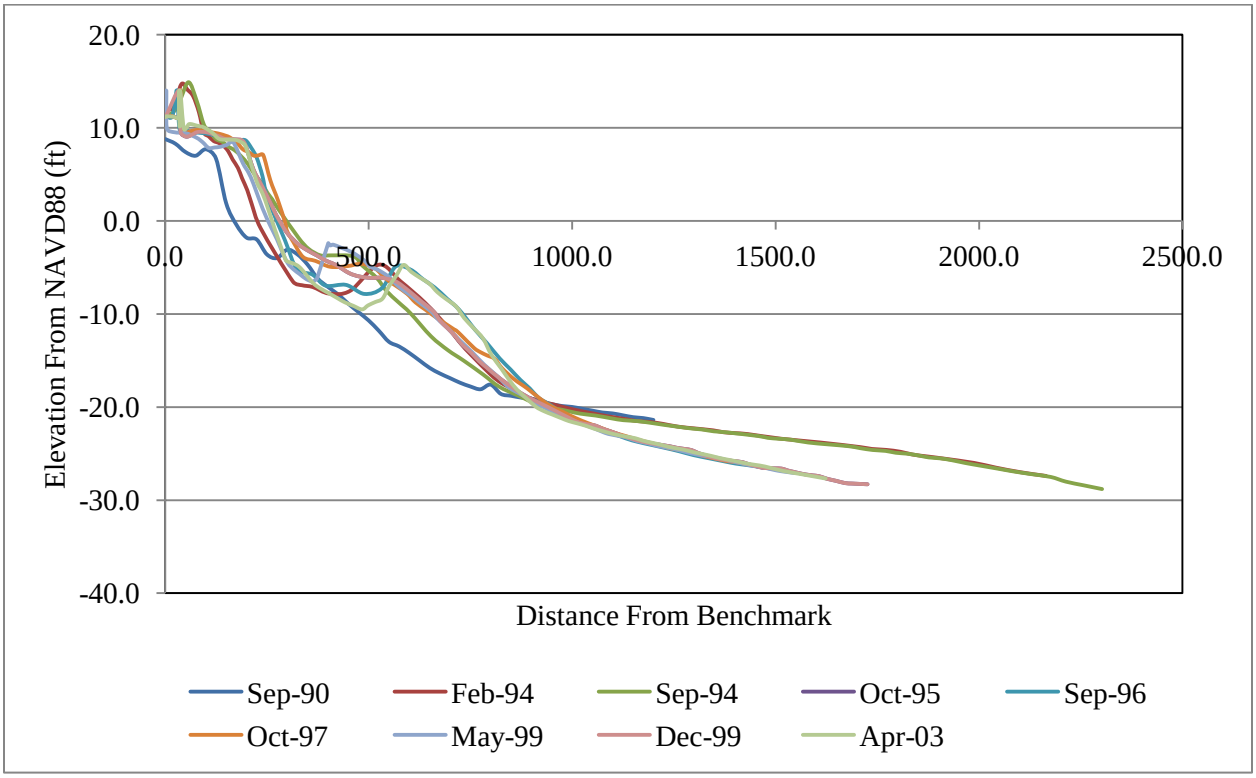

Figure 5.9: Progression of Beach Profiles surveyed at OC 22.

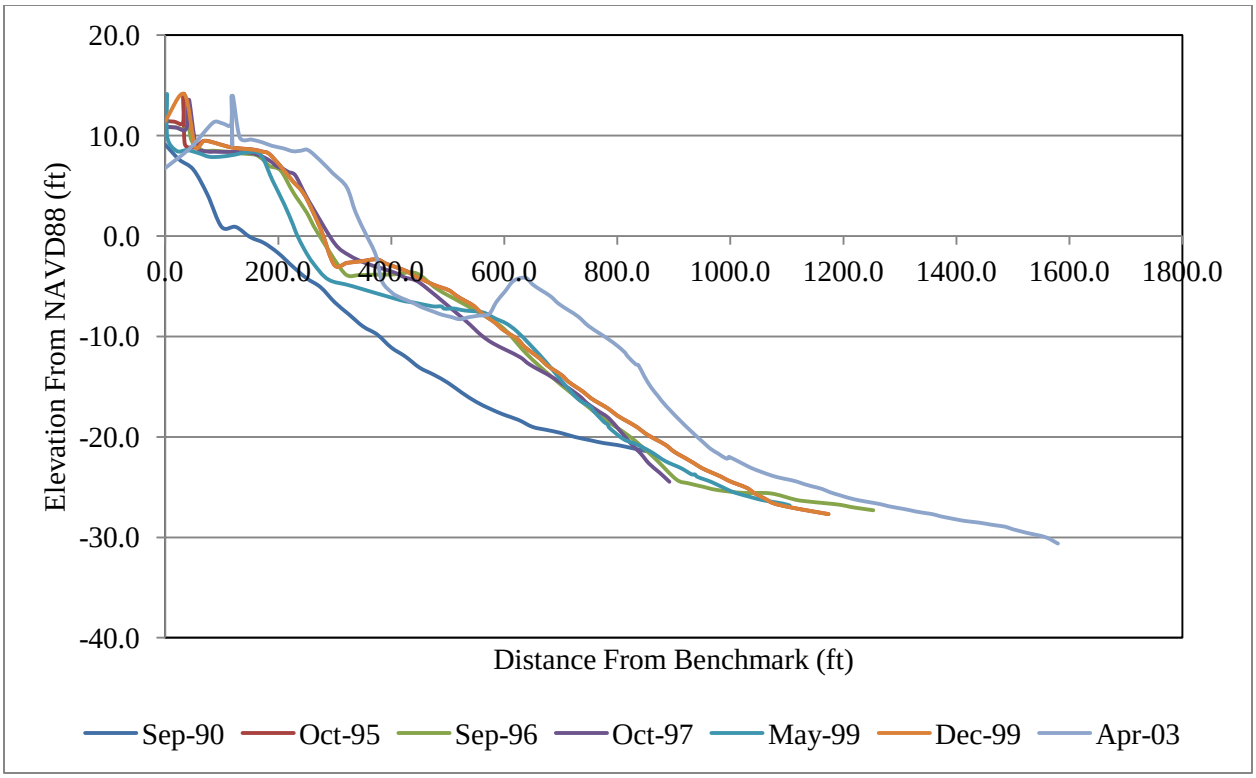

Figure 5.10: Progression of Beach Profiles surveyed at OC 25.

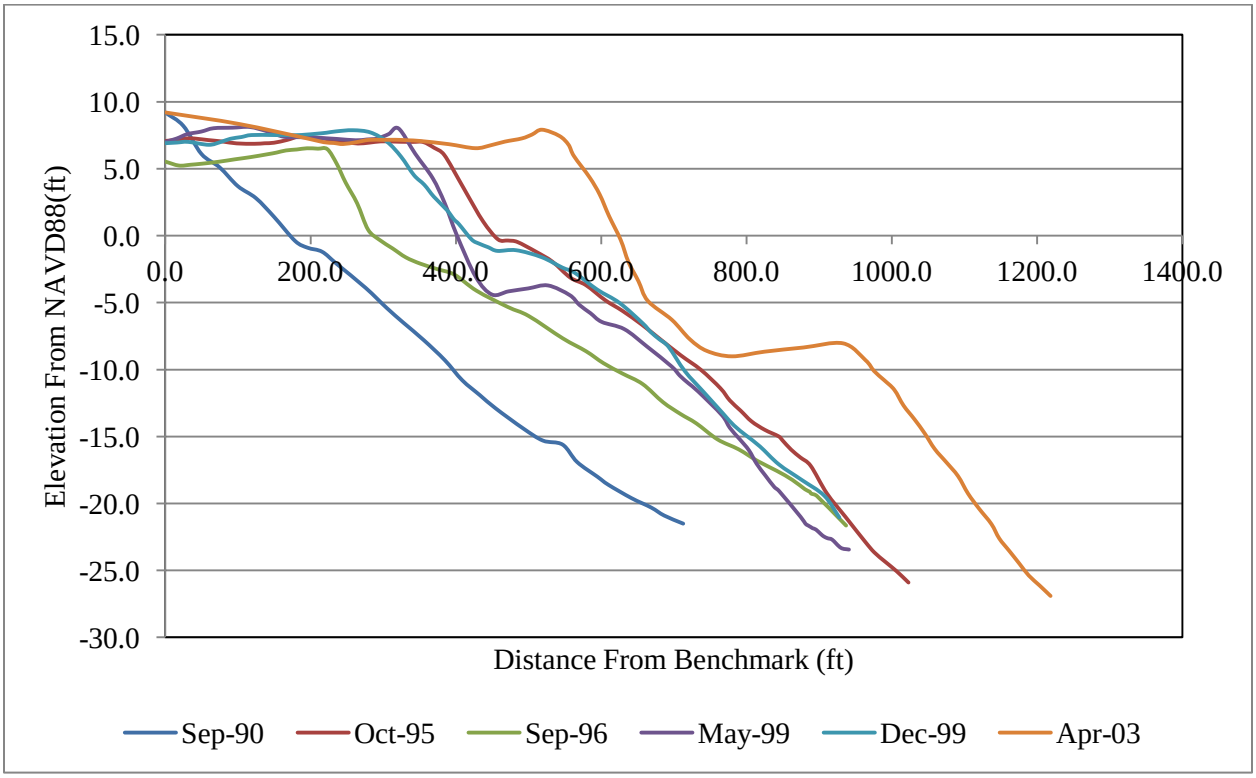

Figure 5.11: Progression of Beach Profiles surveyed at OC 28.

The wave information that is used in the Ocean City analysis was obtained from a hindcast done in 2005 by Offshore & Coastal Technologies. The hindcast used NOAA offshore buoy 44009 as input. The water depth at the output locations varied between 25 and 40 ft deep depending on the location. The water levels used for the SSIM were obtained from NOAA Station 8557380 located in Lewes, Delaware. This station is about 30 miles away from Ocean City, MD which means that the actual water levels at Ocean City may differ slightly depending on the storm track.

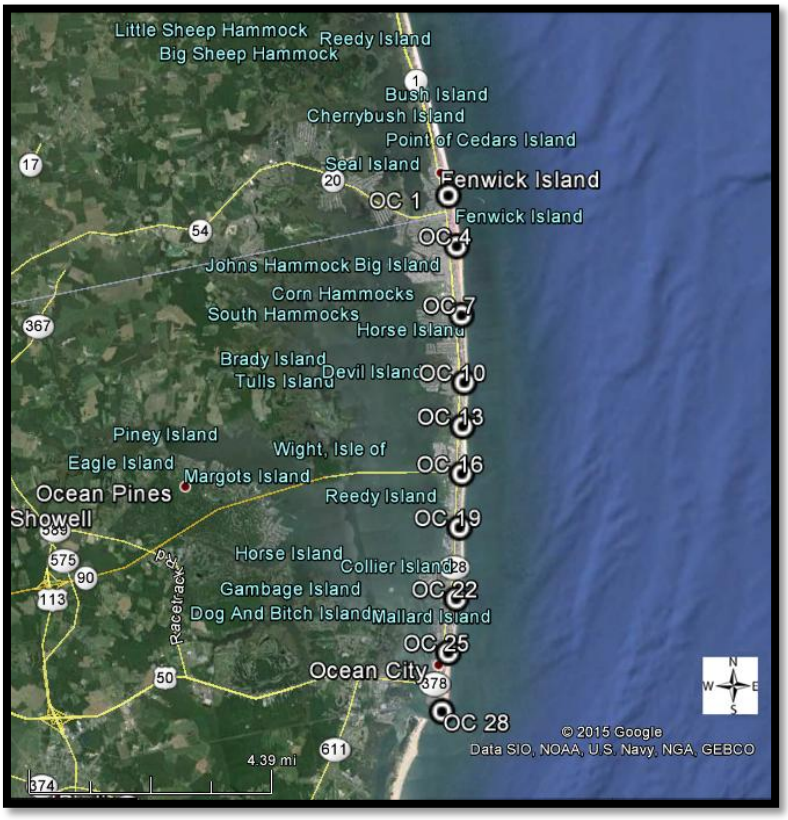

Figure 5.1 shows the wave hindcast from the Christmas 1994 Nor'easter compared to the wave heights recorded at buoy 44009 as an example. One concern, which will be discussed below, is that the hindcast for several storms shows wave heights that are similar to buoy 44009 despite the fact that the buoy was located about 20 miles offshore.

The average results at each location during the storm are included but they should not be used to classify an individual storm. The goal of this SSIM is to create an index for the impact a

storm has on a specific location. Thus, judging the storm by its average will defeat the goal of this SSIM. It has simply been included as a reference point.

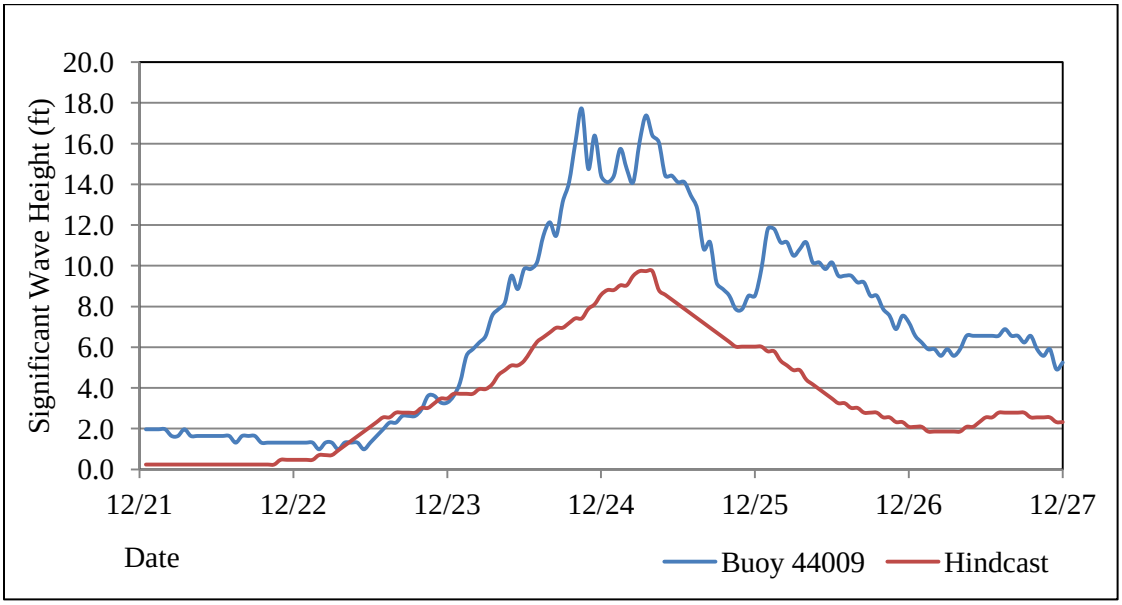

Figure 5.12: Significant Wave Heights during Christmas 1994 Nor'easter.

5.1 DESCRIPTION OF OCEAN CITY STORMS

Out of the 11 storms that were used, 6 of them were tropical systems while the other 5 were extra-tropical systems. The first storm in the record was not able to be identified but because it occurred in August it was assumed to be a tropical system.

TROPICAL STORMS

Hurricane Bob (1991): Hurricane Bob formed in the Bahamas during Mid-August 1991. Bob tracked along the Eastern coast of the United States until finally impacting near Newport, Rhode Island. At its peak, Bob reached Category 3 with 115 MPH winds. Bob dissipated quickly after impacting the North East.

Tropical Storm Josephine (1996): Tropical Storm Josephine formed in October of 1996 in the Gulf of Mexico. It traveled east across Florida and proceeded up the coast of the United States. Josephine reached 70 MPH winds before making landfall in Florida. The extra-tropical remains of the storms produced 77 MPH winds in Maryland.

Hurricane Floyd (1999): Hurricane Floyd originated off the coast of Africa. It strengthened into a tropical storm on September 8th, eventually strengthening to just under Category 5 status while in the Bahamas on September 13th. Floyd accelerated to the northeast along the Florida coast, and weakened to a Category 2 storm by the time it made landfall in North Carolina. The storm continued northward and made landfall again in Long Island.

Tropical Storm Helene (2000): Tropical Storm Helene was formed from a tropical wave off the African coast on September 10. The tropical system traveled east into the Gulf of Mexico. On September 21st, Helene reached its peak intensity of 70 MPH and the next day, it made landfall at Fort Walton Beach, Florida. The system moved Northeast across the southern States. Helene reemerged from the Virginia coast and continued on its way North.

Hurricane Isabel (2003): Hurricane Isabel formed in September of 2003 in the Atlantic Ocean. Isabel fluctuated between Category 4 and Category 5 until finally weakening to a Category 2 storm before making landfall on the outer banks of North Carolina.

EXTRATROPICAL STORMS

January Nor'easter (1992): The January '92 Nor'easter was a small, short-lived storm that struck the Mid Atlantic States. The storm produced 55 MPH winds and a high surf during a new moon.

Maryland Ice Storm (1994): The Maryland Ice Storm of '94 was one of a series of ice storms that struck Maryland in winter of 1993-94. The storm dropped snow and freezing rain across the Mid Atlantic states and damages estimates were near $100 million.

Christmas Nor'easter (1994): The Christmas '94 Nor'easter was an intense cyclone that formed in the Gulf of Mexico in an area of low pressure and moved across the state. It intensified and moved northward as it hit the warm waters of the Gulf Stream. The storm came ashore on Christmas Eve near New York City. The impact in Maryland was fairly minimal with winds around 40 MPH and some damage to dunes.

North American Blizzard (1996): The Blizzard of '96 was a severe nor'easter that struck the U.S. East Coast with up to 4 feet of snow in January of 1996. Winds speeds hit 40 MPH as snow fell for 2 days.

The El Nino Winter (1998): The winter of 1997-98 was one of the warmest and wettest winters on record. A record-breaking El Nino event caused unusual weather all over the country including persistent storms in the winter. The wave record was obtained from early February of 1998 during one of the many storms that occurred during this time period.

5.2 UNKNOWN STORM (1990)

The first earliest storm in the record occurred between August 18th and 24th during 1990. This storm was not identified by name but it is assumed to be a tropical system due to the time of year in which it occurred. The pre-storm conditions of the beach were available at eight different locations. Table 5.2 shows the result from the SSIM. During this storm there was no overwash or inundation due to the low peak power values. The post-storm profiles were only available for Site OC 10 and OC 13. Figure 5.13 and Figure 5.14 show the results from the SSIM for all of the locations during the storm. The storm lasted for 5 days and had an impact during every high tide during this time period. The index numbers at each site are minor but the erosion at the two available sites is significant in magnitude with 9.85 cubic yards of sand per foot of erosion at OC 10 and 20.33 cubic yards per foot of erosion at OC 13. The measurements for the erosion are taken above the zero elevation datum (NAVD88).

Table 5.2: Storm Severity Index Model Results for Unknown Storm

Site	EFI Value (kW-hours/ft)	Peak Power (kW/ft)	Overwash (Cubic ft/ft)	Inundation (Cubic ft/ft)	Sand Lost (Cubic Yards/ft)
OC 7	10.43	0.53	0.0	0.0	N/A
OC 10	10.17	0.53	0.0	0.0	-9.85
OC 13	12.82	0.59	0.0	0.0	-20.33
OC 16	7.46	0.41	0.0	0.0	N/A
OC 19	16.62	0.75	0.0	0.0	N/A
OC 22	11.78	0.58	0.0	0.0	N/A
OC 25	5.93	0.32	0.0	0.0	N/A
OC 28	18.89	0.72	0.0	0.0	N/A
Avg	11.76	0.55	0.0	0.0	-15.09
STDV	4.35	0.14	0.0	0.0	7.41

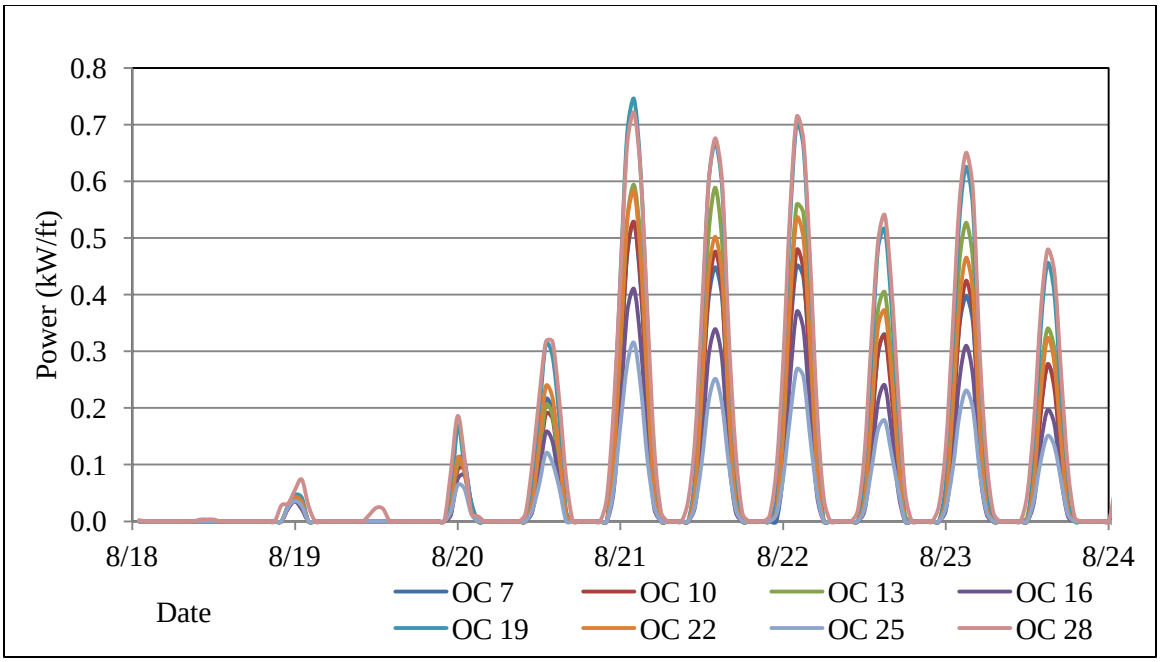

Figure 5.13: Energy Flux Time Series during Unknown Storm (1990).

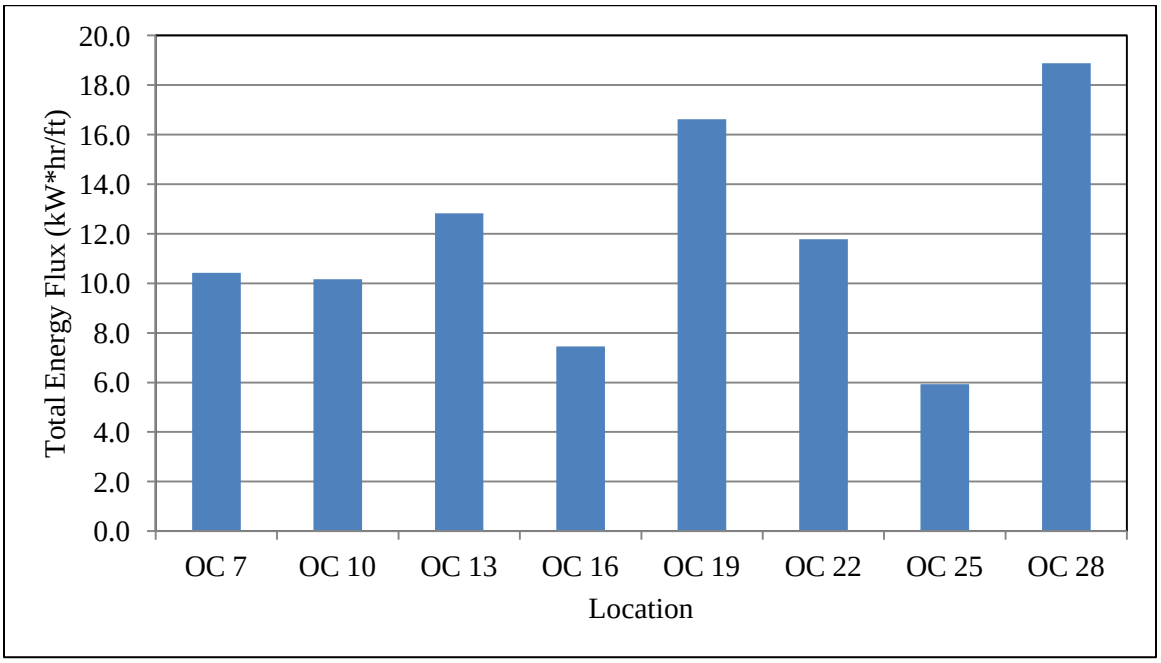

Figure 5.14: Energy Flux Index Numbers for each Location during Unknown Storm.

5.3 HURRICANE BOB (1991)

The second storm that the SSIM was used on was Hurricane Bob in 1991, which occurred on August 19th. There are four profiles from Hurricane Bob. The pre-storm surveys for this location were taken in June of 1991 and the post-storm surveys were done in November of 1991. As seen in Table 5.3, there are three locations where surveys were done. The hindcast (seen in Figure B.9.B) for Hurricane Bob raises some concerns. The hindcast wave heights are very similar to the wave heights from buoy 44009 when they should be lower. This means the results from the SSIM are possibly overestimated. The storm produced similar results at all three locations with index numbers ranging from 1.12 to 1.42 kW-hours per linear foot. There was no overwash at any of the locations the storm. The volume of sand lost at all three locations was similar, OC 4 lost 7.93 cubic yards per foot, OC 10 lost 8.63 cubic yards per foot, and OC 13 lost 12.70 cubic yards per foot. These values are high considering the index numbers did not exceed 1.50 kW-hours per linear foot. The peak powers were also limited and did not exceed 0.31 kW per foot. The EFI values during Hurricane Bob can be seen in Figure 5.15 and the index numbers can be seen in Figure 5.16.

Table 5.3: Storm Severity Index Model Results for Hurricane Bob

Site	EFI Value (kW-hours/ft)	Peak Power (kW/ft)	Overwash (Cubic ft/ft)	Inundation (Cubic ft/ft)	Sand Lost (Cubic Yards/ft)
OC 4	1.12	0.25	0.0	0.0	-7.93
OC 10	1.26	0.25	0.0	0.0	-8.63
OC 13	1.42	0.31	0.0	0.0	-12.70
Avg	1.27	0.27	0.0	0.0	-9.75
STDV	0.15	0.03	0.0	0.0	2.58

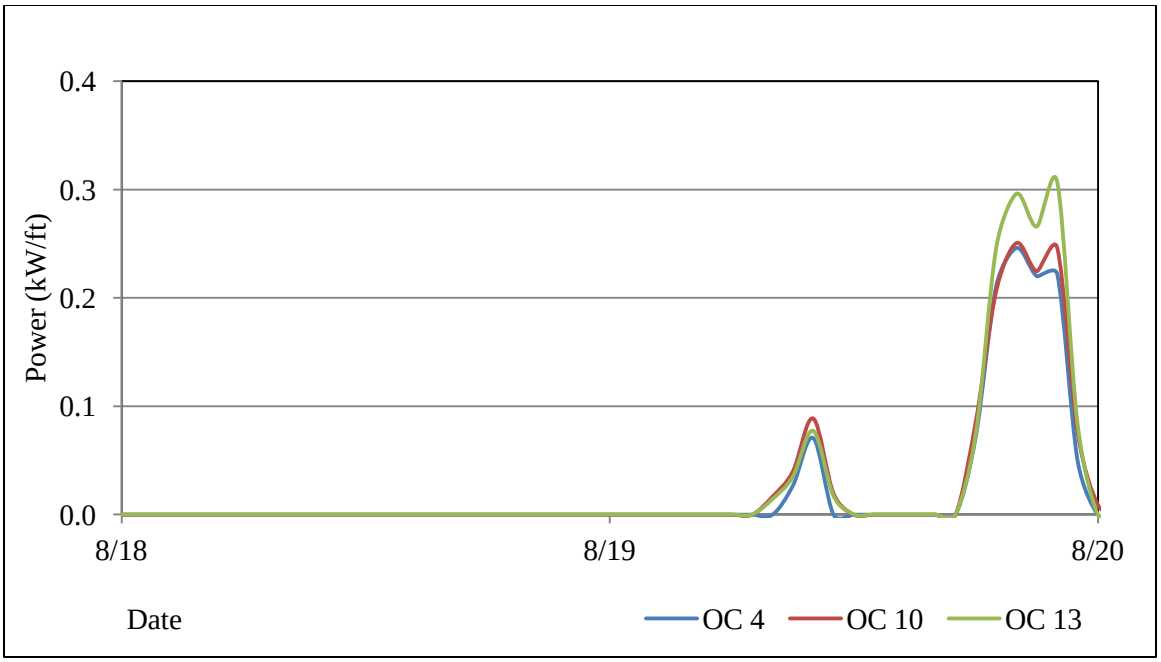

Figure 5.15: Time Series of Energy Flux above the Normal Mean High Water Line during Hurricane Bob (1991).

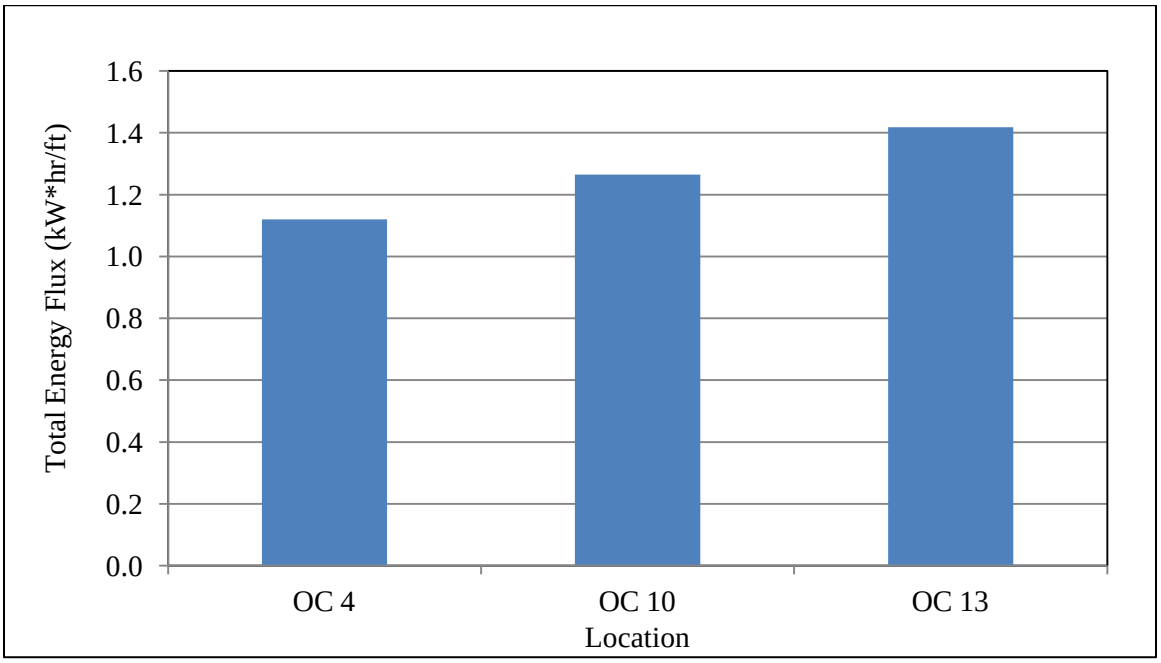

Figure 5.16: Energy Flux Index Numbers for each Location during Hurricane Bob.

5.4 JANUARY NOR'EASTER (1992)

The third storm in this section is the January 1992 Nor'easter which occurred from January 1st to January 8th. The storm struck on New Year's Day and the surveyed profiles bracketed it closely. This was the second storm to hit the area in rapid succession after Hurricane Bob passed in August of 1991. The January 1992 Nor'easter dataset has 3 profiles available. The profiles that were used here include the post-storm profiles of Bob that were taken in November of 1991 as the pre-storm profiles for the January 1992 Nor'easter. The post storm profiles were taken in late January of 1992. The hindcast, which can be seen in Figure B.12.B, once again shows possible overestimation of the wave heights. The results of the SSIM can be seen in graphical form in Figure 5.17 and Figure 5.18 while the quantitative data can be seen below in Table 5.4. Like Bob, this storm also produced similar results in all three locations. The Energy Flux Index values range from 35.35 to 41.66 kW-hours per linear foot. There was overwash during this storm event at all three locations. OC 4 had almost 4000 cubic feet per foot of water, OC 10 had approximately 7400 cubic feet per foot, and OC 13 had 572.8 cubic feet per foot according to the SSIM estimate.

Table 5.4: Storm Severity Index Model Results for January 1992 Nor'easter

Site	EFI Value (kW-hours/ft)	Peak Power (kW/ft)	Overwash (Cubic ft/ft)	Inundation (Cubic ft/ft)	Sand Lost (cubic yards/ft)
OC 4	35.35	3.68	3983.2	0.0	-14.33
OC 10	41.66	4.82	7431.8	0.0	-5.33
OC 13	40.98	4.59	572.8	0.0	-12.70
Avg	39.33	4.36	3995.9	0.0	-10.79
STDV	3.46	0.60	3429.5	0.0	4.80

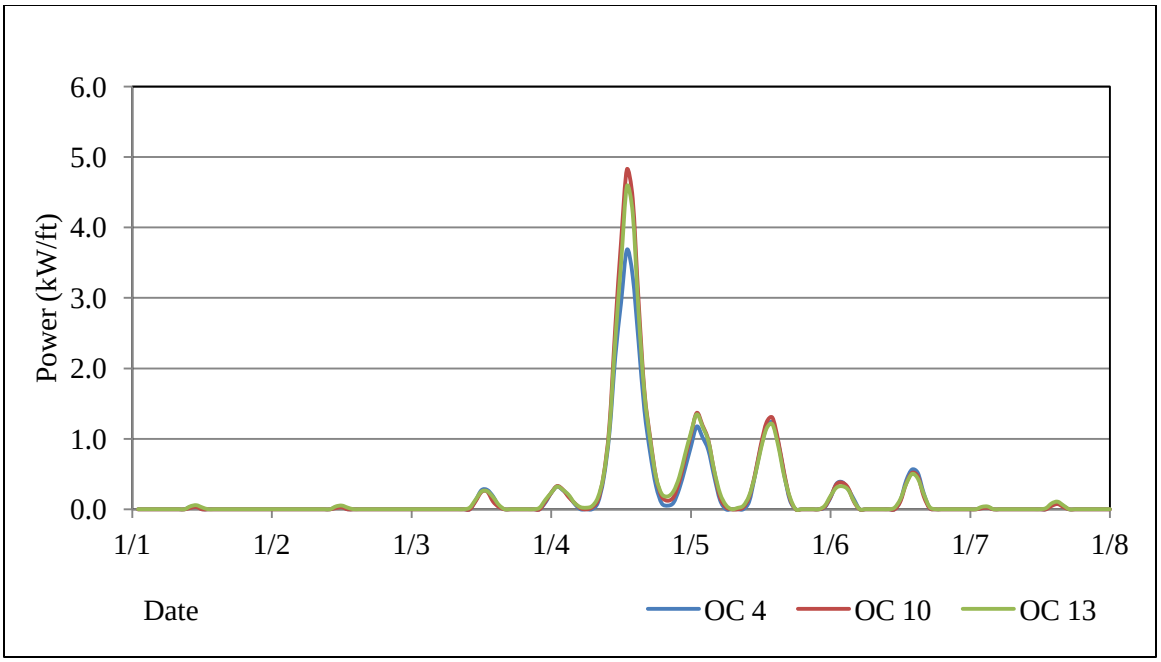

Figure 5.17: Time Series of Energy Flux above Normal Mean High Water Line during January Nor'easter (1992).

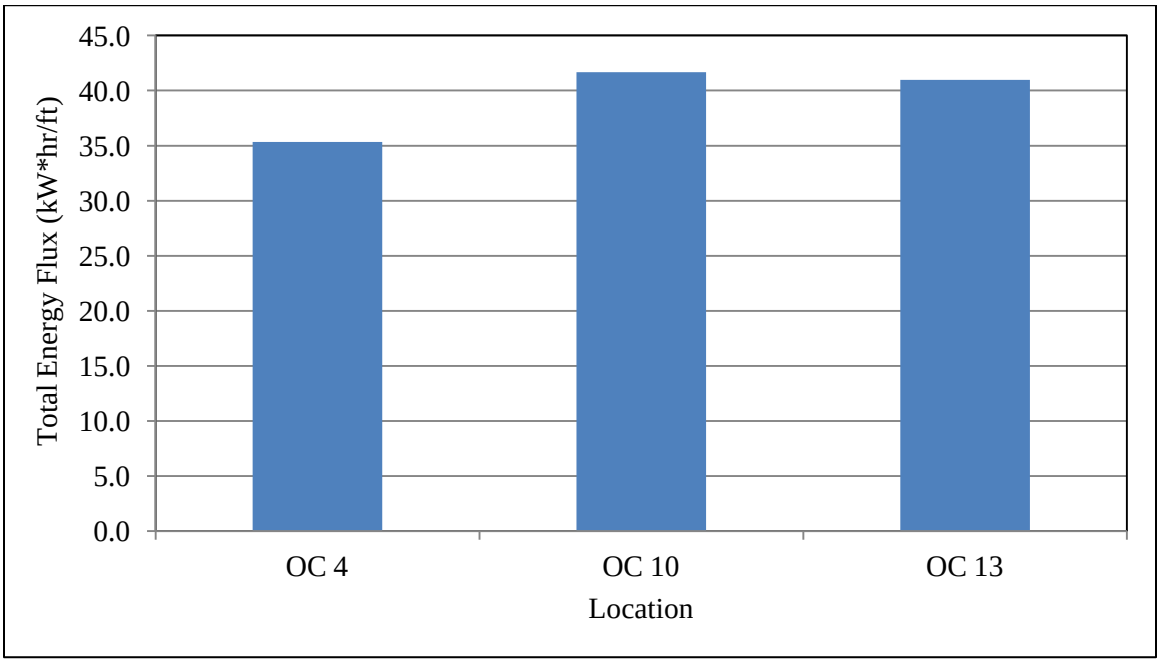

Figure 5.18: Energy Flux Index Numbers for each Location during January 1992 Nor'easter.

5.5 MARYLAND ICE STORM (1994)

The Maryland Ice Storm occurred between February 28th and March 4th in 1994. This storm has profiles at 5 locations and there are both pre- and post-storm beach profiles available (from February and March of 1994). The wave height data from buoy 44009 are not available for this time period but it is possible that the hindcast (seen in Figure B.15.B) is overestimating the wave heights. The time series energy flux above the normal mean high water line can be seen in Figure 5.19 and the EFI numbers are shown in Figure 5.20. The Maryland Ice Storm produced a range of SSIM results. OC 4 only had an index number of 10.60 kW-hours per linear foot but OC 13 had 36.05 kW-hours per linear foot. There was overwash at OC1 and OC 22. There was no inundation during this storm. OC1 lost 36.15 cubic yards of sand per foot above the zero elevation datum (NAVD88). Table 5.5 shows the SSIM results for each of the 5 Ocean City sites.

Table 5.5: Storm Severity Index Model Results for Maryland Ice Storm of 1994

Site	EFI Value (kW-hours/ft)	Peak Power (kW/ft)	Overwash (Cubic ft/ft)	Inundation (Cubic ft/ft)	Sand Lost (cubic yards/ft)
OC 1	19.29	2.76	604.2	0.0	-36.15
OC 4	10.60	1.66	0.0	0.0	-7.59
OC 10	32.54	4.06	0.0	0.0	-3.74
OC 13	36.05	4.24	0.0	0.0	-2.44
OC 22	30.95	3.83	45.0	0.0	-1.44
Avg	25.89	3.31	129.8	0.0	-10.27
STDV	10.61	1.09	265.9	0.0	14.65

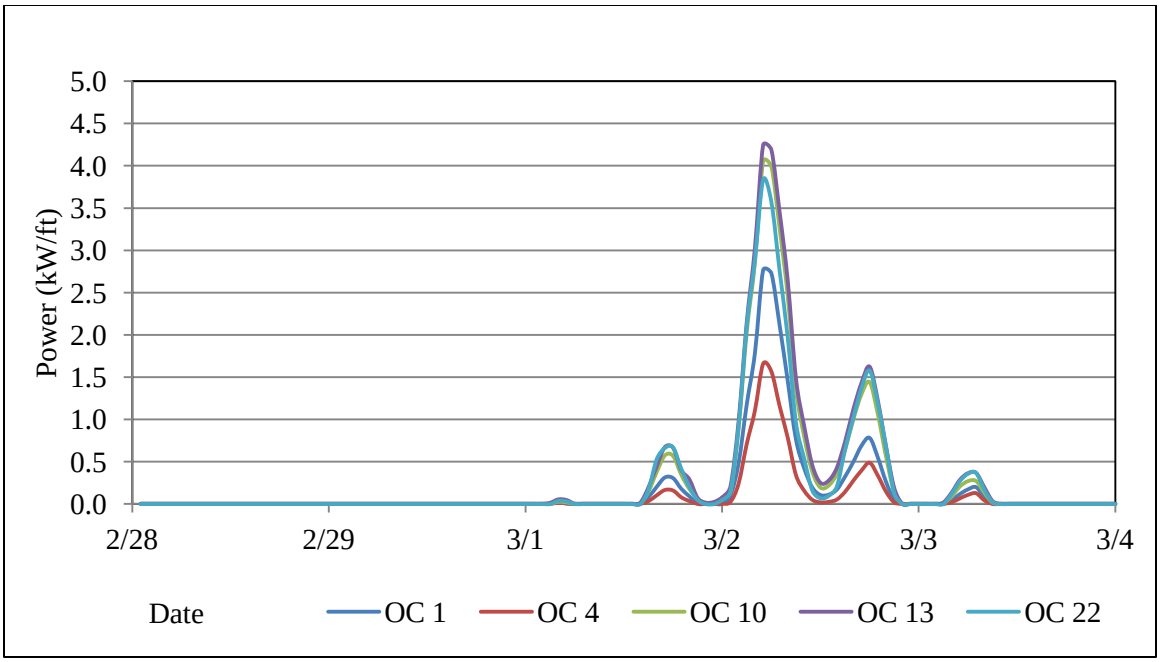

Figure 5.19: Time Series of Energy Flux above Normal Mean High Water Line during Maryland Ice Storm (1994).

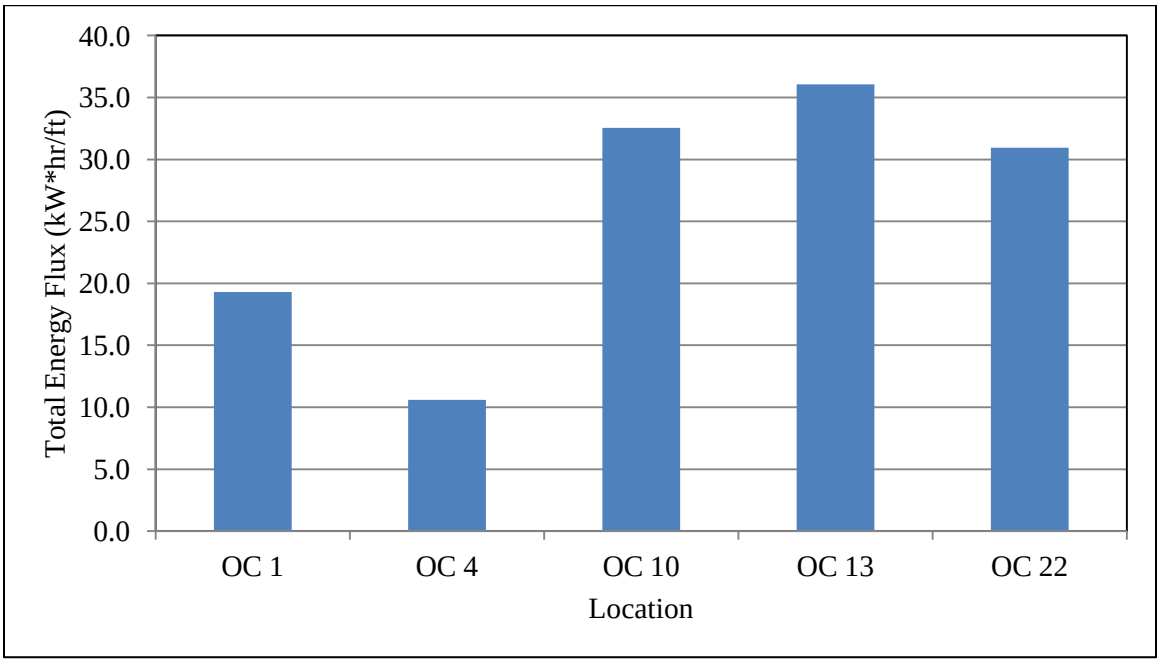

Figure 5.20: Energy Flux Index Numbers for each Location during Maryland Ice Storm.

5.6 CHRISTMAS NOR'EASTER (1994)

The Christmas 1994 Nor'easter struck Maryland between December 22nd and 27th of 1994. There were 5 locations available for this storm. During this time period, the hindcast appears to do a better job of calculating the nearshore wave heights. Unlike during previous storms, the hindcast shows lower wave heights than the offshore buoy does which makes the SSIM results more credible than for the January 1992 Nor'easter. The index numbers during this storm are fairly uniform except for at OC 22. As seen in Table 5.6, OC 22 only has 10.22 kW-hours per foot while the other four locations have between 16.70 and 27.23 kW-hours per foot. The energy flux above the normal mean high water can be viewed in Figure 5.21 while the EFI values can be seen in Figure 5.22. There was some overwash at OC 10 but no inundation. The volume of sand lost is not available due to the lack of post-storm profiles.

Table 5.6: Storm Severity Index Model Results for Christmas 1994 Nor'easter

Site	EFI Value (kW-hours/ft)	Peak Power (kW/ft)	Overwash (Cubic ft/ft)	Inundation (Cubic ft/ft)	Sand Lost (cubic yards/ft)
OC 1	22.32	1.26	0.0	0.0	N/A
OC 4	27.23	1.37	0.0	0.0	N/A
OC 10	16.70	1.08	97.2	0.0	N/A
OC 13	17.70	1.21	0.0	0.0	N/A
OC 22	10.22	0.81	0.0	0.0	N/A
Avg	18.83	1.14	19.4	0.0	N/A
STDV	6.38	0.21	43.5	0.0	N/A

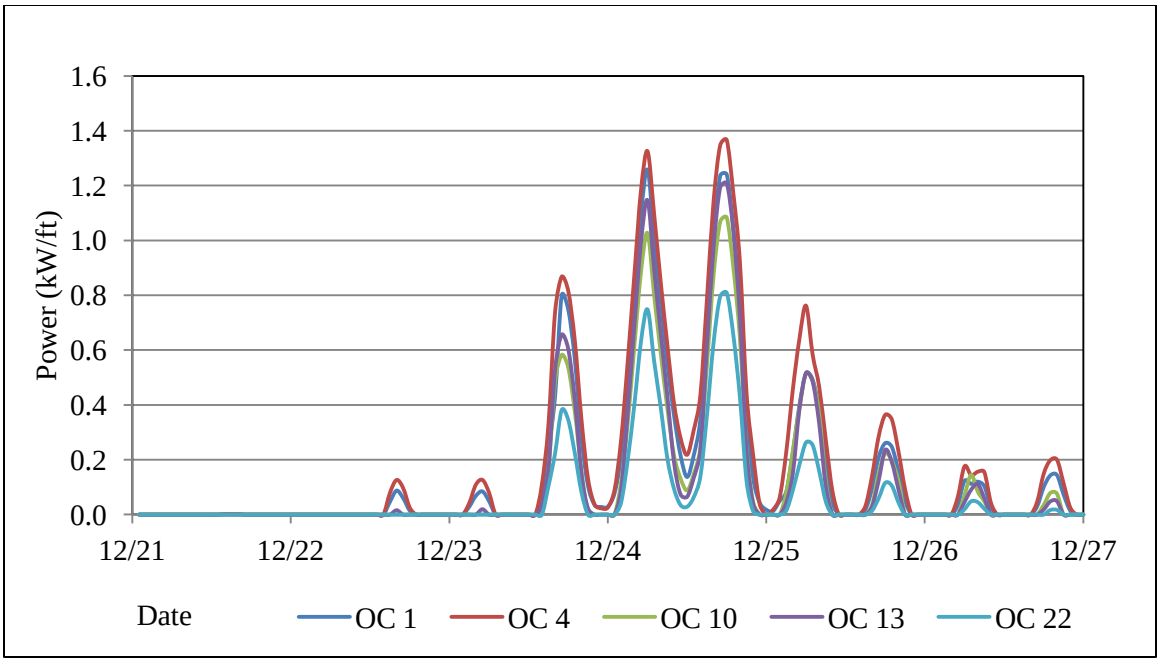

Figure 5.21: Times Series of Energy Flux above Normal Mean High Water Line during Christmas Nor'easter (1994).

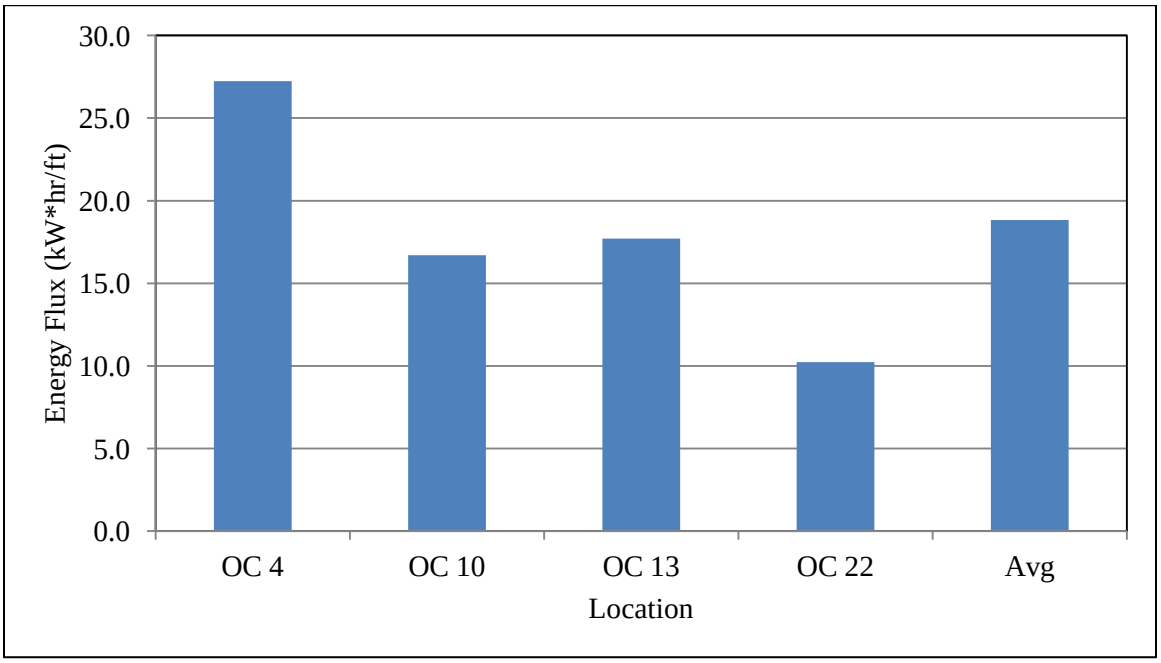

Figure 5.22: Energy Flux Index Numbers for each Location during Christmas 1994 Nor'easter.

5.7 NORTH AMERICAN BLIZZARD (1996)

The North American Blizzard of 1996 occurred in from January 7th to 12th. All 10 sites have available pre-storm surveys during this storm. However, post-storm profiles are only available at sites OC 1, OC 4, OC 7, and OC 10. Figure 5.24 shows that the SSIM results for this storm are very consistent at each location. The hindcast again appeared to do a better job in this case as the peak wave heights were lower than the ones observed by the offshore buoy. The index numbers range from 18 to 24 kW-hours per linear foot with the only exception being at OC 25. OC 25 reports an SSIM result of 33.37 kW-hours per foot. There was some overwash predicted by the SSIM. At OC 13, 539.6 cubic feet per linear foot was reported. OC 25 showed 2,970 cubic feet per linear foot and OC 28 had 3,433 cubic feet per linear foot. OC 28 experienced 4,680 cubic feet per foot of inundation. The summary of results can be seen below in Table 5.7 and the EFI values above the mean high water line can viewed in Figure 5.23.

Table 5.7: Storm Severity Index Model Results for North American Blizzard

Site	EFI Value (kW-hours/ft)	Peak Power (kW/ft)	Overwash (Cubic ft/ft)	Inundation (Cubic ft/ft)	Sand Lost (cubic yards/ft)
OC 1	19.61	1.97	0.00	0.00	-81.00
OC 4	21.57	2.16	0.00	0.00	-178.00
OC 7	22.34	2.15	0.00	0.00	-28.00
OC 10	18.89	1.92	0.00	0.00	-190.00
OC 13	21.04	2.06	539.60	0.00	N/A
OC 16	24.18	2.23	0.00	0.00	N/A
OC 19	22.81	2.16	0.00	0.00	N/A
OC 22	24.71	2.30	0.00	0.00	N/A
OC 25	33.37	2.77	2970.86	0.00	N/A
OC 28	19.35	1.91	3433.97	4680.00	N/A
Avg	22.79	2.16	694.44	468.00	-119.25
STDV	4.21	0.25	1336.95	1479.95	77.99

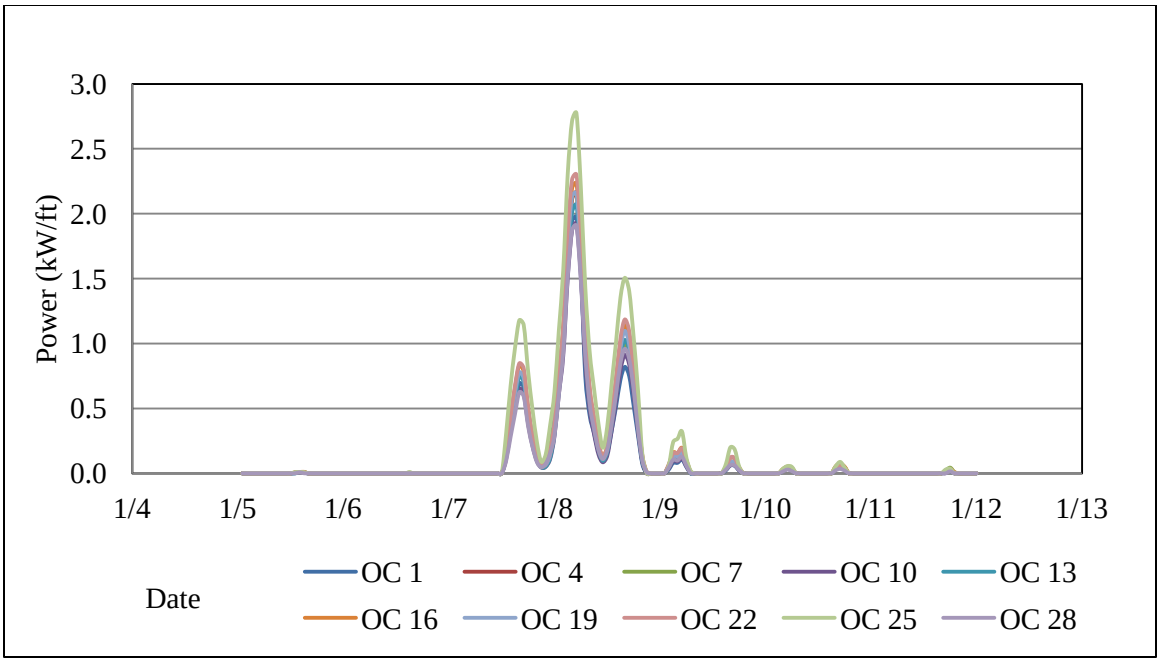

Figure 5.23: Time Series of Energy Flux above Normal Mean High Water Line during North American Blizzard (1996).

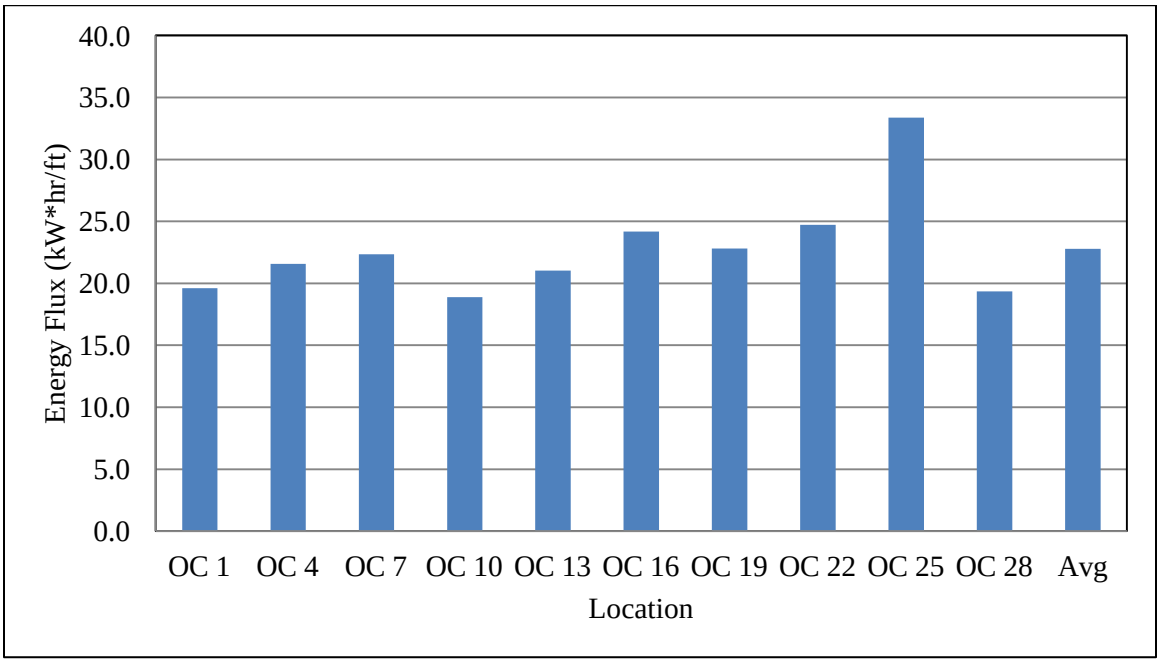

Figure 5.24: Energy Flux Index Numbers for each Location during North American Blizzard.

5.8 TROPICAL STORM JOSEPHINE (1996)

Tropical Storm Josephine passed by Ocean City from October 7th to 11th of 1996. Tropical Storm Josephine has 10 profiles from when the storm occurred. There are no post-storm surveys available for Josephine; however, the pre-storm surveys were recent, having been taken in September of 1996. The SSIM results are found in Table 5.8. The index numbers at each location during Tropical Storm Josephine was very consistent; with values ranging from 10 to 17 kW-hours per linear foot. Figure 5.26 shows the results graphically while Figure 5.25 shows the Energy Flux Index values above the mean high water line. There was overwash at OC 4, OC 7, and OC 28. It ranged from 123 (OC 7) to 2603 cubic feet per linear foot at OC 28. OC 28 had 6120 cubic feet per linear foot of inundation. There was no way to determine the amount of sand lost during the storm due to the lack of post-storm profiles.

Table 5.8: Storm Severity Index Model Results for Tropical Storm Josephine

Site	EFI Value (kW-hours/ft)	Peak Power (kW/ft)	Overwash (Cubic ft/ft)	Inundation (Cubic ft/ft)	Sand Lost (cubic yards/ft)
OC 1	12.93	2.00	0.00	0.00	N/A
OC 4	14.74	2.55	417.82	0.00	N/A
OC 7	15.01	2.55	123.24	0.00	N/A
OC 10	13.94	2.30	0.00	0.00	N/A
OC 13	15.51	2.51	0.00	0.00	N/A
OC 16	15.77	2.64	0.00	0.00	N/A
OC 19	14.84	2.52	7.30	0.00	N/A
OC 22	17.13	2.80	0.00	0.00	N/A
OC 25	10.22	1.85	0.00	0.00	N/A
OC 28	11.66	1.74	1087.98	6120.00	N/A
Avg	14.18	2.35	163.63	612.00	N/A
STDV	2.06	0.36	350.52	1935.31	N/A

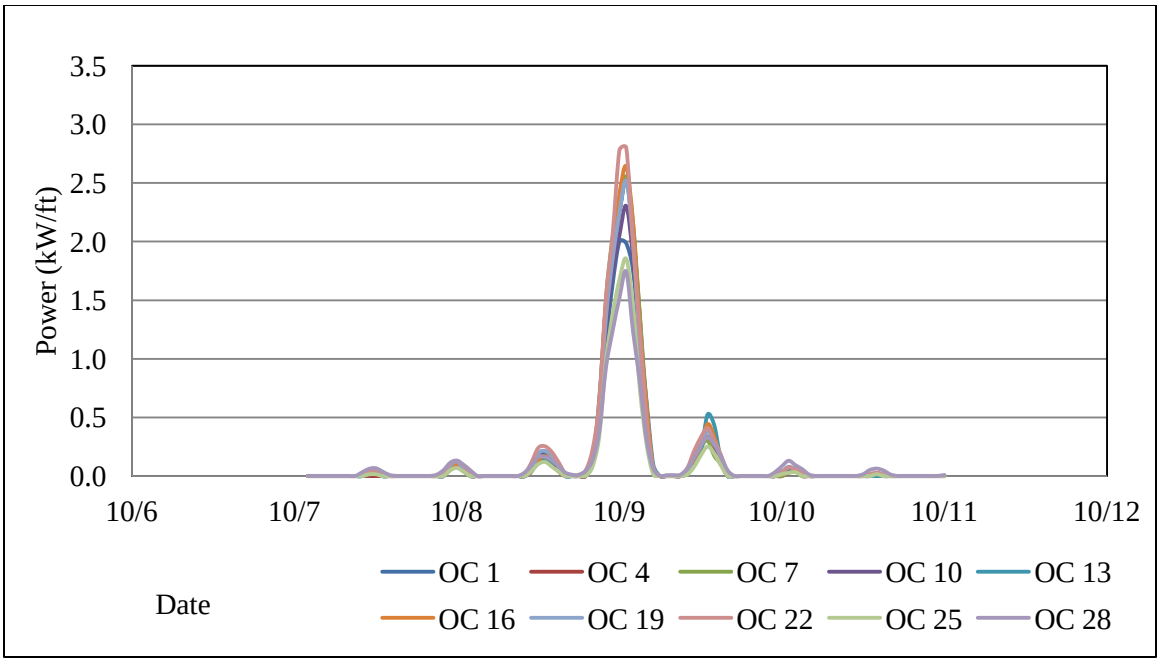

Figure 5.25: Time Series of Energy Flux above Normal Mean High Water Line during Tropical Storm Josephine (1996).

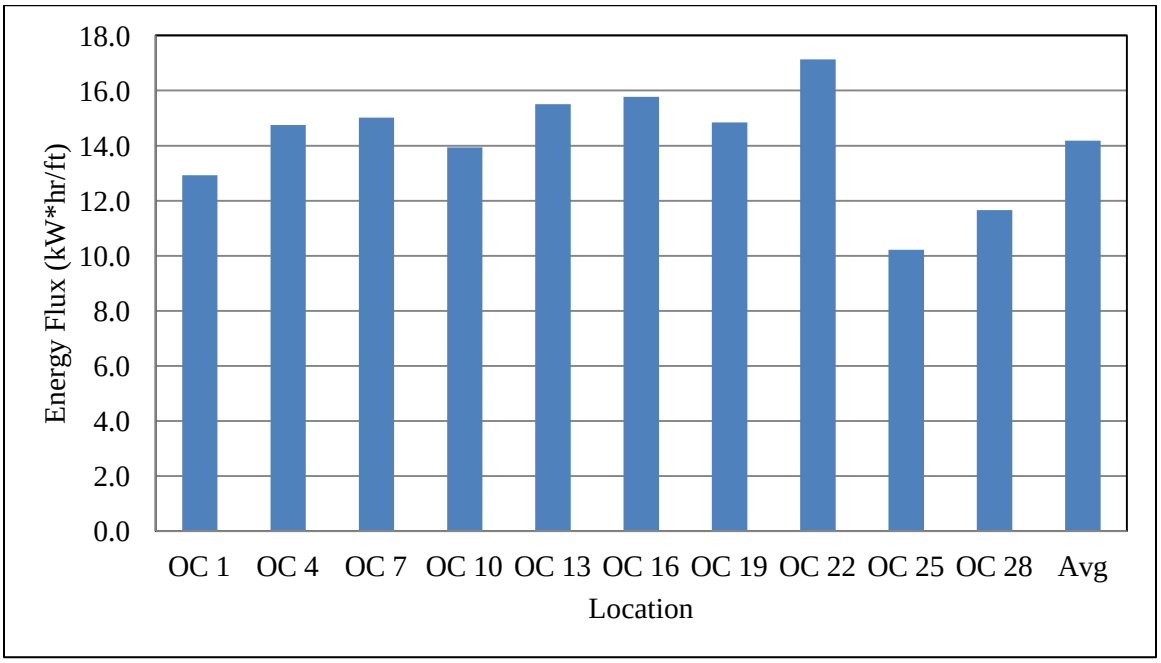

Figure 5.26: Energy Flux Index Numbers for each Location during Tropical Storm Josephine.

5.9 EL NINO WINTER (1998)

The El Nino Winter was a series of nor'easters that formed from January 27th and February 9th of 1998. The El Nino Winter is different from the other storms that are presented in this section because the El Nino Winter consists of two separate storms. The presence of the two storms can be seen in Figure 5.27 as two series of elevated energy flux. The first storm occurred from January 27 to January 31 while the second storm occurred from February 4th to the 9th. For the purposes of this thesis, the two storms have been grouped into a single event due to the short amount of time between them and the lack storm surveys between the two storms. Due to this grouping, the El Nino Winter is by far the longest spanning storm and the SSIM results show a high level of total energy flux above the normal mean high water line. The peak power, as seen in Table 5.9, is only 4.05 kW per foot but the index number at that same location (OC 22) is 150 kW-hours per linear foot. There is a large range of index number values for this event (from 80 to 150 kW-hours per foot) which can be seen in Figure 5.28. There are 8 pre-storm profiles available in this section and no post-storm profiles.

Table 5.9: Storm Severity Index Model Results for the El Nino Winter

Site	EFI Value (kW-hours/ft)	Peak Power (kW/ft)	Overwash (Cubic ft/ft)	Inundation (Cubic ft/ft)	Sand Lost (cubic yards/ft)
OC 4	84.20	2.70	0.00	0.00	-3.00
OC 7	130.08	3.44	194.51	0.00	-6.59
OC 10	93.65	2.97	34.95	0.00	-1.04
OC 13	80.49	2.66	0.00	0.00	-7.04
OC 16	122.03	3.65	5626.07	0.00	N/A
OC 19	110.72	3.34	375.18	0.00	N/A
OC 22	150.52	4.05	2515.25	0.00	N/A
OC 25	108.52	3.34	6358.46	0.00	N/A
Avg	110.03	3.27	1888.05	0.00	-4.42
STDV	23.89	0.47	2674.51	0.00	2.89

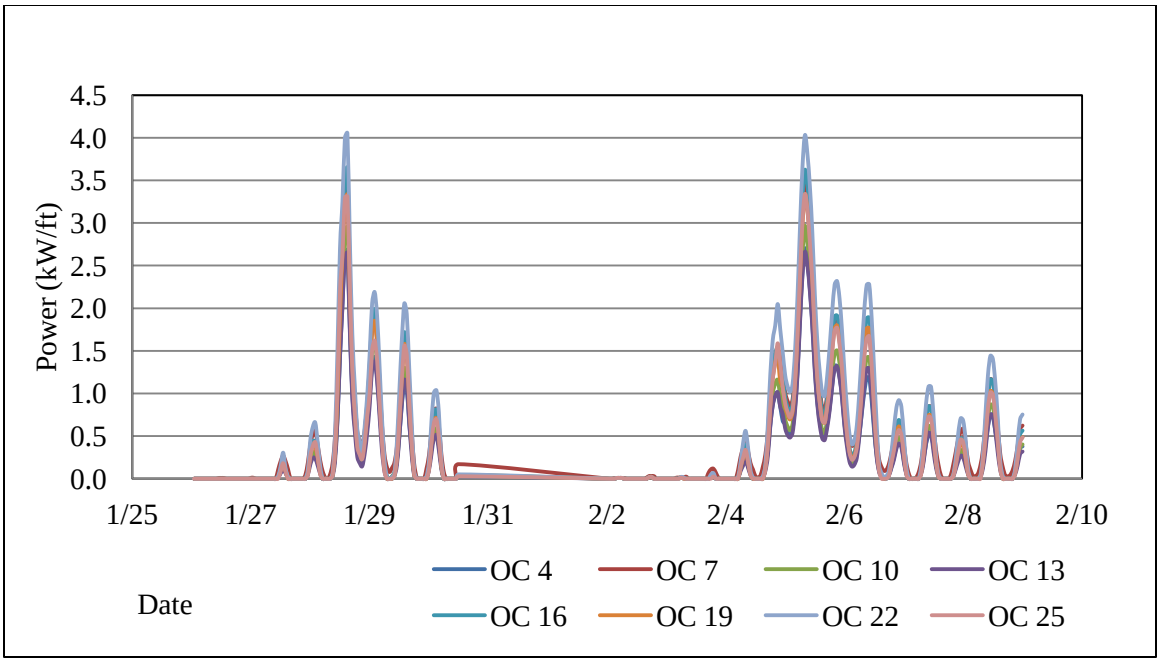

Figure 5.27: Time Series of Energy Flux above Normal Mean High Water Line during the El Nino Winter (1998).

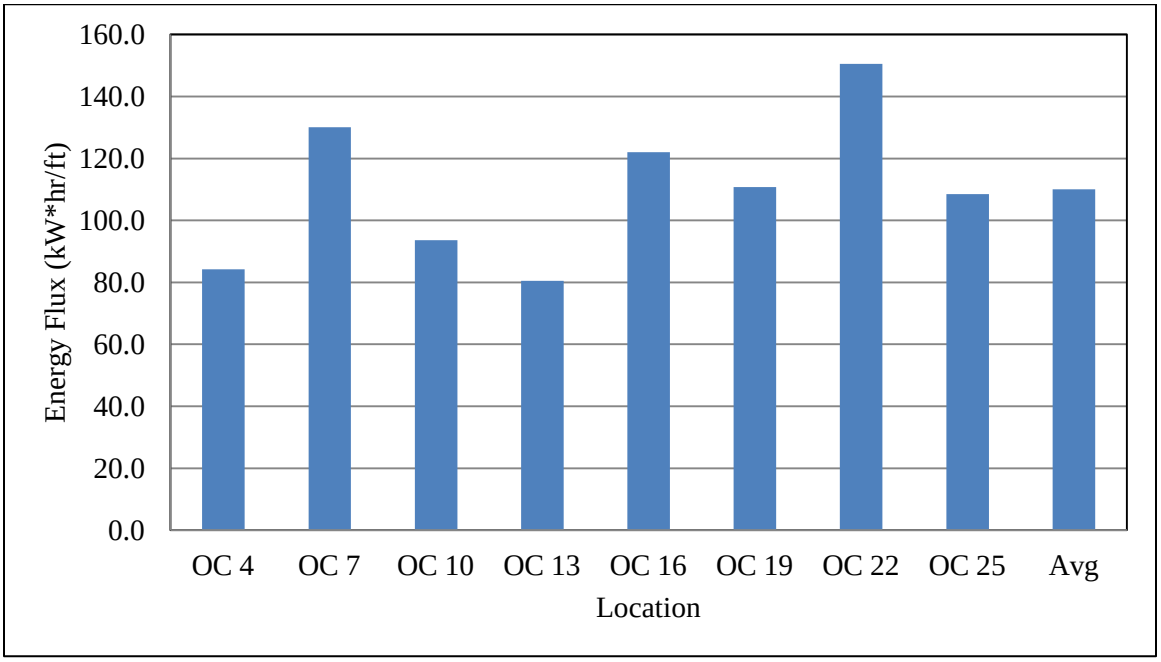

Figure 5.28: Energy Flux Index Numbers for each Location during the El Nino Winter.

5.10 HURRICANE FLOYD (1999)

Hurricane Floyd was a large hurricane that passed up the east coast of the United States between September 15th and 17th of 1999. The pre-storm profiles are from May of 1999 at all 10 locations, but there are no post-storm profiles available. The energy flux time series above the normal mean high water line is shown in Figure 5.29. The index numbers at each site can be seen in Figure 5.30. There is overwash at one location during this storm (OC 28). These results are presented in Table 5.10. Hurricane Floyd was a very strong storm but its fast movement speed limited the amount of energy that was produced at Ocean City.

Table 5.10: Storm Severity Index Model Results during Hurricane Floyd

Site	EFI Value (kW-hours/ft)	Peak Power (kW/ft)	Overwash (Cubic ft/ft)	Inundation (Cubic ft/ft)	Sand Lost (cubic yards/ft)
OC 1	5.40	1.12	0.00	0.00	N/A
OC 4	4.33	0.96	0.00	0.00	N/A
OC 7	6.11	1.27	0.00	0.00	N/A
OC 10	7.18	1.30	0.00	0.00	N/A
OC 13	4.46	0.81	0.00	0.00	N/A
OC 16	8.37	1.57	0.00	0.00	N/A
OC 19	5.19	1.08	0.00	0.00	N/A
OC 22	5.15	1.04	0.00	0.00	N/A
OC 25	6.41	1.23	0.00	0.00	N/A
OC 28	6.37	1.30	1071.57	0.00	N/A
Avg	5.90	1.17	107.16	0.00	N/A
STDV	1.25	0.21	338.86	0.00	N/A

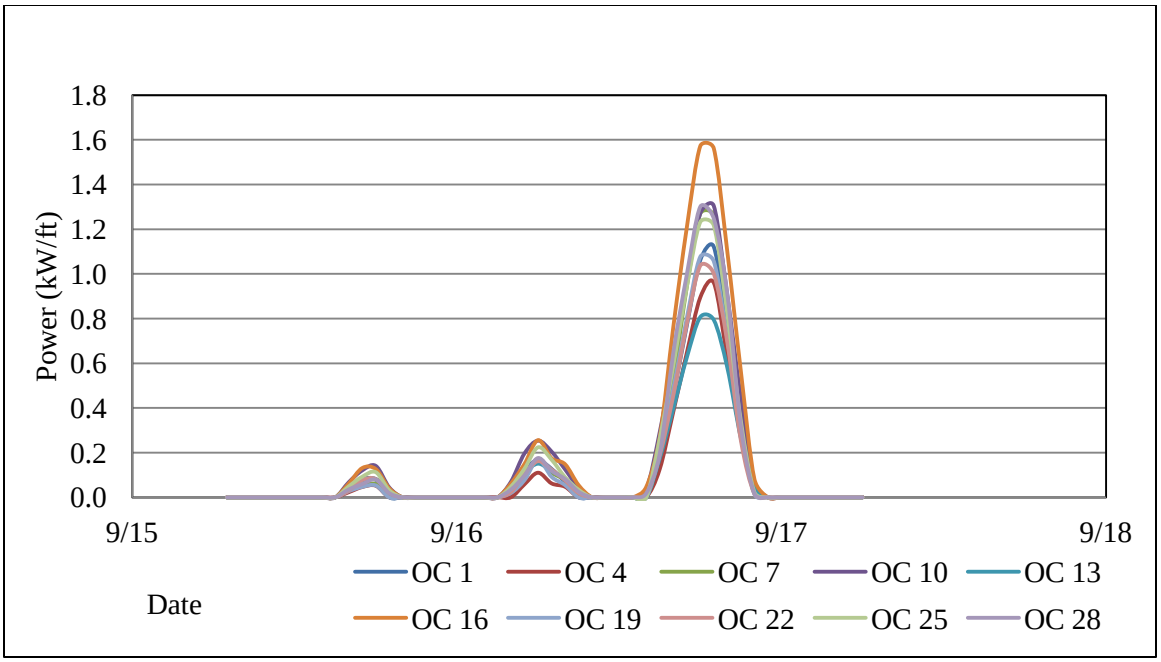

Figure 5.29: Time Series of Energy Flux above Normal Mean High Water Line during Hurricane Floyd (1999).

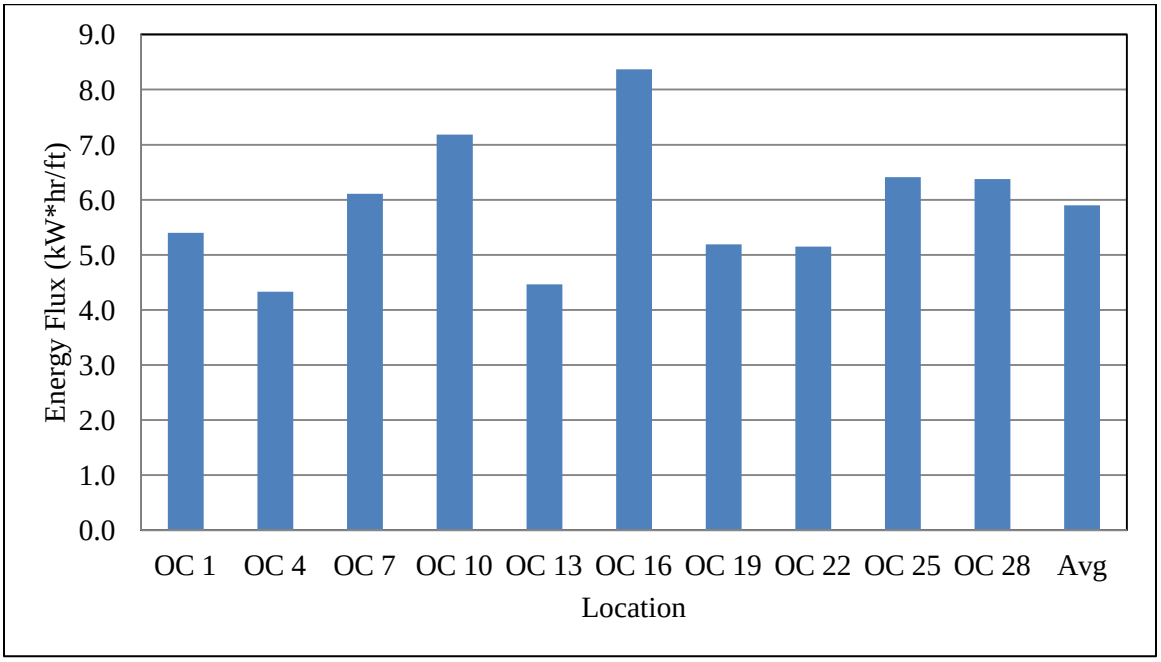

Figure 5.30: Energy Flux Index Numbers for each Location during Hurricane Floyd.

5.11 TROPICAL STORM HELENE (2000)

Tropical Storm Helene had both pre- and post-storm profiles available. There are 10 profiles during this storm. The pre-storm profiles are from December of 1999 and the post-storm profiles were taken in November of 2000, one month after the storm, which struck between September 22nd and 28th. The amount of sand lost can be seen in Table 5.11. All of the sites lost between 97.0 and 170.0 cubic yards of sand per foot above the zero elevation datum (NAVD88). Figure 5.31 shows the time series of energy flux above the normal mean high water line. From the chart, it is possible to conclude that the energy flux was significant only during times of high tide due to the oscillations that occur twice a day. Figure 5.32 presents the index numbers at each site during for the storm. Most of the sites were impacted by between 5.0 and 7.0 kW-hours per linear foot. There was overwash that occurred at OC 16 and OC 28 but no inundation.

Table 5.11: Storm Severity Index Model Results during Tropical Storm Helene

Site	EFI Value (kW-hours/ft)	Peak Power (kW/ft)	Overwash (Cubic ft/ft)	Inundation (Cubic ft/ft)	Sand Lost (cubic yards/ft)
OC 1	11.89	1.03	0.00	0.00	-6.19
OC 4	9.84	0.87	0.00	0.00	-6.30
OC 7	8.61	0.86	0.00	0.00	-3.89
OC 10	14.64	1.28	0.00	0.00	-5.59
OC 13	12.13	1.00	0.00	0.00	-4.85
OC 16	31.07	2.30	25.46	0.00	-5.30
OC 19	21.03	1.80	0.00	0.00	-5.19
OC 22	24.87	1.80	0.00	0.00	-5.33
OC 25	21.01	1.68	0.00	0.00	-3.59
OC 28	9.81	0.89	44.07	0.00	-3.89
Avg	16.49	1.35	6.95	0.00	-5.01
STDV	7.59	0.51	15.30	0.00	0.95

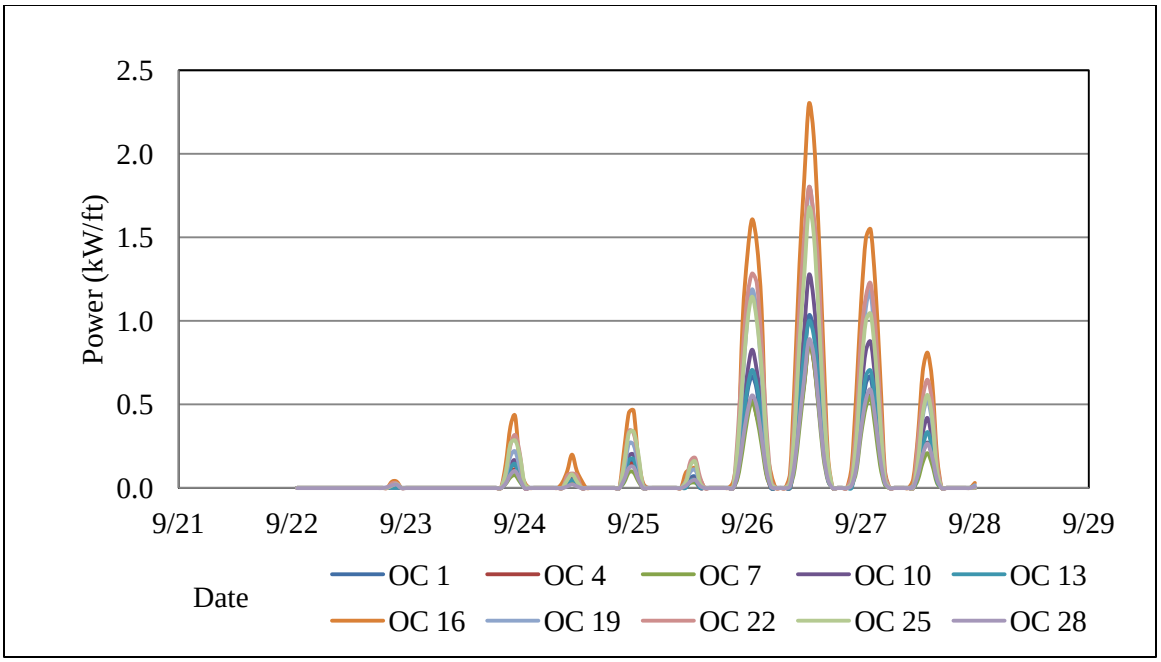

Figure 5.31: Time Series of Energy Flux above Normal Mean High Water Line during Tropical Storm Helene (2000).

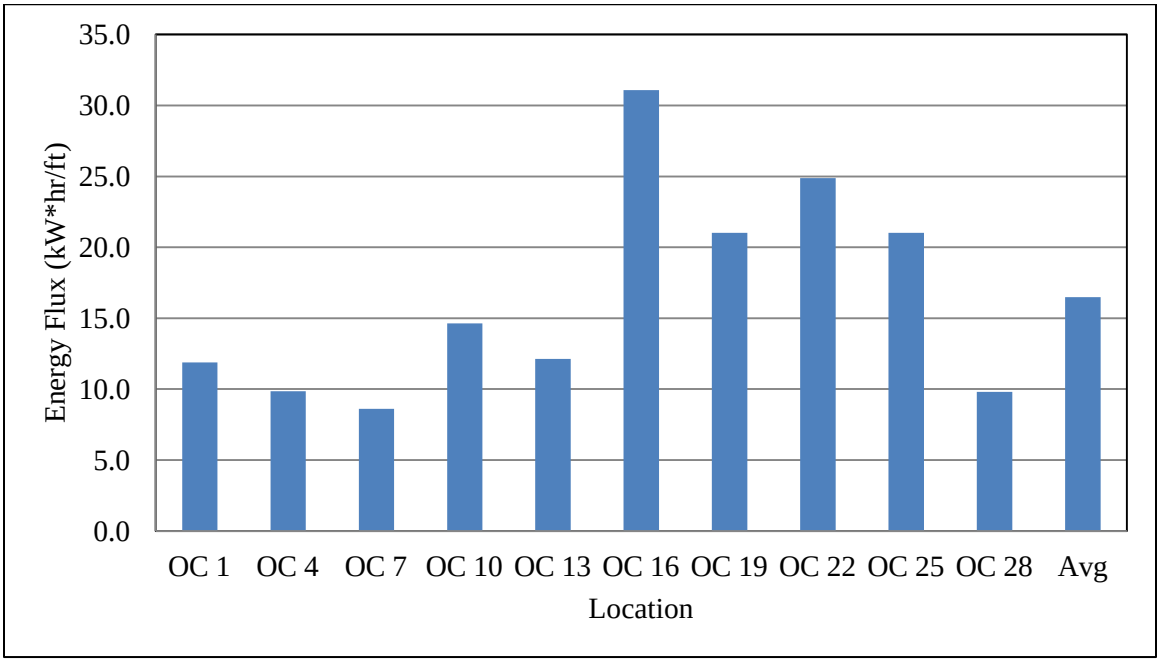

Figure 5.32: Energy Flux Index Numbers for each Location during Tropical Storm Helene.

5.12 HURRICANE ISABEL (2003)

Hurricane Isabel is the final storm presented in the Ocean City chapter. Isabel struck Ocean City from September 12th to 19th in 2003. This is a large amount of time for a hurricane to impact an area but prior to the 18th the amount of energy flux was minor. It was only during the 18th and 19th that significant amount of energy flux above the normal mean high water line was recorded. There are 10 profiles available from this storm. The pre-storm profiles are from April of that year and there are no post-storm profiles available. According to the SSIM, there was overwash at OC 7 and OC 16 during this event. The results of the SSIM can be seen in Table 5.12. Figure 5.33 shows the energy flux above the mean high water level while Figure 5.34 shows the Energy Flux Index at the beach during this storm.

Table 5.12: Storm Severity Index Model Results during Hurricane Isabel

Site	EFI Value (kW-hours/ft)	Peak Power (kW/ft)	Overwash (Cubic ft/ft)	Inundation (Cubic ft/ft)	Sand Lost (cubic yards/ft)
OC 1	5.26	0.36	0.00	0.00	N/A
OC 4	6.99	0.51	0.00	0.00	N/A
OC 7	6.96	0.51	151.61	0.00	N/A
OC 10	14.03	1.43	0.00	0.00	N/A
OC 13	8.40	0.59	0.00	0.00	N/A
OC 16	11.60	0.82	40.28	0.00	N/A
OC 19	21.85	1.63	0.00	0.00	N/A
OC 22	17.50	1.22	0.00	0.00	N/A
OC 25	17.20	1.09	0.00	0.00	N/A
OC 28	18.93	1.09	0.02	0.00	N/A
Avg	12.87	0.93	19.19	0.00	N/A
STDV	5.85	0.43	48.22	0.00	N/A

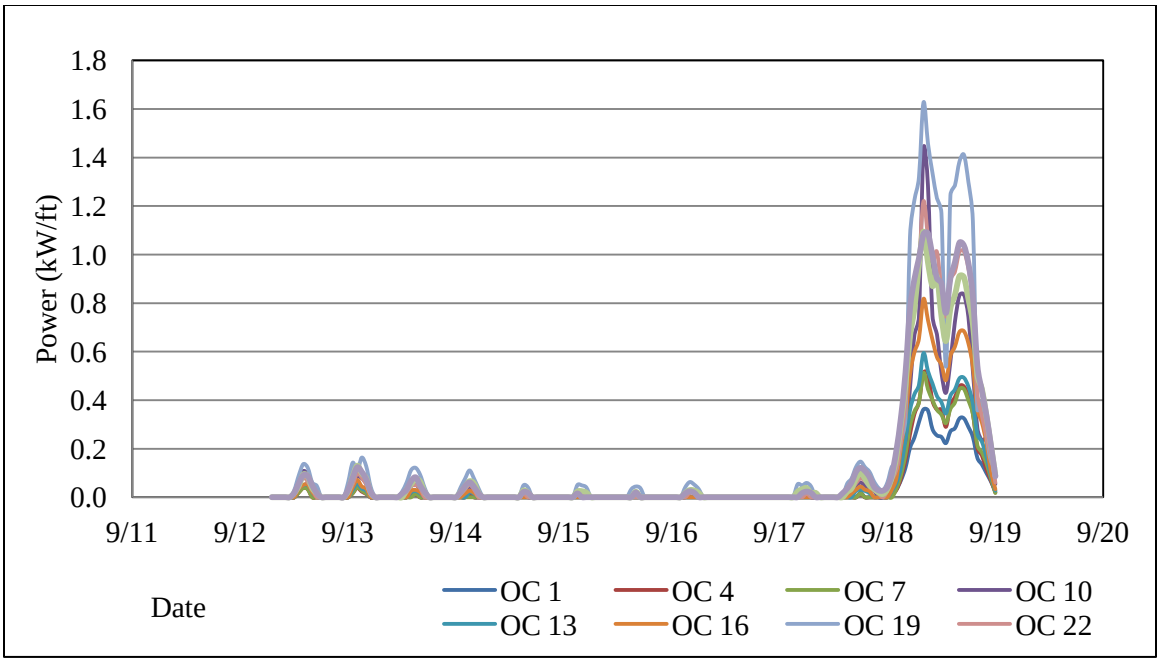

Figure 5.33 Time Series of Energy Flux above Normal Mean High Water Line during Hurricane Isabel (2003).

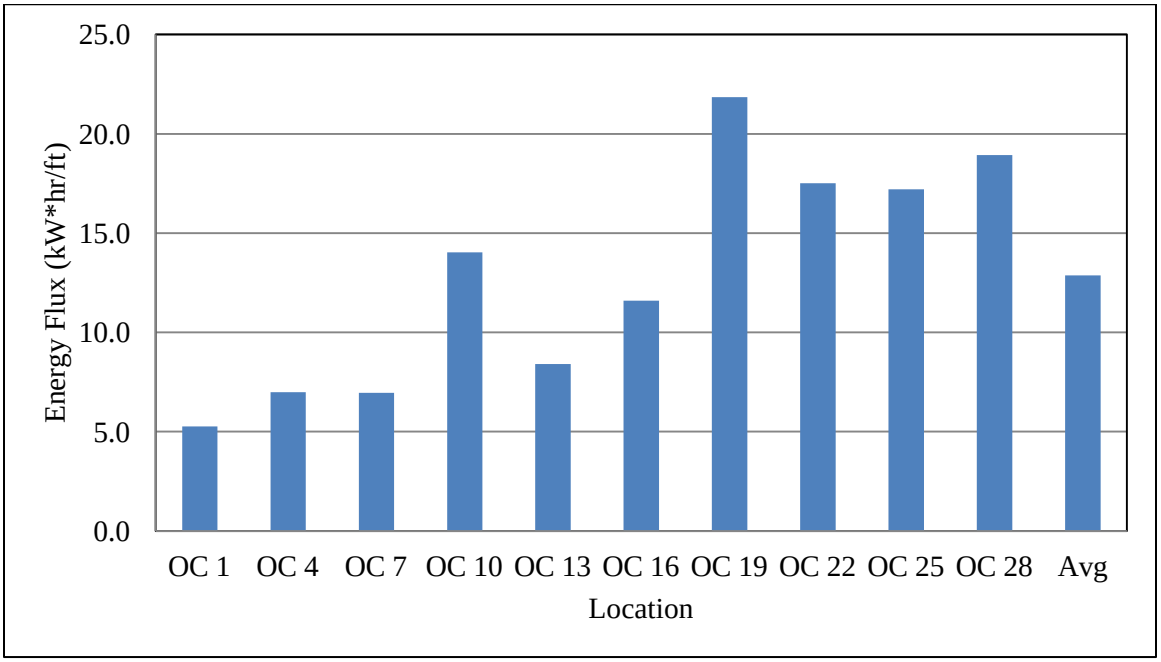

Figure 5.34: Energy Flux Index Numbers for each Location during Hurricane Isabel.

5.13 ANALYSIS OF STORM SEVERITY INDEX MODEL AT OCEAN CITY

In the Hurricane Sandy section, the SSIM was used to compare the impact of one storm at multiple locations in a large area. In this section, the SSIM was run on smaller area but it compared multiple storms within that area. The most efficient way of doing this comparison is by comparing the impact at each survey location from each storm. Table 5.13 shows the number of profiles that are available per location. Out of the 11 storms, each location has a minimum of 6 profiles. Five locations have 7 profiles, one location has 9 profiles, and one location has 10 profiles. Only OC 10 and OC 13 have profiles for every possible storm.

Table 5.13: Number of Profiles at each Ocean City Location

Location	Number of Profiles
OC 1	7
OC 4	10
OC 7	7
OC 10	11
OC 13	11
OC 16	7
OC 19	7
OC 22	9
OC 25	7
OC 28	6

The first step of the analysis is to rank the storms at each location by their index numbers. Table 5.14 shows the rankings for each storm at each of the Ocean City sites. From this table, some conclusions can be drawn; first, the El Nino Winter is clearly the strongest storm since it tops all of the locations for which profiles were available. Second, the January 1992 Nor'easter is the second strongest storm, and third, Hurricane Bob is the weakest storm, followed by Hurricane Floyd.

Table 5.14: Rank of Strongest Storm by SSIM Value at each Location

Rank	OC 1	OC 4	OC 7	OC 10	OC 13	OC 16	OC 19	OC 22	OC 25	OC 28
1	Christmas 1994	El Nino Winter	El Nino Winter	El Nino Winter	El Nino Winter	El Nino Winter	El Nino Winter	El Nino Winter	El Nino Winter	N.A. Blizzard
2	N.A. Blizzard	January 1992 N.E.	N.A. Blizzard	January 1992 N.E.	January 1992 N.E.	T.S. Helene	N.A. Blizzard	Maryland Ice Storm	N.A. Blizzard	Hurricane Isabel
3	Maryland Ice Storm	Christmas 1994	T.S. Josephine	Maryland Ice Storm	Maryland Ice Storm	N.A. Blizzard	Hurricane Isabel	T.S. Helene	T.S. Helene	Unknown Storm
4	T.S. Josephine	N.A. Blizzard	Unknown Storm	N.A. Blizzard	N.A. Blizzard	T.S. Josephine	T.S. Helene	N.A. Blizzard	Hurricane Isabel	T.S. Josephine
5	T.S. Helene	T.S. Josephine	T.S. Helene	Christmas 1994	Christmas 1994	Hurricane Isabel	Unknown Storm	Hurricane Isabel	T.S. Josephine	T.S. Helene
6	Hurricane Floyd	Maryland Ice Storm	Hurricane Isabel	T.S. Helene	T.S. Josephine	Hurricane Floyd	T.S. Josephine	T.S. Josephine	Hurricane Floyd	Hurricane Floyd
7	Hurricane Isabel	T.S. Helene	Hurricane Floyd	Hurricane Isabel	Unknown Storm	Unknown Storm	Hurricane Floyd	Unknown Storm	Unknown Storm	
8		Hurricane Isabel		T.S. Josephine	T.S. Helene			Christmas 1994		
9		Hurricane Floyd		Unknown Storm	Hurricane Isabel			Hurricane Floyd		
10		Hurricane Bob		Hurricane Floyd	Hurricane Floyd					
11				Hurricane Bob	Hurricane Bob					

While the strongest two storms and the weakest two storms are easy to identify, the remaining 7 storms are a bit harder to rank. Instead of giving them rigid ranks, it is more appropriate to divide them into small groups. The storms within each group are fairly interchangeable within the group depending on which Ocean City section that is affected. The first group consists of the North American Blizzard, the Christmas 1994 Nor'easter, and the Maryland Ice Storm of 1994. This is the group that is just below the two highest storms (the El Nino Event and the January 1992 Nor'easter) and the storms interchange in severity depending on the location. The next group of storms is made up of Tropical Storm Josephine and Tropical Storm Helene. In both of these events there is a wide disparity in the rankings depending on the location but overall both of these storms fall below the higher ranked storms. The last group is made up of Hurricane Isabel and the Unknown Storm. These storms interchange rankings but are consistently below the Josephine and Helene group and above Hurricanes Floyd and Bob. After taking account of the groups of storms, the final rankings for the storm severity according to the SSIM are presented in Table 5.15.

Table 5.15: Storm Severity Index Model Ranks of Ocean City Storms

Group	Storm
1	El Nino Winter
2	January 1992 Nor'easter
3	Maryland Ice Storm
	North American Blizzard
	Christmas 1994 Nor'easter
4	Tropical Storm Helene
	Tropical Storm Josephine
5	Hurricane Isabel
	Unknown Storm
6	Hurricane Floyd
7	Hurricane Bob

After ranking the SSIM results it is necessary to check if they are consistent with the conditions after each storm. The El Nino winter was characterized by extremes in weather so it makes sense that it is the strongest storm according to the SSIM. The January 1992 Nor'easter occurred a few months after the Perfect Storm which meant that the beach was already eroded. This resulted in a lot overwash which was matched by the SSIM results. The Christmas 1994 Nor'easter, the Maryland Ice Storm, and the North American Storm were all characterized as strong nor'easters but not as strong as the January 1992 storm.

Tropical Storm Josephine was a strong storm that passed just off the coast of Maryland, but due to its speed, it only had a strong impact during one high tide, which limited the amount of energy flux above the normal mean high water line. Tropical Storm Helene weakened after passing inland over the southern states but because it was slower than Josephine, it lasted for about 2 days which meant that it had more time to impact the coast. As a result, the two storms ended up with about the EFI value.

Hurricane Isabel was a very strong hurricane that reached Category 5 status on the Saffir-Simpson Scale. However, the storm made landfall in the Outer Banks of North Carolina and traveled north-west which meant that it passed well west of Ocean City. It was a very fast moving storm that was dissipating over land by the time it impacted Maryland which lowered the amount of energy that it produced.

The Unknown Storm was not identified so there is no way to find out if the SSIM results are consistent with damage reports. Hurricane Floyd was another storm that weakened prior to approaching Ocean City. It was also a fast moving storm that only had a large impact during one high tide. Hurricane Bob also weakened dramatically and because it passed 90 miles off the coast of Maryland, the wave impacts were limited.

Overall the SSIM results are consistent with the reports available for the storms. However, ranking the storms by their average total energies does not use the SSIM appropriately. Instead, the results should be ranked individually by location. The rankings for these results can be seen in Table 5.16, Table 5.17, and Table 5.18. The rankings confirm that the El Nino Winter is clearly the strongest storm and Hurricane Bob is clearly the weakest.

One thing to note is that the volume of overwash is not directly proportional to the amount of total energy that an area absorbs. The shape of the beach plays a role in the susceptibility of an area to get flooded. OC 28 consistently is one of the lower dunes and as a result, it is the location that has overwash the most often. The beach shapes have changed often over time which is a factor of determining exactly when a beach will experience overwash or inundation.

The next step is to compare the Ocean City storm to the devastation of Hurricane Sandy. Table 5.19 has the highest third of the Ocean City storms (Table 5.16) with the Hurricane Sandy results added in. It is clear that the only Ocean City storm that rivals Sandy is the El Nino Winter. Only Cape May County and Atlantic County are outside of the top third of all the Ocean City storms.

Table 5.16: Ocean County Storm Severity Index Model Result Ranks pt. 1

Name	OC	Index Number (kW-hr/ft)	Peak Power (kW/ft)	Volume of Overwash (cubic feet/foot)
El Nino Winter	OC 22	150.52	4.05	2515.25
El Nino Winter	OC 7	130.08	3.44	194.51
El Nino Winter	OC 16	122.03	3.65	5626.07
El Nino Winter	OC 19	110.72	3.34	375.18
El Nino Winter	OC 25	108.52	3.34	6358.46
El Nino Winter	OC 10	93.65	2.97	34.95
El Nino Winter	OC 4	84.20	2.70	0.00
El Nino Winter	OC 13	80.49	2.66	0.00
January 1992 Nor'easter	OC 10	41.66	4.82	7431.78
January 1992 Nor'easter	OC 13	40.98	4.59	572.76
Maryland Ice Storm	OC 13	36.05	4.24	0.00
January 1992 Nor'easter	OC 4	35.35	3.68	3983.19
North American Blizzard	OC 25	33.37	2.77	2970.86
Maryland Ice Storm	OC 10	32.54	4.06	0.00
Tropical Storm Helene	OC 16	31.07	2.30	25.46
Maryland Ice Storm	OC 22	30.95	3.83	45.04
Christmas 1994 Nor'easter	OC 4	27.23	1.37	0.00
Tropical Storm Helene	OC 22	24.87	1.80	0.00
North American Blizzard	OC 22	24.71	2.19	0.00
North American Blizzard	OC 16	24.18	2.10	0.00
North American Blizzard	OC 19	22.81	2.24	0.00
North American Blizzard	OC 7	22.34	2.61	0.00
Christmas 1994 Nor'easter	OC 1	22.32	1.26	0.00
Hurricane Isabel	OC 19	21.85	1.63	0.00
North American Blizzard	OC 4	21.57	2.37	0.00
North American Blizzard	OC 13	21.04	2.06	539.60
Tropical Storm Helene	OC 19	21.03	1.80	0.00

Table 5.17: Ocean County Storm Severity Index Model Result Ranks pt.2

Name	OC	Index Number (kW-hr/ft)	Peak Power (kW/ft)	Volume of Overwash (cubic feet/foot)
Tropical Storm Helene	OC 25	21.01	1.68	0.00
North American Blizzard	OC 1	19.61	2.93	0.00
North American Blizzard	OC 28	19.35	1.91	8156.70
Maryland Ice Storm	OC 1	19.29	2.76	604.20
Hurricane Isabel	OC 28	18.93	1.09	0.02
North American Blizzard	OC 10	18.89	2.19	0.00
Unknown Storm	OC 28	18.89	0.72	0.00
Christmas 1994 Nor'easter	OC 13	17.70	1.21	0.00
Hurricane Isabel	OC 22	17.50	1.22	0.00
Hurricane Isabel	OC 25	17.20	1.09	0.00
Tropical Storm Josephine	OC 22	17.13	2.80	0.00
Christmas 1994 Nor'easter	OC 10	16.70	1.08	97.23
Unknown Storm	OC 19	16.62	0.75	0.00
Tropical Storm Josephine	OC 16	15.77	2.64	0.00
Tropical Storm Josephine	OC 13	15.51	2.51	0.00
Tropical Storm Josephine	OC 7	15.01	2.55	123.24
Tropical Storm Josephine	OC 19	14.84	2.52	7.30
Tropical Storm Josephine	OC 4	14.74	2.55	417.82
Tropical Storm Helene	OC 10	14.64	1.28	0.00
Hurricane Isabel	OC 10	14.03	1.43	0.00
Tropical Storm Josephine	OC 10	13.94	2.30	0.00
Tropical Storm Josephine	OC 1	12.93	2.00	0.00
Unknown Storm	OC 13	12.82	0.59	0.00
Tropical Storm Helene	OC 13	12.13	1.00	0.00
Tropical Storm Helene	OC 1	11.89	1.03	0.00
Unknown Storm	OC 22	11.78	0.58	0.00
Tropical Storm Josephine	OC 28	11.66	1.74	2603.39

Table 5.18: Ocean County Storm Severity Index Model Result Ranks pt. 3

Name	OC	Index Number (kW-hr/ft)	Peak Power (kW/ft)	Volume of Overwash (cubic feet/foot)
Hurricane Isabel	OC 16	11.60	0.82	40.28
Maryland Ice Storm	OC 4	10.60	1.66	0.00
Unknown Storm	OC 7	10.43	0.53	0.00
Christmas 1994 Nor'easter	OC 22	10.22	0.81	0.00
Tropical Storm Josephine	OC 25	10.22	1.85	0.00
Unknown Storm	OC 10	10.17	0.53	0.00
Tropical Storm Helene	OC 4	9.84	0.87	0.00
Tropical Storm Helene	OC 28	9.81	0.89	44.07
Tropical Storm Helene	OC 7	8.61	0.86	0.00
Hurricane Isabel	OC 13	8.40	0.59	0.00
Hurricane Floyd	OC 16	8.37	1.57	0.00
Unknown Storm	OC 16	7.46	0.41	0.00
Hurricane Floyd	OC 10	7.18	1.30	0.00
Hurricane Isabel	OC 4	6.99	0.51	0.00
Hurricane Isabel	OC 7	6.96	0.51	151.61
Hurricane Floyd	OC 25	6.41	1.23	0.00
Hurricane Floyd	OC 28	6.37	1.30	1071.57
Hurricane Floyd	OC 7	6.11	1.27	0.00
Unknown Storm	OC 25	5.93	0.32	0.00
Hurricane Floyd	OC 1	5.40	1.12	0.00
Hurricane Isabel	OC 1	5.26	0.36	0.00
Hurricane Floyd	OC 19	5.19	1.08	0.00
Hurricane Floyd	OC 22	5.15	1.04	0.00
Hurricane Floyd	OC 13	4.46	0.81	0.00
Hurricane Floyd	OC 4	4.33	0.96	0.00
Hurricane Bob	OC 13	1.42	0.31	0.00
Hurricane Bob	OC 10	1.26	0.25	0.00
Hurricane Bob	OC 4	1.12	0.25	0.00

Table 5.19: Compare Ocean City Storms to Hurricane Sandy

Name	Location	Index Number (kW-hr/ft)	Peak Power (kW/ft)	Volume of Overwash (cubic feet/foot)
El Nino Winter	OC 22	150.52	4.05	2515.25
Hurricane Sandy	NJBPN 150	147.59	9.34	0.00
El Nino Winter	OC 7	130.08	3.44	194.51
Hurricane Sandy	NJBPN 171	123.42	11.04	464.26
El Nino Winter	OC 16	122.03	3.65	5626.07
Hurricane Sandy	NJBPN 173	120.12	11.00	631.34
El Nino Winter	OC 19	110.72	3.34	375.18
El Nino Winter	OC 25	108.52	3.34	6358.46
El Nino Winter	OC 10	93.65	2.97	34.95
Hurricane Sandy	NJBPN 183	91.42	9.14	2113.18
Hurricane Sandy	NJBPN 177	86.76	8.76	2473.91
El Nino Winter	OC 4	84.20	2.70	0.00
El Nino Winter	OC 13	80.49	2.66	0.00
Hurricane Sandy	NJBPN 138	66.86	4.35	0.00
Hurricane Sandy	NJBPN 167	63.59	6.57	13285.73
Hurricane Sandy	NJBPN 168	60.99	6.74	290.83
Hurricane Sandy	NJBPN 153	60.45	5.59	1336.29
Hurricane Sandy	NJBPN 141	56.66	4.25	0.00
Hurricane Sandy	NJBPN 145	53.69	4.11	8.52
Hurricane Sandy	NJBPN 248	49.65	3.74	9134.05
January 1992 Nor'easter	OC 10	41.66	4.82	7431.78
January 1992 Nor'easter	OC 13	40.98	4.59	572.76
Hurricane Sandy	NJBPN 163	39.66	4.65	2018.16
Maryland Ice Storm	OC 13	36.05	4.24	0.00
January 1992 Nor'easter	OC 4	35.35	3.68	3983.19
North American Blizzard	OC 25	33.37	2.77	2970.86
Maryland Ice Storm	OC 10	32.54	4.06	0.00
Tropical Storm Helene	OC 16	31.07	2.30	25.46
Maryland Ice Storm	OC 22	30.95	3.83	45.04
Hurricane Sandy	NJBPN 133	29.43	2.40	0.00
Hurricane Sandy	NJBPN 109	28.82	1.74	0.00
Christmas 1994 Nor'easter	OC 4	27.23	1.37	0.00
Tropical Storm Helene	OC 22	24.87	1.80	0.00

CHAPTER 6: GULF OF MEXICO STORMS

The sixth chapter of this thesis focuses on five tropical systems that had an impact in the Gulf of Mexico. There are two specific parts of Florida that are featured. The first is the panhandle region where two of the storms (Hurricanes Georges and Ivan) caused damage. The second region is the Clearwater/Tampa Bay region where the other three storms passed. All of the wave information obtained in this section was obtained from the U.S. Army Corps of Engineers Wave Information studies hindcast (USACE WIS). The wave heights in the panhandle were taken from WIS Station 73354 while the wave heights for Clearwater are from WIS station 73362. The hindcast obtained from the WIS stations were then used as input for a version of the Steady State Spectral Wave model (STWAVE) that is modified to include bottom friction (Smith, Sherlock, & Resio, 1999). The results from STWAVE are then used in the SSIM. All of the beach profiles have pre- and post-storm surveys so the amount of sand lost can be found at each location. This chapter contains summaries of the results from the five storms. The storms are presented geographically; the panhandle region of Florida is highlighted first, followed by Pinellas County. The detailed results, along with water levels, wave heights, and beach profiles, from Hurricane Ivan at S6SJ2 are highlighted in the body of the chapter while the detailed results from the other sites can be found in Appendix D. Figure 6.1 shows the site locations and the storm tracks from all of the storms. The tracks were retrieved from the website Weather Underground (2015).

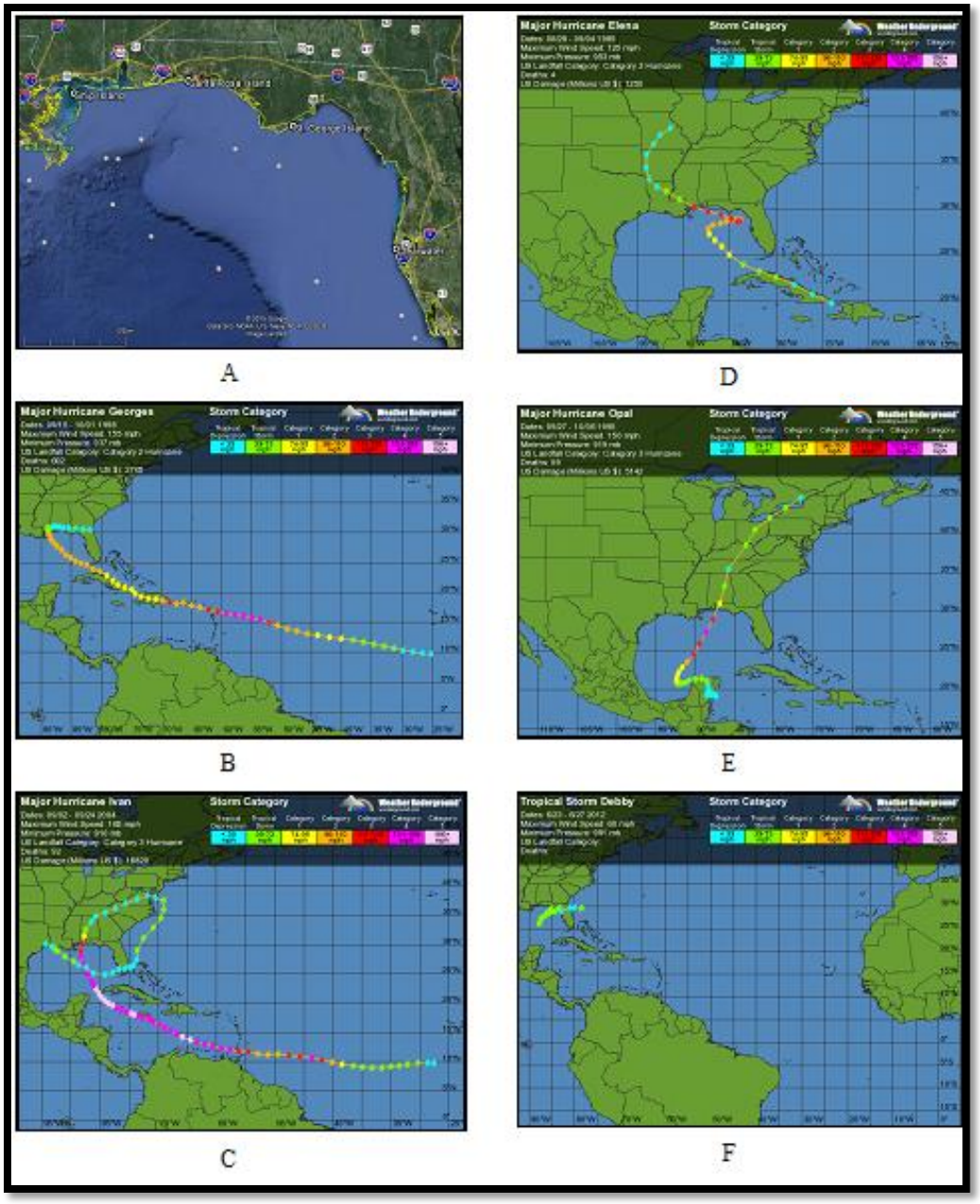

Figure 6.1: Gulf of Mexico Storm Tracks. Gulf of Mexico beach profile survey locations. B) Hurricane Georges storm track. C) Hurricane Ivan storm track. D) Hurricane Elena storm track. E) Hurricane Opal storm track. F) Tropical Storm Debby storm track (The Weather Channel, 2015).

6.1 HURRICANE GEORGES (1998)

The first storm in this section is Hurricane Georges. Hurricane Georges made landfall near Biloxi, Mississippi in late September (26^{th}-30^{th}) of 1998. Hurricane Georges was a September storm that caused a lot of damage in the Gulf region. Georges maxed out as a Category 4 hurricane with winds upwards of 150 MPH. One of the locations from which a beach profile was available was from Santa Rosa Island, Florida, which is located approximately 130 miles to the east of the landfall point. The other was from West Ship Island, Mississippi, which is about 12 miles southwest of Biloxi. The profiles were obtained from Stone and Liu (2004). As will be described below, despite being further from the landfall point, Santa Rosa Island produced a larger index number then West Ship Island. This is because Santa Rosa Island was located on the eastward, or stronger, side of the hurricane while West Ship Island was on the back side of the storm. The tide information was found from NOAA Station 8729840 located at Pensacola, FL and NOAA Station 8747766 near Gulfport, MS. The wave information was obtained from WIS Station 73354 which is about 30 miles offshore and at a depth of 100 m and WIS Station 73349 which is at a depth of 130 m and located 75 miles south of West Ship Island.

Table 6.1 shows the impact that Georges had at both locations. Overall, most of the statistics are similar with the exception of the overwash value at Santa Rosa Island. While West Ship Island did not have any overwash, Santa Rosa Island had approximately 7000 cubic feet per linear foot of shoreline. The main difference was that the beach at Santa Rosa Island had a crest elevation of 6 feet whereas the beach crest at West Ship Island was close to 11 feet which made it less susceptible to water damage. The beach profiles are presented in Appendix D. Both sites lost approximately 19.30 cubic yards per foot of beach of sand above the zero elevation datum

(NAVD88) during the storm. Figure 6.2 shows the energy flux time series and the energy flux index numbers are provided in the table.

Table 6.1: Storm Severity Index Model Results for Hurricane Georges

Site	EFI Value (kW-hours/ft)	Peak Power (kW/ft)	Overwash (Cubic ft/ft)	Inundation (Cubic ft/ft)	Sand Lost (Cubic Yards/ft)
Santa Rosa Island	41.81	1.86	7052.66	0.00	-19.30
West Ship Island	23.70	1.32	0.00	0.00	-19.48
Avg	32.76	1.59	3526.33	0.00	-19.39
STDV	12.80	0.38	4986.98	0.00	0.13

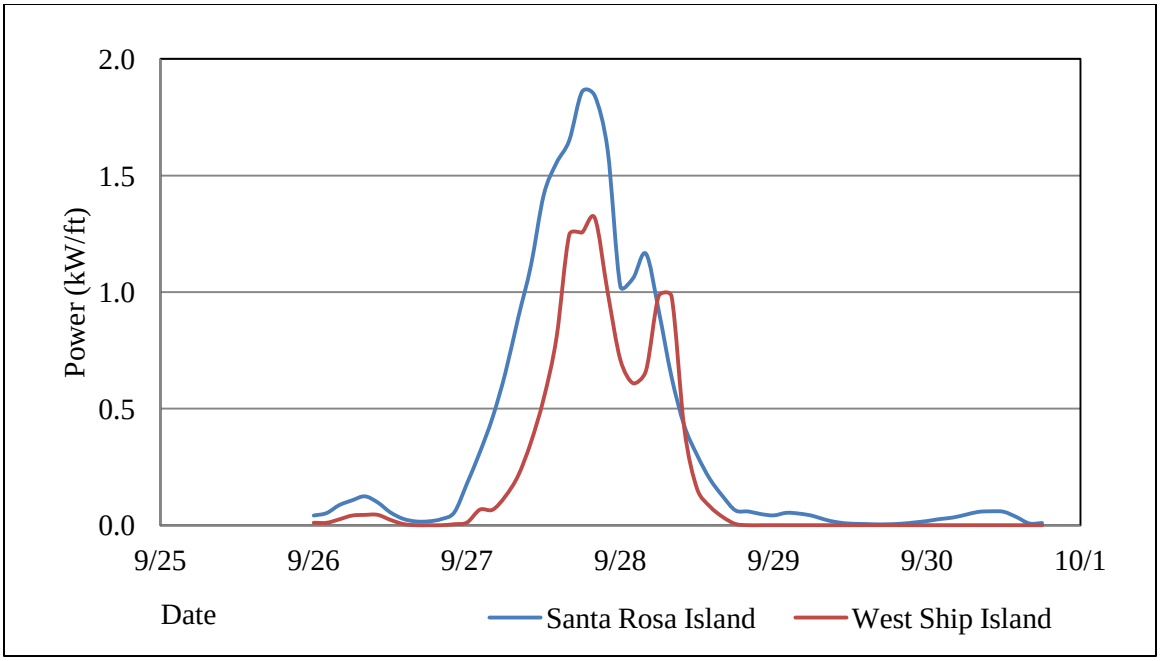

Figure 6.2: Time Series of Energy Flux above the Normal Mean High Water Line during Hurricane Georges (1998).

6.2 HURRICANE IVAN (2004)

Hurricane Ivan was the second Tropical system in this thesis to have an impact in the panhandle region of Florida. Hurricane Ivan formed in the Atlantic Ocean and made its way through the Caribbean. At its peak, Ivan became a Category 5 storm but weakened to a Category 3 when it struck Pensacola, FL. Ivan struck Florida twice as it cut across the Southeast into the Atlantic Ocean where it reformed and came back to strike southern Florida. The beach profiles that were studied are from the Pensacola region. They were obtained from a paper written by Wang and Kirby (2006). Ivan struck between September 15th and 17th of 2004. The wave record used was obtained from WIS Station 73354 which is located 30 miles off the coast of Pensacola at a depth of 100 m. The tide information was obtained from NOAA Station 8729210 at Panama City Beach, FL.

There are eight locations for which the SSIM was computed, extending from Destin to St. George Island, Florida, and they are presented in Table 6.2 from west to east. Hurricane Ivan made landfall just west of Pensacola. Based strictly on location relative to landfall, it is expected that the EFI should decrease from west to east as the sites get farther from the landfall point. However, this does not occur. The sites have similar index numbers and peak powers which are due to the sheer size of Ivan. Ivan was a very strong hurricane but due to high elevation of the dunes, there was only minor overwash in two of the locations, as well as no inundation. Figure 6.3 shows the energy flux time series during the storm. There was erosion experienced at all of the locations, ranging from 6.63 to 39.00 cubic yards of sand per foot above the zero elevation datum (NAVD88). One important feature of Ivan was that, unlike Hurricane Sandy, Ivan struck directly and quickly. Ivan was a very strong storm but due to its short duration, there was less coastal erosion and potential overwash then there might have been otherwise.

Site S6SJ2 had the highest EFI value out of all of the sites in the Gulf of Mexico chapter. Figures of the beach profile, the water levels, the significant wave heights, and the instantaneous energy flux have been included. They can be seen below in Figure 6.4.

Table 6.2: Storm Severity Index Model Results for Hurricane Ivan

Site	EFI Value (kW-hours/ft)	Peak Power (kW/ft)	Overwash (Cubic ft/ft)	Inundation (Cubic ft/ft)	Sand Lost (Cubic yards/ft)
S1BP1	49.10	2.90	0.00	0.00	-23.78
S1BP2	62.23	3.88	0.00	0.00	-39.00
S4IB1	61.21	3.81	0.00	0.00	-14.67
S4IB2	82.05	4.95	493.10	0.00	-19.89
S6SJ1	74.47	5.00	0.00	0.00	-22.74
S6SJ2	88.05	5.81	0.00	0.00	-13.85
S7SG1	70.17	4.80	0.46	0.00	-6.63
S7SG2	58.05	4.08	0.00	0.00	-7.33
Avg	68.17	4.40	61.70	0.00	-18.49
STDV	12.99	0.91	174.31	0.00	10.49

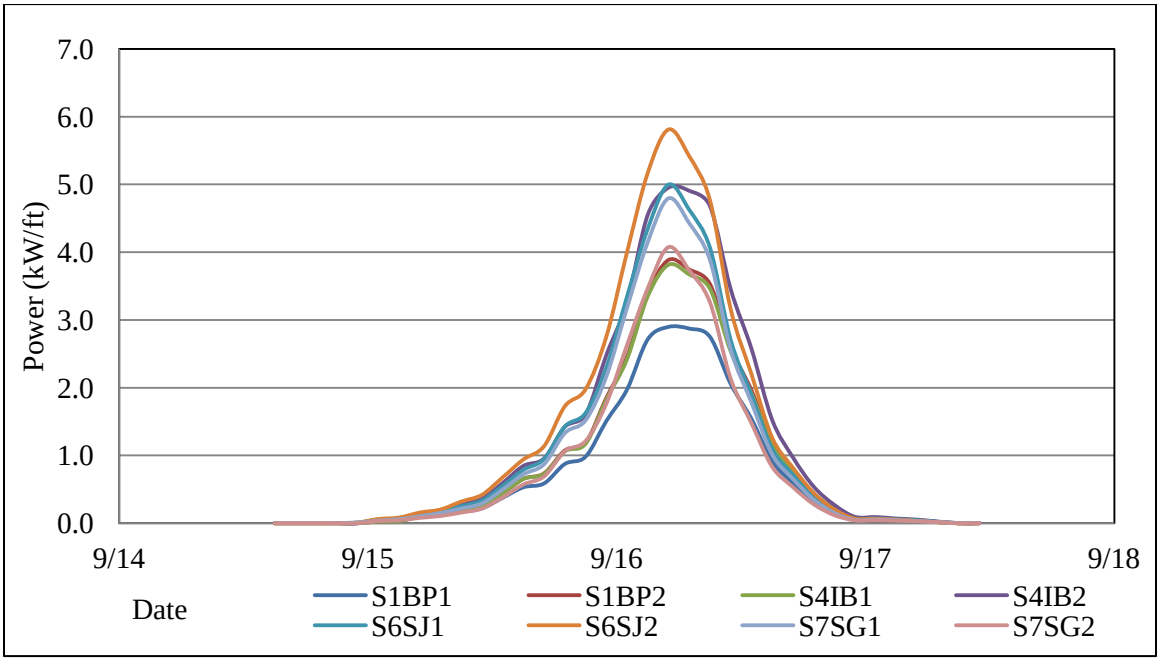

Figure 6.3: Time Series of Energy Flux above the Normal Mean High Water Line during Hurricane Ivan (2004).

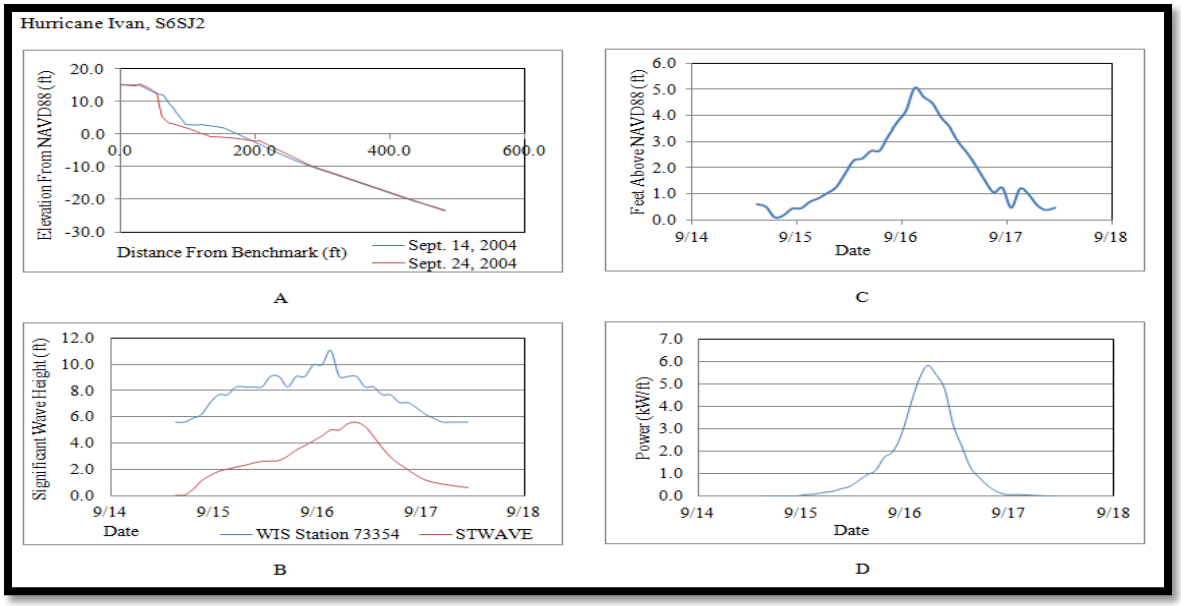

Figure 6.4: S6SJ2 Conditions and Results. A) The pre- and post-Hurricane Ivan profiles. B) Hurricane Ivan wave heights. C) Water levels at S6SJ2. D) SSIM Results at S6SJ2 during Hurricane Ivan.

6.3 HURRICANE ELENA (1984)

The first storm to impact the Pinellas County region in this thesis is Hurricane Elena which struck the area from August 29th to September 2nd. The storm stalled for several days off the west coast of Florida which resulted in severe beach erosion. Storm winds reached 125 MPH and Elena reached Category 3 status on the Saffir-Simpson Scale. Beach profile information was information was obtained for Sand Key Beach, which is located just south of Clearwater, Florida, from Bodge and Kriebel (1985). Hurricane Elena initially passed well westward of the region but then doubled back and stalled in the north-eastern part of the Gulf of Mexico. Water level information was also obtained from the report which stated that the water levels were taken from the Florida Coastal Data Network Station at Clearwater. The wave height information was developed from hindcast wave information obtained from USACE WIS Station 73362. WIS Station 73362 is located about 100 miles off the coast of Sand Key Beach in about 110 m. of water.

The time series of energy flux above the normal mean high water line is reflected in Figure 6.5. Table 6.3 shows the impact that Elena had on site R-58 and R-59. Both sites had similar index numbers and peak powers and neither site had any overwash, due to the fact that both sites have very similar beach profiles. R-59 lost over 13 cubic yards per foot of shoreline of sand above the zero elevation datum while site R-58 actually gained a small amount. Both sites experienced the same pattern of erosion, however, the erosion at R-59 occurred slightly higher on the profile resulting in more erosion above the zero elevation datum (NAVD88) at this location. Elena lasted 5 days and delivered energy to the beach during each high tide cycle. Even though the peak power during Elena was not large, the duration of the storm caused a significant amount of energy to be delivered to the beach.

Table 6.3: Storm Severity Index Model Results for Hurricane Elena

Site	EFI Value (kW-hours/ft)	Peak Power (kW/ft)	Overwash (Cubic ft/ft)	Inundation (Cubic ft/ft)	Sand Lost (Cubic Yards/ft)
R-58	29.63	1.43	0.00	0.00	0.19
R-59	28.71	1.42	0.00	0.00	-13.30
Avg	29.17	1.43	0.00	0.00	-6.56
STDV	0.65	0.01	0.00	0.00	9.53

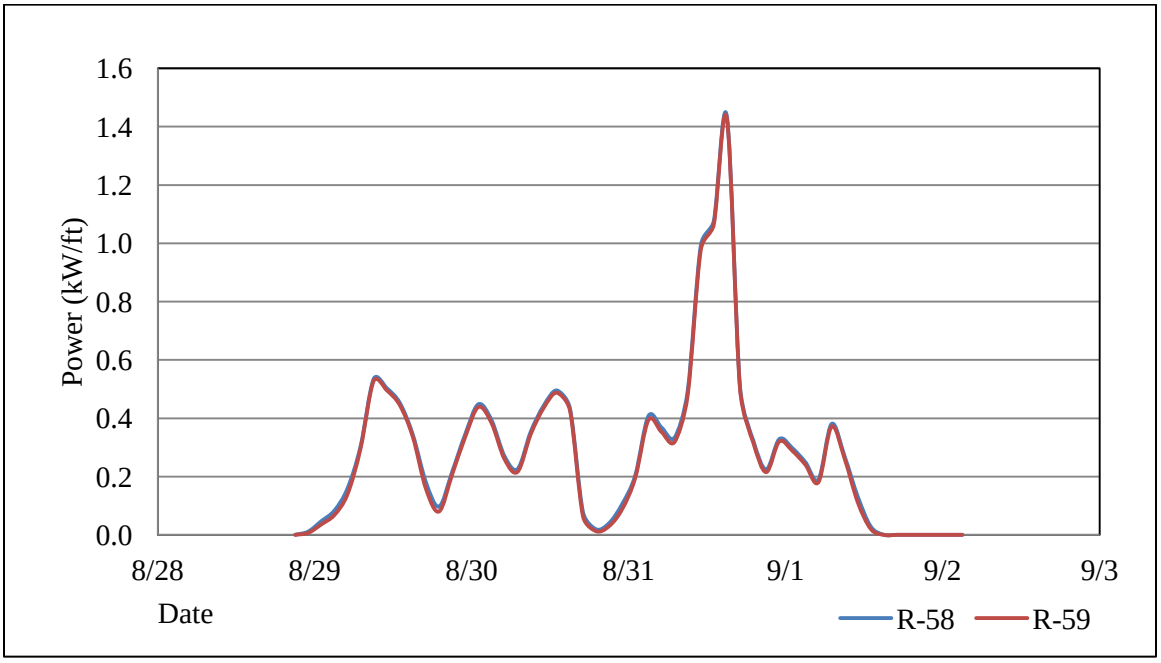

Figure 6.5: Time Series of Energy Flux above the Normal Mean High Water Line during Hurricane Elena (1985).

6.4 HURRICANE OPAL (1995)

Hurricane Opal is another storm that impacted Pinellas County. Opal lasted from October 4th to 7th in 1995. The storm formed in the Gulf of Mexico in September of 1995. It became a Category 4 hurricane with 115 MPH winds and made landfall near Pensacola, FL. The beach profile information was obtained from Davis and Wang (1996) and depicts Indian Rocks Beach and Redington Beach, FL. The impressive feature of Opal is that despite passing 300 miles offshore of the area, it produced minor inundation in some places. Sites R-74 and R-80 are located at Indian Rocks Beach while site R-106 is located at Redington Beach, Florida. The tide information is from the NOAA Station 8726724 at Clearwater, FL and the wave hindcast information is from WIS Station 73362 which is located approximately 100 miles from the coast of Sand Key Beach at a depth of 110 m.

Figure 6.6 shows the time series of energy fluxes above the normal mean high water line over the duration of the storm and Table 6.4 presents the totals for each site. The sites are listed order from north to south in the table. There were high amounts of overwash at all three locations and there was minor inundation at site R-106. This correlates well with reports of coastal flooding in the area after the storm. The most notable thing about Opal was its impact when it comes to overwash. The beaches in this region are susceptible due to their lack of elevation. The highest dune elevation at all three sites is less than 10 feet above NAVD88. There was not much erosion or accretion at these locations. Site R-74 had accretion of 1.56 cubic yards per foot of shoreline above the zero elevation datum (NAVD88) while the other two sites experienced less than 2.40 cubic yards per foot of erosion.

Table 6.4: Storm Severity Index Model Results for Hurricane Opal

Site	EFI Value (kW-hours/ft)	Peak Power (kW/ft)	Overwash (Cubic ft/ft)	Inundation (Cubic ft/ft)	Sand Lost (Cubic Yards/ft)
R-74	36.18	1.72	3479.94	0.00	1.56
R-80	29.90	1.45	3986.66	0.00	-2.37
R-106	26.10	1.18	1349.28	47520	-1.11
Avg	30.73	1.45	2938.63	15840.00	-0.64
STDV	5.09	0.27	1399.54	27435.68	2.00

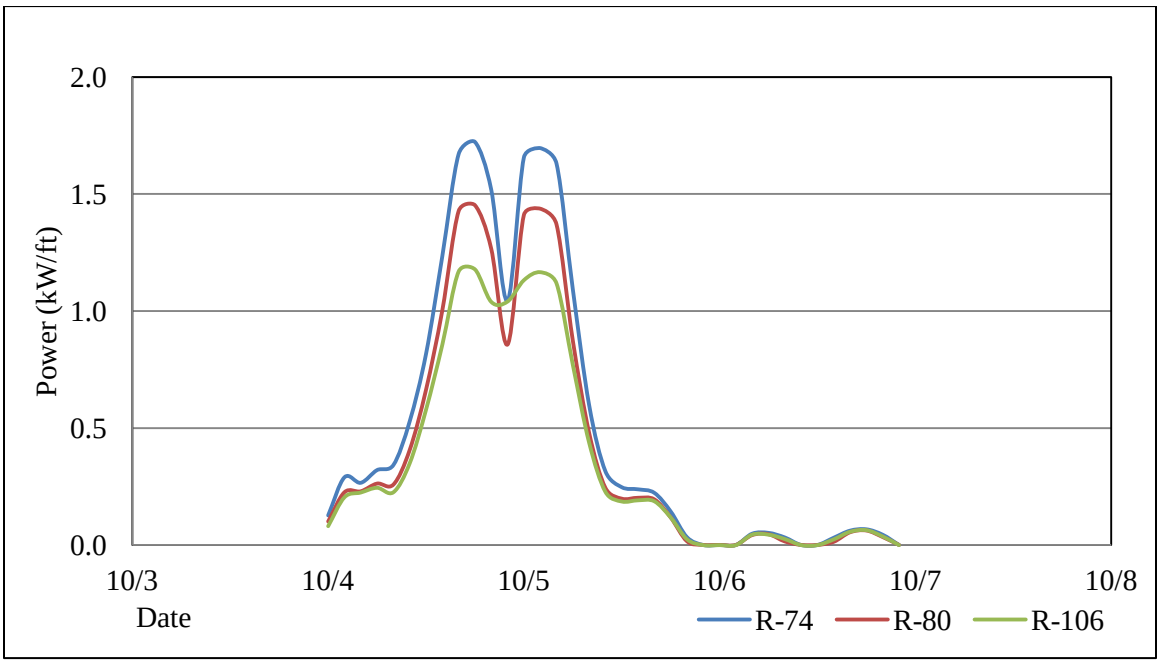

Figure 6.6: Time Series of Energy Flux above the Normal Mean High Water Line during Hurricane Opal (1995).

6.5 TROPICAL STORM DEBBY (2012)

Tropical Storm Debby is the final storm to be examined and was also the weakest of the five. The storm developed in the Gulf of Mexico in June of 2012. Debby was an early storm and it occurred between June 3rd and June 7th. Despite a projected track towards Louisiana, the storm headed northeast towards Florida. Debbie was a weak tropical storm with maximum winds of 65 MPH. The beach profiles were obtained from the report titled: Volume and Shoreline Changes along Pinellas County Beaches during Tropical Storm Debby by Wang and Roberts (2012). The SSIM analysis was applied to five locations during the storm. These locations are listed in order from north to south. The wave record was obtained from WIS Station 73362 which is 100 miles of the coast of Clearwater at a depth of 110 m. The tide information was obtained from NOAA Station 8726724 at Clearwater Beach, FL

As seen, in Table 6.5, the average peak power between the five sites is only 0.20 kW per foot. The time series of energy flux above the normal mean high water line over time during Tropical Storm Debby are presented in Figure 6.7. The most notable aspect of Tropical Storm Debby was the amount of erosion that occurred at the beaches in the Clearwater area. R-66 had minor accretion but the other four sites lost between 1.50 and 7.50 cubic yards of sand per foot of beach above the zero elevation datum (NAVD88). These are large values of erosion compared to how little energy flux was present during this storm. It is important to note that this value is only measured above the zero elevation datum and does not take into account any erosion or accretion below this elevation. The EFI values range from 4.25 to 5.84 kW-hours per linear foot of shoreline which indicates a weak storm. The SSIM modeling did not indicate any overwash or inundation during this storm.

Table 6.5: Storm Severity Index Model Results for Tropical Storm Debby

Site	EFI Value (kW-hours/ft)	Peak Power (kW/ft)	Overwash (Cubic ft/ft)	Inundation (Cubic ft/ft)	Sand Lost (Cubic Yards/ft)
R-66	4.25	0.18	0.00	0.00	0.93
R-75	4.36	0.18	0.00	0.00	-1.52
R-108	4.90	0.21	0.00	0.00	-3.33
R-140	5.72	0.22	0.00	0.00	-5.44
R-160	5.84	0.23	0.00	0.00	-7.41
Avg	5.01	0.20	0.00	0.00	-3.36
STDV	0.74	0.02	0.00	0.00	3.26

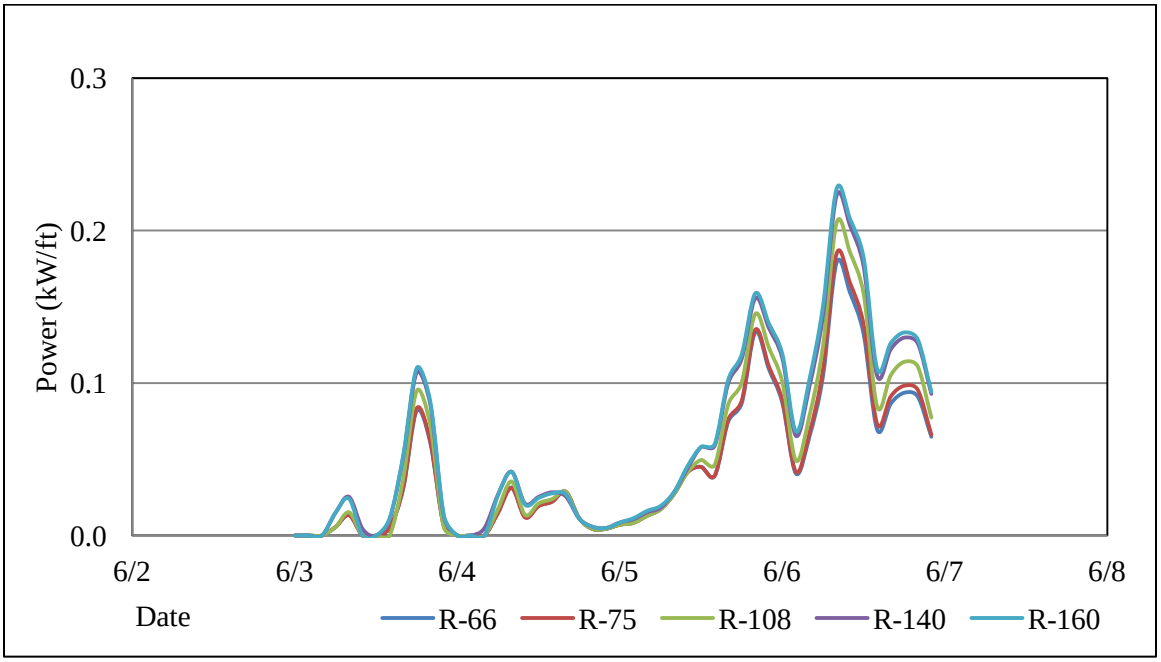

Figure 6.7: Time Series of Energy Flux above the Normal Mean High Water Line during Tropical Storm Debby (2012).

6.6 ANALYSIS OF STORM SEVERITY INDEX MODEL FOR GULF OF MEXICO STORMS

In Chapter 5, which dealt with Ocean City storms, the application and analysis of the Storm Severity Index Model was conducted by comparing the impact of multiple storms at the same transects. However, it is not possible to emulate this for the Gulf of Mexico storms because each storm utilized different beach profile locations. Instead, in order to judge the veracity of the SSIM results, they will be quantitatively compared using the Saffir-Simpson Scale, the duration, and the distance that the storm passed from each location. Table 6.6 summarizes these characteristics for all five storms.

Table 6.6: Characteristics of Gulf of Mexico Storms

Storm	Peak Category	Category at Impact	Approx. Storm Distance from Sites	Duration (Days)
Hurricane Georges	4	2	100 miles	2
Hurricane Ivan	5	3	100 miles	1
Hurricane Elena	3	1	80 miles	4
Hurricane Opal	4	4	300 miles	2
Tropical Storm Debby	T.S.	T.S.	50 miles	4

Judging from the characteristics of each storm, it is reasonable to expect that Hurricane Ivan will be the most severe storm because, although it is the second strongest category storm after Hurricane Opal, it passed much closer to the profile locations. After Ivan it is expected that Hurricanes Georges and Opal will be next most severe, followed by Hurricane Elena and Tropical Storm Debby.

When looking at the results of the SSIM, they confirm with what is expected from the qualitative information. As shown in Figure 6.8, Hurricane Ivan does have the highest SSIM values, followed by Hurricane Georges, Hurricane Opal, Hurricane Elena, and Tropical Storm

Debby. The only unexpected result is that the severity of Opal is closer to Elena instead of Georges.

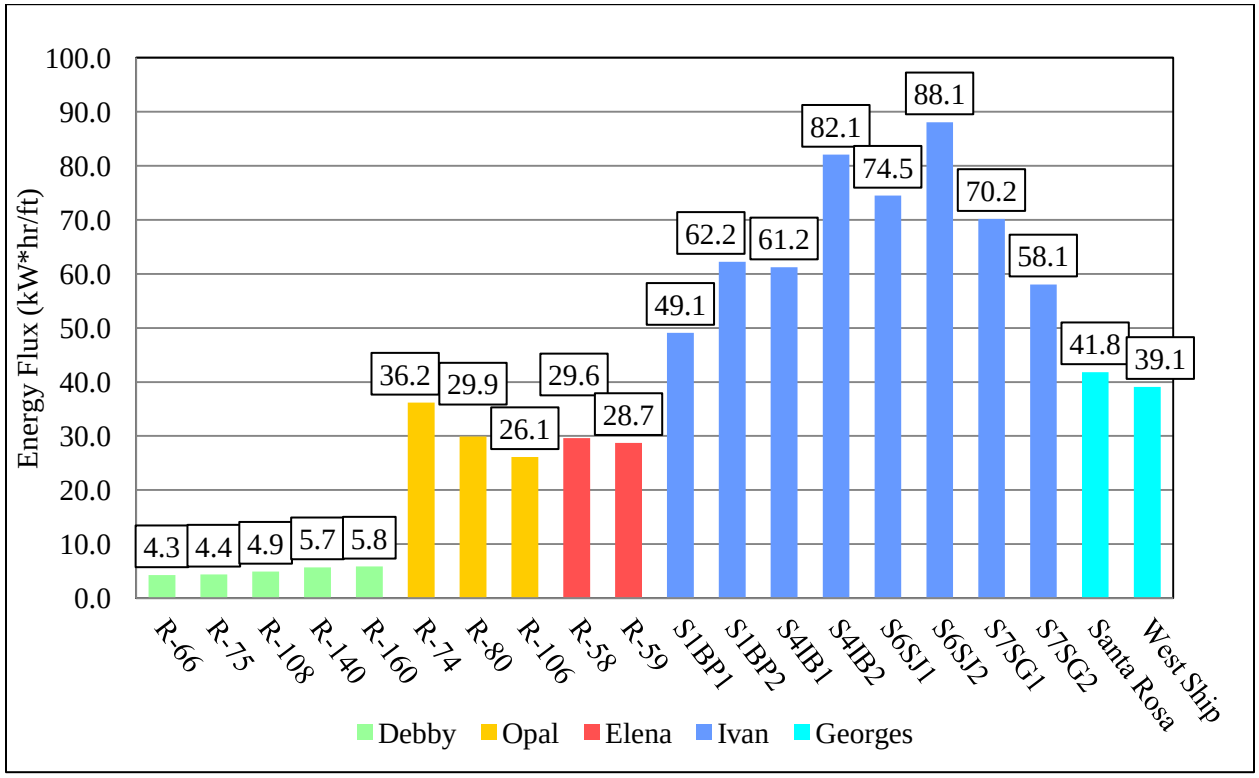

Figure 6.8: Energy Flux Index Values for Each Gulf of the Mexico Storms.

Although Figure 6.8 confirms that Hurricane Ivan is the strongest of the five storms when it comes to wave energy flux, and Tropical Storm Debby is clearly the weakest, with the other three storms in the middle, in order to create a more comprehensive storm severity scale, the energy flux is not the only factor that needs to be taken into account. The amount of overwash and any inundation also need to be included. Consequently, the following section outlines the creation of a new combined storm severity scale that is based on both the potential water damage due to wave overtopping and flooding inundation as well as energy flux above the normal mean high water line.

CHAPTER 7: TWENTY-FOUR POINT STORM SEVERITY SCALE

A somewhat subjective "Twenty-Four Point Storm Severity Scale (SSS)" combines the Energy Flux Index number, the amount of overwash, and the inundation that a site suffers in order to create a single value that qualitatively estimates the impact a storm will have on a region. There are two parts to this scale. The first part of the scale relates to the Energy Flux Index number. For each storm, a category of severity for the Energy Flux Index is determined by using Table 7.1. The table is split into twelve categories, each of which corresponds to a range of index numbers. In order to use the scale, it is simply necessary to compare the number produced by the SSIM to the table to find its corresponding category. For example, Hurricane Ivan site S4IB1 has an index value of 61.21 kW-hours per linear foot, which falls in category 6.

Table 7.1: Energy Flux Index Categories

Category	Min Index Number	Max Index Number	Rank
1	0	10	Low
2	10	20	
3	20	30	Moderate
4	30	40	
5	40	60	
6	60	80	High
7	80	100	
8	100	125	
9	125	150	
10	150	175	Extreme
11	175	200	
12	>200		

It is noted that the range between min and max increases as the category numbers become larger. Originally, an exponential scale was tried but it was found that the index numbers rose too

quickly to have enough definitive categories. The opposite was found when attempting categories with uniform spacing. In that case, there were too many categories to create a scale that is simple to understand. The last column of Table 7.1 gives a one-word description of how strong the category is compared to the others. Categories 1 and 2, for example, are considered to be locally low energy storms. It is important to note that the higher values of energy flux above the normal mean high water line are produced by lower probability storms in close proximity. This means that the lower categories are more likely to be seen then the higher ones, and as a result, when a higher category is seen, perhaps a non-linear increase in damage should be expected.

The second part of the Twenty-Four Point Scale is related to the amount of water that gets beyond the dune. This part is slightly more complex because it takes into account two separate types of water damage rather than simply looking at one index number. Like the first part, the procedure to determine the category is to use the wave model and water level record to obtain the overwash and inundation estimations for a given storm. Next, Table 1.2 is used to separate the overwash and inundation into categories. In a case where there is both overwash and inundation, whichever value produces the greater category is used. Thus, if there is a case where the total overwash is 16,000 cubic feet per foot and the inundation is 11,000 cubic feet per foot, the value for overwash is used because its corresponding category is 9 whereas the category corresponding to the inundation is 8. However, if there is a case with 7,000 cubic feet per foot of overwash and the same amount of inundation, the category would still be 8 because it is the higher of the two numbers. The development of this part of the scale is similar to the first part. At first, evenly separated magnitudes of volume were tried, but they produced too many

categories to be functional. Next, an exponential scale was used with the opposite result. In the end, the scale was created with overlap in categories between inundation and overwash.

Table 1.2: Overwash and Inundation Categories

Overwash			Inundation		
Water Index	Min Overwash Volume	Max Overwash Volume	Min Inundation Volume	Max Inundation Volume	Rank
0	0	1	-	-	Low
1	1	10	-	-	
2	10	100	-	-	
3	100	500	-	-	
4	500	1000	-	-	Moderate
5	1000	3000	-	-	
6	3000	6500	0	5000	High
7	6500	10000	5000	10000	
8	10000	15000	10000	50000	
9	15000	20000	50000	100000	Extreme
10	20000	30000	100000	500000	
11	>30000		500000	1000000	
12			>1000000		

- Note: any inundation results in a minimum category of 6.
-- All values are in units of cubic feet per foot of shoreline.

Once the category for the water damage is determined, the next step is simply to add that number to the category number that was determined for the wave energy flux above the normal mean high water line. This new number is a storm's final category number for a given location. Using site R-106 from Hurricane Opal as an example; the index number for this site is 26.10 kW-hours per linear foot which falls into category 3 in Table 7.1. There is 6443.43 cubic feet per foot of overwash which corresponds to category 6 in Table 1.2. The inundation at this location is 18.60 cubic feet per foot which also corresponds to category 6. Thus, category 6 is selected from Table 1.2. Next, the two values are added to create the final category number of 9.

The Twenty-Four Point Storm Severity Scale is shown below in Table 1.3. Each category has a description associated with it that describes the basic attributes that a storm has at a given location. Because there is some overlap in the category descriptions, a system of seven classifications was also added to the scale. These classifications group the categories that have similar descriptions in order to make it easier to understand. A description of the different classifications can be seen below:

A--Low SSIM Index with little chance of overwash.

B--Low to moderate SSIM Index with no or low overwash.

C--Up to high SSIM Index with a chance of reaching high water overwash volumes. Inundation is now possible but unlikely.

D--SSIM Index is in moderate to high range. Water volumes are likely in the moderate range with a chance of being high. Inundation is possible.

E--Both SSIM Index and water volumes are in the high range with one of them likely to be extreme. Inundation likely.

F--SSIM Index is in the high range with a chance of becoming extreme. Water volumes are at least high with large chance of being extreme. Inundation almost certain.

G--SSIM Index and water volumes are both extreme. One or both can be off the chart.

Class A storms are the most minor ones of the selection but even some of these storms are capable of creating overwash depending on the shape of the beach. The classifications give a general indicator of the impact that can occur but in order to better understand any potential danger, it is better to look at SSIM and Water Volume Indices rather than just the classifications.

Table 1.3: Twenty-Four Point Storm Severity Scale

Class	Cat.	Description
A	1	SSIM Index under 10 and no overwash.
	2	Has a low SSIM Index with a chance of low overwash.
	3	Has a low or moderate SSIM Index with a chance of low overwash.
B	4	Either moderate SSIM Index with no overwash or low SSIM Index with low overwash.
	5	Either moderate SSIM Index with little to no overwash or low SSIM Index with moderate overwash.
C	6	Either high SSIM Index with little to no overwash or moderate SSIM Index with low overwash.
	7	Up to high SSIM Index or moderate volume of overwash.
	8	Up to high SSIM Index or high volume of water. Inundation is possible.
	9	Up to high SSIM Index or high water volume. Possibility of some inundation.
D	10	Up to High SSIM Index with chance of reaching extreme or moderate to high water volumes with some chance of inundation.
	11	At least moderate SSIM Index, likely in the high range with a chance of reaching extreme. Water volumes will be low to moderate with a small chance of reaching high. There is some chance of inundation.
	12	At least moderate SSIM Index, likely in the high range. The water volumes are in the moderate to high range. Some chance of inundation.
	13	High SSIM Index. The water volumes are in the moderate to high range. Inundation is possible.
E	14	At least high SSIM Index with a chance of reaching extreme levels. The water volumes are at least moderate but likely in the high range. Inundation is possible.
	15	At least high SSIM Index with a chance of reaching extreme levels. The water volumes are possibly moderate but likely high with inundation possible.
	16	At least high SSIM Index with a chance of reaching extreme. Likely high water volumes with chance of extreme. Inundation is possible.
F	17	Both the SSIM Index and water volume are in the high category with a large chance of one of them reaching extreme. Likely to have inundation.
	18	Both the SSIM Index and water volume are in the high category with likely of one of them reaching extreme. There is likely to be inundation.
	19	One of the SSIM Index or water volume is at the extreme level. There is likely inundation.
	20	At least one of the SSIM Index or water volume is at the extreme level.
G	21	Both SSIM Index and water volume are extreme.
	22	Both SSIM Index and water volume are extreme with a chance of being off the chart.
	23	Off the charts for both SSIM Index and water volume.
	24	Off the charts for both SSIM Index and inundation.

The Twenty-Four Point Scale was applied to all of the storms examined in this study. Table 1.4 contains the top 25 ranked locations. As seen below, Hurricane Sandy and the El Nino Winter make up the top ten, and sixteen of the top twenty-five spots which makes it clear that they are the two strongest storms in the locations studied.

Table 1.4: Greatest 25 Storm Severity Scale Results

Rank	Storm	Location	SSIM Index	Water Index	Category
1	Hurricane Sandy	NJBPN 167	6	10	16
2	Hurricane Sandy	NJBPN 153	6	10	16
3	El Nino Winter	OC 22	10	5	15
4	El Nino Winter	OC 16	8	6	14
5	El Nino Winter	OC 25	8	6	14
6	El Nino Winter	OC 7	9	3	12
7	Hurricane Sandy	NJBPN 173	8	4	12
8	Hurricane Sandy	NJBPN 183	7	5	12
9	Hurricane Sandy	NJBPN 177	7	5	12
10	Hurricane Sandy	NJBPN 248	5	7	12
11	January 1992 Nor'easter	OC 10	5	7	12
12	Hurricane Georges	Santa Rosa Island	5	7	12
13	Hurricane Sandy	NJBPN 171	8	3	11
14	El Nino Winter	OC 19	8	3	11
15	Hurricane Opal	R-106	3	8	11
16	January 1992 Nor'easter	OC 4	4	6	10
17	Hurricane Opal	R-74	4	6	10
18	Hurricane Ivan	S4IB2	7	3	10
19	Hurricane Sandy	NJBPN 150	9	0	9
20	El Nino Winter	OC 10	7	2	9
21	Hurricane Sandy	NJBPN 168	6	3	9
22	January 1992 Nor'easter	OC 13	5	4	9
23	Hurricane Sandy	NJBPN 163	4	5	9
24	North American Blizzard	OC 25	4	5	9
25	Hurricane Opal	R-80	3	6	9

Table 1.5: Breakdown of Classifications

Classification	Number of Locations
A	61
B	11
C	24
D	12
E	5
F	0
G	0
Total	113

Table 1.5 shows the number of locations that are in each classification for all of the events utilized herein. Classification A holds the most with 61 locations, followed by Classification C with 24. One object of note is that classes F and G do not have any locations out of this dataset. Even the locations from Hurricane Sandy only managed to reach Classification E. The scale does not rise linearly so it is important to note that it becomes more difficult to reach the higher levels than the lower ones. And even the low levels can have a large impact. The scale was made to rank the impact of storms on locations and any storm that can produce an impact category greater than 2 can produce overwash.

CHAPTER 8: CONCLUSIONS

The Twenty-Four Point Storm Severity Scale is a new hydrodynamics-based storm severity index. Unlike previous indices, the scale focuses on providing a rank for a particular location, rather than for an entire storm. This allows individual communities the opportunity to determine the impact a storm will have on their specific location. The scale is based on the idea that the wave energy flux above the normal mean high water line is related to the amount of damage that a beach will sustain. The water level and wave runup are also factored into the scale because of the damage that runup-induced overwash and flooding-induced inundation can potentially cause. In this thesis, 17 tropical and extratropical events were studied at 113 locations in order to develop and verify the effectiveness of the Twenty-Four Point Scale against the expected impact of the storms.

The SSS is divided into three parts. The first part is the Energy Flux Index which is the time series of energy flux above the normal mean high water line integrated over time. The second part is the overwash and the third part is the inundation. When combined, these three factors provide a subjective estimation of the damage that an area will receive during a storm.

Chapter 4 focused on Hurricane Sandy in order to establish a benchmark for the validity of using the Energy Flux Index to classify a storm. The chapter looked at twenty beach profile locations that extended along the coast of New Jersey with the expectation that the EFI values would be larger in the northern part of the state. As presented in Figure 4.6, this expectation was met which confirmed that using EFI values to qualitatively rank the severity of a storm is valid.

The EFI values are a valid way of ranking the storm severity but alone they are not sufficient in predicting the amount of potential damage an area will receive. The volume of overwash and the volume of flood-induced inundation added to the SSIM because an area's damage potential is directly tied to the shape of a beach and the height of the beach crest.

Chapter 5 looked at the same factors as Chapter 4 but instead of looking at one storm over a large area, Chapter 5 focused on multiple storms that impacted one area. There were ten profile locations located near Ocean City, Maryland. These ten profiles were observed during eleven storm events between 1990 and 2003. Chapter 5 expanded the work that was started in Chapter 4 but only one storm out the eleven was able to rival Hurricane Sandy. The El Nino Winter storm was the second most severe storm out of those included in this thesis but the only reason it rivaled Sandy was due to its long duration rather than its strength. This highlights one of the strengths of using the EFI. The duration of a storm is inherently factored into the ranking process which is something other indices fail to take into account. The duration of a storm is one of the most important factors when determining the impact a storm will have on an area.

This principal is demonstrated again in Chapter 6. Chapter 6 focuses on 5 storms that had an impact in the Gulf of Mexico. The strongest of these storms was Hurricane Ivan. However, because it was such a fast-moving storm, Ivan did not have as large an impact as some of the other storms such as Hurricane Opal.

When looking at Table 1.4, it is possible to note that there are two kinds of storms that made the top 25 list. The first kind of storm is the storms that have very large Energy Flux Index values and the second kind of storm is the storms that have large Water Index (WI) values. The storms with large Water Index values that have moderate or low EFI values, including Hurricane

Opal, are the ones that struck areas that have low beach crest elevations. This emphasizes the importance that the pre-existing beach profile has in determining the potential damage of an area.

There are some areas of concern that were present during this thesis. The first is the wave information that was used in Chapter 4. In Chapter 4, the wave information used came from a SWAN model. The concern in this chapter is that the wave heights appear to show tidal variation. This tidal variation may have impacted the results of the SSIM slightly.

Another concern involving wave heights was in Chapter 5. For a few storms in Chapter 5, the hindcast wave heights are similar to the wave heights from buoy 44009 when they should be less than the buoy wave heights. This means the SSIM results are possibly overestimated.

One of the goals of this thesis was to find a link between erosion and energy flux. In an attempt to determine this, the Energy Flux Index was plotted against the change in volume at each of the sites at which a pre- and post-storm survey was available. The results of this attempt are located in Appendix F. Unfortunately, a linear correlation between the two was not found. One factor that may have had an impact is that some of the beach profiles are not taken directly after the storm which can impact the amount of change in sand volume that is recorded. This is one area in which this thesis can be improved.

Another area in which the model can be improved in further studies is by using a variable beach profile rather than a static one. If a model can be created to model the change of a beach profile over time then its application to the SSIM could improve the accuracy of the output. Despite this area of improvement, this new scale can be an effective tool to rank potential damage that both tropical and extratropical systems can cause.

This work can potentially be furthered in multiple ways. The first is that the SSIM and Twenty-Four Point Scale can be coupled with storm forecasting in order to create a predictive

index for potential damage. Another way is that this methodology can be expanded to include coastal areas other than sandy beaches. A study on boardwalks, sea walls, and other structures can also be implemented to further the range of uses of the SSIM. Finally, the SSIM and Twenty-Four Point Scale can be coupled with social factors and estimates of infrastructure in order to create a vulnerability scale. A vulnerability scale would incorporate the SSIM output and population density in order to determine the vulnerability of a coastal area.

Despite the concerns that arose within this thesis, the Twenty-Four Point Storm Severity Scale provides a location-based qualitative scale for describing the potential damage that an area may receive during a storm. Unlike other storm severity scales, this one takes into account the four major factors for determining the storm damage potential and provides a site-specific ranking for use by individual coastal communities.

APPENDIX A: HURRICANE SANDY

Appendix A contains site information for Hurricane Sandy. Each site has a site summary which includes a description of the site along with the results from the SSIM. Each site also has four figures which include the water levels at the site, the significant wave heights, the pre- and post-storm beach profiles, and the energy flux above the normal mean high water line during the event. The nearshore wave information used was obtained from an Advanced Circulation Model (ADCIRC) and Simulating Waves Nearshore Model (SWAN) run by Atkins Engineering. The waves were produced offshore of the survey locations and include the significant wave height (H_{mo}), the wave period (in seconds), and the mean wave direction. The water levels were obtained from the National Oceanic and Atmospheric Administration (NOAA) gauge number 8519483 located at Bergen Point, NY, NOAA gauge 8534720 located at Atlantic City, NJ, and NOAA gauge 8536110 located at Cape May, NJ (National Oceanic and Atmospheric Administration, 2015). The beach profiles were obtained from reports from the Richard Stockton College of New Jersey Coastal Research Center (CRC).

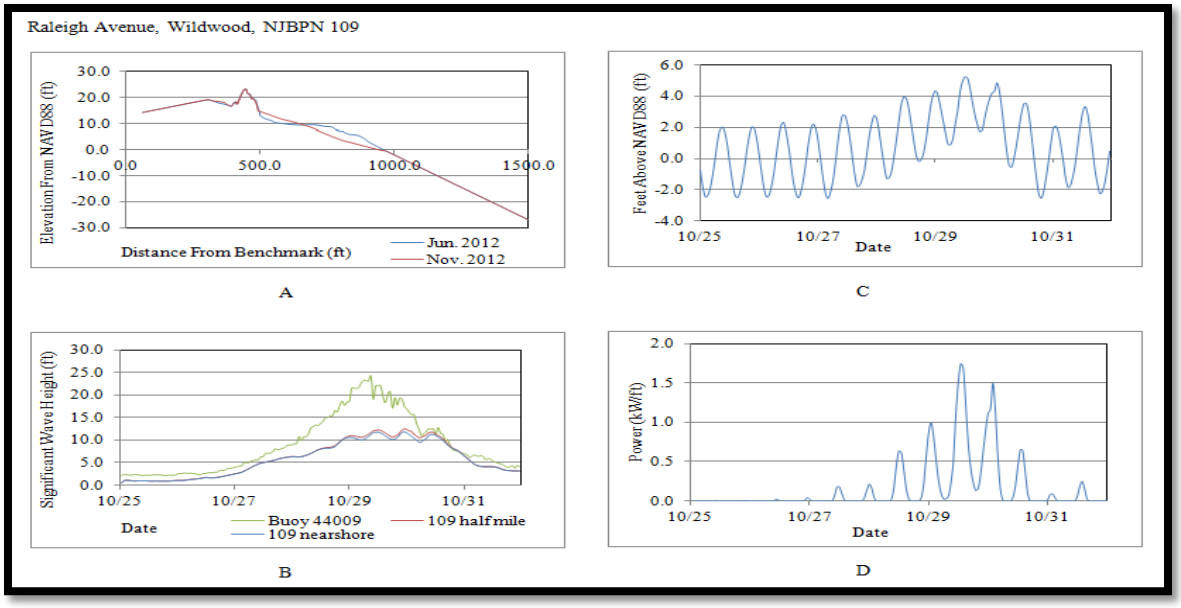

Figure A.1: NJBPN Site 109 Conditions and Results during Hurricane Sandy. A) The pre- and post-Hurricane Sandy profiles. B) Hurricane Sandy wave heights. C) Water levels at NJBPN 109. D) SSIM Results at NJBPN Site 109 during Hurricane Sandy.

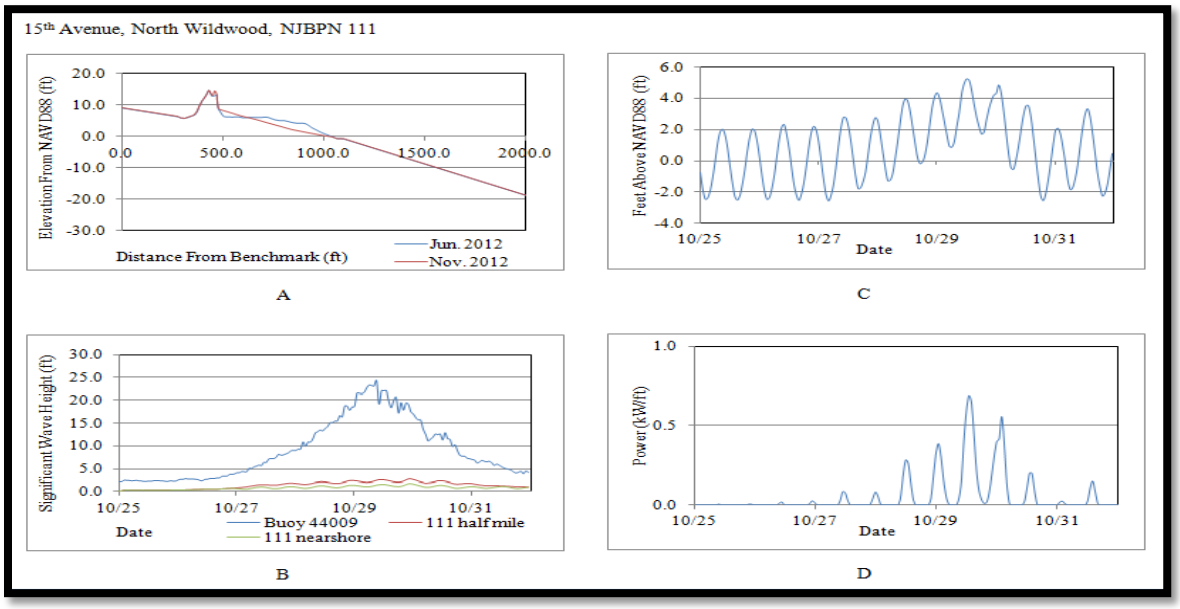

Figure A.2: NJBPN Site 111 Conditions and Results during Hurricane Sandy. A) The pre- and post-Hurricane Sandy profiles. B) Hurricane Sandy wave heights. C) Water levels at NJBPN 111. D) SSIM Results at NJBPN Site 111 during Hurricane Sandy.

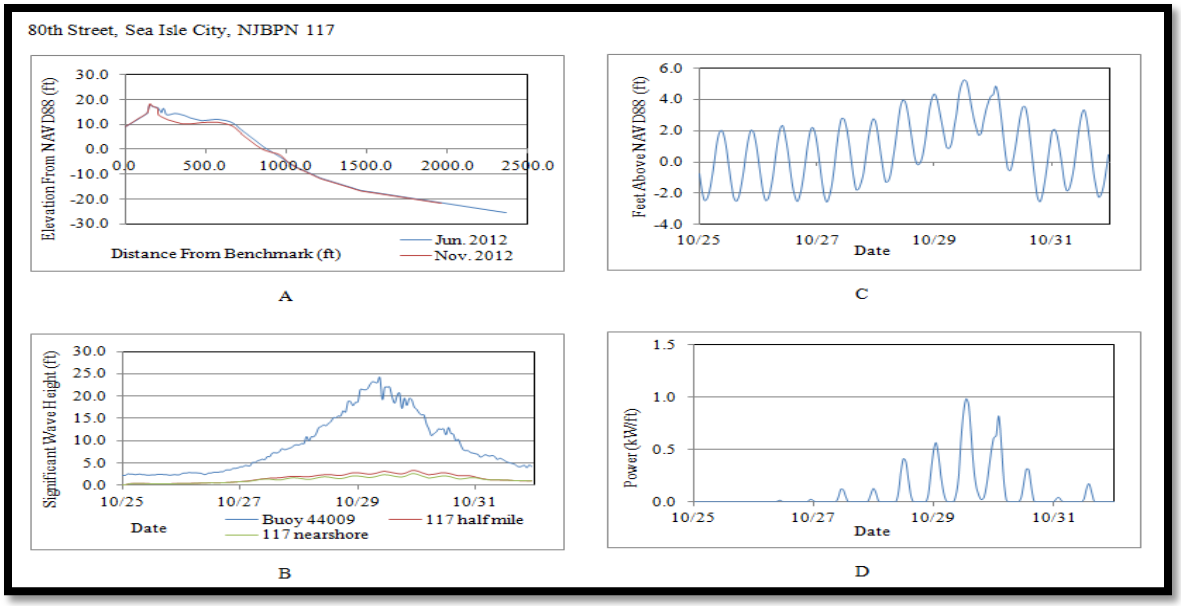

Figure A.3: NJBPN Site 117 Conditions and Results during Hurricane Sandy. A) The pre- and post-Hurricane Sandy profiles. B) Hurricane Sandy wave heights. C) Water levels at NJBPN 117. D) SSIM Results at NJBPN Site 117 during Hurricane Sandy.

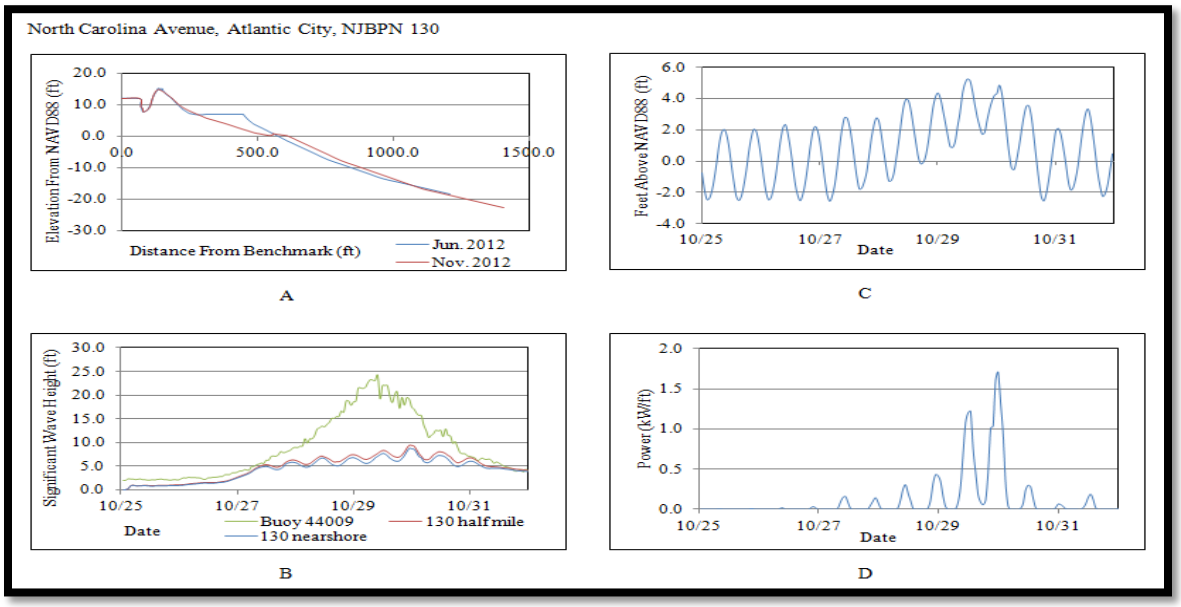

Figure A.4: NJBPN Site 130 Conditions and Results during Hurricane Sandy. A) The pre- and post-Hurricane Sandy profiles. B) Hurricane Sandy wave heights. C) Water levels at NJBPN 130. D) SSIM Results at NJBPN Site 130 during Hurricane Sandy.

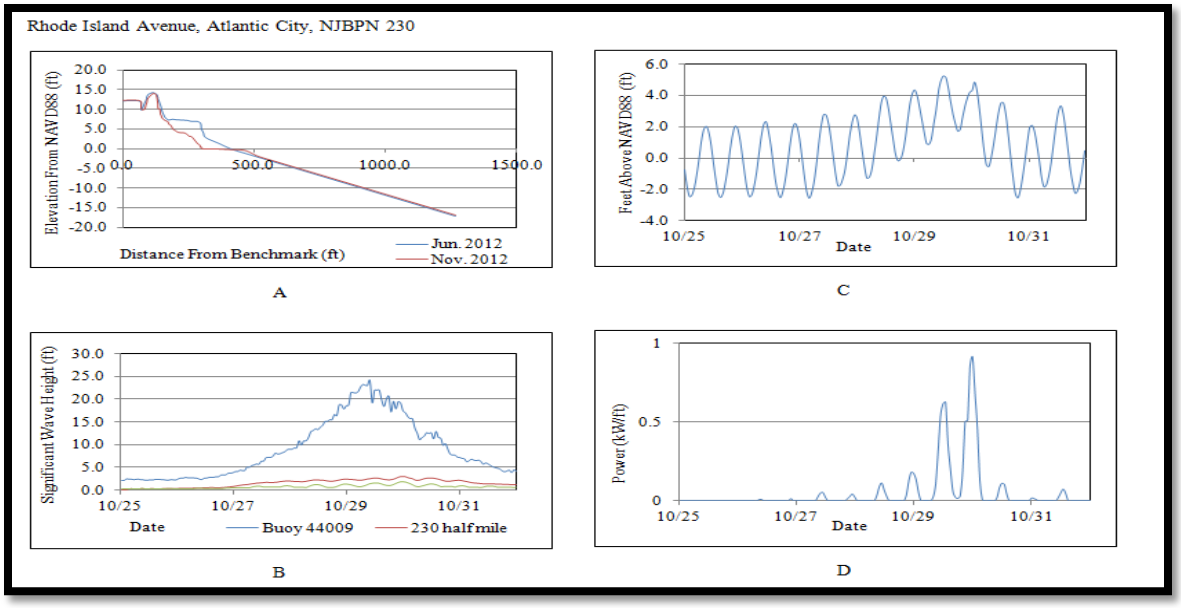

Figure A.5: NJBPN Site 230 Conditions and Results during Hurricane Sandy. A) The pre- and post-Hurricane Sandy profiles. B) Hurricane Sandy wave heights. C) Water levels at NJBPN 230. D) SSIM Results at NJBPN Site 230 during Hurricane Sandy.

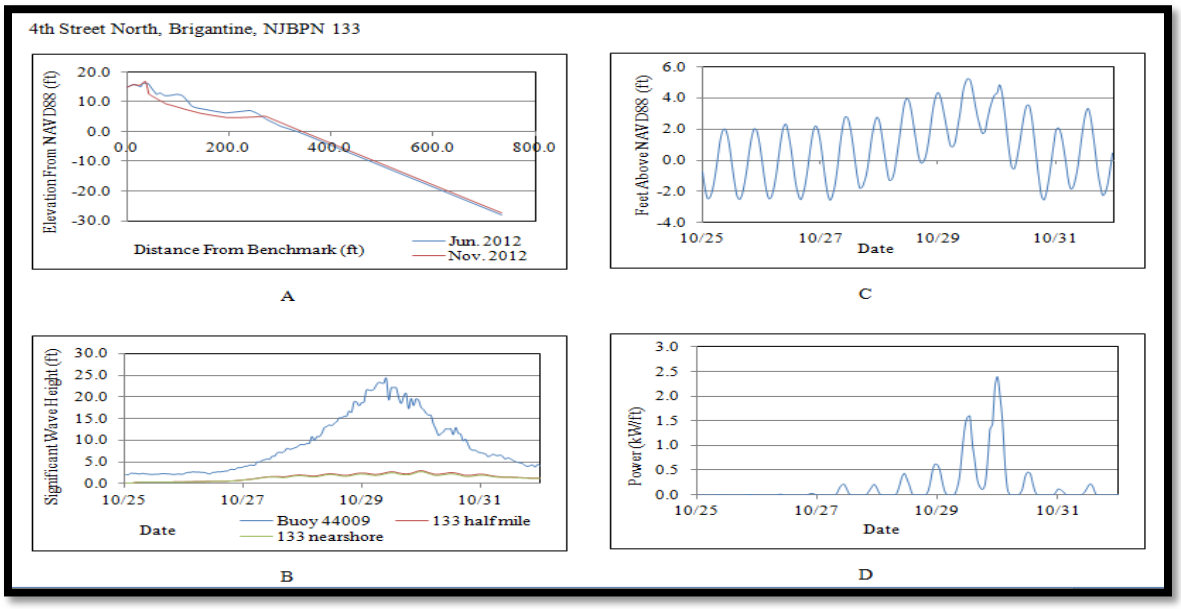

Figure A.6: NJBPN Site 133 Conditions and Results during Hurricane Sandy. A) The pre- and post-Hurricane Sandy profiles. B) Hurricane Sandy wave heights. C) Water levels at NJBPN 133. D) SSIM Results at NJBPN Site 133 during Hurricane Sandy.

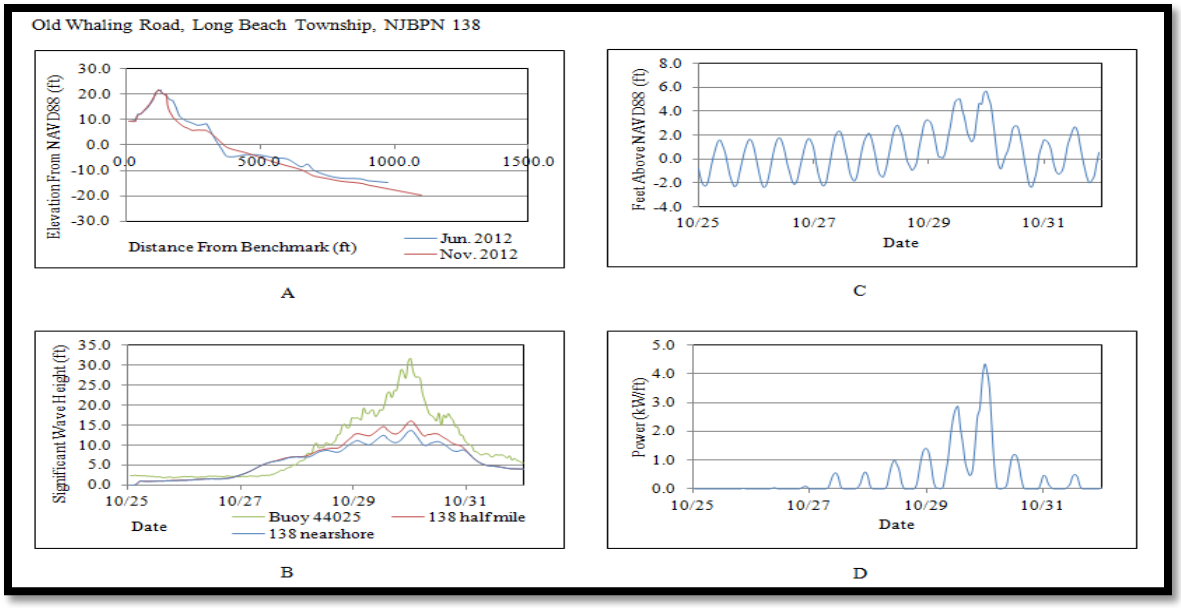

Figure A.7: NJBPN Site 138 Conditions and Results during Hurricane Sandy. A) The pre- and post-Hurricane Sandy profiles. B) Hurricane Sandy wave heights. C) Water levels at NJBPN 138. D) SSIM Results at NJBPN Site 138 during Hurricane Sandy.

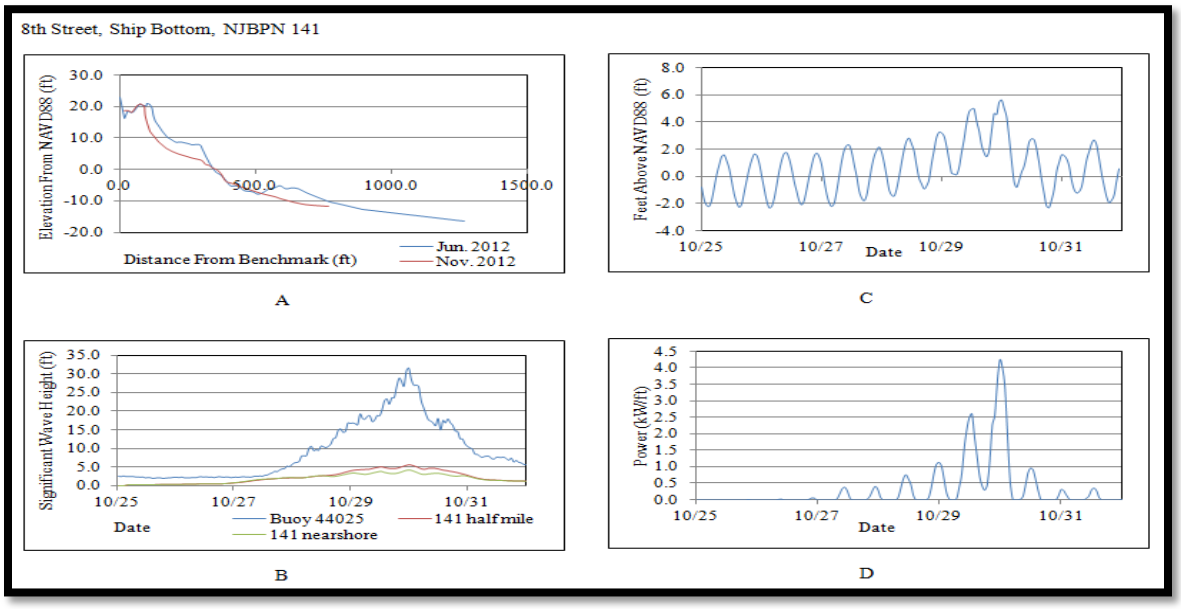

Figure A.8: NJBPN Site 141 Conditions and Results during Hurricane Sandy. A) The pre- and post-Hurricane Sandy profiles. B) Hurricane Sandy wave heights. C) Water levels at NJBPN 141. D) SSIM Results at NJBPN Site 141 during Hurricane Sandy.

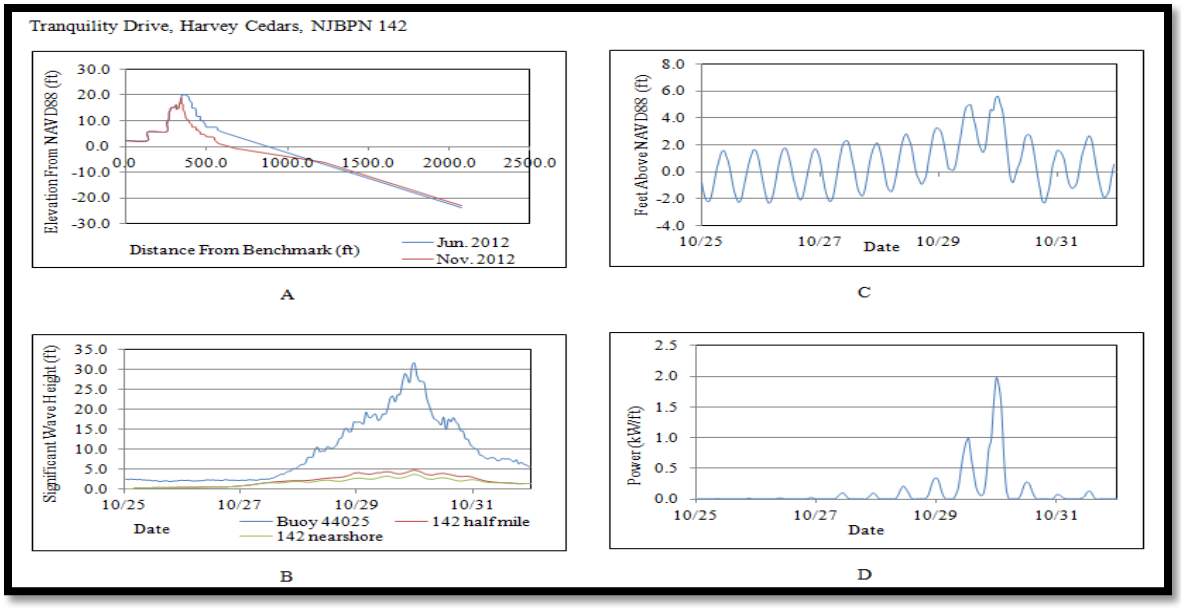

Figure A.9: NJBPN Site 142 Conditions and Results during Hurricane Sandy. A) The pre- and post-Hurricane Sandy profiles. B) Hurricane Sandy wave heights. C) Water levels at NJBPN 142. D) SSIM Results at NJBPN Site 142 during Hurricane Sandy.

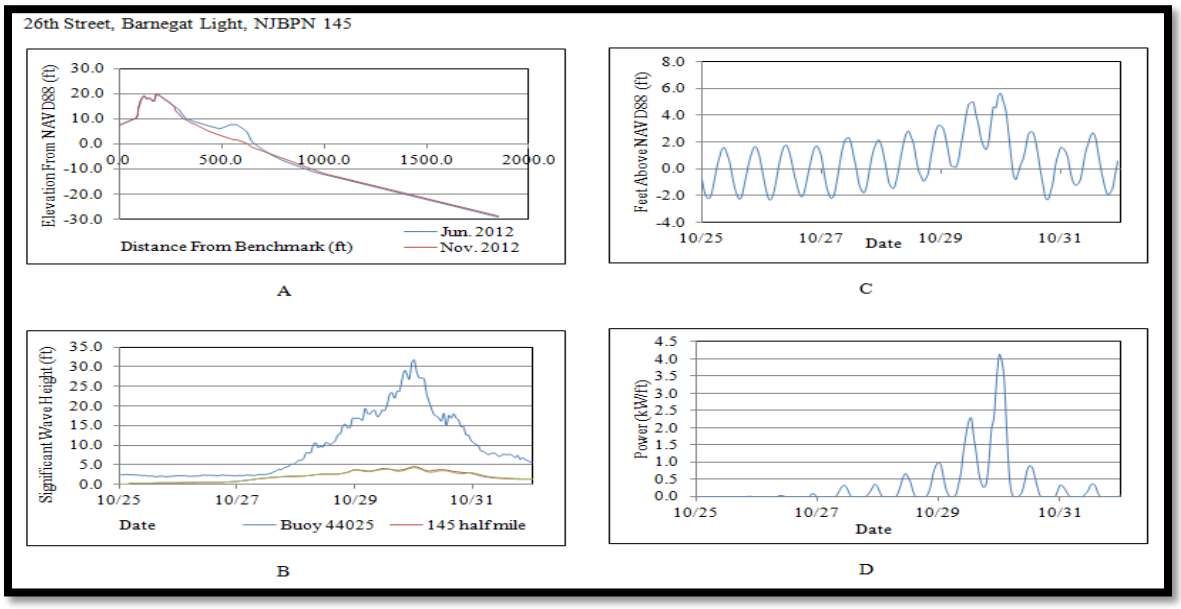

Figure A.10: NJBPN Site 145 Conditions and Results during Hurricane Sandy. A) The pre- and post-Hurricane Sandy profiles. B) Hurricane Sandy wave heights. C) Water levels at NJBPN 145. D) SSIM Results at NJBPN Site 145 during Hurricane Sandy.

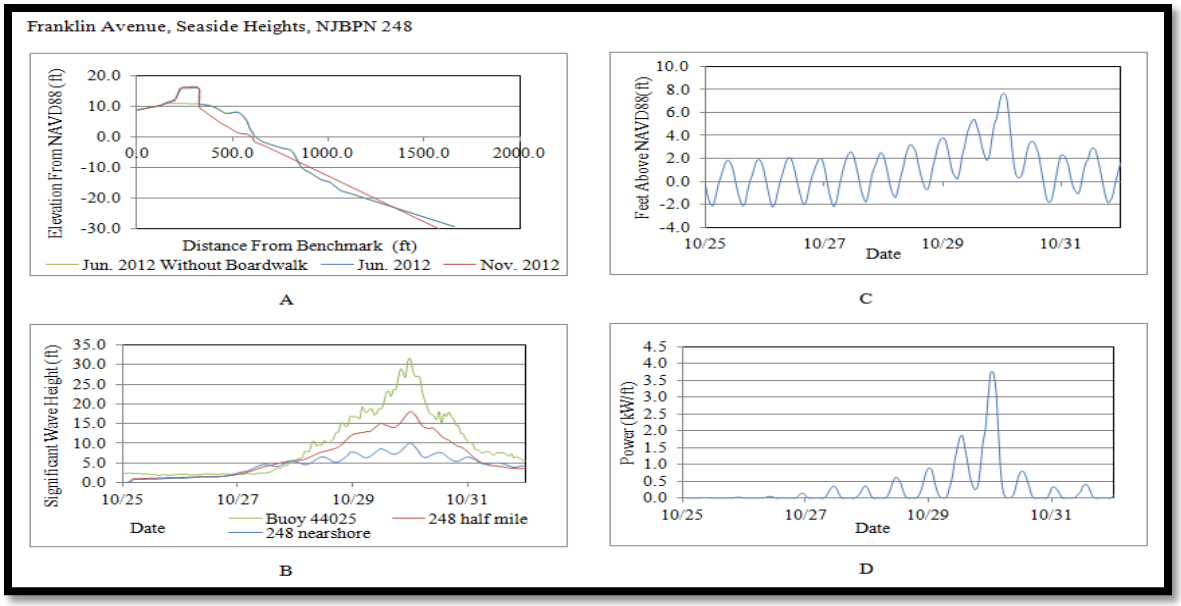

Figure A.11: NJBPN Site 248 Conditions and Results during Hurricane Sandy. A) The pre- and post-Hurricane Sandy profiles. B) Hurricane Sandy wave heights. C) Water levels at NJBPN 248. D) SSIM Results at NJBPN Site 248 during Hurricane Sandy.

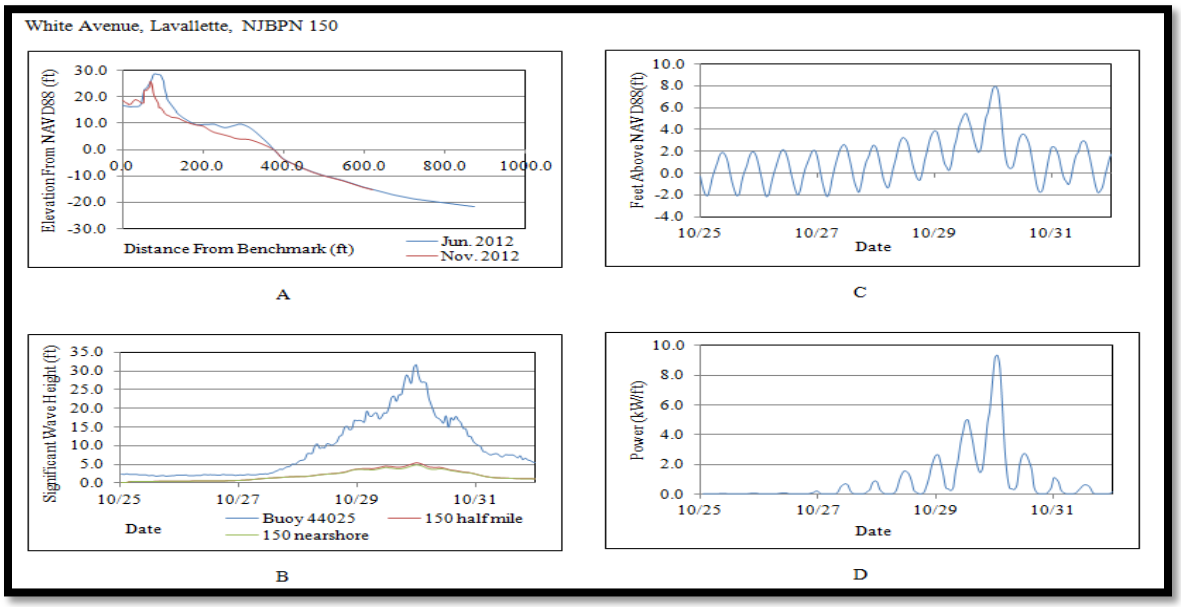

Figure A.12: NJBPN Site 150 Conditions and Results during Hurricane Sandy. A) The pre- and post-Hurricane Sandy profiles. B) Hurricane Sandy wave heights. C) Water levels at NJBPN 150. D) SSIM Results at NJBPN Site 150 during Hurricane Sandy.

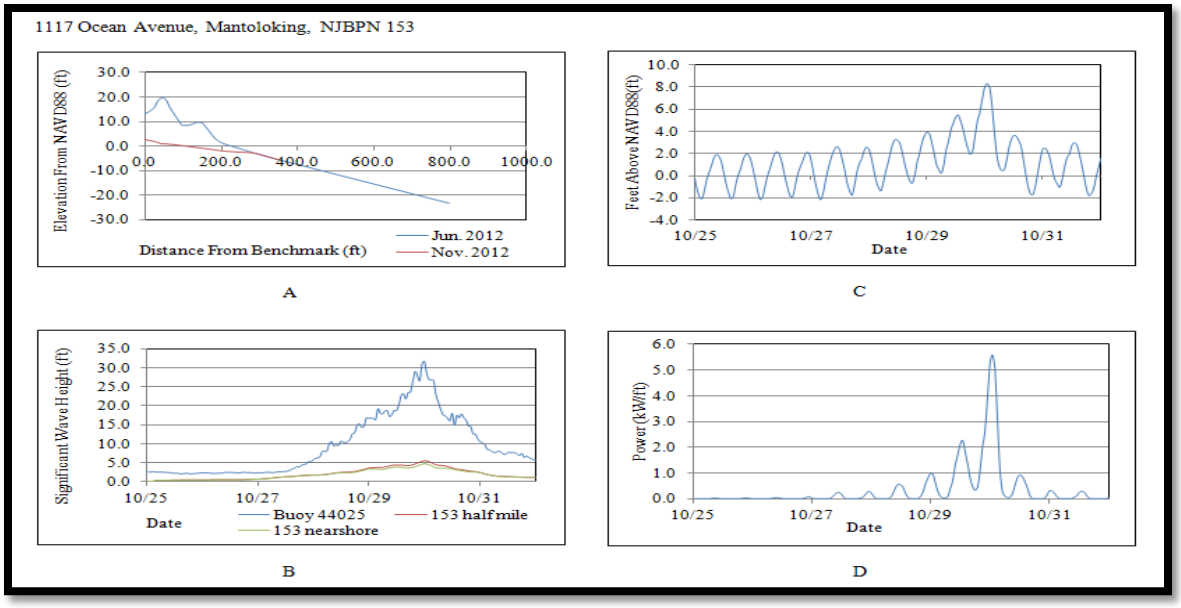

Figure A.13: NJBPN Site 153 Conditions and Results during Hurricane Sandy. A) The pre- and post-Hurricane Sandy profiles. B) Hurricane Sandy wave heights. C) Water levels at NJBPN 153. D) SSIM Results at NJBPN Site 153 during Hurricane Sandy.

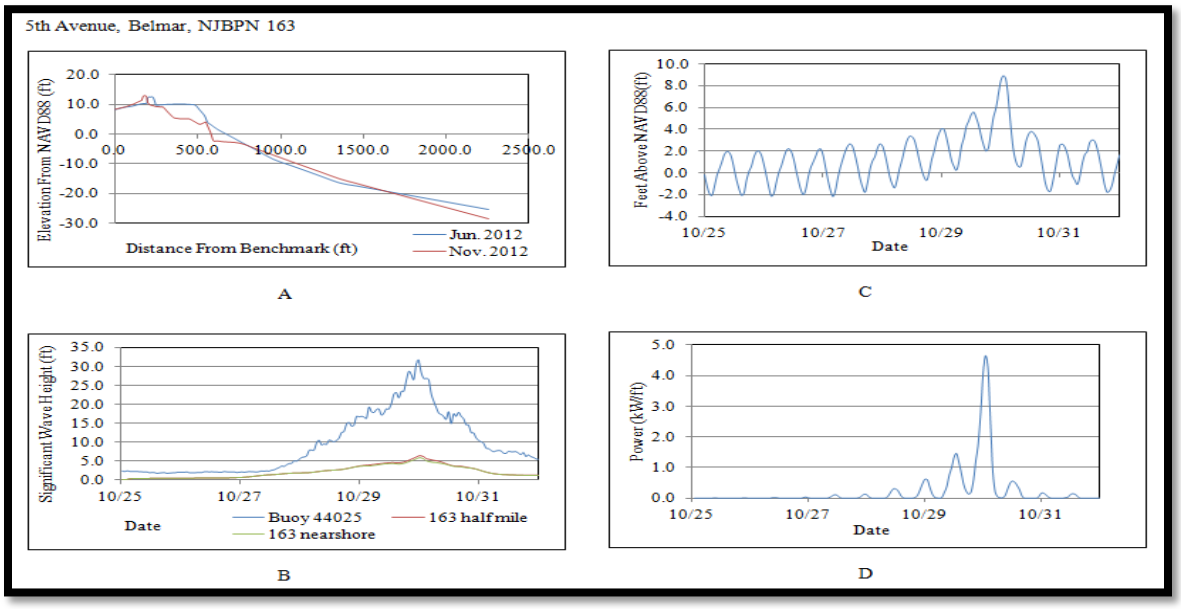

Figure A.14: NJBPN Site 163 Conditions and Results during Hurricane Sandy. A) The pre- and post-Hurricane Sandy profiles. B) Hurricane Sandy wave heights. C) Water levels at NJBPN 163. D) SSIM Results at NJBPN Site 163 during Hurricane Sandy.

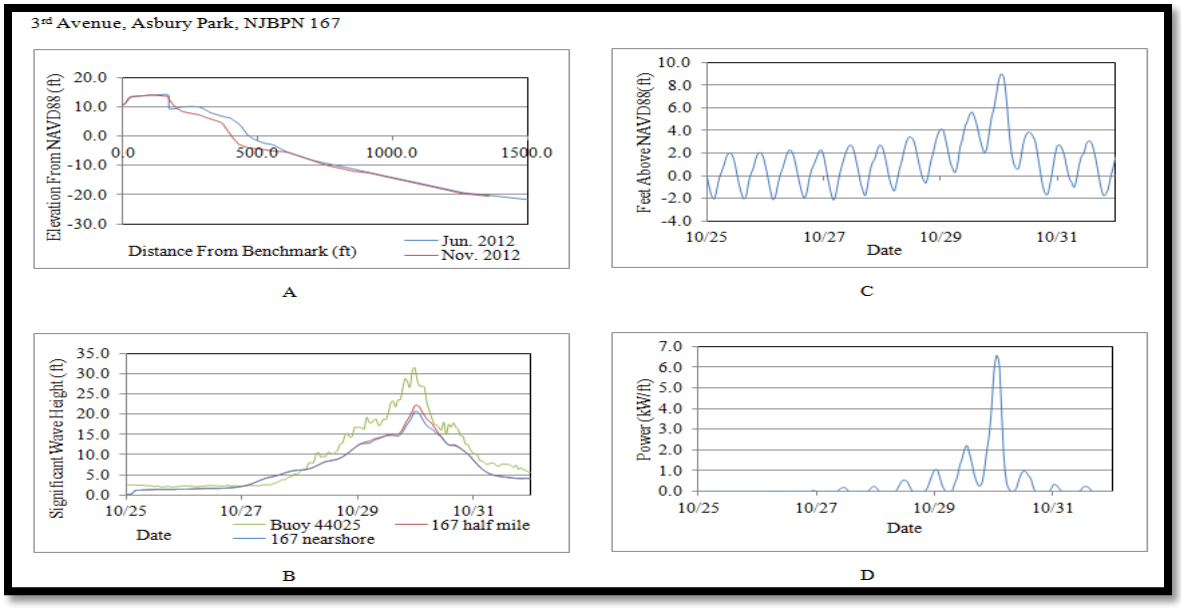

Figure A.15: NJBPN Site 167 Conditions and Results during Hurricane Sandy. A) The pre- and post-Hurricane Sandy profiles. B) Hurricane Sandy wave heights. C) Water levels at NJBPN 167. D) SSIM Results at NJBPN Site 167 during Hurricane Sandy.

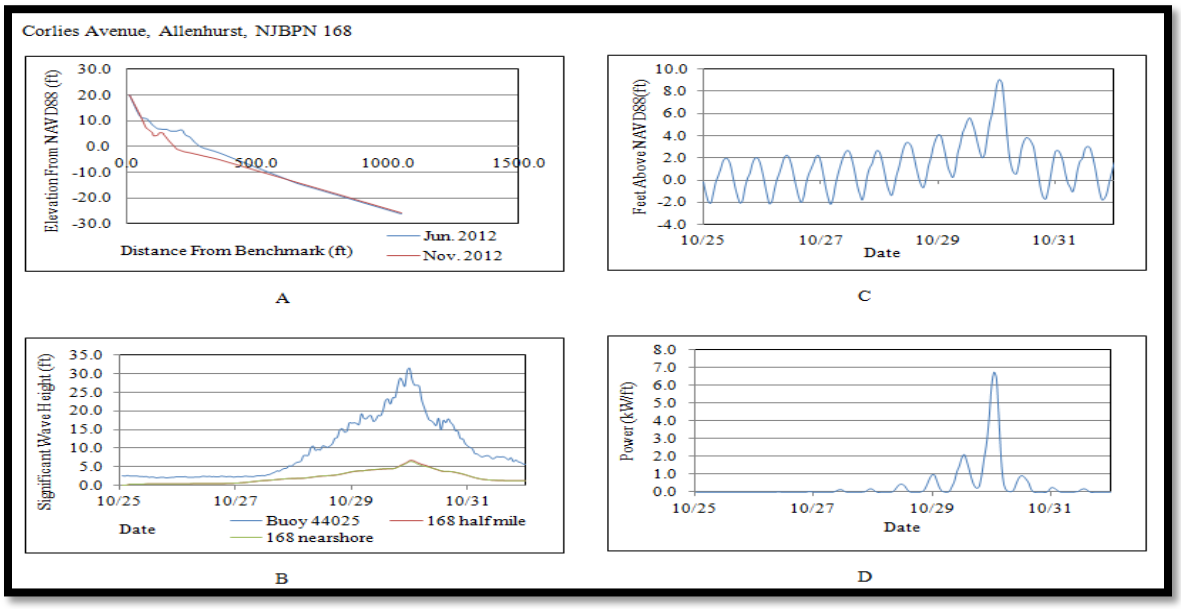

Figure A.16: NJBPN Site 168 Conditions and Results during Hurricane Sandy. A) The pre- and post-Hurricane Sandy profiles. B) Hurricane Sandy wave heights. C) Water levels at NJBPN 168. D) SSIM Results at NJBPN Site 168 during Hurricane Sandy.

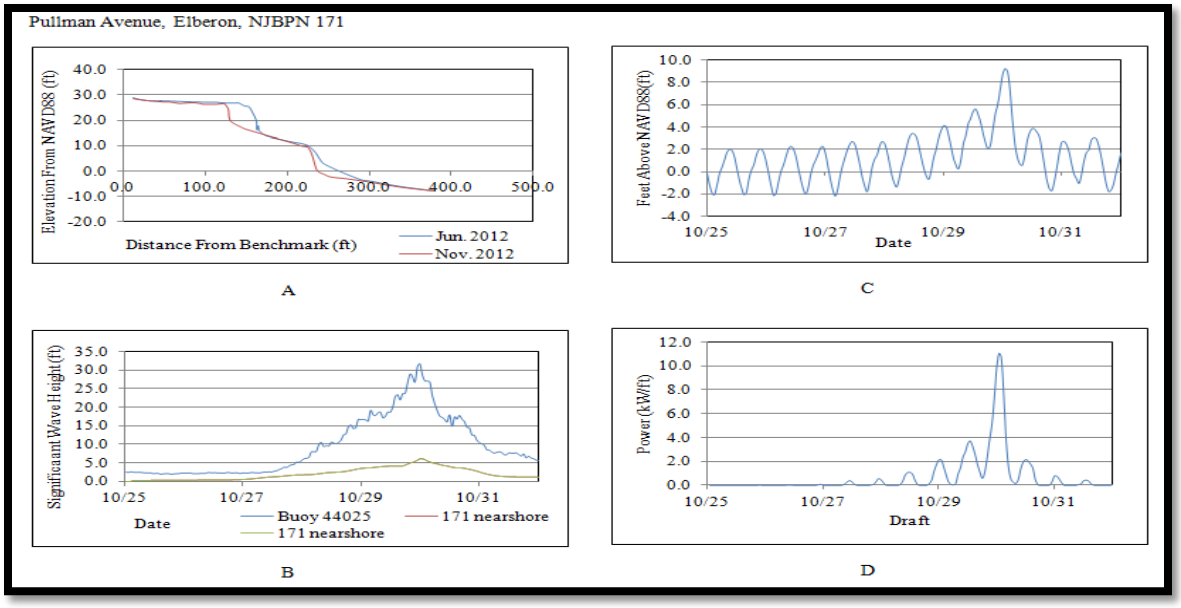

Figure A.17: NJBPN Site 171 Conditions and Results during Hurricane Sandy. A) The pre- and post-Hurricane Sandy profiles. B) Hurricane Sandy wave heights. C) Water levels at NJBPN 171. D) SSIM Results at NJBPN Site 171 during Hurricane Sandy.

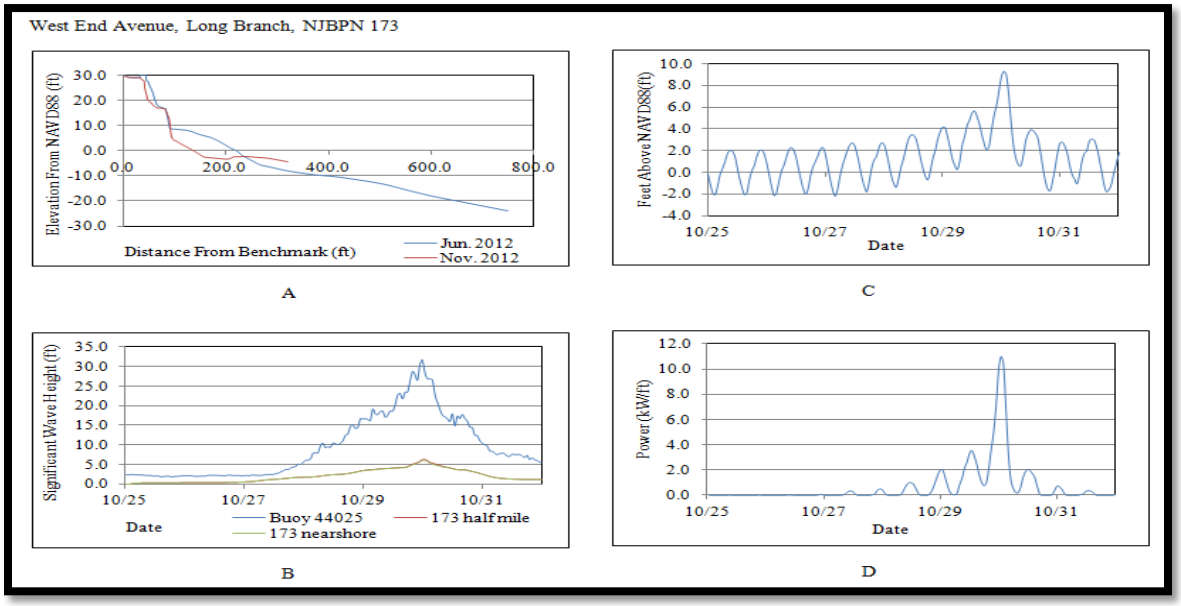

Figure A.18: NJBPN Site 173 Conditions and Results during Hurricane Sandy. A) The pre- and post-Hurricane Sandy profiles. B) Hurricane Sandy wave heights. C) Water levels at NJBPN 173. D) SSIM Results at NJBPN Site 173 during Hurricane Sandy.

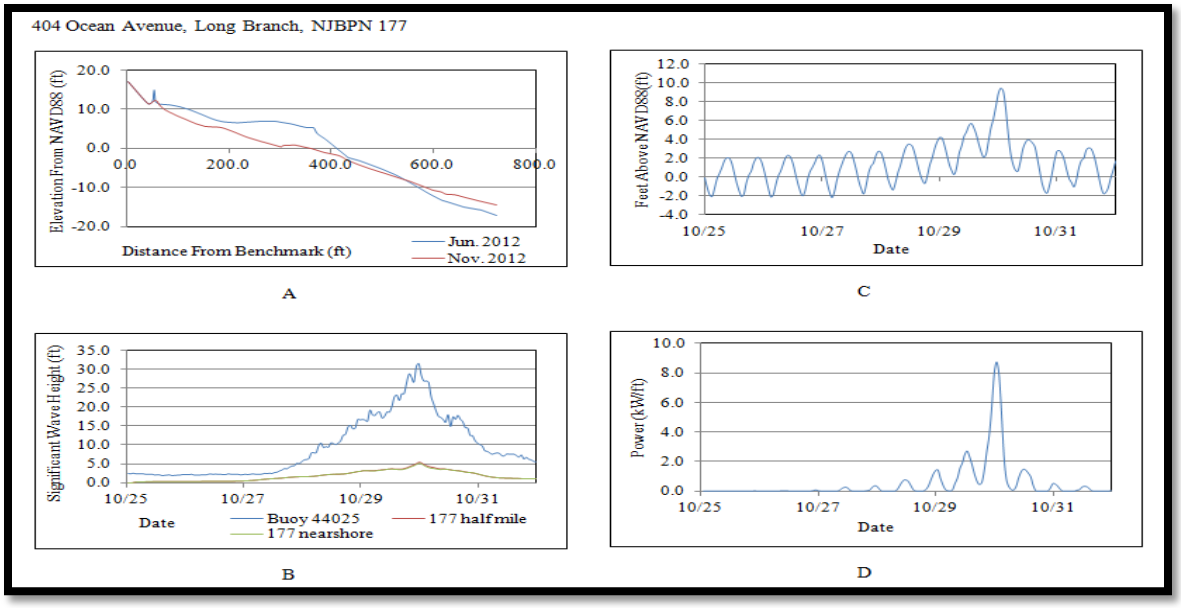

Figure A.19: NJBPN Site 177 Conditions and Results during Hurricane Sandy. A) The pre- and post-Hurricane Sandy profiles. B) Hurricane Sandy wave heights. C) Water levels at NJBPN 177. D) SSIM Results at NJBPN Site 177 during Hurricane Sandy.

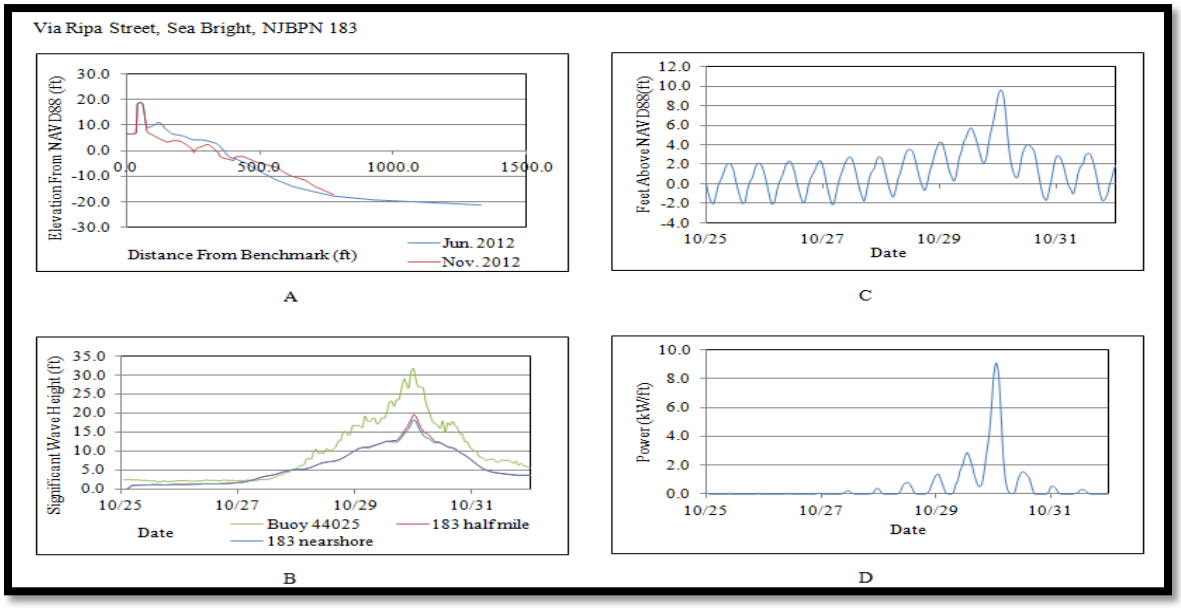

Figure A.20: NJBPN Site 183 Conditions and Results during Hurricane Sandy. A) The pre- and post-Hurricane Sandy profiles. B) Hurricane Sandy wave heights. C) Water levels at NJBPN 183. D) SSIM Results at NJBPN Site 183 during Hurricane Sandy.

.

APPENDIX B: OCEAN CITY

This appendix contains all of the individual beach profiles that were impacted during the storms that struck Ocean City, Maryland between 1990 and 2003. Some of these profiles only have a pre-storm profile and not a post-storm profile because the surveys taken at the time were not intended to measure the impact of the storms. The water levels were all taken from NOAA Station number 8557380 located in Lewes, Delaware. The wave heights were obtained from NOAA offshore buoy 44009 when available. These wave heights were plotted on the same graph as the hindcast data that were received from William Grosskopf at Offshore & Coastal Technologies, Inc. Table B.1 has a summary of the storms to strike Ocean City.

Table B.1: Ocean City Summary

Storm	Dates	# of Profiles	Locations	Distance	Wave Data	Water Level
Unknown	8/19/1990-8/24/1990	8	Ocean City, MD	-	NOAA 44009	NOAA 8557380
Hurricane Bob	8/19/1991-8/20/1991	3	Ocean City, MD	90 Miles E.	NOAA 44009	NOAA 8557380
January Nor'easter	1/3/1992-1/7/1992	3	Ocean City, MD	150 Miles W.	NOAA 44009	NOAA 8557380
Maryland Ice Storm	3/2/1994-3/5/1994	5	Ocean City, MD	80 Miles West	NOAA 44009	NOAA 8557380
Christmas Nor'easter	12/23/1994-12/27/1994	5	Ocean City, MD	30 Miles East	NOAA 44009	NOAA 8557380
N. A. Blizzard	1/7/1996-1/11/1996	10	Ocean City, MD	70 Miles N.W.	NOAA 44009	NOAA 8557380
T.S. Josephine	10/7/1996-10/11/1996	10	Ocean City, MD	80 Miles East	NOAA 44009	NOAA 8557380
El Nino Winter	1/27/1998-2/10/1998	8	Ocean City, MD	-	NOAA 44009	NOAA 8557380
Hurricane Floyd	9/15/1999-9/17/1999	10	Ocean City, MD	0 Miles	NOAA 44009	NOAA 8557380
T.S. Helene	9/24/2000-9/28/2000	10	Ocean City, MD	80 Miles East	NOAA 44009	NOAA 8557380
Hurricane Isabel	9/18/2003-9/20/2003	10	Ocean City, MD	100 Miles W.	NOAA 44009	NOAA 8557380

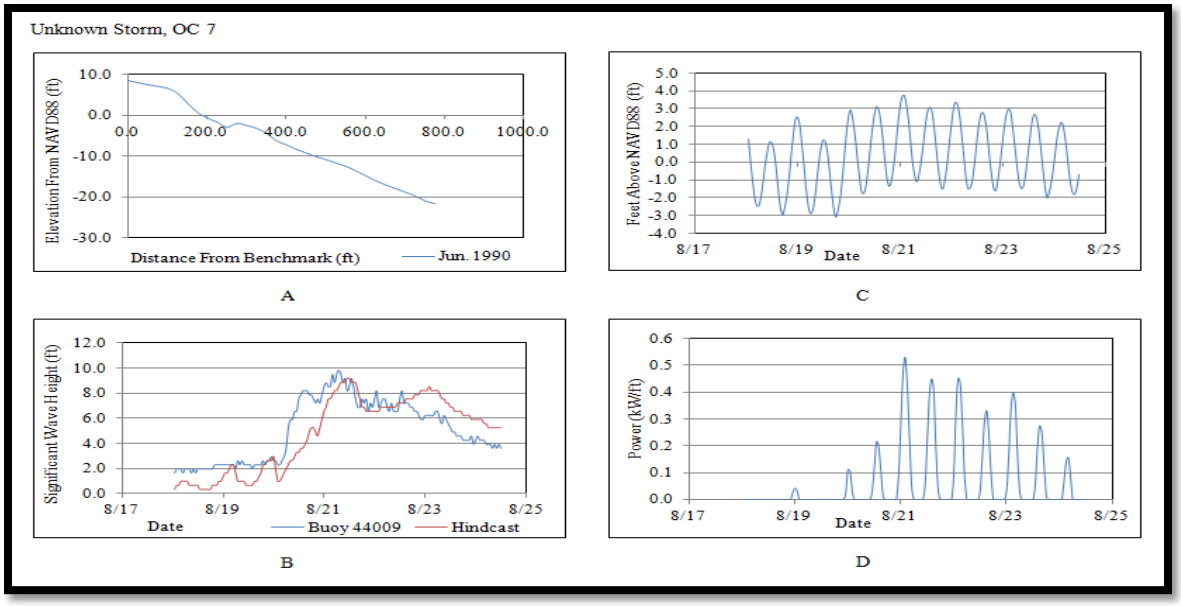

Figure B.1: OC 7 Conditions and Results during Unknown Storm. A) The pre-Unknown Storm profile. B) Unknown Storm wave heights. C) Water levels at OC 7. D) SSIM Results at OC 7 during Unknown Storm.

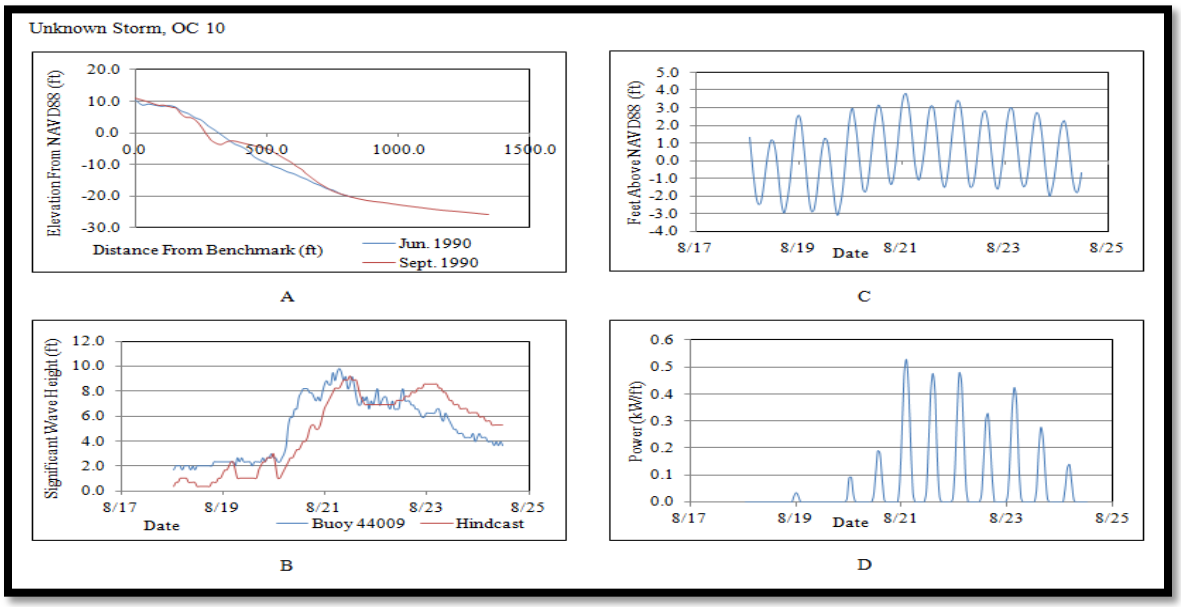

Figure B.2: OC 10 Conditions and Results during Unknown Storm. A) The pre- and post-Unknown Storm profiles. B) Unknown Storm wave heights. C) Water levels at OC 10. D) SSIM Results at OC 10 during Unknown Storm.

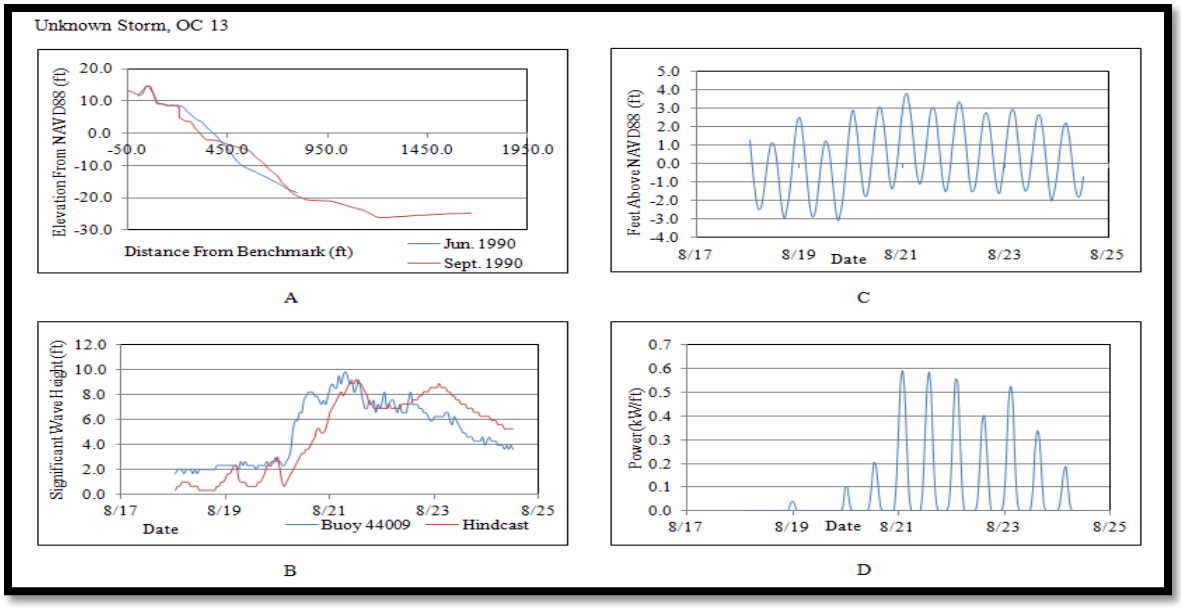

Figure B.3: OC 13 Conditions and Results during Unknown Storm. A) The pre- and post-Unknown Storm profiles. B) Unknown Storm wave heights. C) Water levels at OC 13. D) SSIM Results at OC 13 during Unknown Storm.

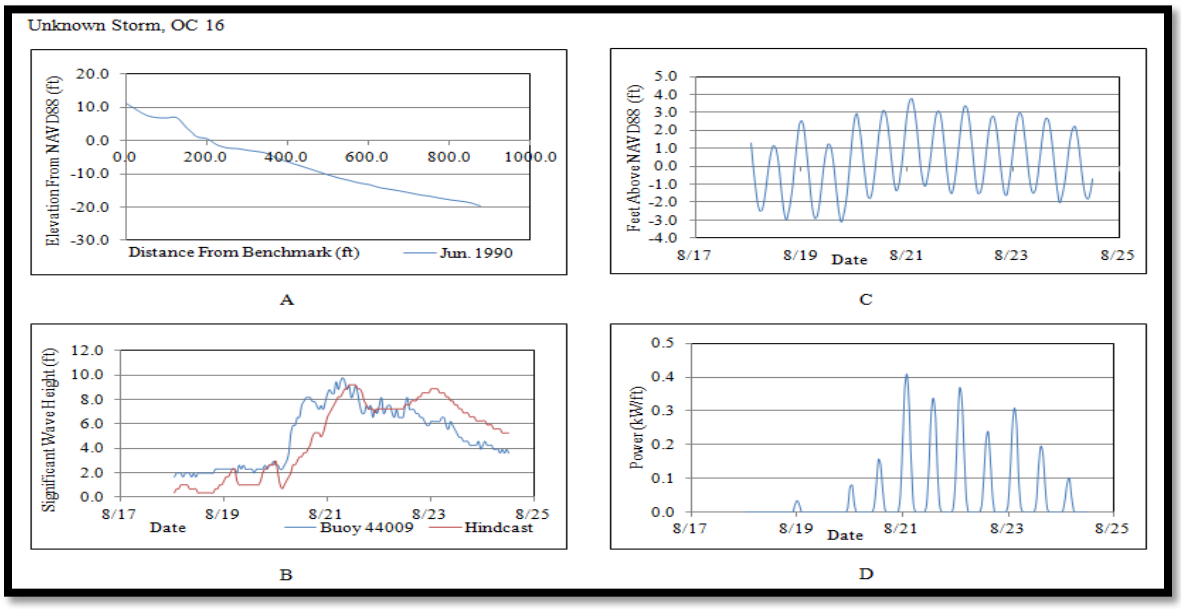

Figure B.4: OC 16 Conditions and Results during Unknown Storm. A) The pre-Unknown Storm profile. B) Unknown Storm wave heights. C) Water levels at OC 16. D) SSIM Results at OC 16 during Unknown Storm.

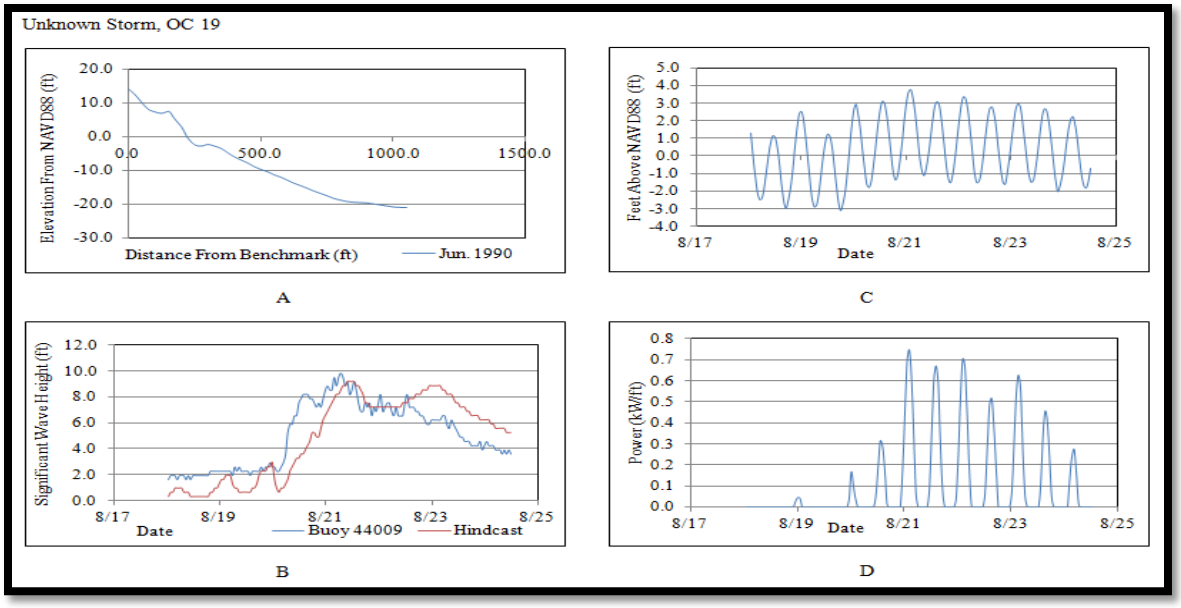

Figure B.5: OC 19 Conditions and Results during Unknown Storm. A) The pre- Unknown Storm profile. B) Unknown Storm wave heights. C) Water levels at OC 19. D) SSIM Results at OC 19 during Unknown Storm.

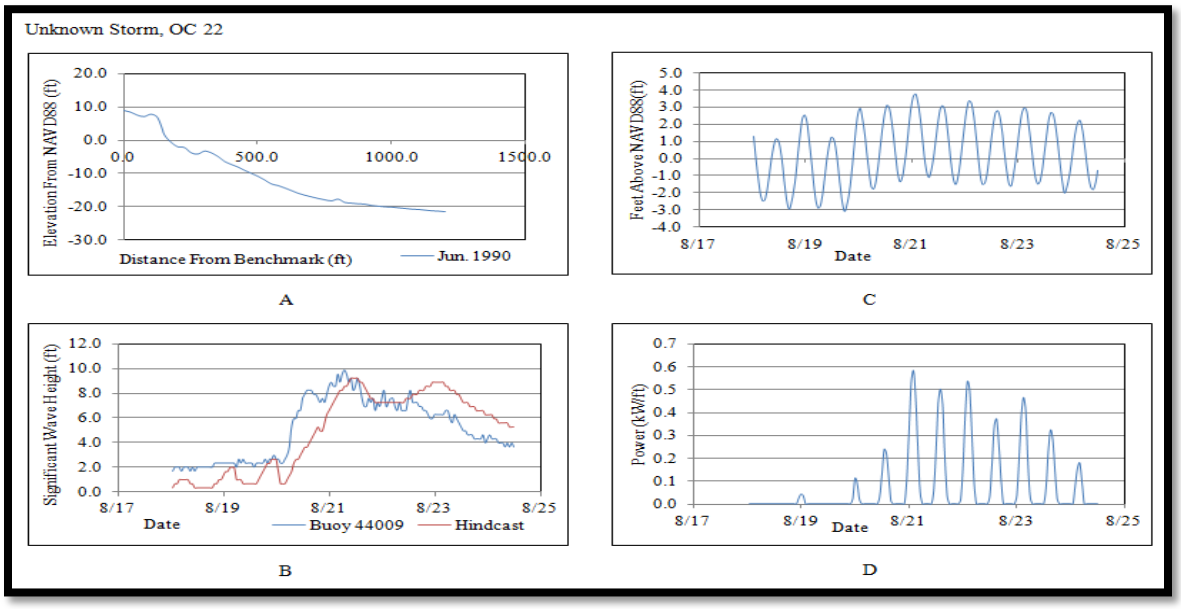

Figure B.6: OC 22 Conditions and Results during Unknown Storm. A) The pre-Unknown Storm profile. B) Unknown Storm wave heights. C) Water levels at OC 22. D) SSIM Results at OC 22 during Unknown Storm.

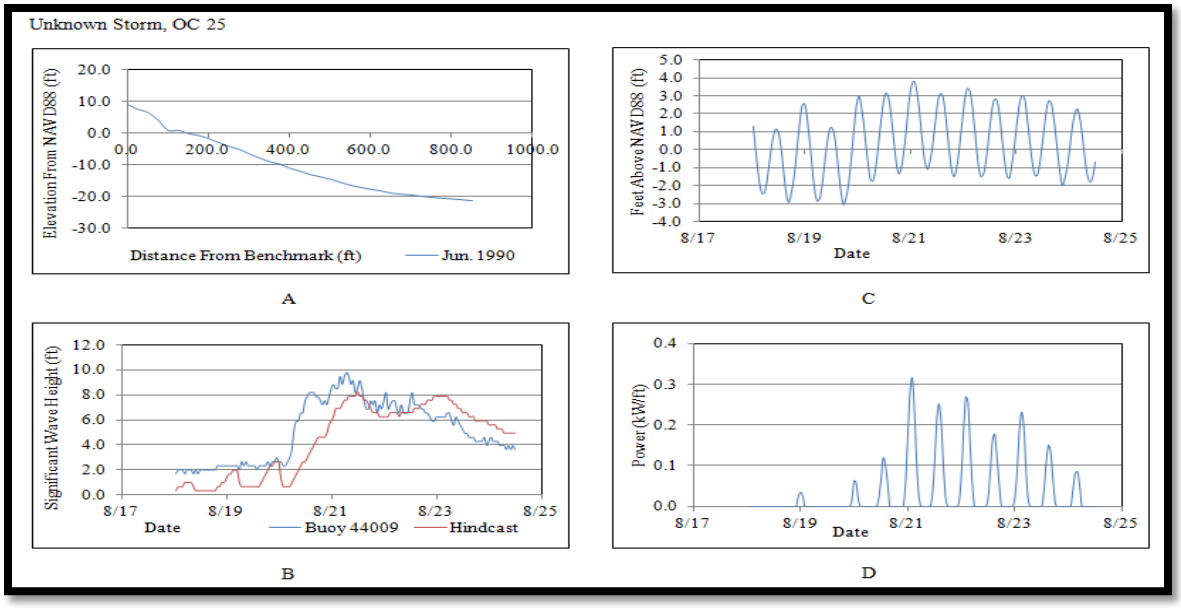

Figure B.7: OC 25 Conditions and Results during Unknown Storm. A) The pre-Unknown Storm profile. B) Unknown Storm wave heights. C) Water levels at OC 25. D) SSIM Results at OC 25 during Unknown Storm.

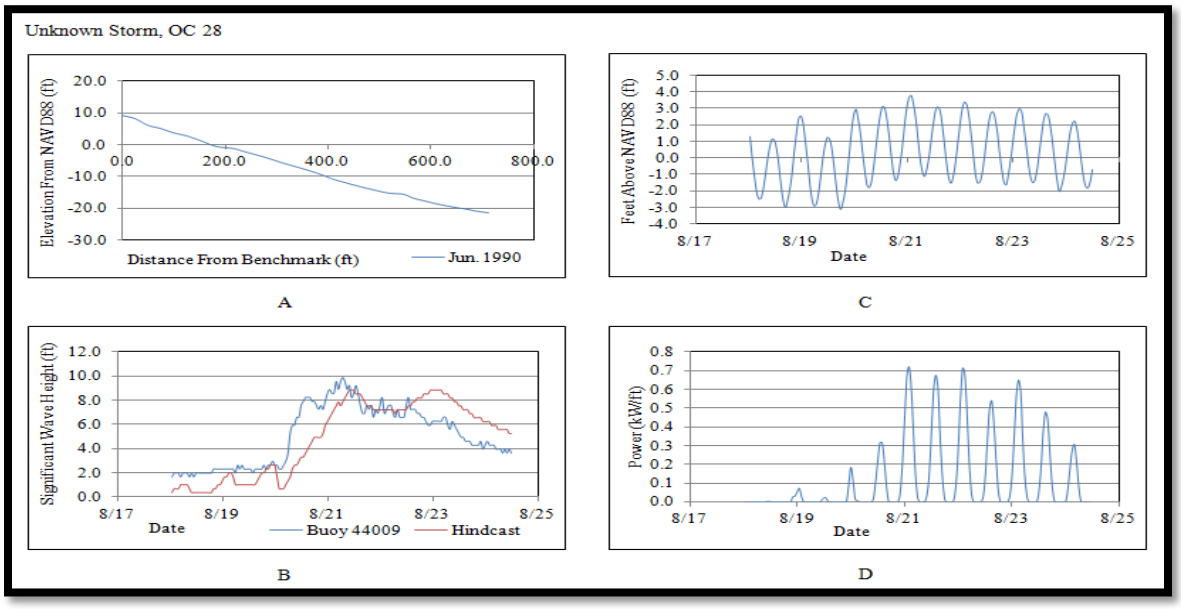

Figure B.8: OC 28 Conditions and Results during Unknown Storm. A) The pre-Unknown Storm profile. B) Unknown Storm wave heights. C) Water levels at OC 28. D) SSIM Results at OC 28 during Unknown Storm.

.

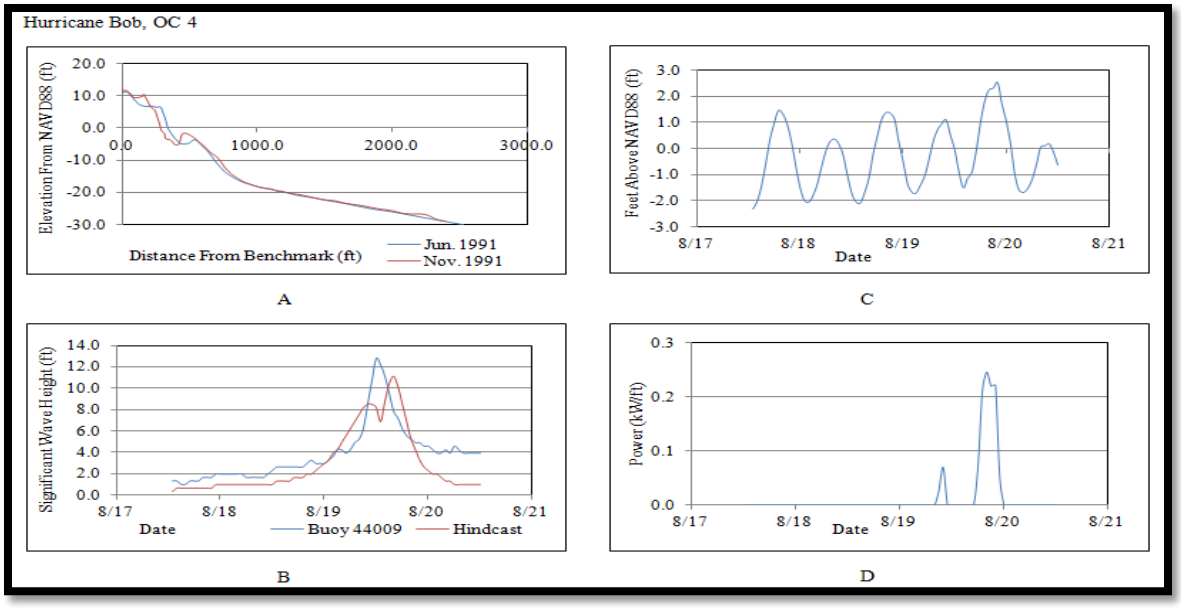

Figure B.9: OC 4 Conditions and Results during Hurricane Bob. A) The pre- and post-Hurricane Bob profiles. B) Hurricane Bob wave heights. C) Water levels at OC 4. D) SSIM Results at OC 4 during Hurricane Bob.

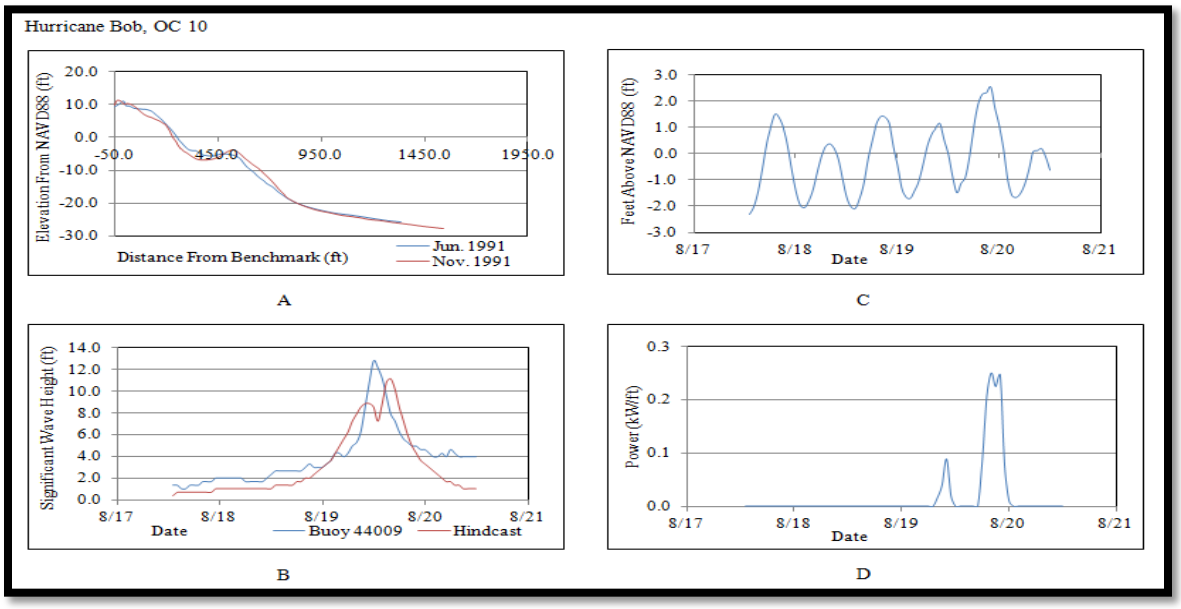

Figure B.10: OC 10 Conditions and Results during Hurricane Bob. A) The pre- and post-Hurricane Bob profiles. B) Hurricane Bob wave heights. C) Water levels at OC 10. D) SSIM Results at OC 10 during Hurricane Bob.

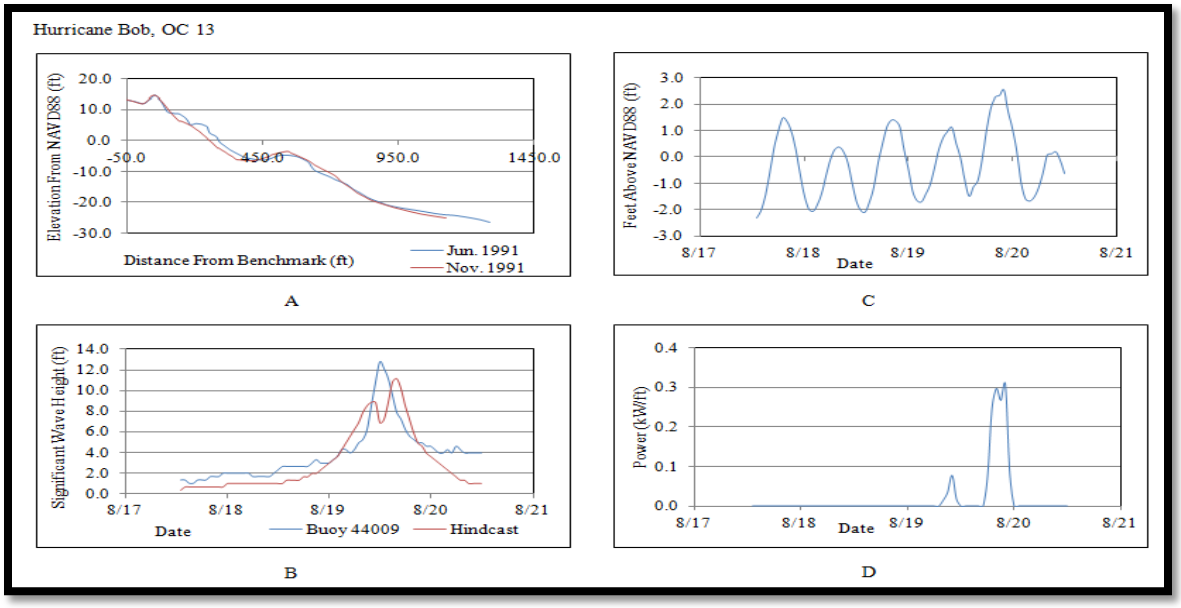

Figure B.11: OC 13 Conditions and Results during Hurricane Bob. A) The pre- and post-Hurricane Bob profiles. B) Hurricane Bob wave heights. C) Water levels at OC 13. D) SSIM Results at OC 13 during Hurricane Bob.

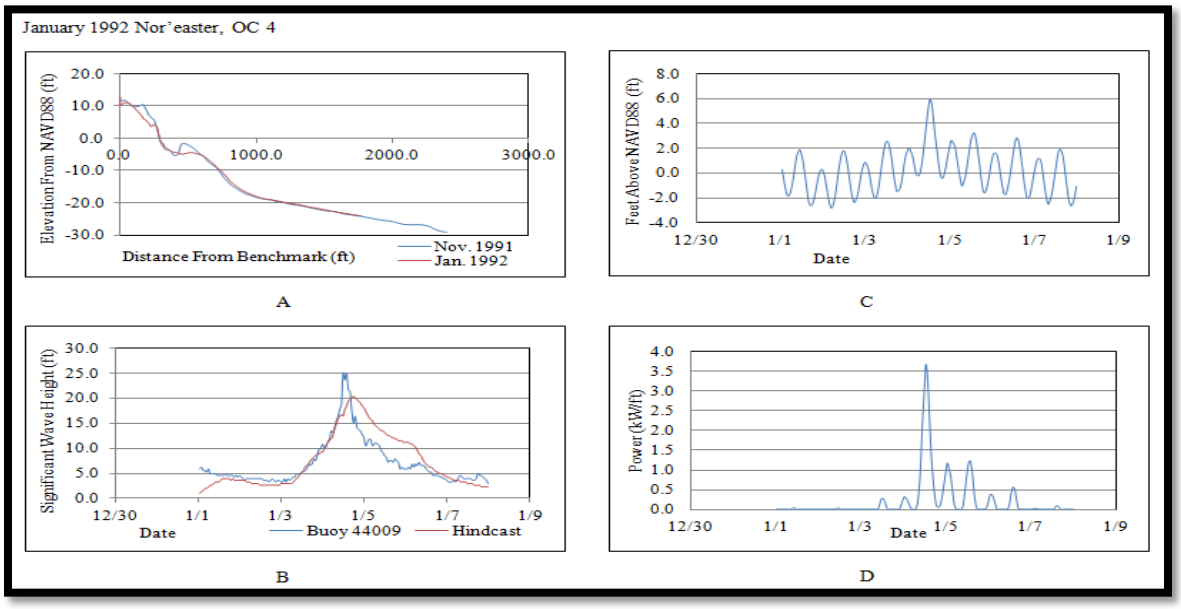

Figure B.12: OC 4 Conditions and Results during January 1992 Nor'easter. A) The pre- and post-January 1992 Nor'easter profiles. B) January 1992 Nor'easter wave heights. C) Water levels at OC 4. D) SSIM Results at OC 4 during January 1992 Nor'easter.

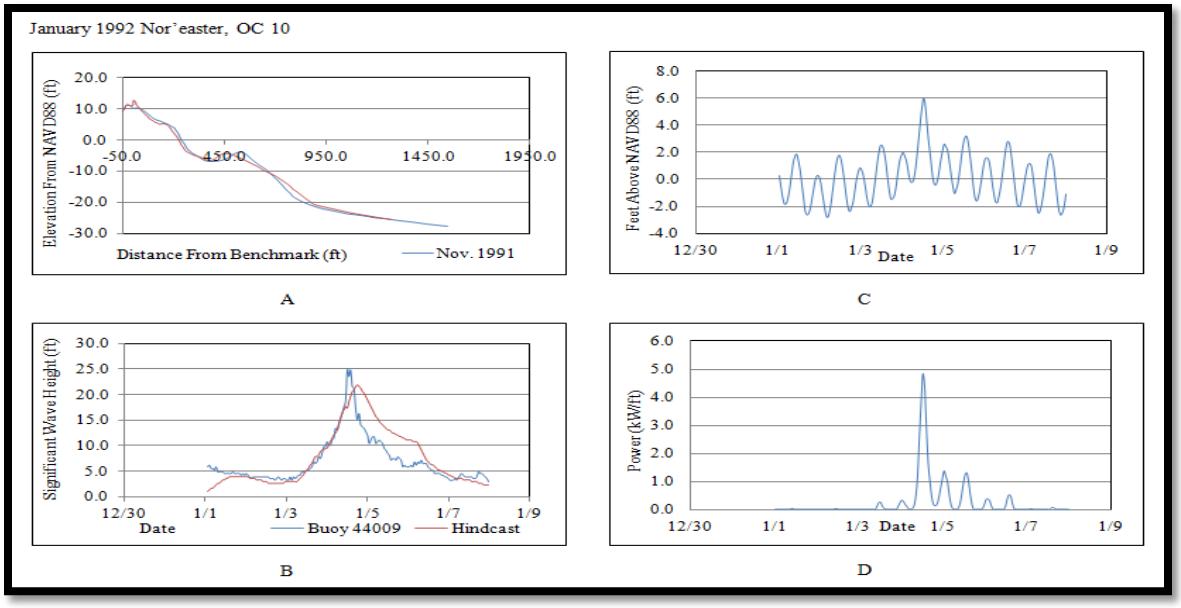

Figure B.13: OC 10 Conditions and Results during January 1992 Nor'easter. A) The pre- and post-January 1992 Nor'easter profiles. B) January 1992 Nor'easter wave heights. C) Water levels at OC 10. D) SSIM Results at OC 10 during January 1992 Nor'easter.

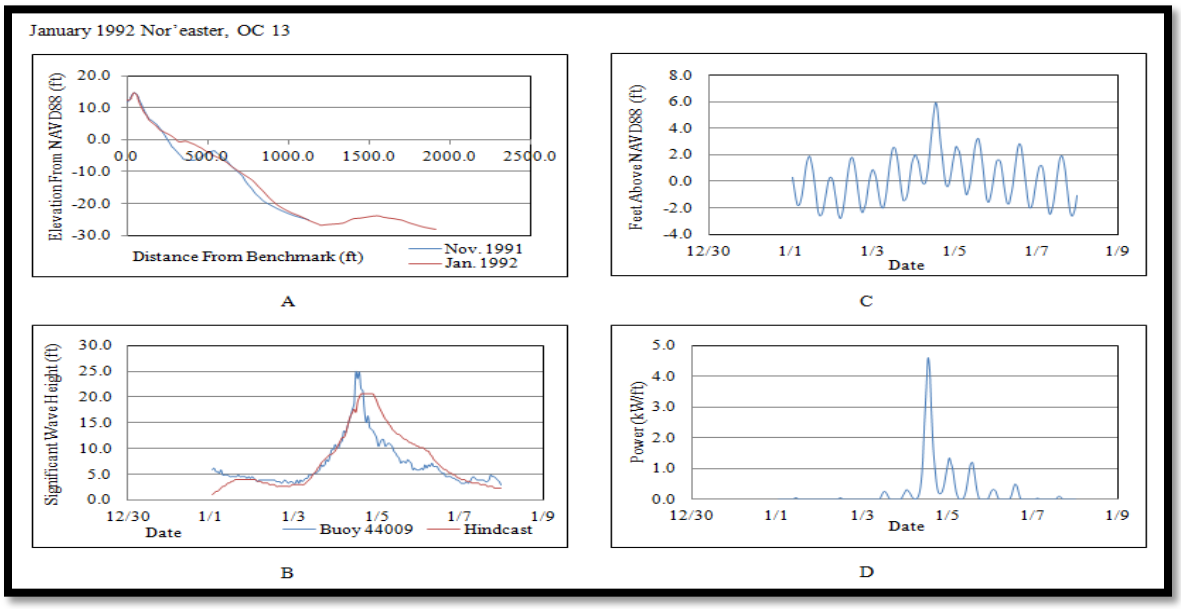

Figure B.14: OC 13 Conditions and Results during January 1992 Nor'easter. A) The pre- and post-January 1992 Nor'easter profiles. B) January 1992 Nor'easter wave heights. C) Water levels at OC 13. D) SSIM Results at OC 13 during January 1992 Nor'easter.

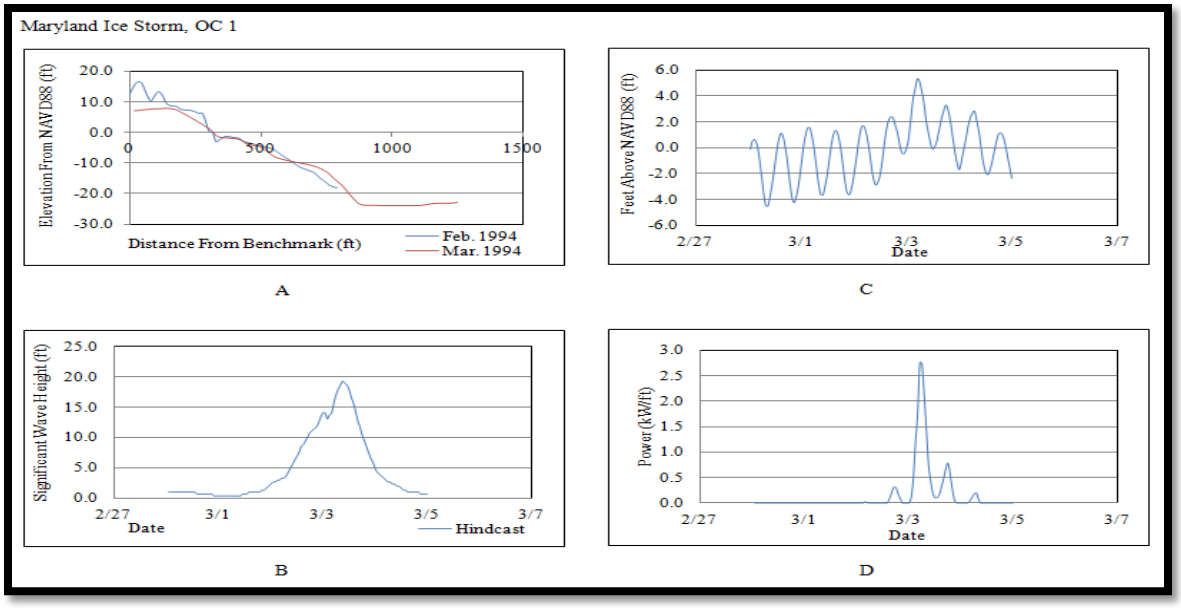

Figure B.15: OC 1 Conditions and Results during Maryland Ice Storm. A) The pre- and post-Maryland Ice Storm profiles. B) Maryland Ice Storm wave heights. C) Water levels at OC 1. D) SSIM Results at OC 1 during Maryland Ice Storm.

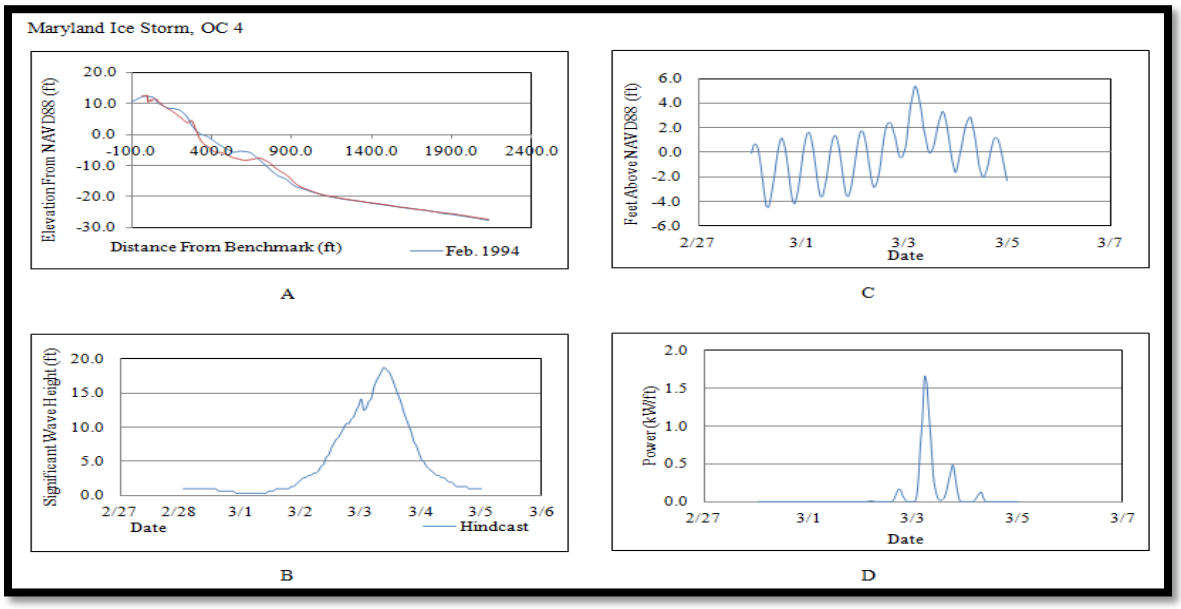

Figure B.16: OC 4 Conditions and Results during Maryland Ice Storm. A) The pre- and post-Maryland Ice Storm profiles. B) Maryland Ice Storm wave heights. C) Water levels at OC 4. D) SSIM Results at OC 4 during Maryland Ice Storm.

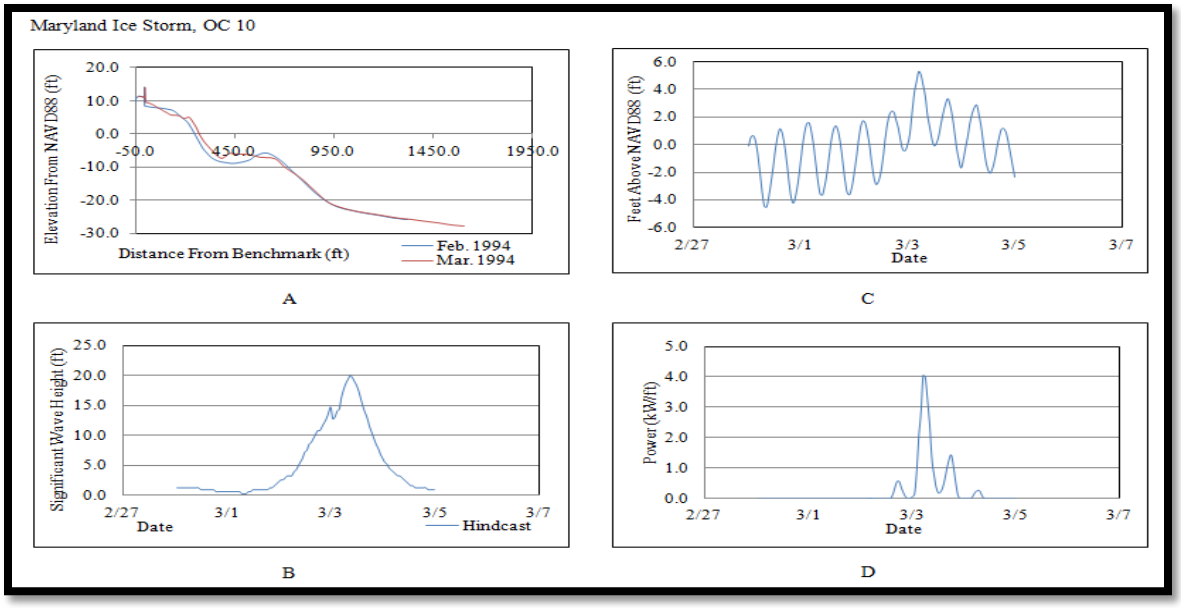

Figure B.17: OC 10 Conditions and Results during Maryland Ice Storm. A) The pre- and post-Maryland Ice Storm profiles. B) Maryland Ice Storm wave heights. C) Water levels at OC 10. D) SSIM Results at OC 10 during Maryland Ice Storm.

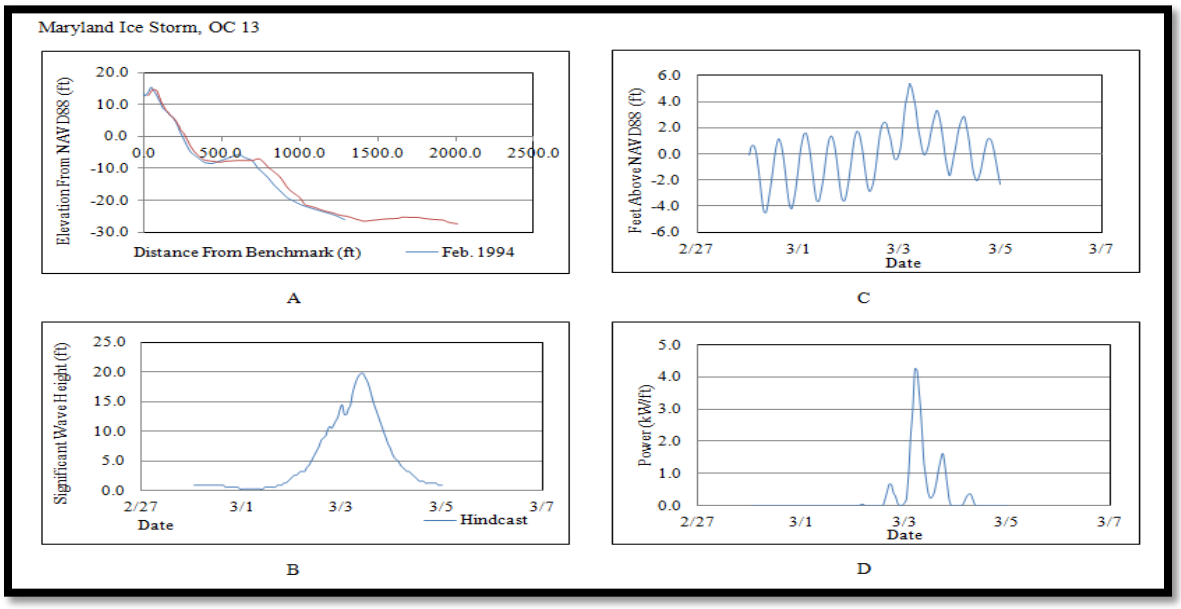

Figure B.18: OC 13 Conditions and Results during Maryland Ice Storm. A) The pre- and post-Maryland Ice Storm profiles. B) Maryland Ice Storm wave heights. C) Water levels at OC 13. D) SSIM Results at OC 13 during Maryland Ice Storm.

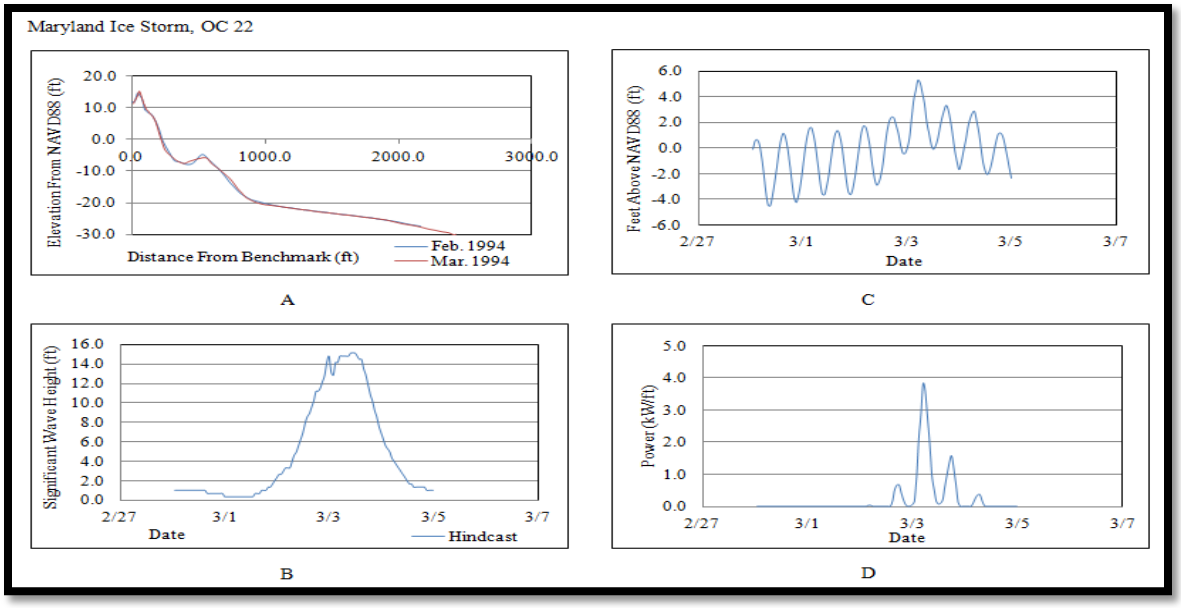

Figure B.19: OC 22 Conditions and Results during Maryland Ice Storm. A) The pre- and post-Maryland Ice Storm profiles. B) Maryland Ice Storm wave heights. C) Water levels at OC 22. D) SSIM Results at OC 22 during Maryland Ice Storm.

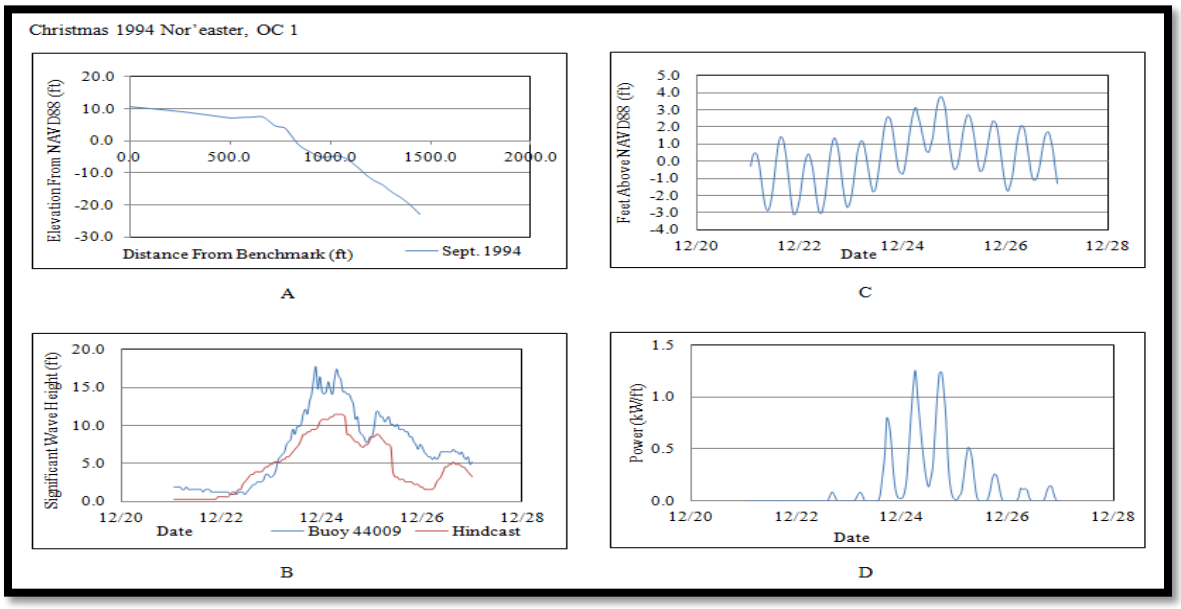

Figure B.20: OC 1 Conditions and Results during Christmas 1994 Nor'easter. A) The pre-Christmas 1994 Nor'easter profile. B) Christmas 1994 Nor'easter wave heights. C) Water levels at OC 1. D) SSIM Results at OC 1 during Christmas 1994 Nor'easter.

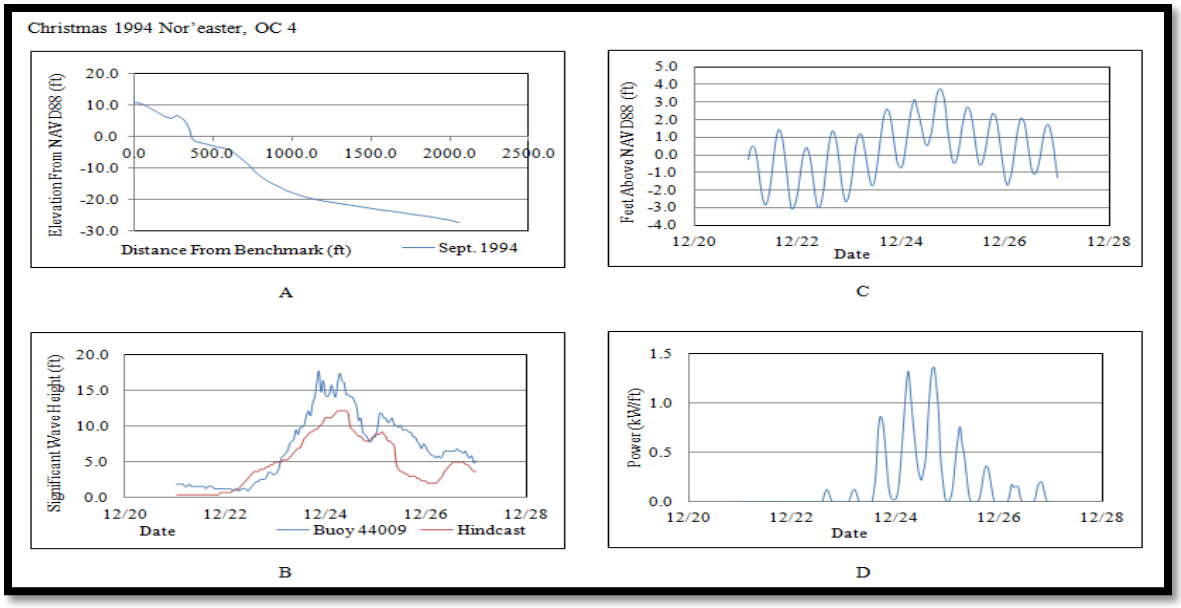

Figure B.21: OC 4 Conditions and Results during Christmas 1994 Nor'easter. A) The pre-Christmas 1994 Nor'easter profile. B) Christmas 1994 Nor'easter wave heights. C) Water levels at OC 4. D) SSIM Results at OC 4 during Christmas 1994 Nor'easter.

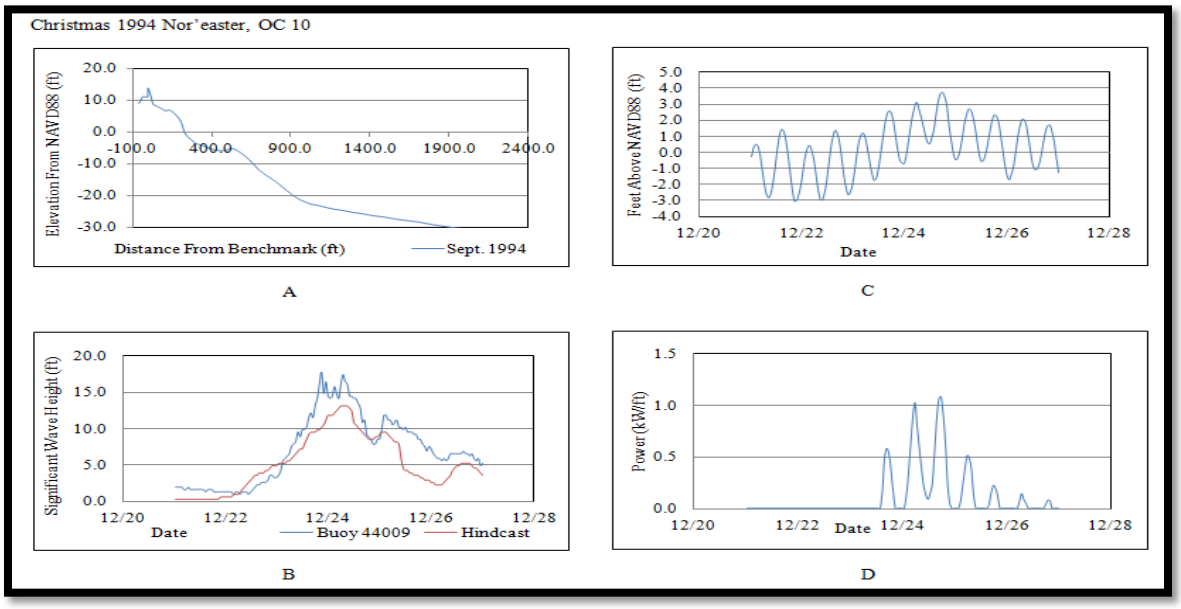

Figure B.22: OC 10 Conditions and Results during Christmas 1994 Nor'easter. A) The pre-Christmas 1994 Nor'easter profile. B) Christmas 1994 Nor'easter wave heights. C) Water levels at OC 10. D) SSIM Results at OC 10 during Christmas 1994 Nor'easter.

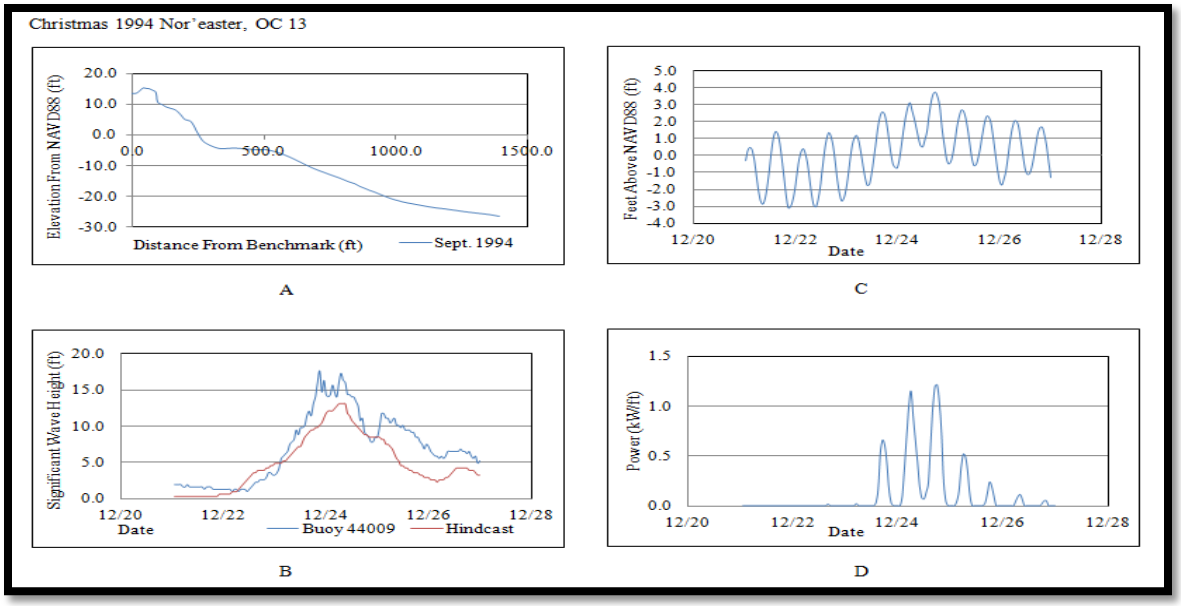

Figure B.23: OC 13 Conditions and Results during Christmas 1994 Nor'easter. A) The pre-Christmas 1994 Nor'easter profile. B) Christmas 1994 Nor'easter wave heights. C) Water levels at OC 13. D) SSIM Results at OC 13 during Christmas 1994 Nor'easter.

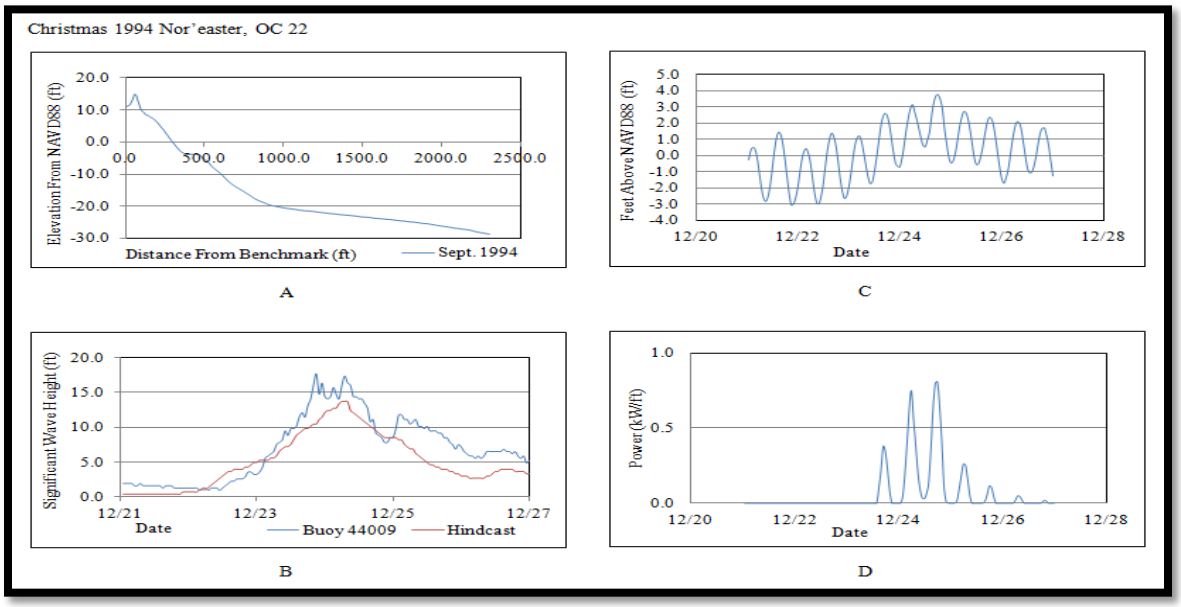

Figure B.24: OC 22 Conditions and Results during Christmas 1994 Nor'easter. A) The pre-Christmas 1994 Nor'easter profile. B) Christmas 1994 Nor'easter wave heights. C) Water levels at OC 22. D) SSIM Results at OC 22 during Christmas 1994 Nor'easter.

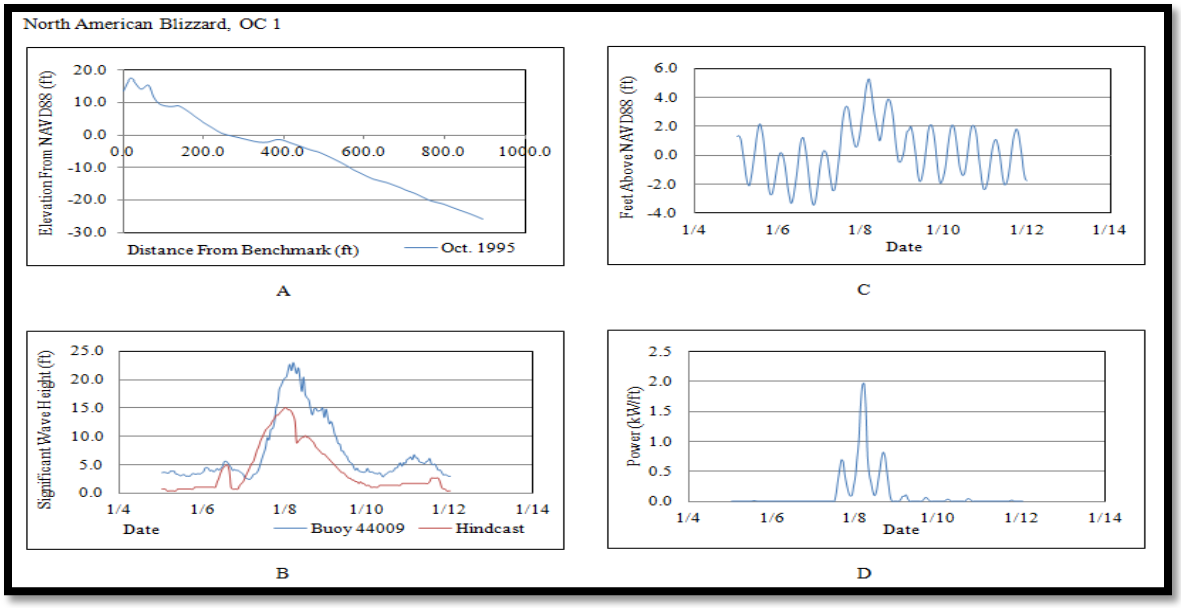

Figure B.25: OC 1 Conditions and Results during North American Blizzard. A) The pre-North American Blizzard profile. B) North American Blizzard wave heights. C) Water levels at OC 1. D) SSIM Results at OC 1 during North American Blizzard.

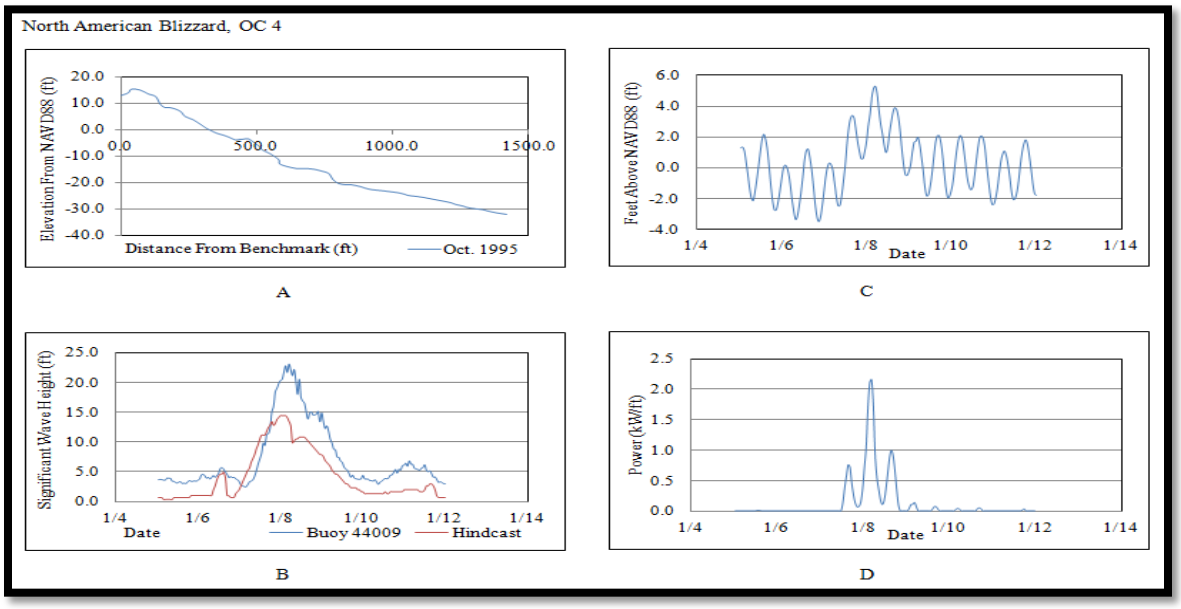

Figure B.26: OC 4 Conditions and Results during North American Blizzard. A) The pre-North American Blizzard profile. B) North American Blizzard wave heights. C) Water levels at OC 4. D) SSIM Results at OC 4 during North American Blizzard.

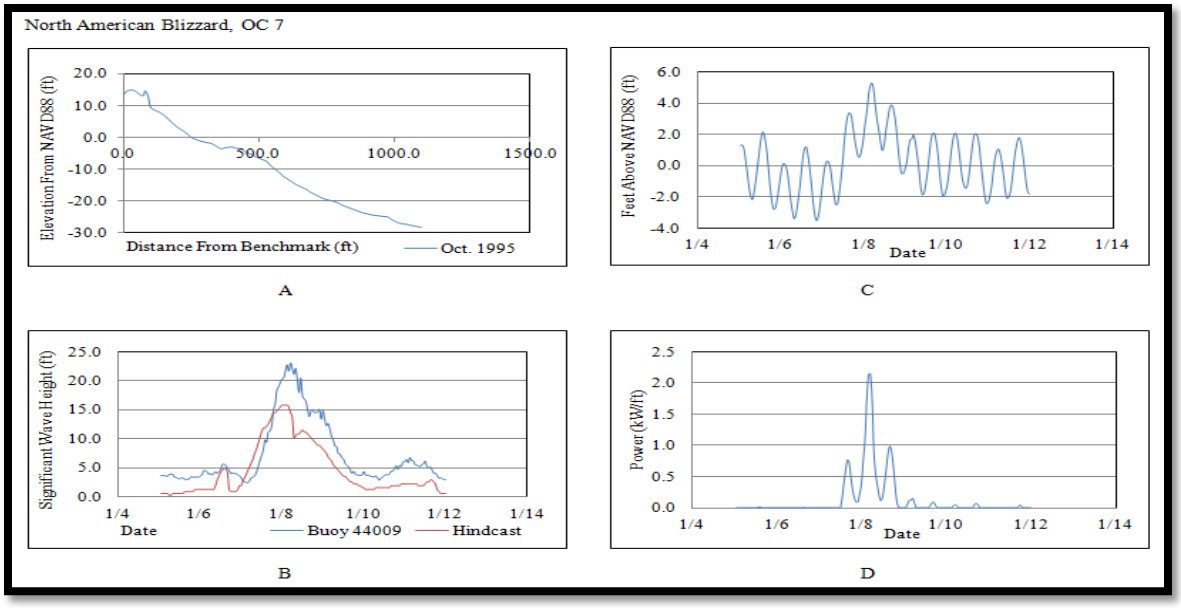

Figure B.27: OC 7 Conditions and Results during North American Blizzard. A) The pre-North American Blizzard profile. B) North American Blizzard wave heights. C) Water levels at OC 7. D) SSIM Results at OC 7 during North American Blizzard.

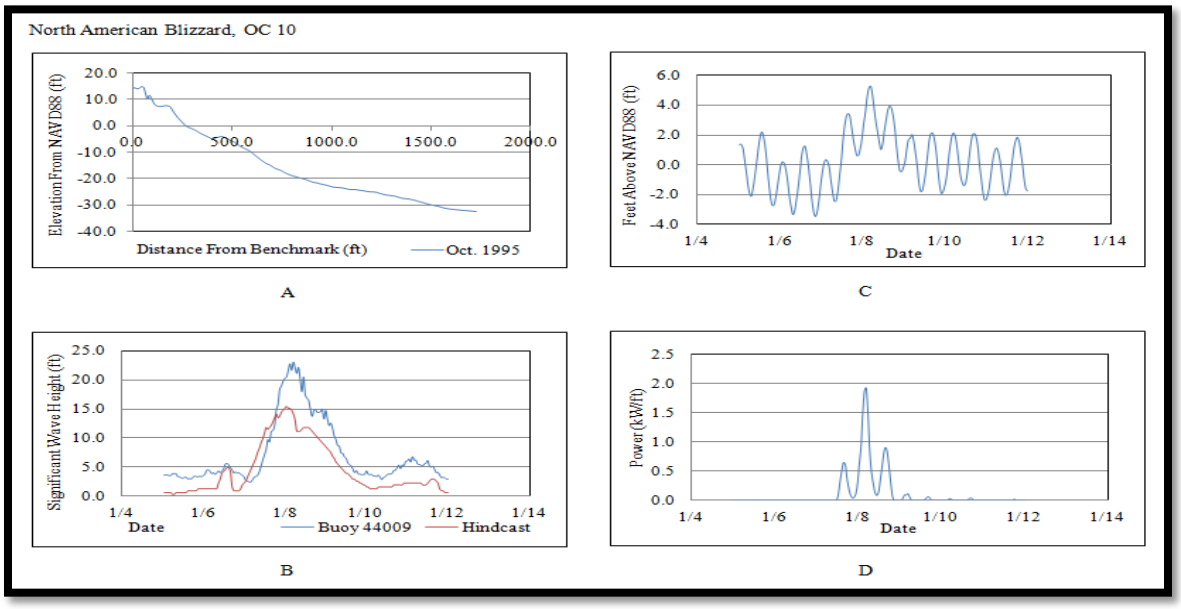

Figure B.28: OC 10 Conditions and Results during North American Blizzard. A) The pre-North American Blizzard profile. B) North American Blizzard wave heights. C) Water levels at OC 10. D) SSIM Results at OC 10 during North American Blizzard.

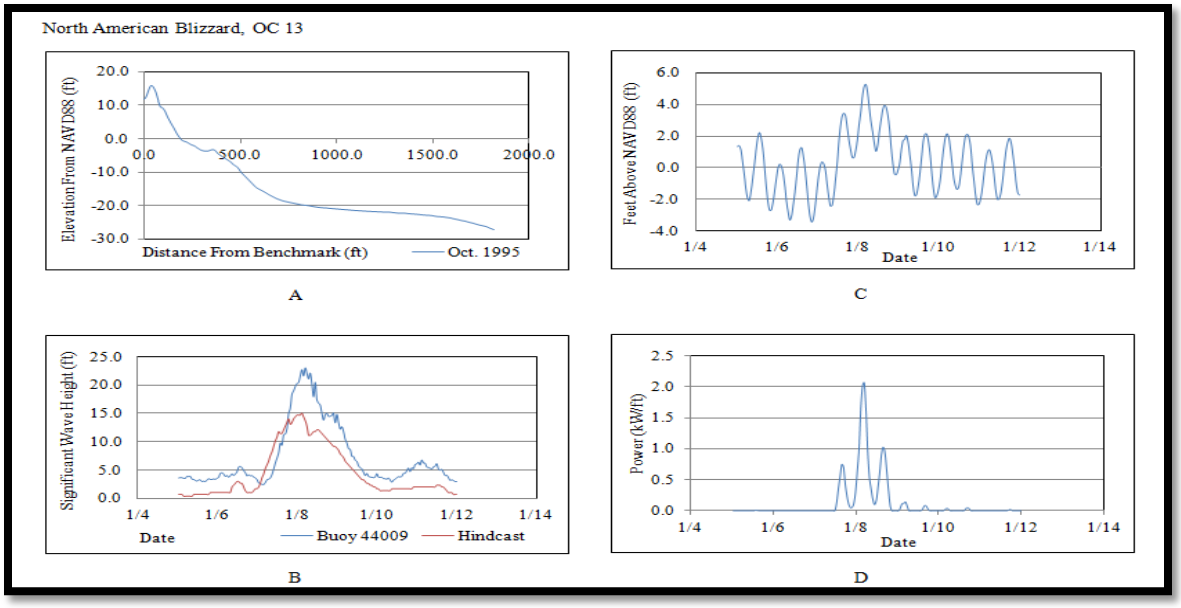

Figure B.29: OC 13 Conditions and Results during North American Blizzard. A) The pre-North American Blizzard profile. B) North American Blizzard wave heights. C) Water levels at OC 13. D) SSIM Results at OC 13 during North American Blizzard.

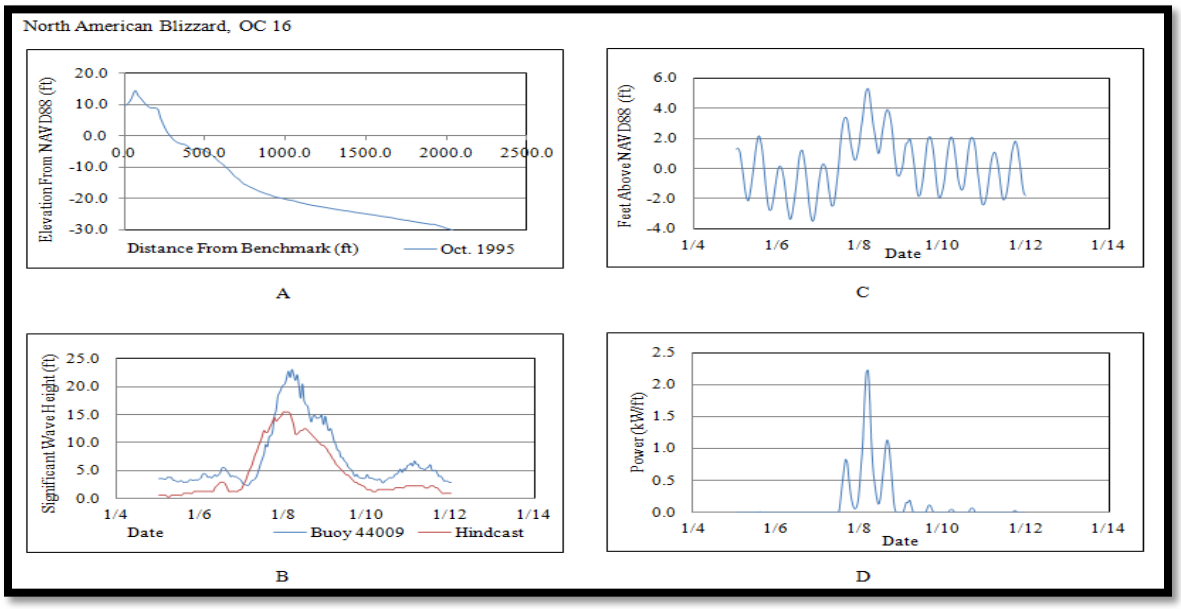

Figure B.30: OC 16 Conditions and Results during North American Blizzard. A) The pre-North American Blizzard profile. B) North American Blizzard wave heights. C) Water levels at OC 16. D) SSIM Results at OC 16 during North American Blizzard.

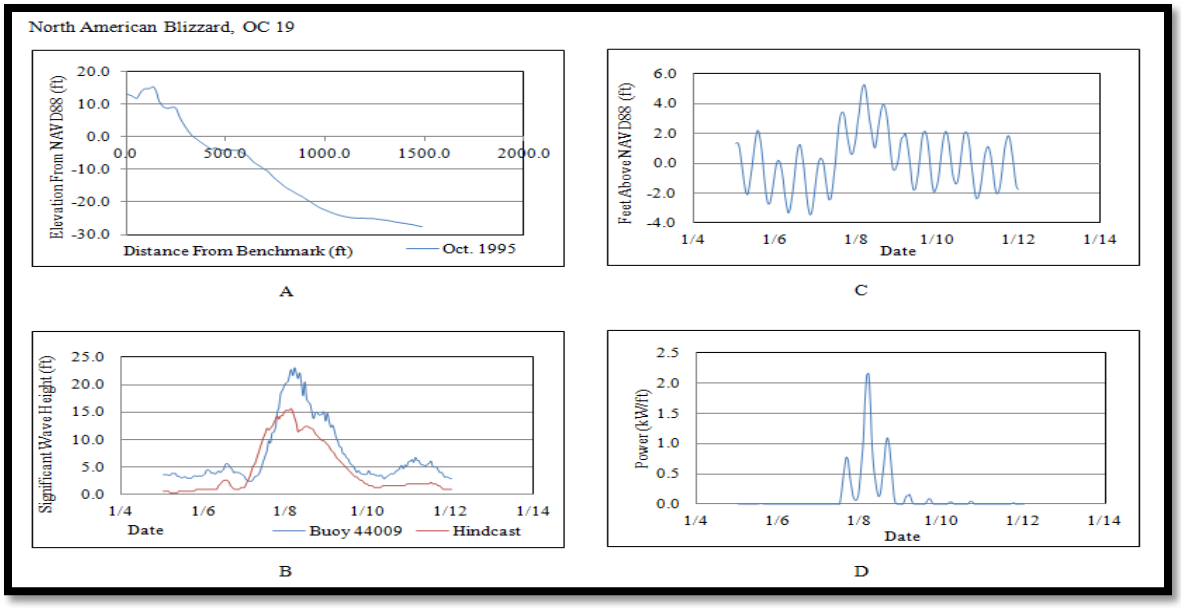

Figure B.31: OC 19 Conditions and Results during North American Blizzard. A) The pre-North American Blizzard profile. B) North American Blizzard wave heights. C) Water levels at OC 19. D) SSIM Results at OC 19 during North American Blizzard.

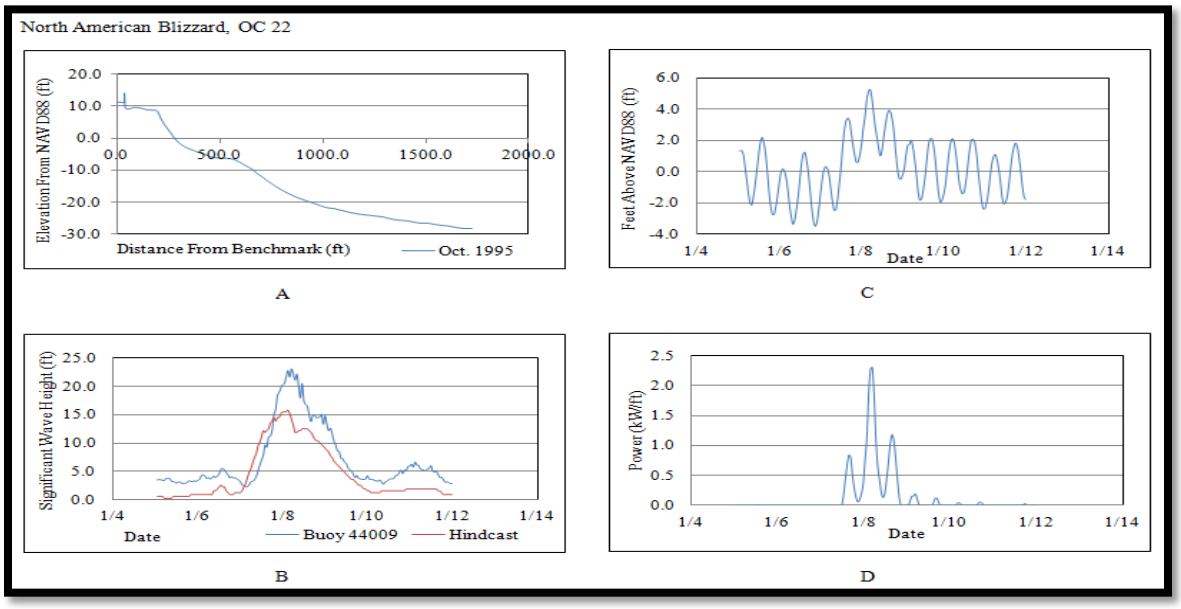

Figure B.32: OC 22 Conditions and Results during North American Blizzard. A) The pre-North American Blizzard profile. B) North American Blizzard wave heights. C) Water levels at OC 22. D) SSIM Results at OC 22 during North American Blizzard.

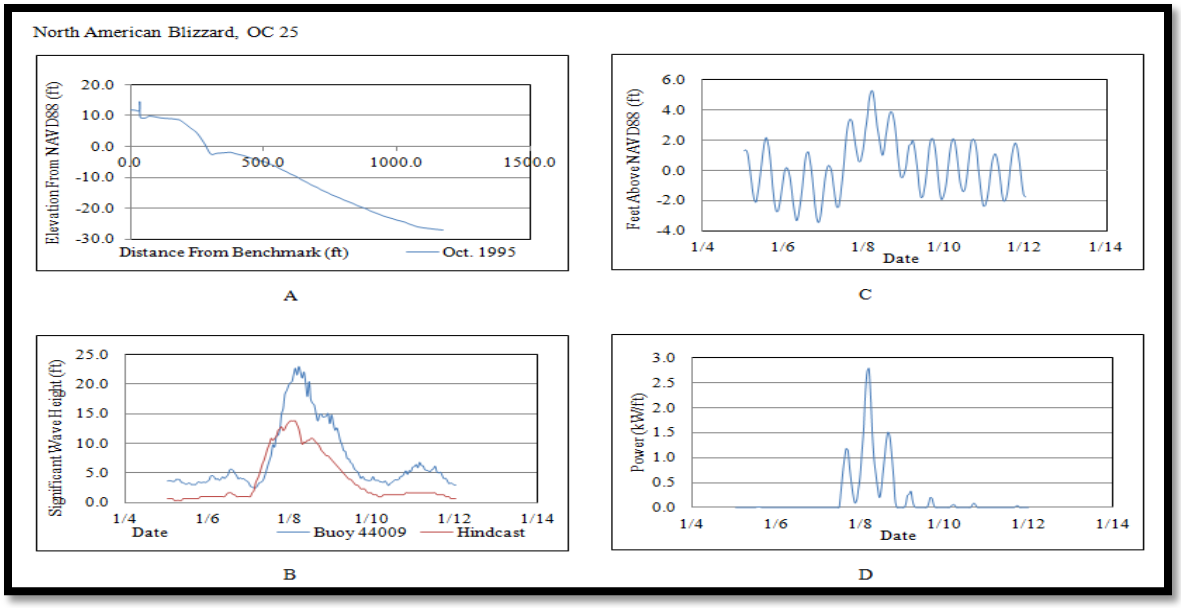

Figure B.33: OC 25 Conditions and Results during North American Blizzard. A) The pre-North American Blizzard profile. B) North American Blizzard wave heights. C) Water levels at OC 25. D) SSIM Results at OC 25 during North American Blizzard.

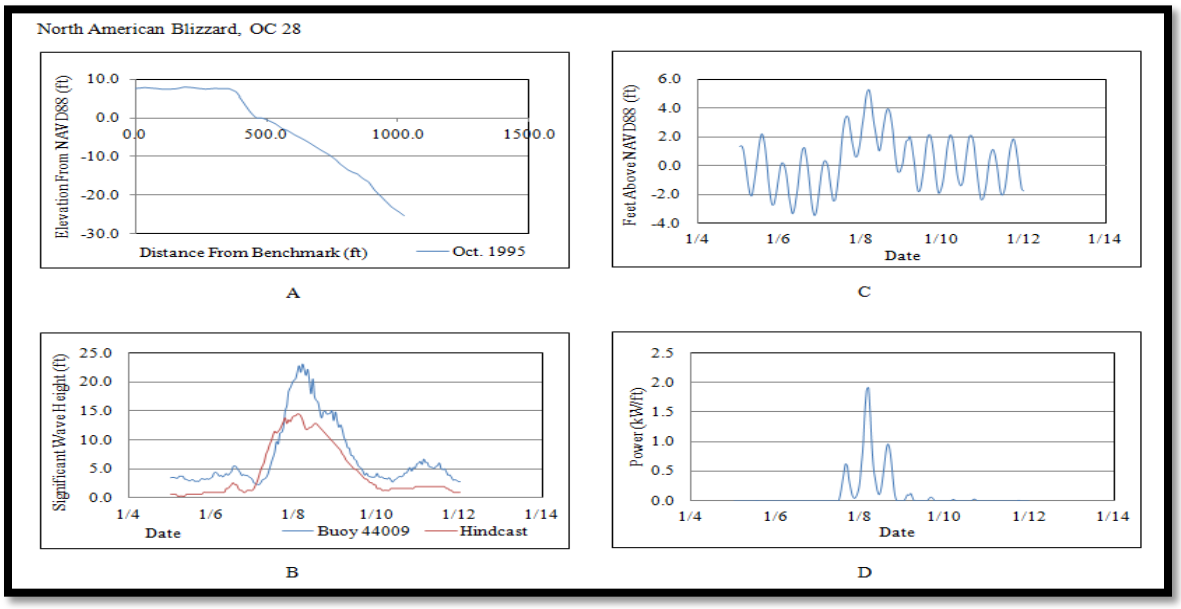

Figure B.34: OC 28 Conditions and Results during North American Blizzard. A) The pre-North American Blizzard profile. B) North American Blizzard wave heights. C) Water levels at OC 28. D) SSIM Results at OC 28 during North American Blizzard.

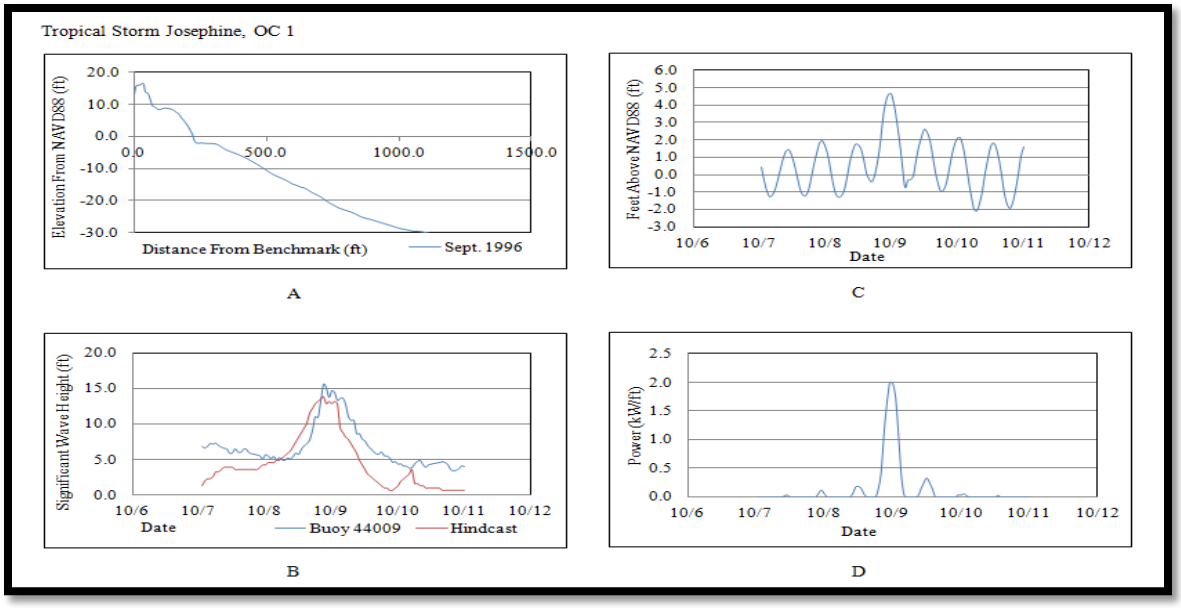

Figure B.35: OC 1 Conditions and Results during Tropical Storm Josephine. A) The pre-Tropical Storm Josephine profile. B) Tropical Storm Josephine wave heights. C) Water levels at OC 1. D) SSIM Results at OC 1 during Tropical Storm Josephine.

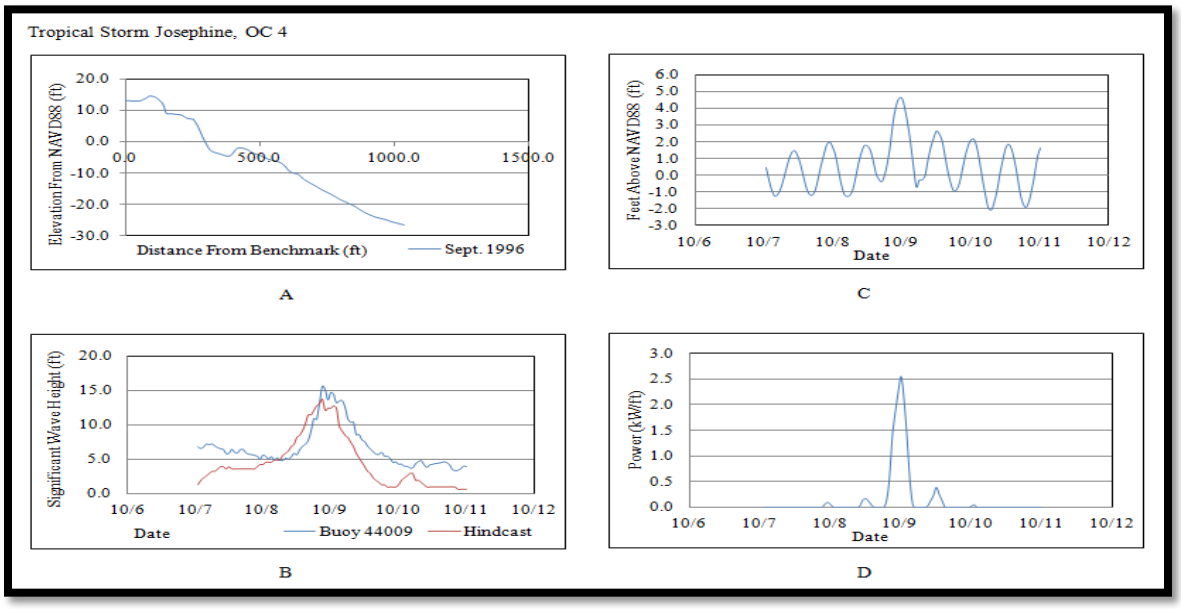

Figure B.36: OC 4 Conditions and Results during Tropical Storm Josephine. A) The pre-Tropical Storm Josephine profile. B) Tropical Storm Josephine wave heights. C) Water levels at OC 4. D) SSIM Results at OC 4 during Tropical Storm Josephine.

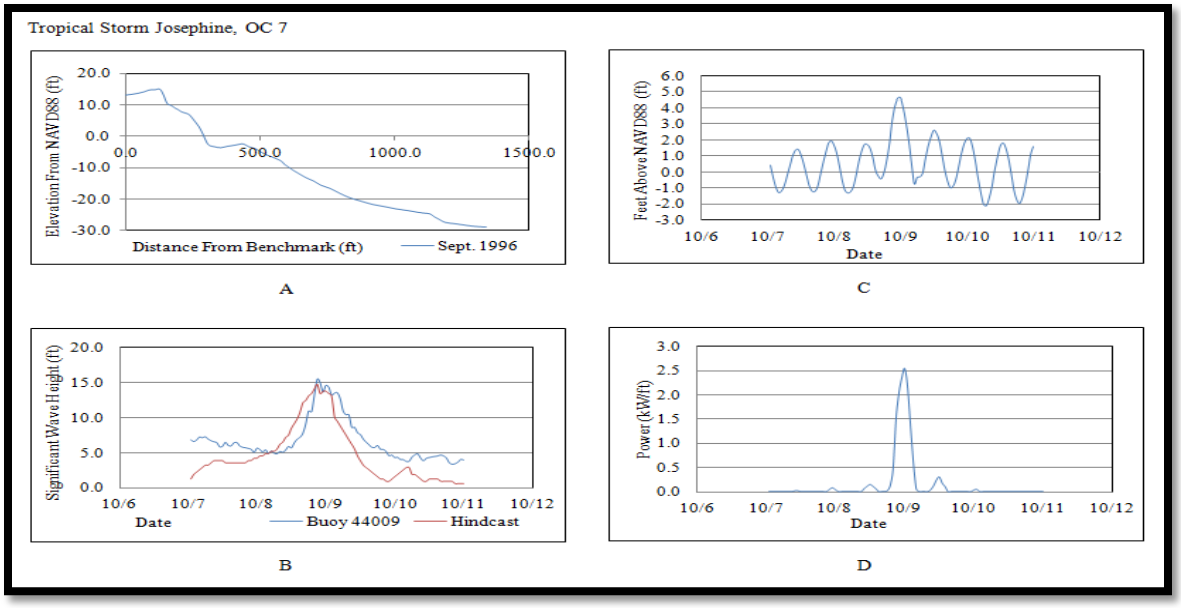

Figure B.37: OC 7 Conditions and Results during Tropical Storm Josephine. A) The pre-Tropical Storm Josephine profile. B) Tropical Storm Josephine wave heights. C) Water levels at OC 7. D) SSIM Results at OC 7 during Tropical Storm Josephine.

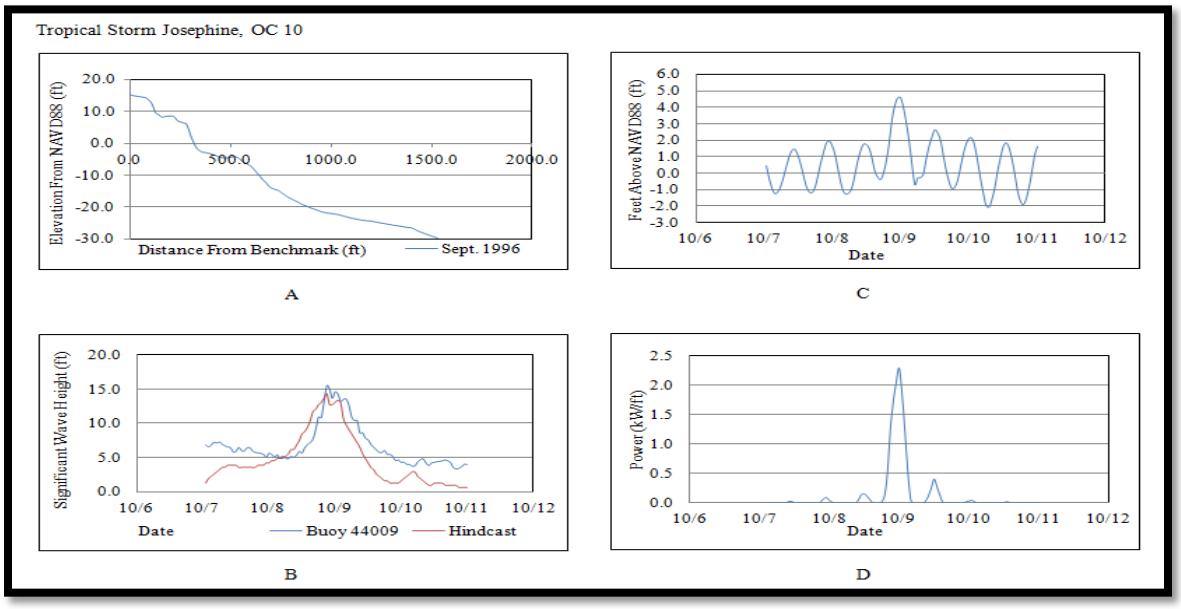

Figure B.38: OC 10 Conditions and Results during Tropical Storm Josephine. A) The pre-Tropical Storm Josephine profile. B) Tropical Storm Josephine wave heights. C) Water levels at OC 10. D) SSIM Results at OC 10 during Tropical Storm Josephine.

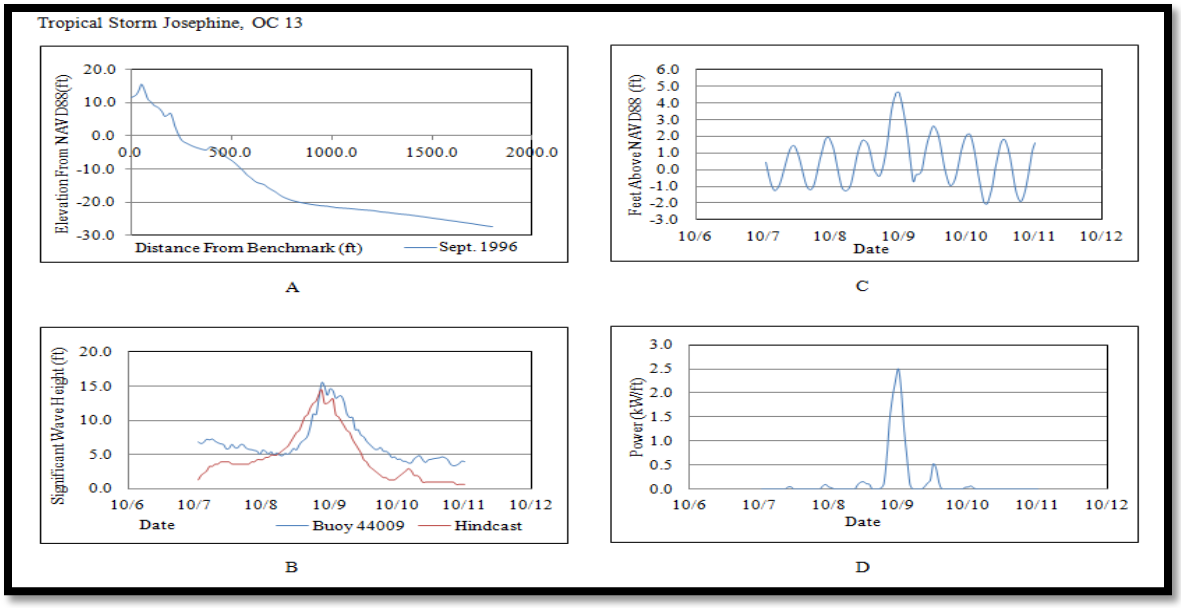

Figure B.39: OC 13 Conditions and Results during Tropical Storm Josephine. A) The pre-Tropical Storm Josephine profile. B) Tropical Storm Josephine wave heights. C) Water levels at OC 1. D) SSIM Results at OC 1 during Tropical Storm Josephine.

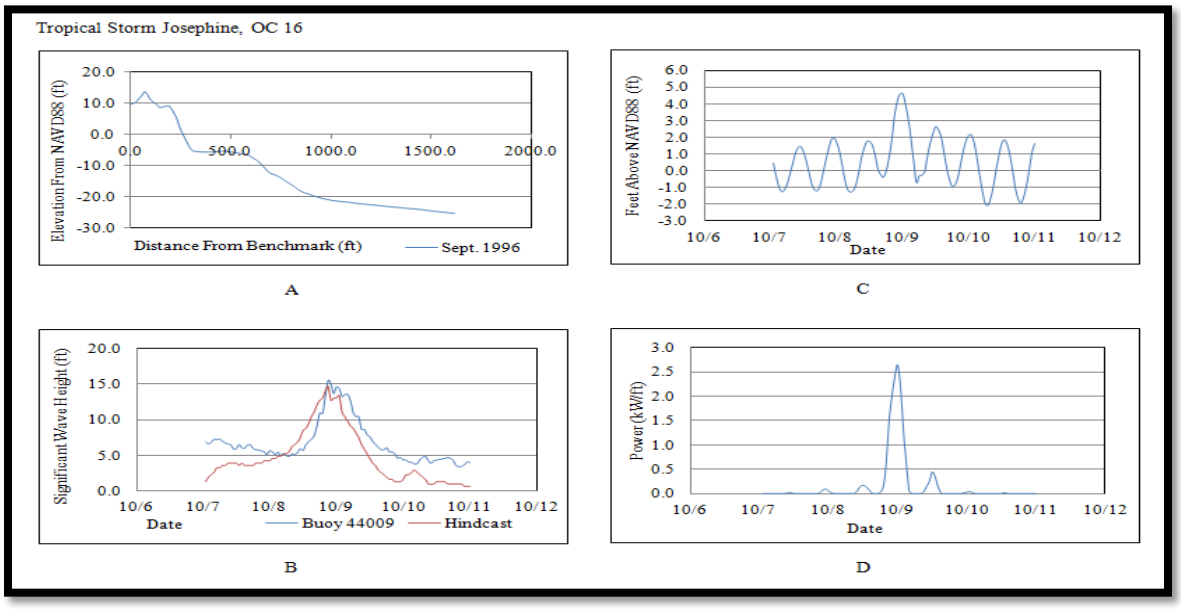

Figure B.40: OC 16 Conditions and Results during Tropical Storm Josephine. A) The pre-Tropical Storm Josephine profile. B) Tropical Storm Josephine wave heights. C) Water levels at OC 16. D) SSIM Results at OC 16 during Tropical Storm Josephine.

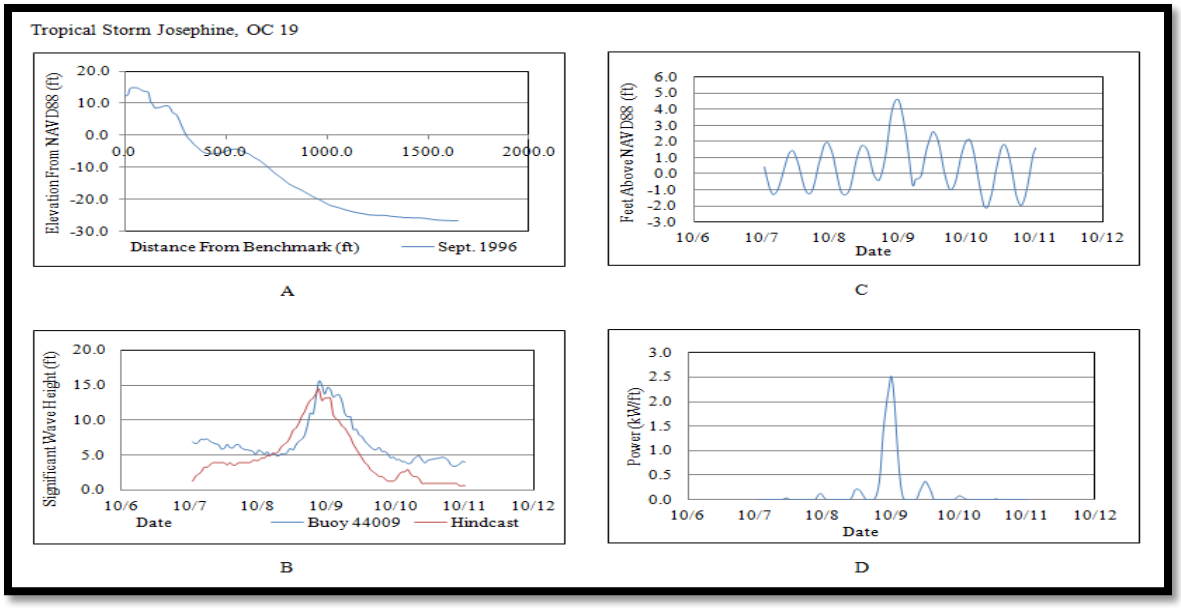

Figure B.41: OC 19 Conditions and Results during Tropical Storm Josephine. A) The pre-Tropical Storm Josephine profile. B) Tropical Storm Josephine wave heights. C) Water levels at OC 19. D) SSIM Results at OC 19 during Tropical Storm Josephine.

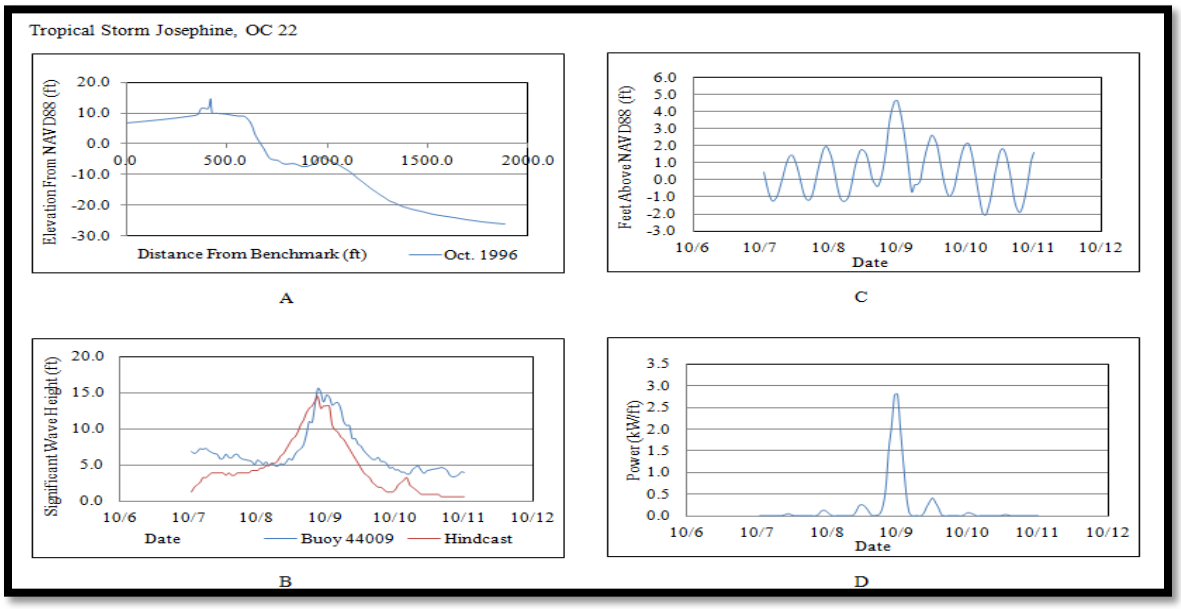

Figure B.42: OC 22 Conditions and Results during Tropical Storm Josephine. A) The pre-Tropical Storm Josephine profile. B) Tropical Storm Josephine wave heights. C) Water levels at OC 22. D) SSIM Results at OC 22 during Tropical Storm Josephine.

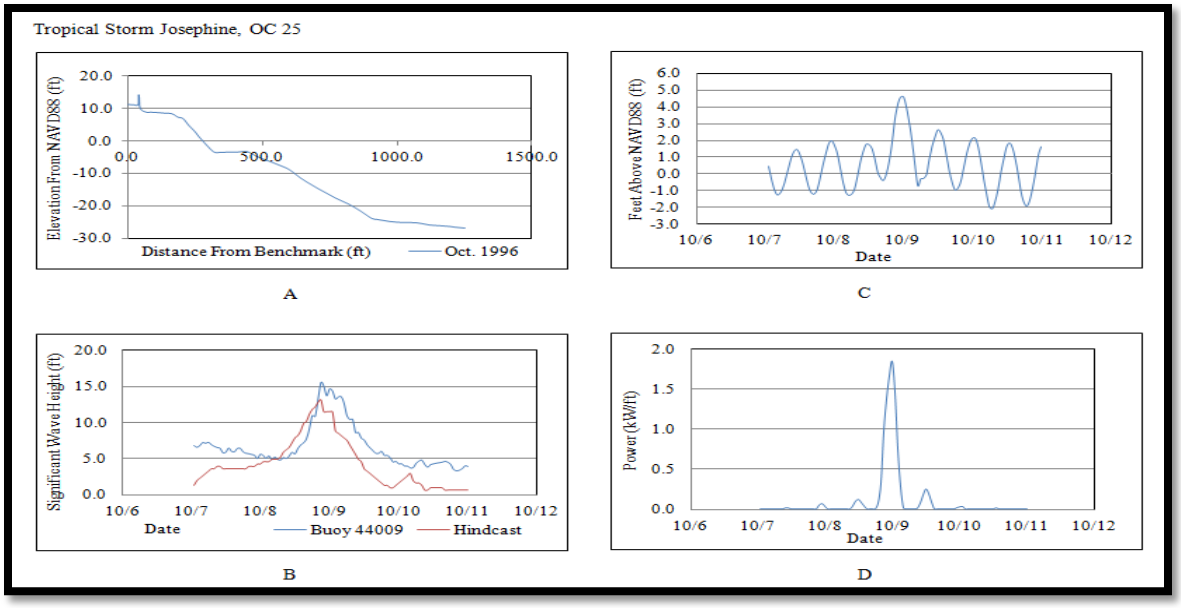

Figure B.43: OC 25 Conditions and Results during Tropical Storm Josephine. A) The pre-Tropical Storm Josephine profile. B) Tropical Storm Josephine wave heights. C) Water levels at OC 25. D) SSIM Results at OC 25 during Tropical Storm Josephine.

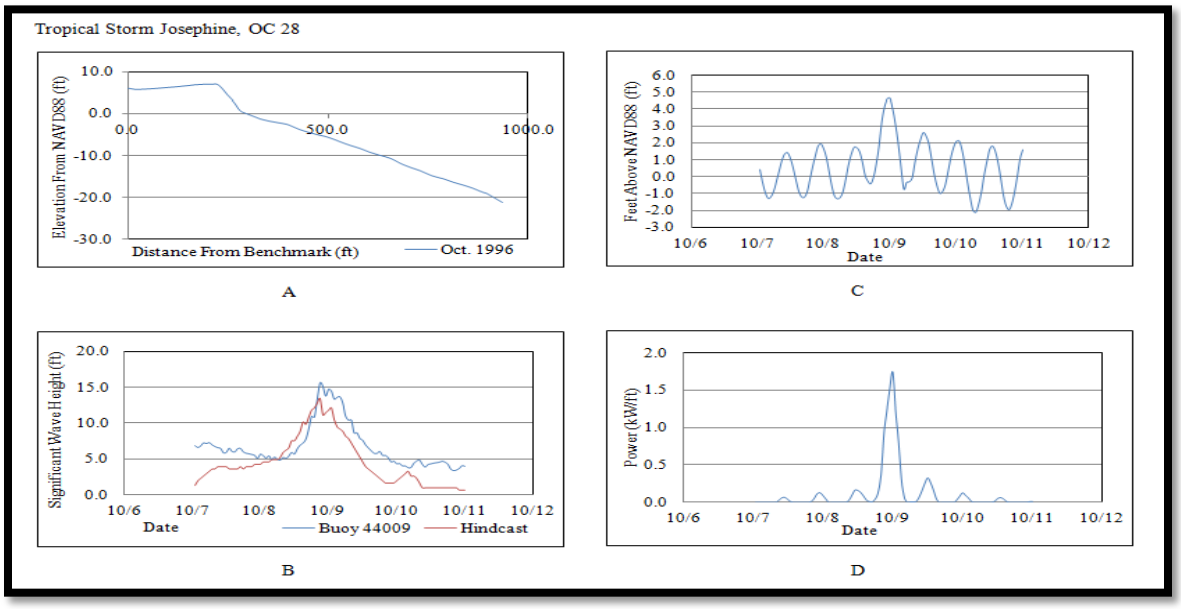

Figure B.44: OC 28 Conditions and Results during Tropical Storm Josephine. A) The pre-Tropical Storm Josephine profile. B) Tropical Storm Josephine wave heights. C) Water levels at OC 28. D) SSIM Results at OC 28 during Tropical Storm Josephine.

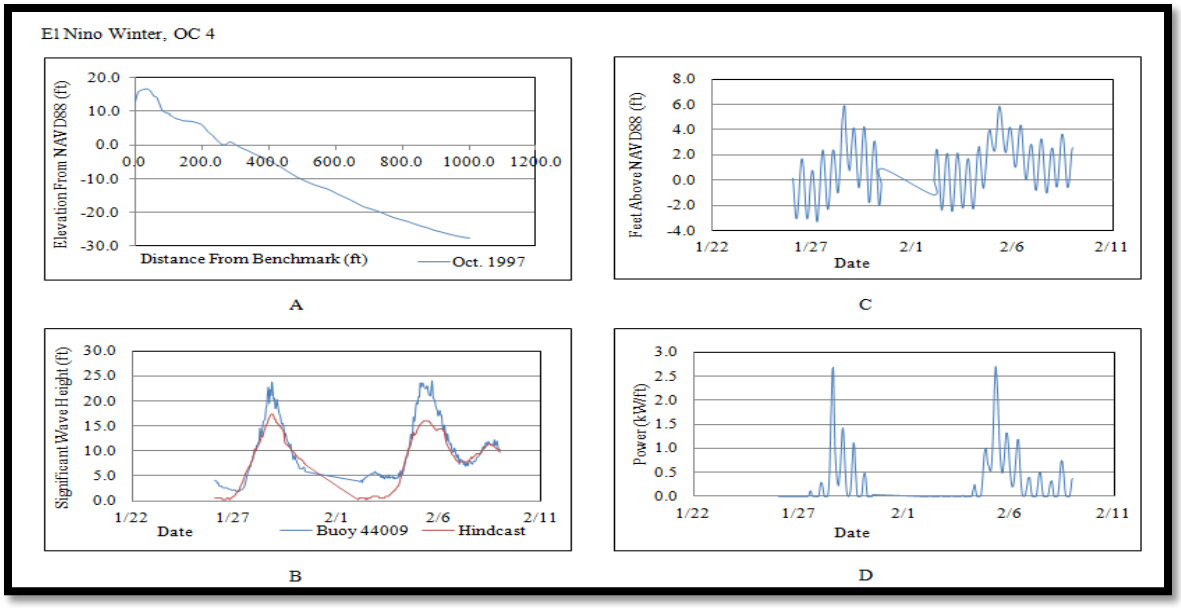

Figure B.45: OC 4 Conditions and Results during El Nino Winter. A) The pre-El Nino Winter profile. B) El Nino Winter wave heights. C) Water levels at OC 4. D) SSIM Results at OC 4 during El Nino Winter.

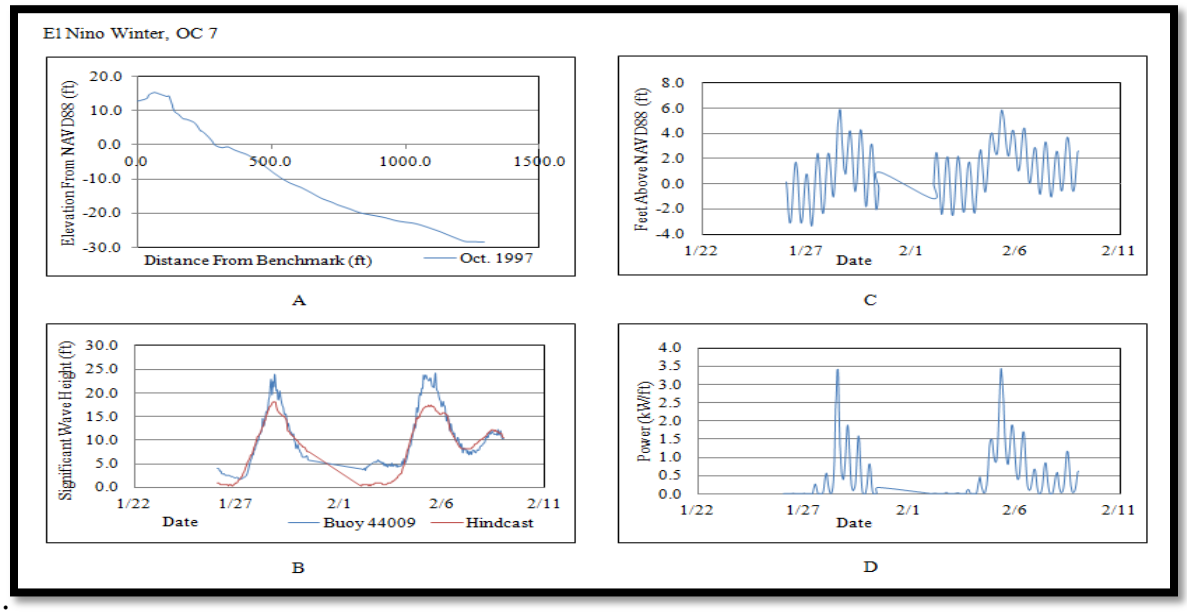

Figure B.46: OC 7 Conditions and Results during El Nino Winter. A) The pre-El Nino Winter profile. B) El Nino Winter wave heights. C) Water levels at OC 7. D) SSIM Results at OC 7 during El Nino Winter.

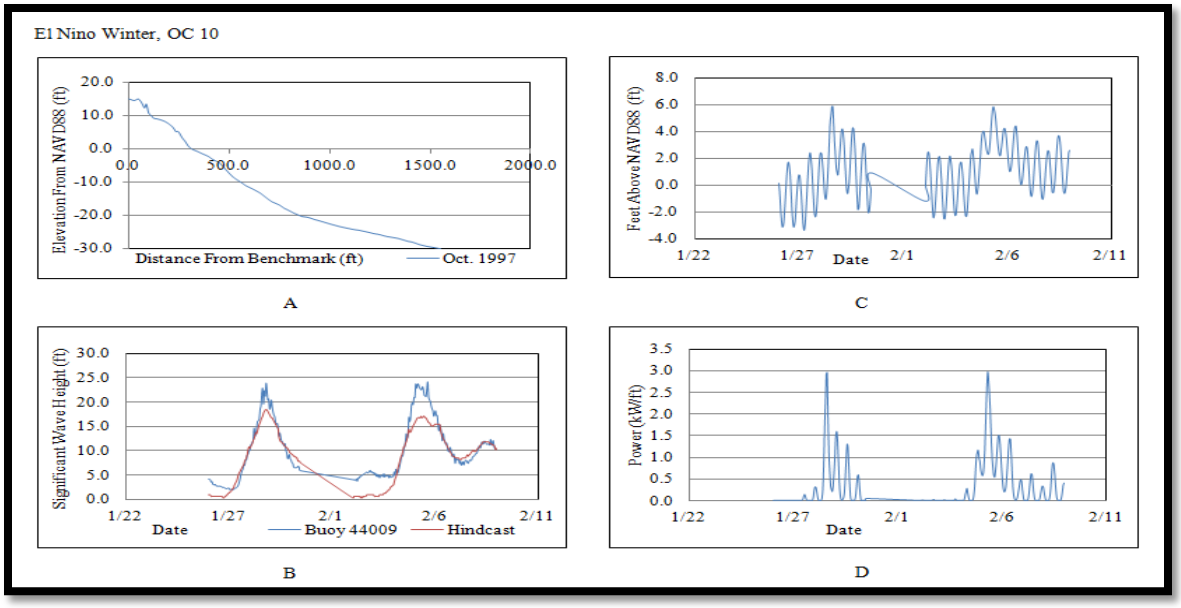

Figure B.47: OC 10 Conditions and Results during El Nino Winter. A) The pre-El Nino Winter profile. B) El Nino Winter wave heights. C) Water levels at OC 10. D) SSIM Results at OC 10 during El Nino Winter.

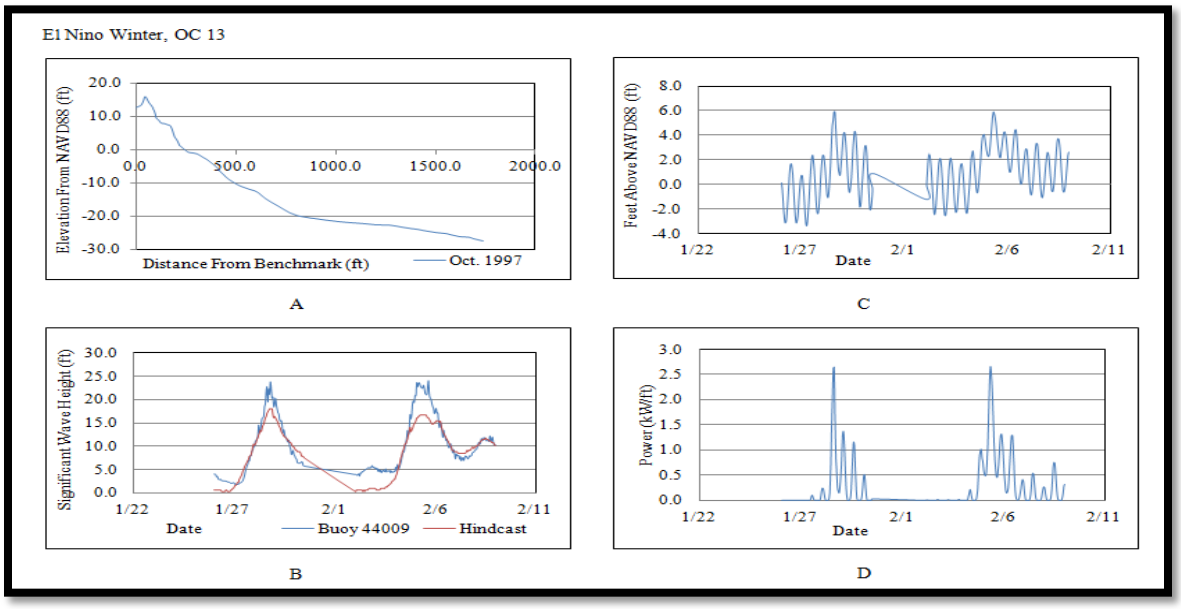

Figure B.48: OC 13 Conditions and Results during El Nino Winter. A) The pre-El Nino Winter profile. B) El Nino Winter wave heights. C) Water levels at OC 13. D) SSIM Results at OC 13 during El Nino Winter.

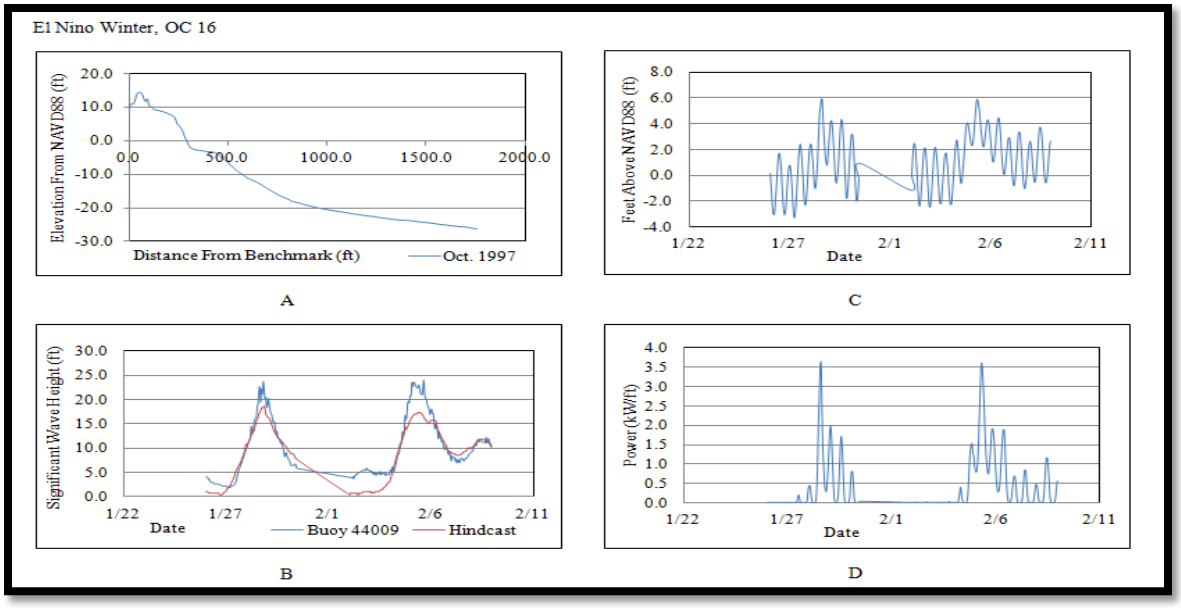

Figure B.49: OC 16 Conditions and Results during the El Nino Winter. A) The pre-El Nino Winter profile. B) El Nino Winter wave heights. C) Water levels at OC 16. D) SSIM Results at OC 16 during El Nino Winter.

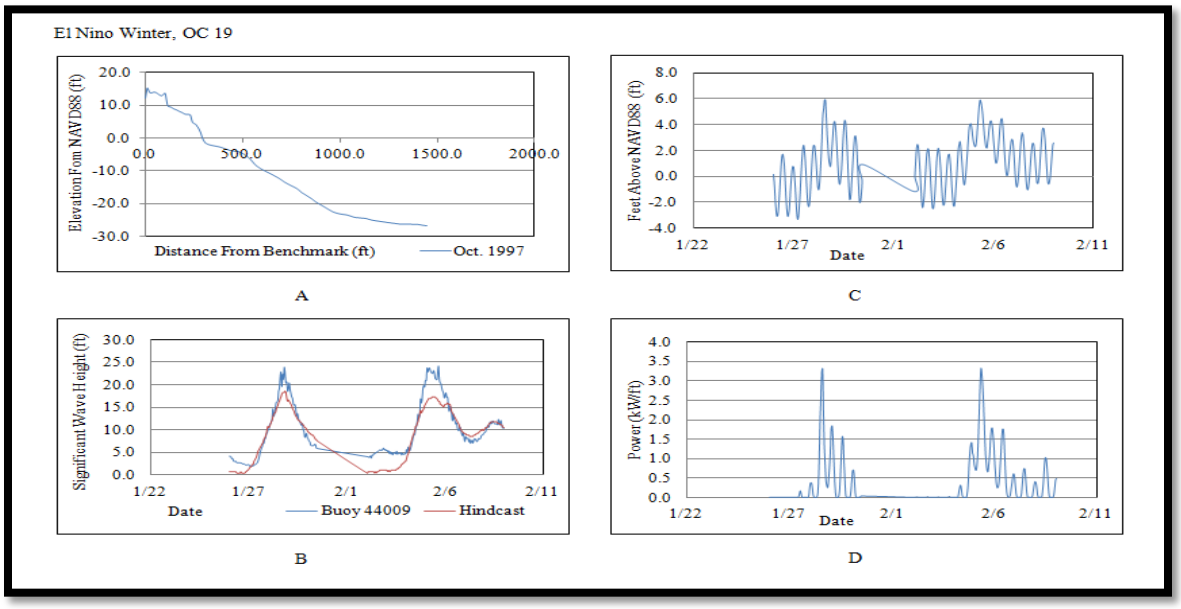

Figure B.50: OC 19 Conditions and Results during El Nino Winter. A) The pre-El Nino Winter profile. B) El Nino Winter wave heights. C) Water levels at OC 19. D) SSIM Results at OC 19 during El Nino Winter.

.

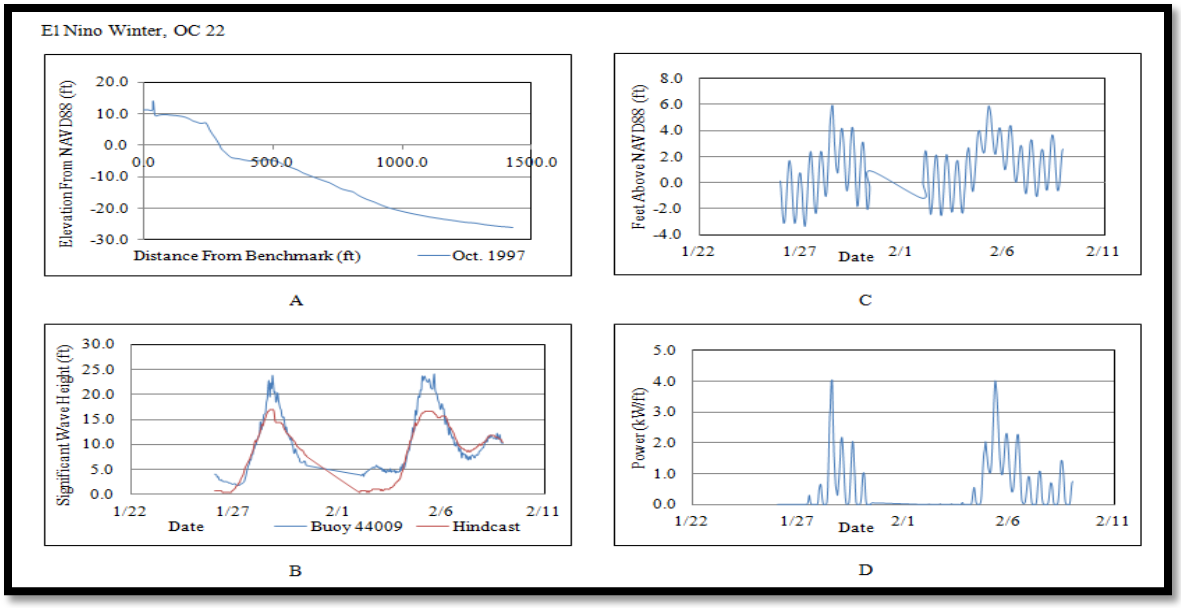

Figure B.51: OC 22 Conditions and Results during El Nino Winter. A) The pre-El Nino Winter profile. B) El Nino Winter wave heights. C) Water levels at OC 22. D) SSIM Results at OC 22 during El Nino Winter.

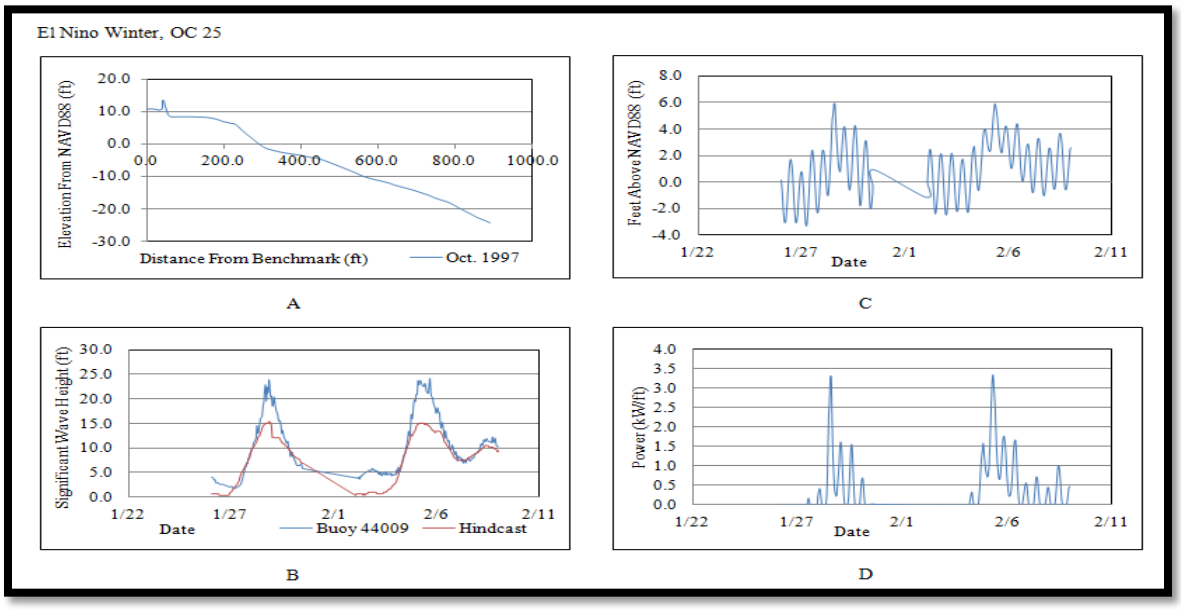

Figure B.52: OC 25 Conditions and Results during El Nino Winter. A) The pre-El Nino Winter profile. B) El Nino Winter wave heights. C) Water levels at OC 25. D) SSIM Results at OC 25 during El Nino Winter.

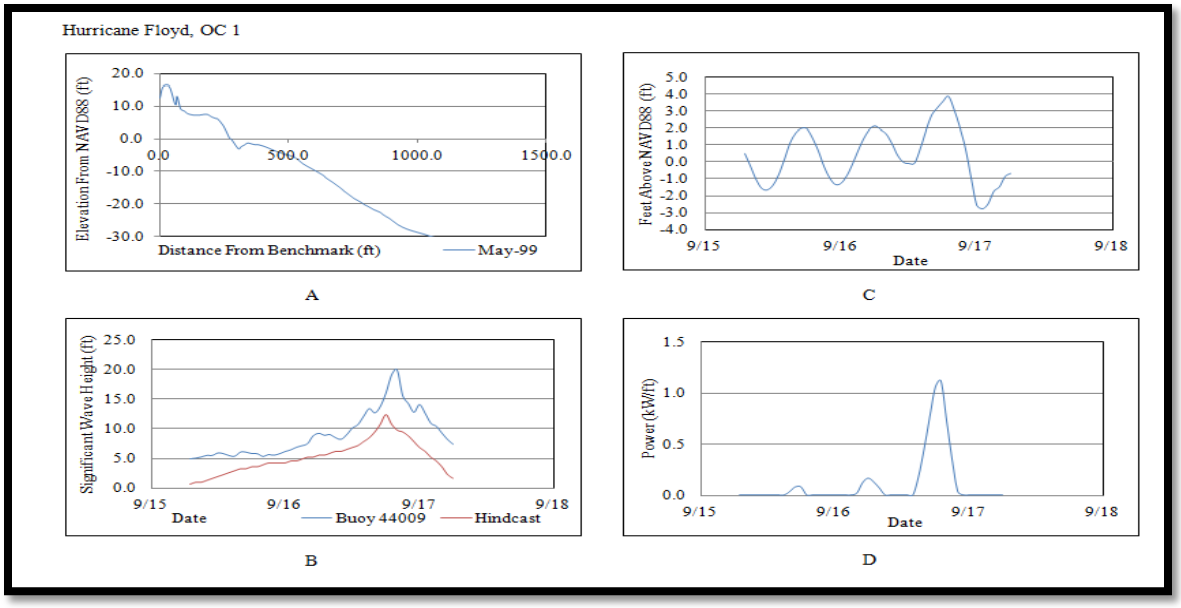

Figure B.53: OC 1 Conditions and Results during Hurricane Floyd. A) The pre-Hurricane Floyd profile. B) Hurricane Floyd wave heights. C) Water levels at OC 1. D) SSIM Results at OC 1 during Hurricane Floyd.

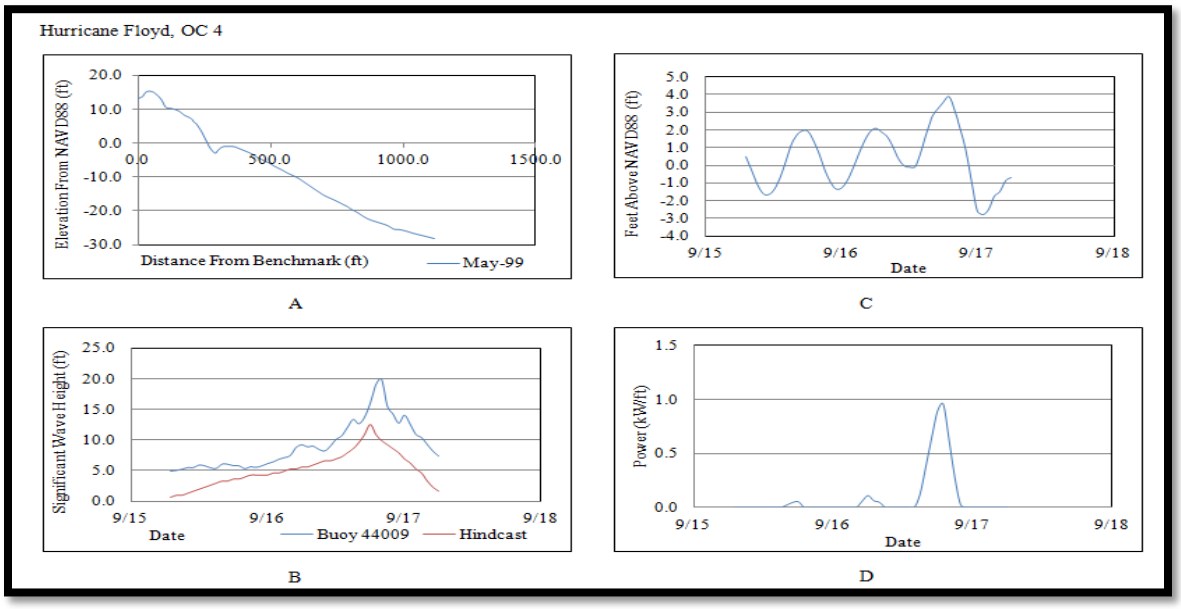

Figure B.54: OC 4 Conditions and Results during Hurricane Floyd. A) The pre-Hurricane Floyd profile. B) Hurricane Floyd wave heights. C) Water levels at OC 4. D) SSIM Results at OC 4 during Hurricane Floyd.

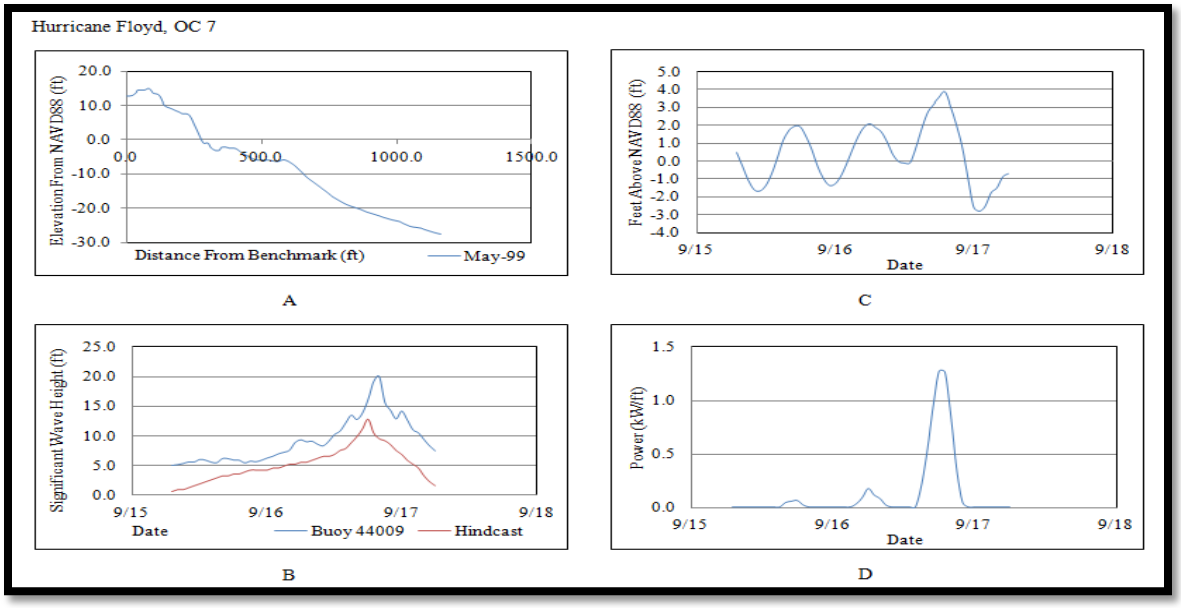

Figure B.55: OC 7 Conditions and Results during Hurricane Floyd. A) The pre-Hurricane Floyd profile. B) Hurricane Floyd wave heights. C) Water levels at OC 7. D) SSIM Results at OC 7 during Hurricane Floyd.

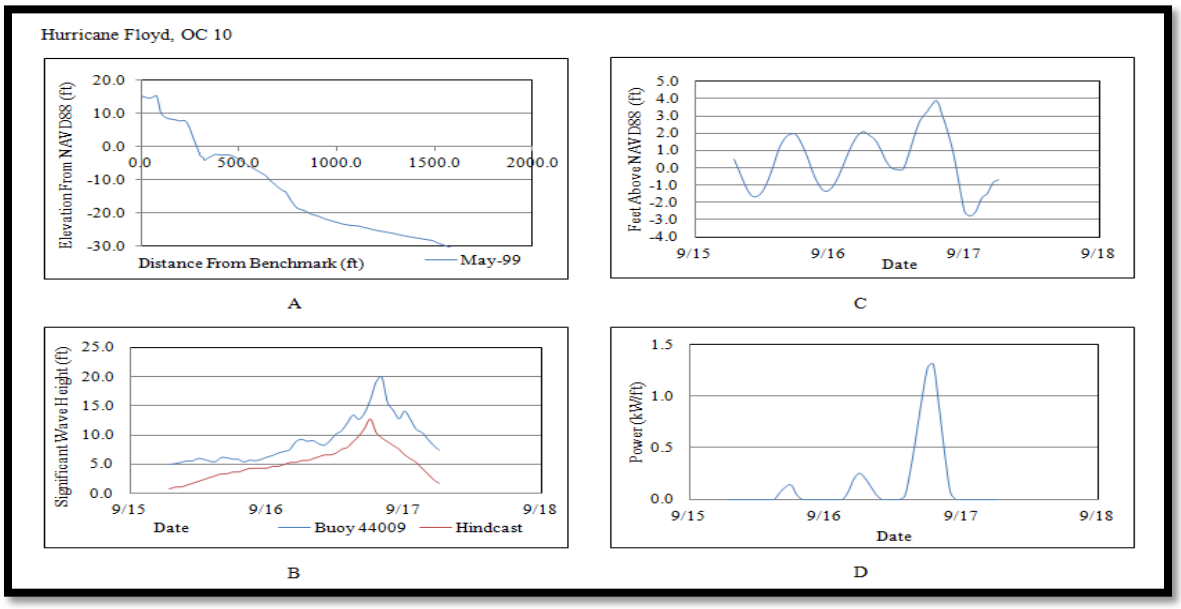

Figure B.56: OC 10 Conditions and Results during Hurricane Floyd. A) The pre-Hurricane Floyd profile. B) Hurricane Floyd wave heights. C) Water levels at OC 10. D) SSIM Results at OC 10 during Hurricane Floyd.

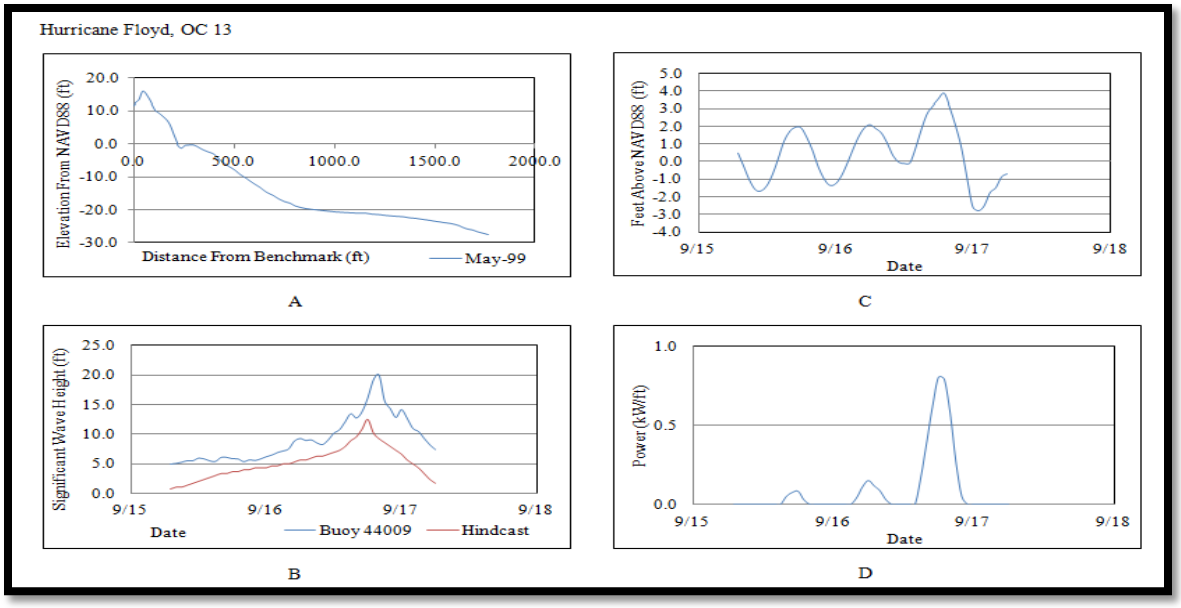

Figure B.57: OC 13 Conditions and Results during Hurricane Floyd. A) The pre-Hurricane Floyd profile. B) Hurricane Floyd wave heights. C) Water levels at OC 13. D) SSIM Results at OC 13 during Hurricane Floyd.

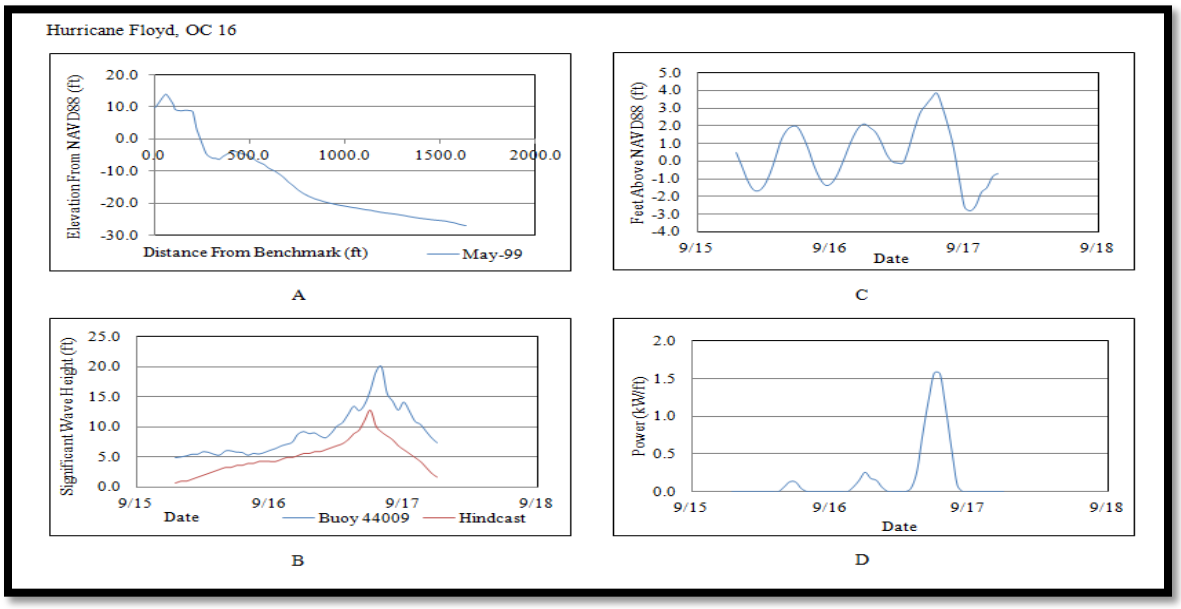

Figure B.58: OC 16 Conditions and Results during Hurricane Floyd. A) The pre-Hurricane Floyd profile. B) Hurricane Floyd wave heights. C) Water levels at OC 16. D) SSIM Results at OC 16 during Hurricane Floyd.

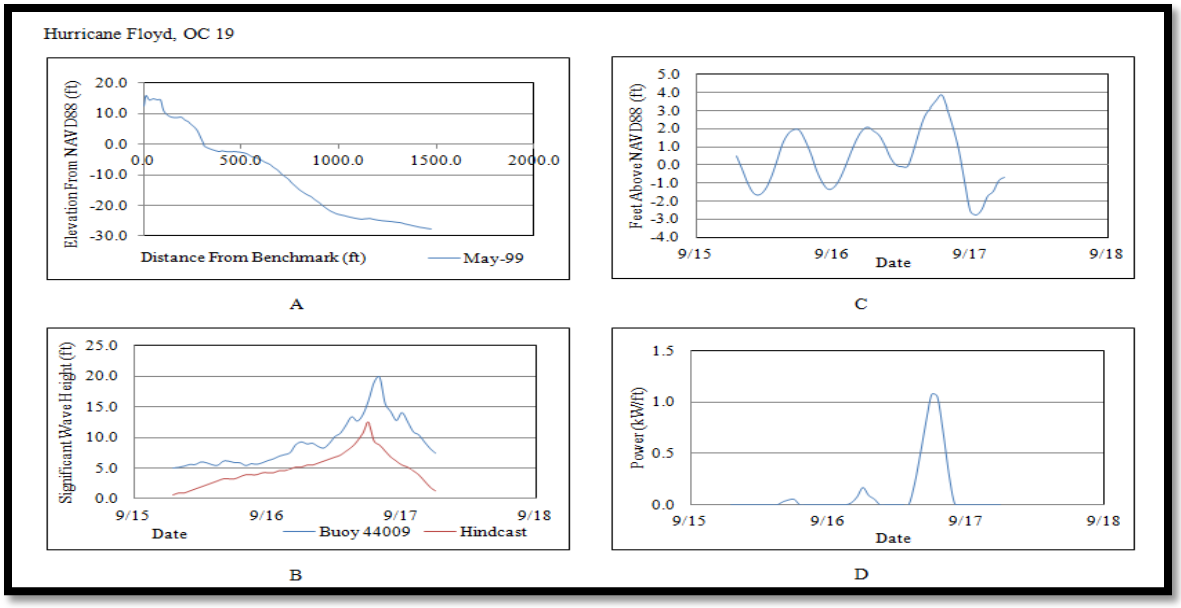

Figure B.59: OC 19 Conditions and Results during Hurricane Floyd. A) The pre-Hurricane Floyd profile. B) Hurricane Floyd wave heights. C) Water levels at OC 19. D) SSIM Results at OC 19 during Hurricane Floyd.

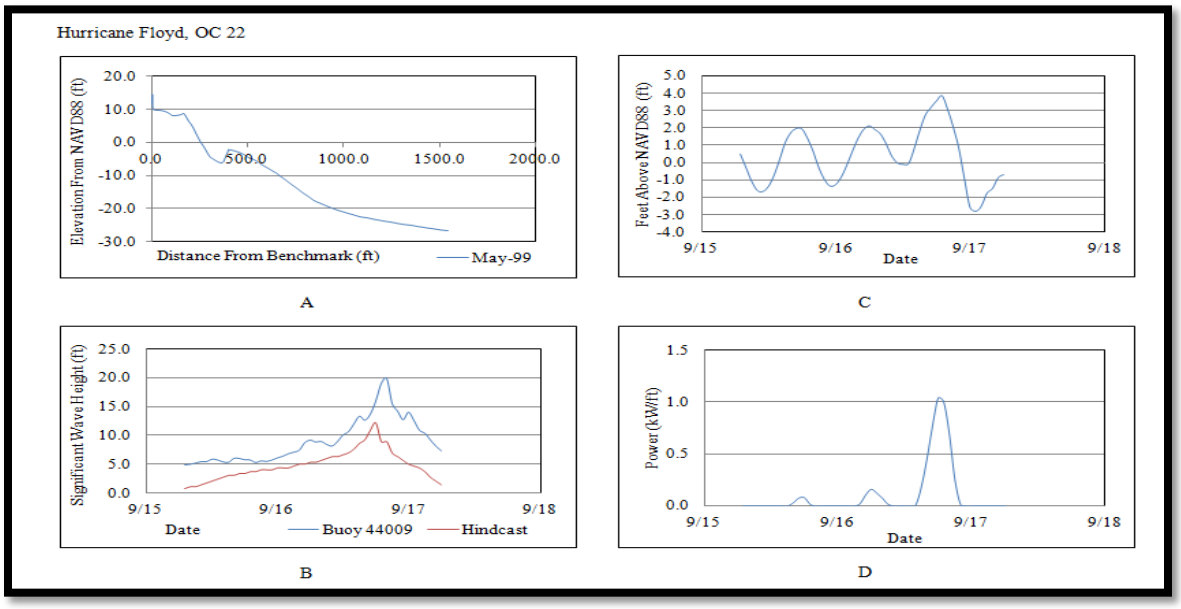

Figure B.60: OC 22 Conditions and Results during Hurricane Floyd. A) The pre-Hurricane Floyd profile. B) Hurricane Floyd wave heights. C) Water levels at OC 22. D) SSIM Results at OC 22 during Hurricane Floyd.

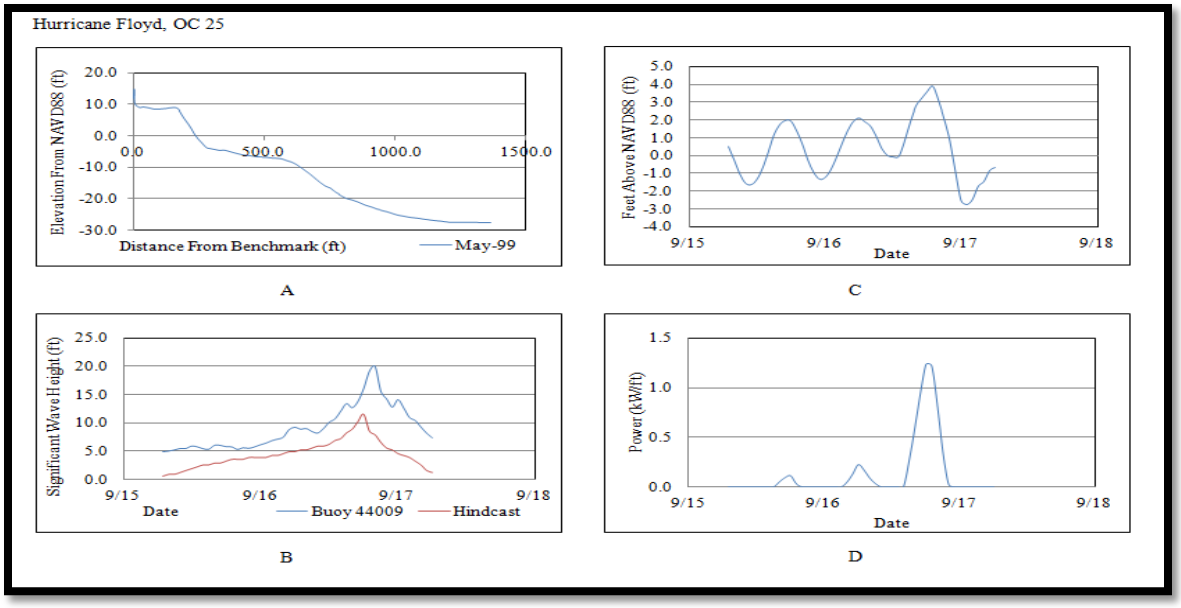

Figure B.61: OC 25 Conditions and Results during Hurricane Floyd. A) The pre-Hurricane Floyd profile. B) Hurricane Floyd wave heights. C) Water levels at OC 25. D) SSIM Results at OC 25 during Hurricane Floyd.

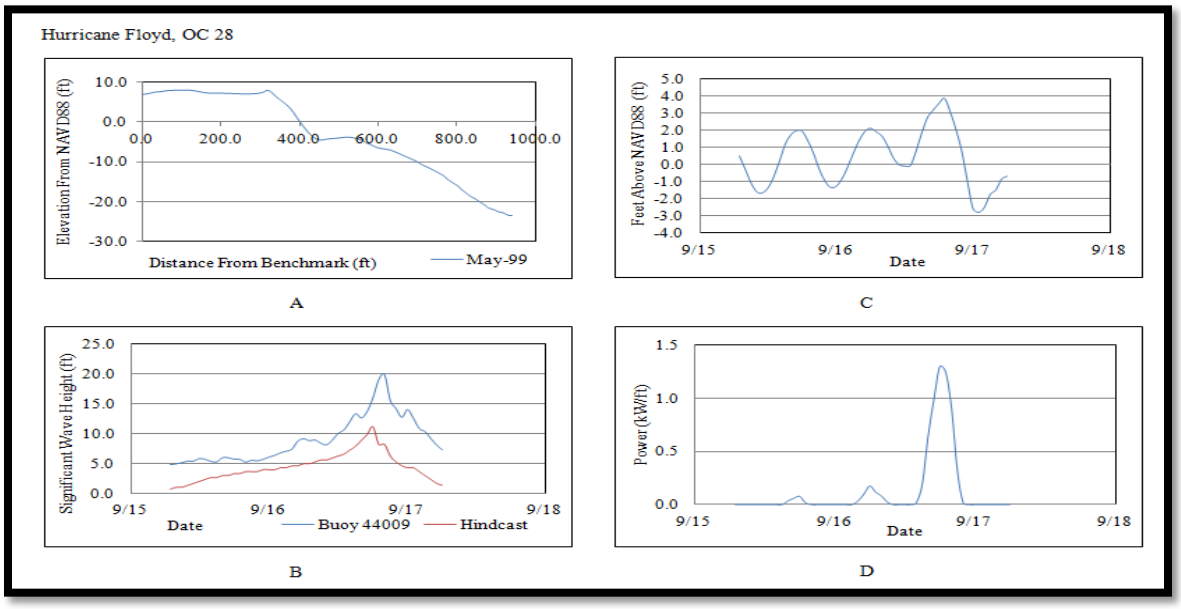

Figure B.62: OC 28 Conditions and Results during Hurricane Floyd. A) The pre-Hurricane Floyd profile. B) Hurricane Floyd wave heights. C) Water levels at OC 28. D) SSIM Results at OC 28 during Hurricane Floyd.

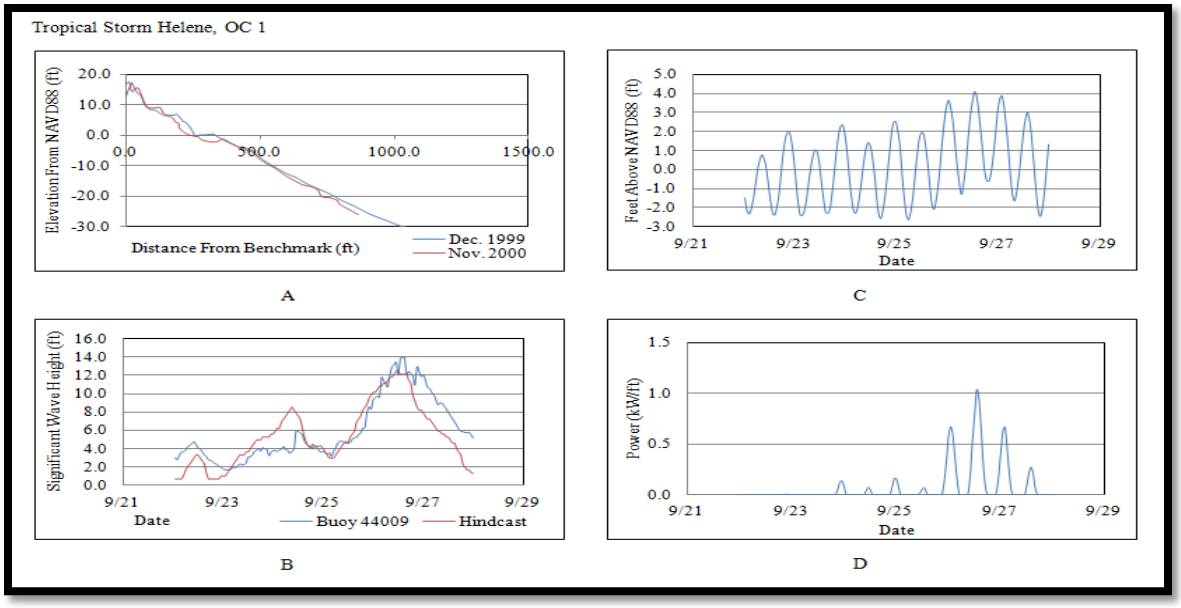

Figure B.63: OC 1 Conditions and Results during Tropical Storm Helene. A) The pre- and post-Tropical Storm Helene profiles. B) Tropical Storm Helene wave heights. C) Water levels at OC 1. D) SSIM Results at OC 1 during Tropical Storm Helene.

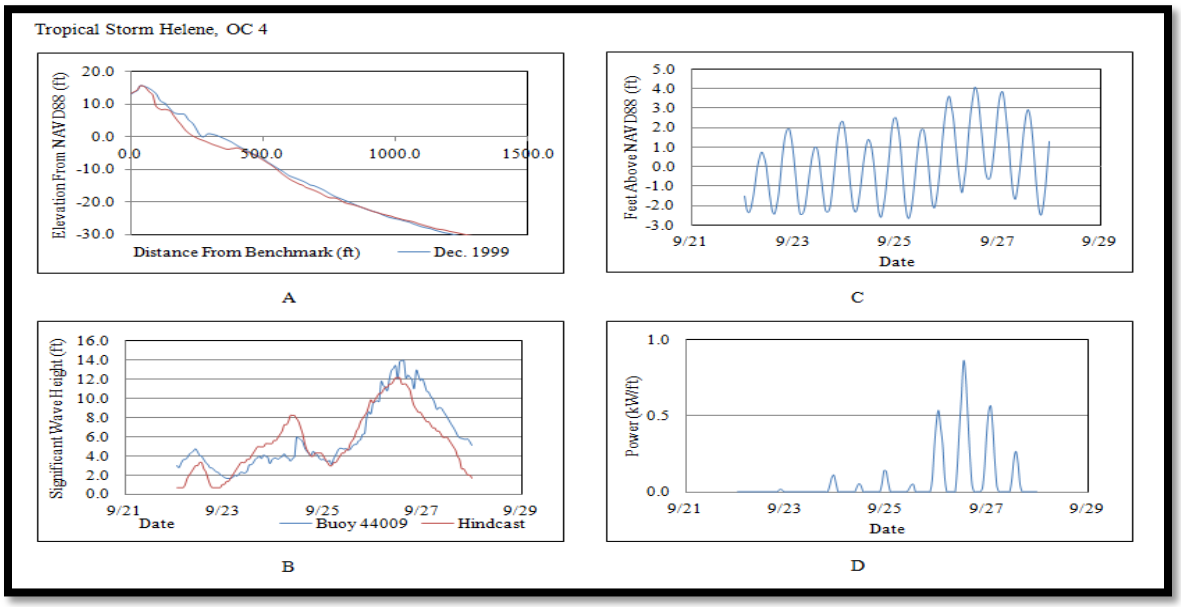

Figure B.64: OC 4 Conditions and Results during Tropical Storm Helene. A) The pre- and post-Tropical Storm Helene profiles. B) Tropical Storm Helene wave heights. C) Water levels at OC 4. D) SSIM Results at OC 4 during Tropical Storm Helene.

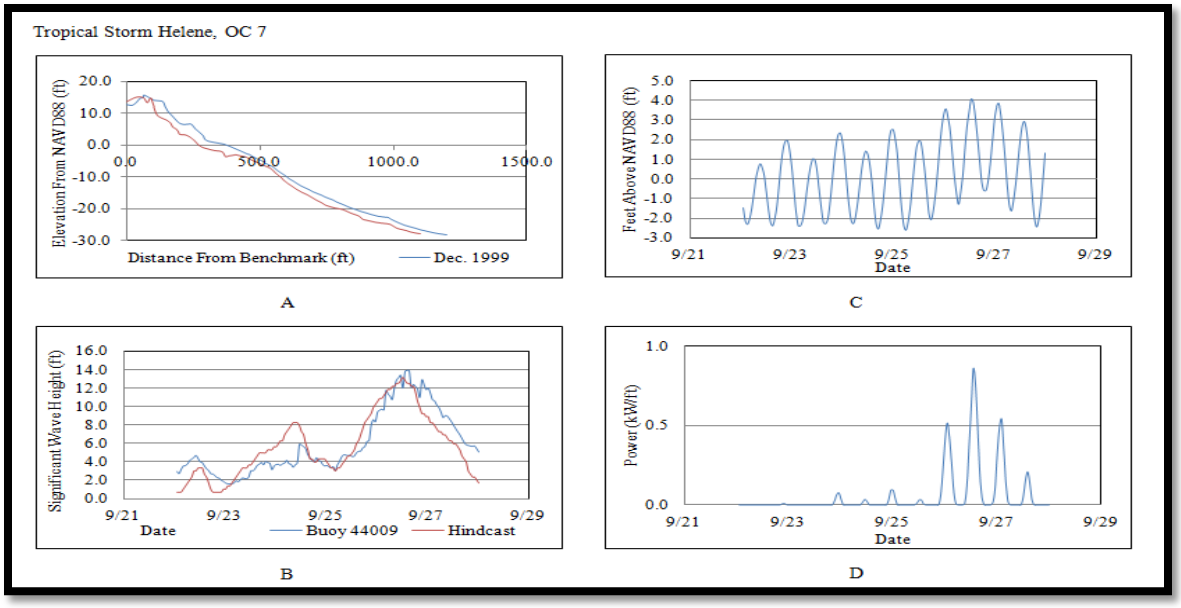

Figure B.65: OC 7 Conditions and Results during Tropical Storm Helene. A) The pre- and post-Tropical Storm Helene profiles. B) Tropical Storm Helene wave heights. C) Water levels at OC 7. D) SSIM Results at OC 7 during Tropical Storm Helene.

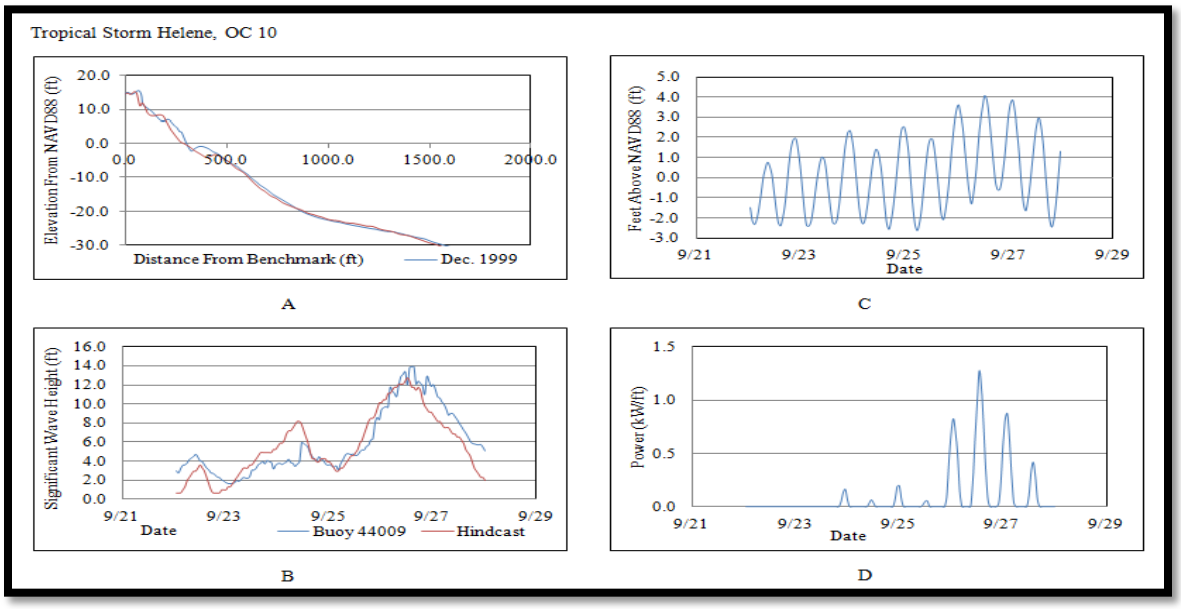

Figure B.66: OC 10 Conditions and Results during Tropical Storm Helene. A) The pre- and post-Tropical Storm Helene profiles. B) Tropical Storm Helene wave heights. C) Water levels at OC 10. D) SSIM Results at OC 10 during Tropical Storm Helene.

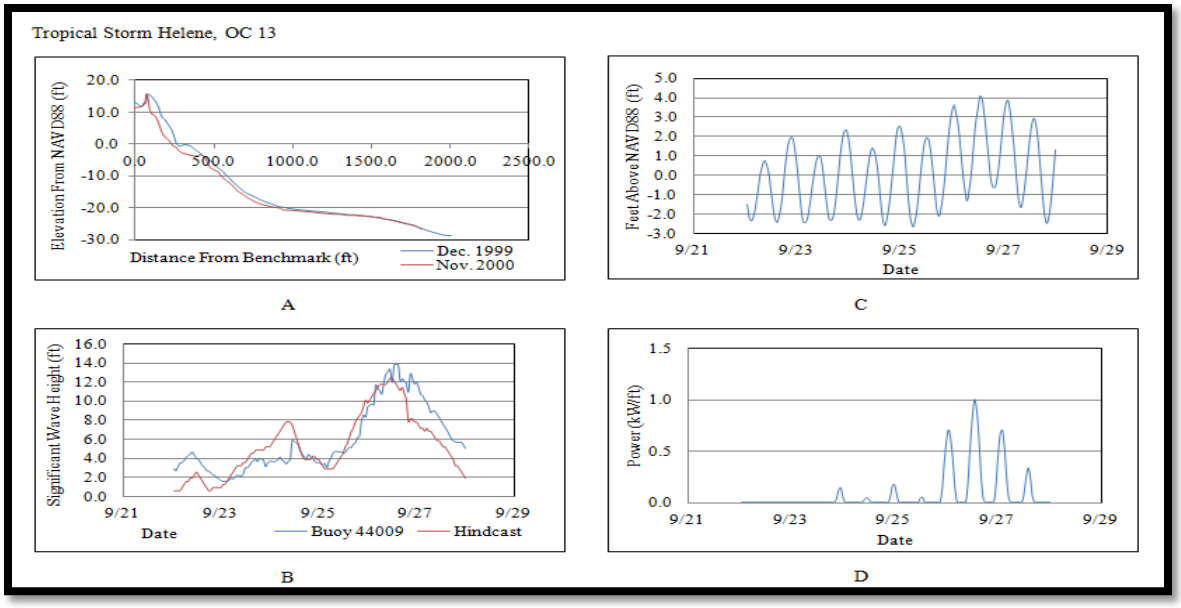

Figure B.67: OC 13 Conditions and Results during Tropical Storm Helene. A) The pre- and post-Tropical Storm Helene profiles. B) Tropical Storm Helene wave heights. C) Water levels at OC 13. D) SSIM Results at OC 13 during Tropical Storm Helene.

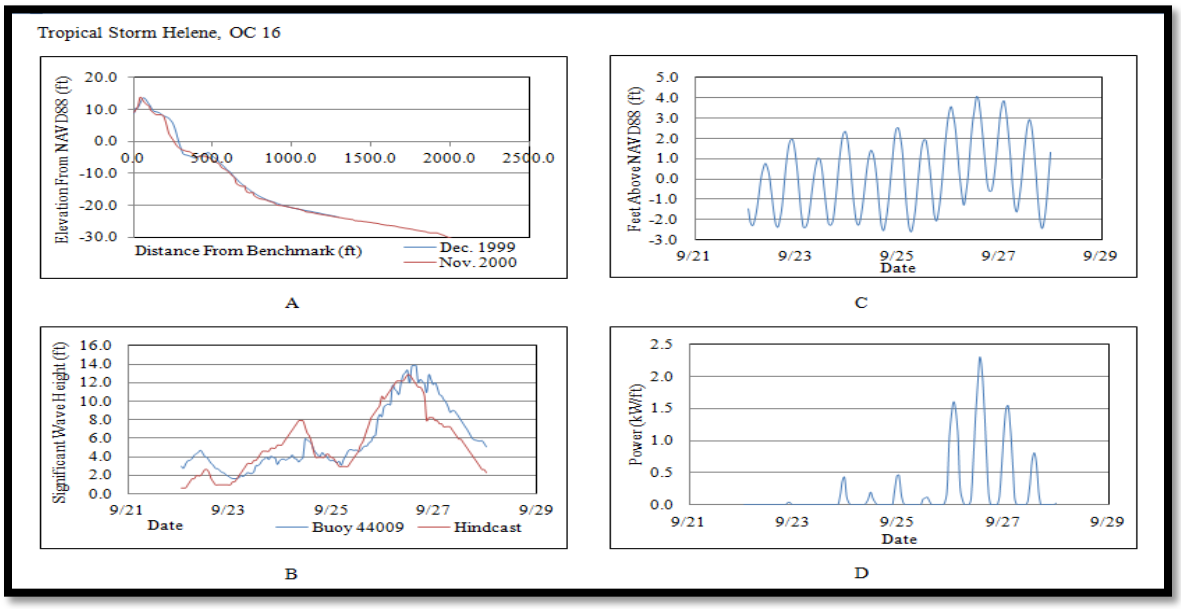

Figure B.68: OC 16 Conditions and Results during Tropical Storm Helene. A) The pre- and post-Tropical Storm Helene profiles. B) Tropical Storm Helene wave heights. C) Water levels at OC 16. D) SSIM Results at OC 16 during Tropical Storm Helene.

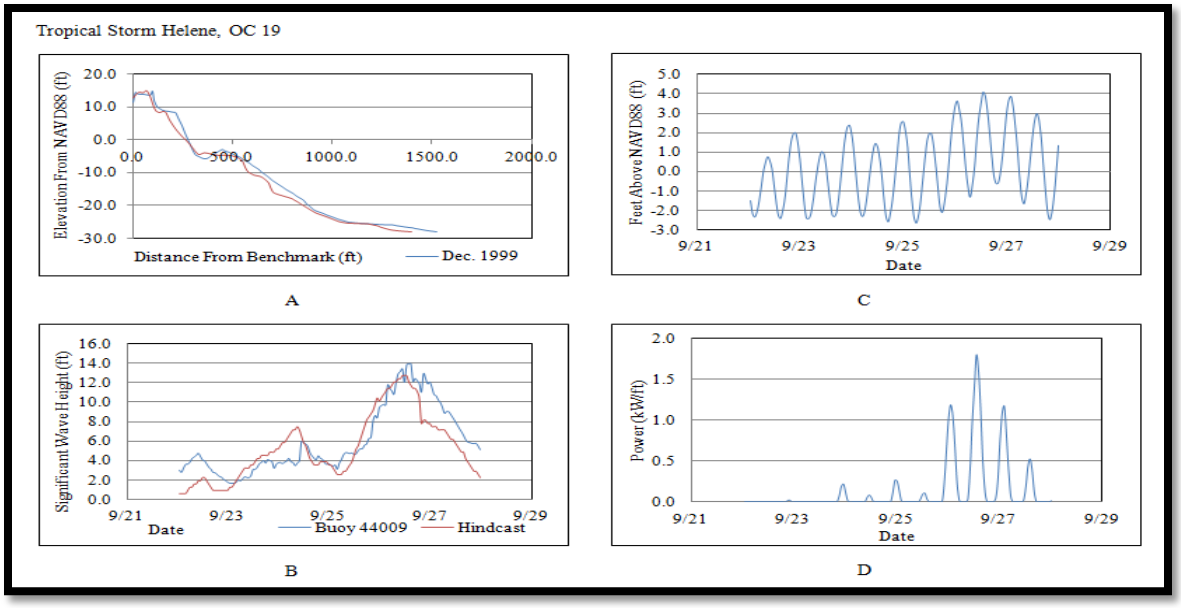

Figure B.69: OC 19 Conditions and Results during Tropical Storm Helene. A) The pre- and post-Tropical Storm Helene profiles. B) Tropical Storm Helene wave heights. C) Water levels at OC 19. D) SSIM Results at OC 19 during Tropical Storm Helene.

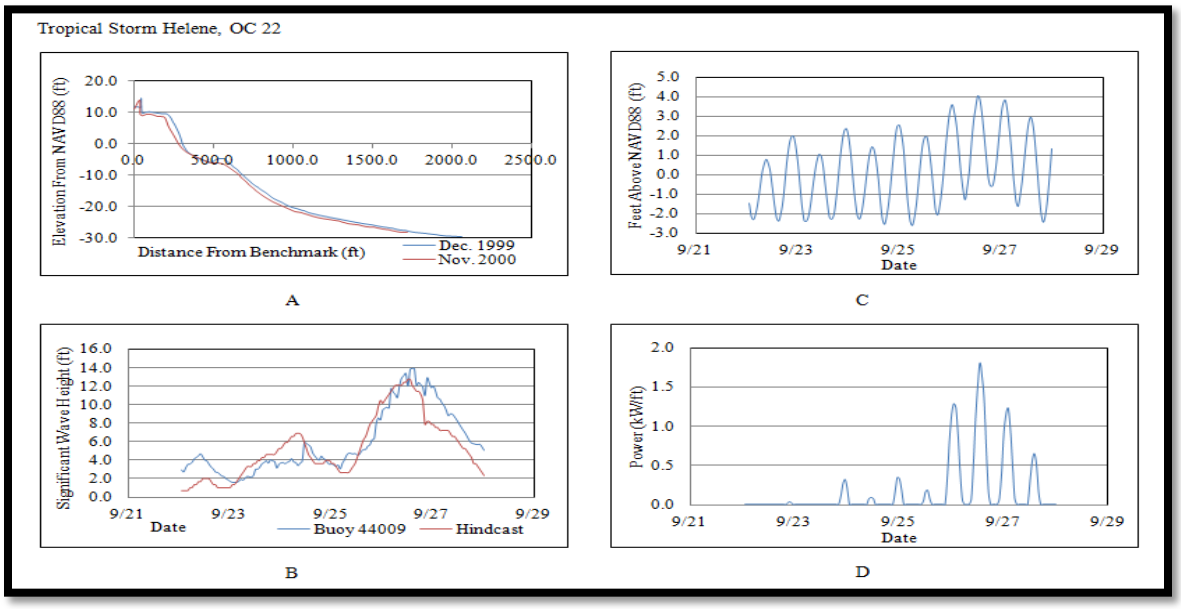

Figure B.70: OC 22 Conditions and Results during Tropical Storm Helene. A) The pre- and post-Tropical Storm Helene profiles. B) Tropical Storm Helene wave heights. C) Water levels at OC 22. D) SSIM Results at OC 22 during Tropical Storm Helene.

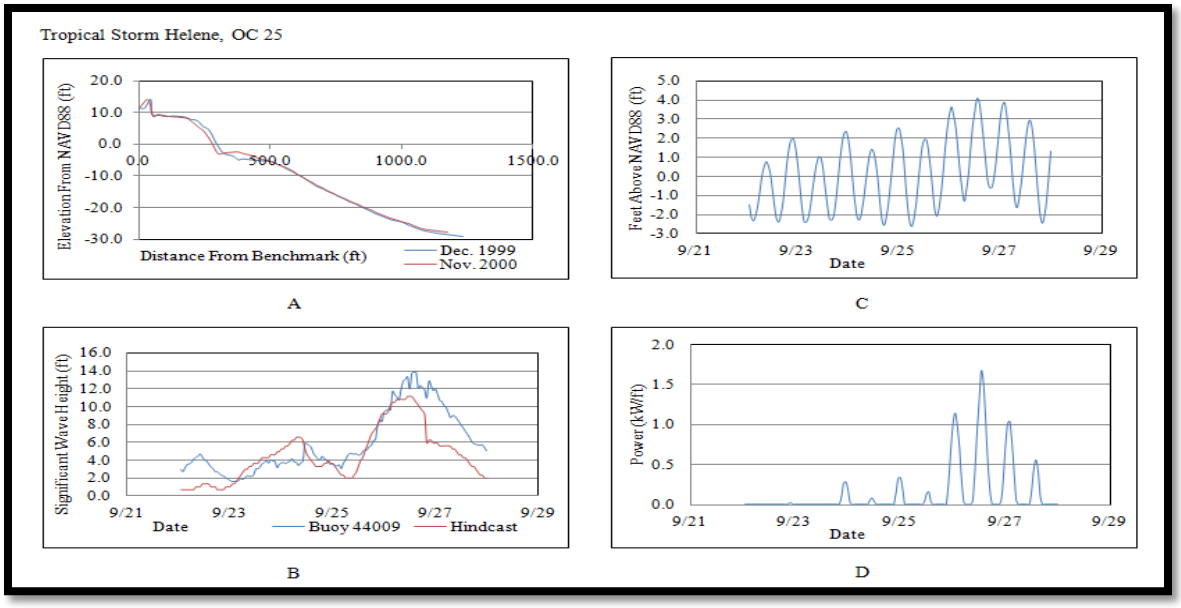

Figure B.71: OC 25 Conditions and Results during Tropical Storm Helene. A) The pre- and post-Tropical Storm Helene profiles. B) Tropical Storm Helene wave heights. C) Water levels at OC 25. D) SSIM Results at OC 25 during Tropical Storm Helene.

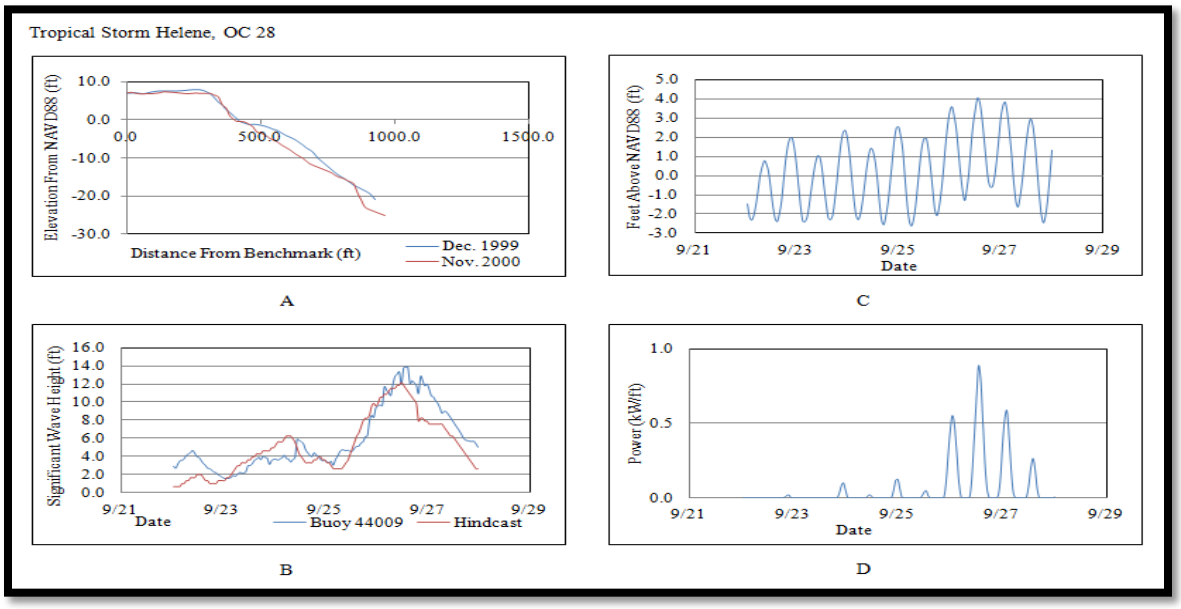

Figure B.72: OC 28 Conditions and Results during Tropical Storm Helene. A) The pre- and post-Tropical Storm Helene profiles. B) Tropical Storm Helene wave heights. C) Water levels at OC 28. D) SSIM Results at OC 28 during Tropical Storm Helene.

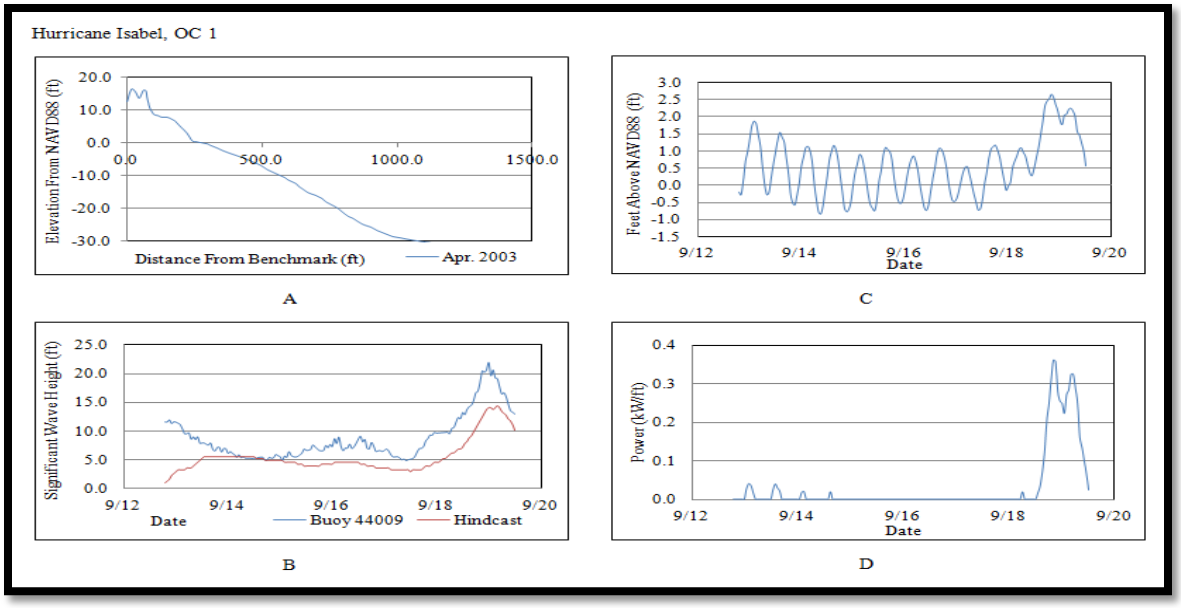

Figure B.73: OC 1 Conditions and Results during Hurricane Isabel. A) The pre-Hurricane Isabel profile. B) Hurricane Isabel wave heights. C) Water levels at OC 1. D) SSIM Results at OC 1 during Hurricane Isabel.

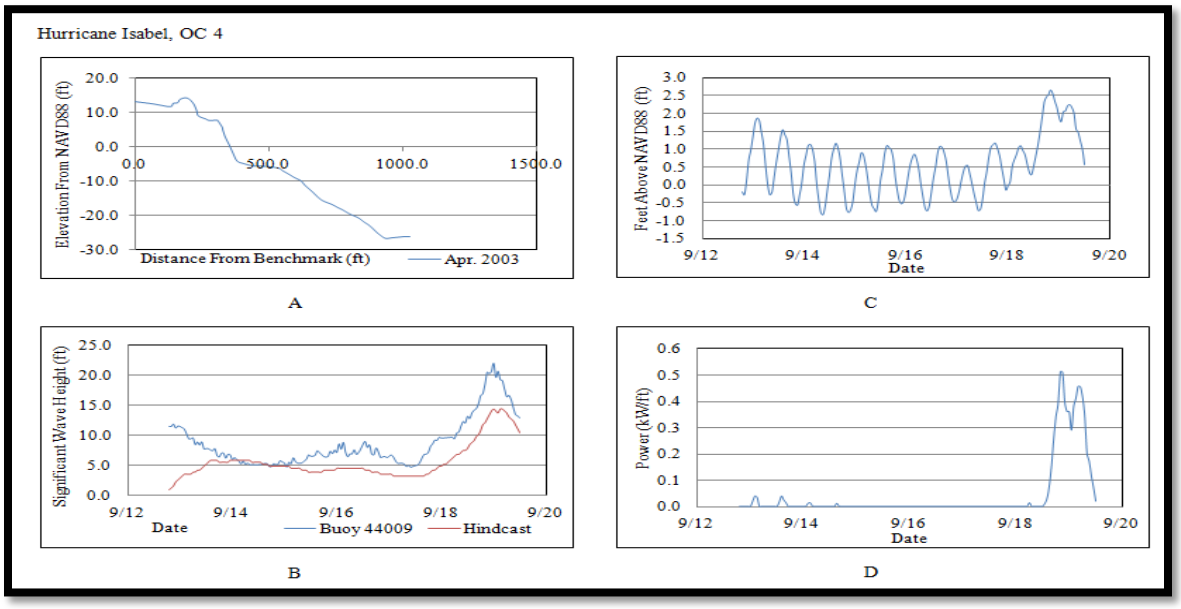

Figure B.74: OC 4 Conditions and Results during Hurricane Isabel. A) The pre-Hurricane Isabel profile. B) Hurricane Isabel wave heights. C) Water levels at OC 4. D) SSIM Results at OC 4 during Hurricane Isabel.

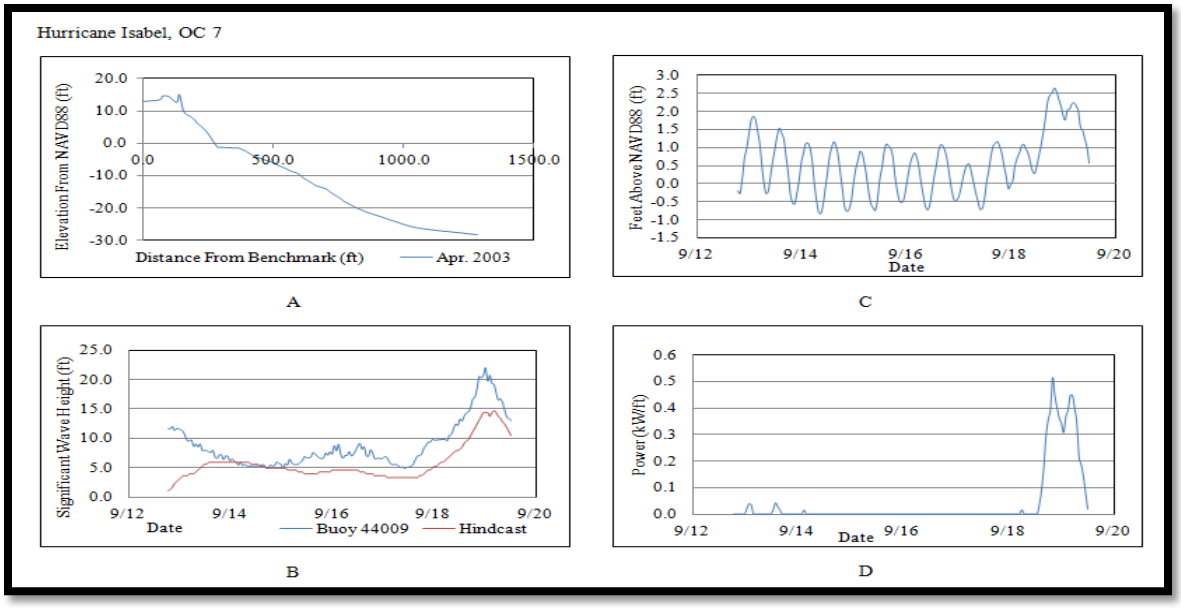

Figure B.75: OC 7 Conditions and Results during Hurricane Isabel. A) The pre-Hurricane Isabel profile. B) Hurricane Isabel wave heights. C) Water levels at OC 7. D) SSIM Results at OC 7 during Hurricane Isabel.

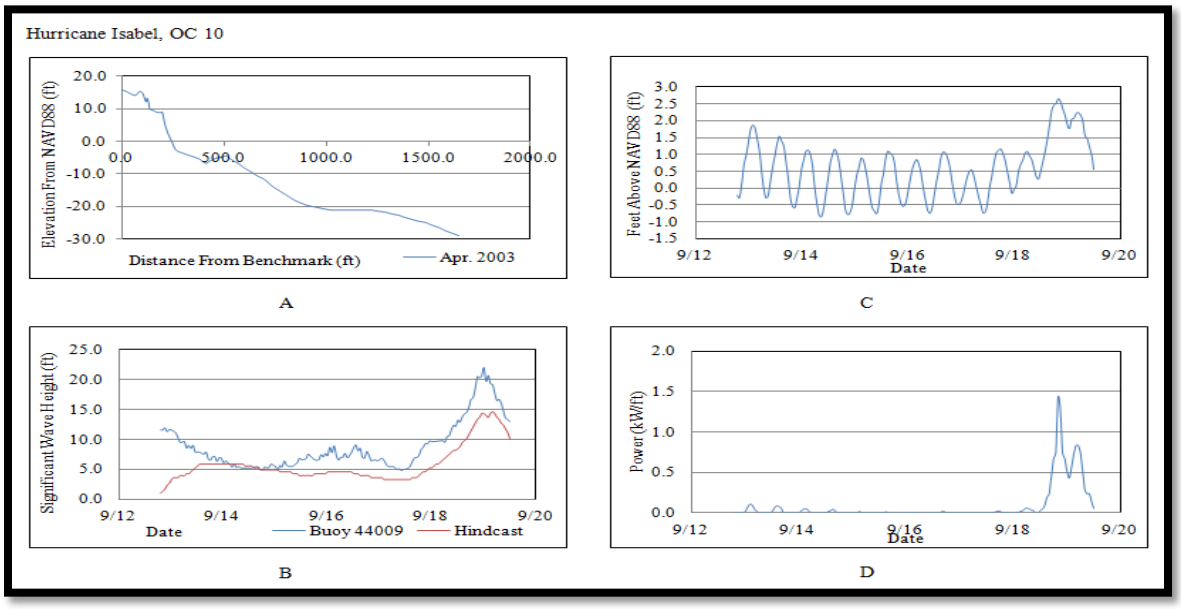

Figure B.76: OC 10 Conditions and Results during Hurricane Isabel. A) The pre-Hurricane Isabel profile. B) Hurricane Isabel wave heights. C) Water levels at OC 10. D) SSIM Results at OC 10 during Hurricane Isabel.

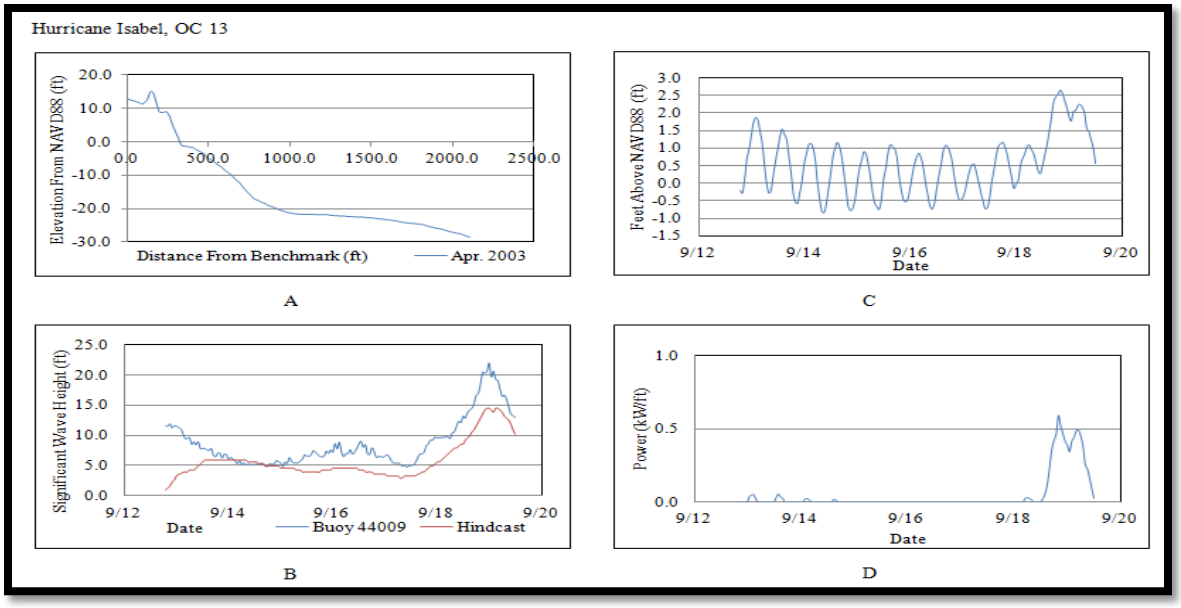

Figure B.77: OC 13 Conditions and Results during Hurricane Isabel. A) The pre-Hurricane Isabel profile. B) Hurricane Isabel wave heights. C) Water levels at OC 13. D) SSIM Results at OC 13 during Hurricane Isabel.

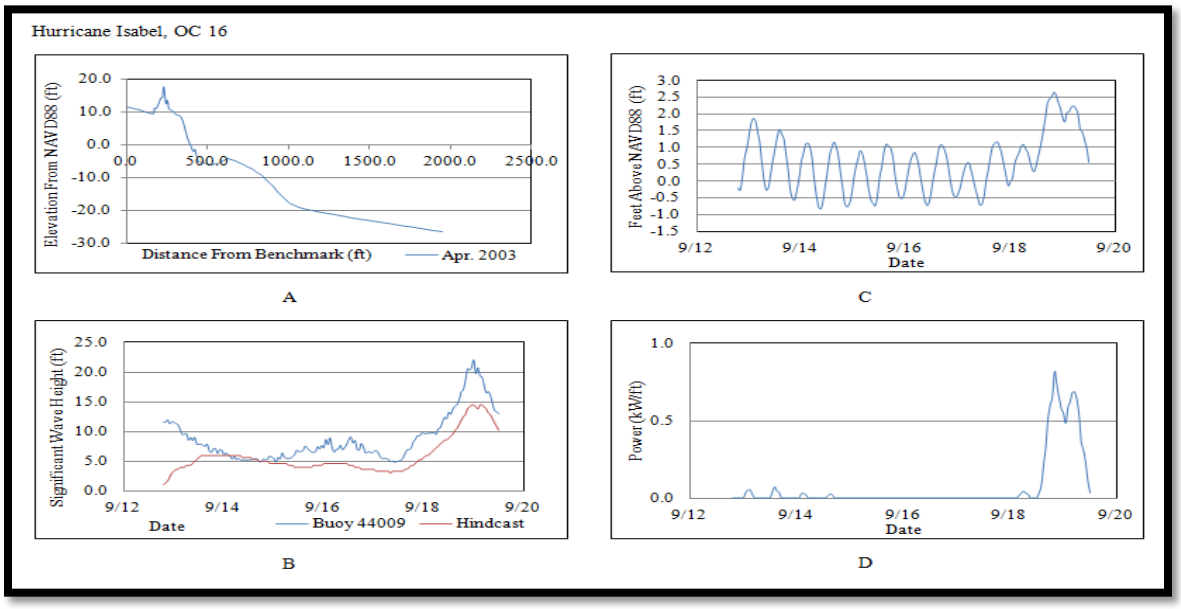

Figure B.78: OC 16 Conditions and Results during Hurricane Isabel. A) The pre-Hurricane Isabel profile. B) Hurricane Isabel wave heights. C) Water levels at OC 16. D) SSIM Results at OC 16 during Hurricane Isabel.

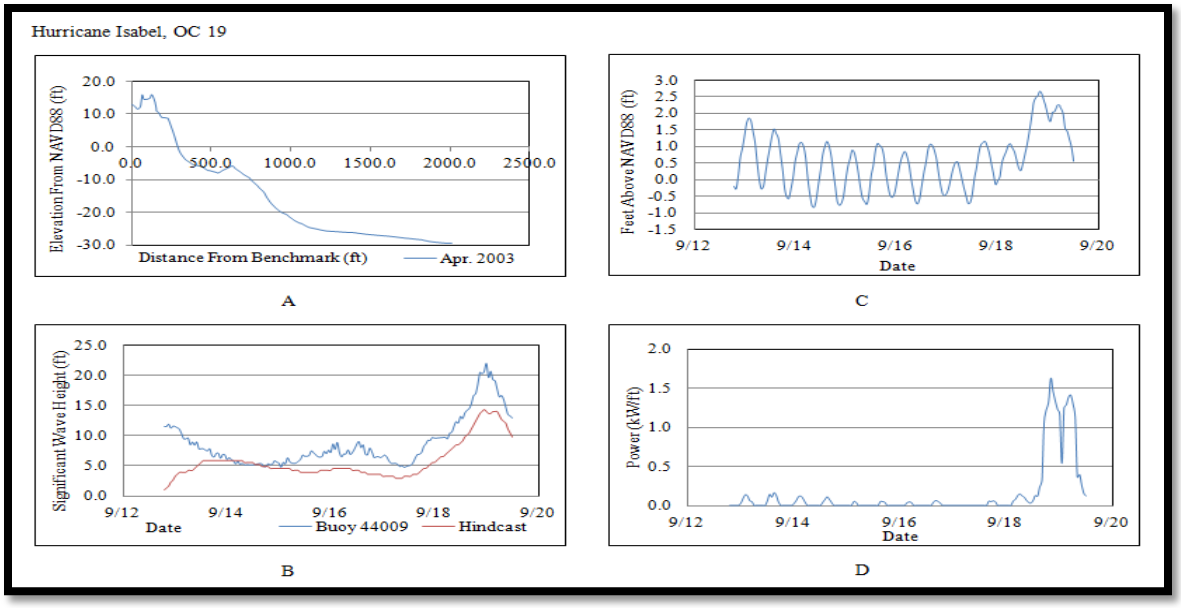

Figure B.79: OC 19 Conditions and Results during Hurricane Isabel. A) The pre-Hurricane Isabel profile. B) Hurricane Isabel wave heights. C) Water levels at OC 19. D) SSIM Results at OC 19 during Hurricane Isabel.

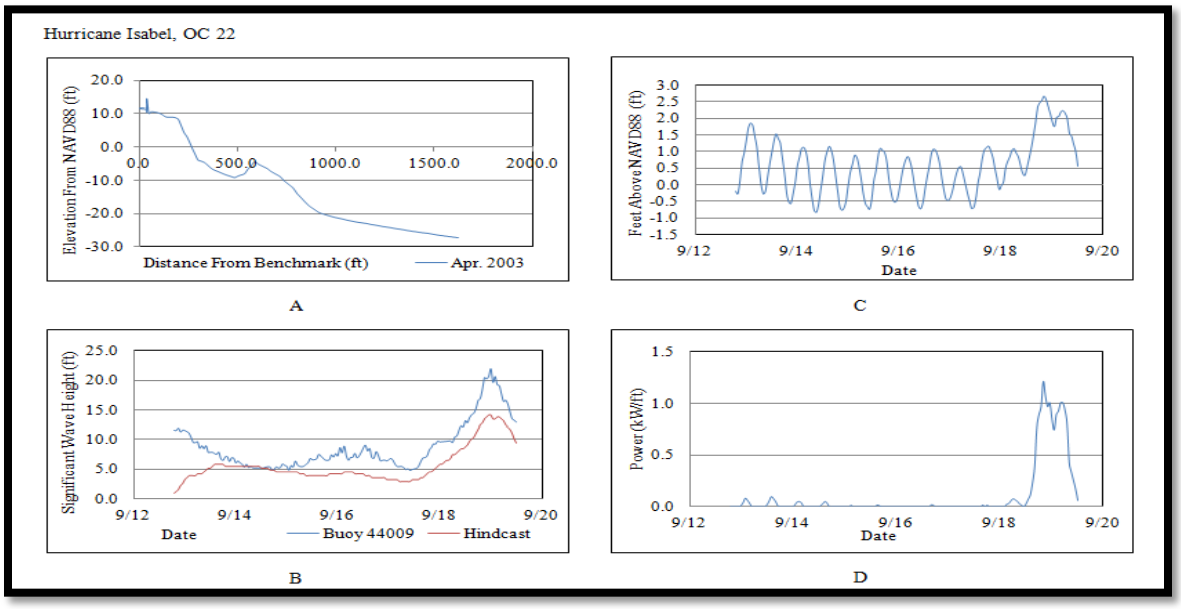

Figure B.80: OC 22 Conditions and Results during Hurricane Isabel. A) The pre-Hurricane Isabel profile. B) Hurricane Isabel wave heights. C) Water levels at OC 22. D) SSIM Results at OC 22 during Hurricane Isabel.

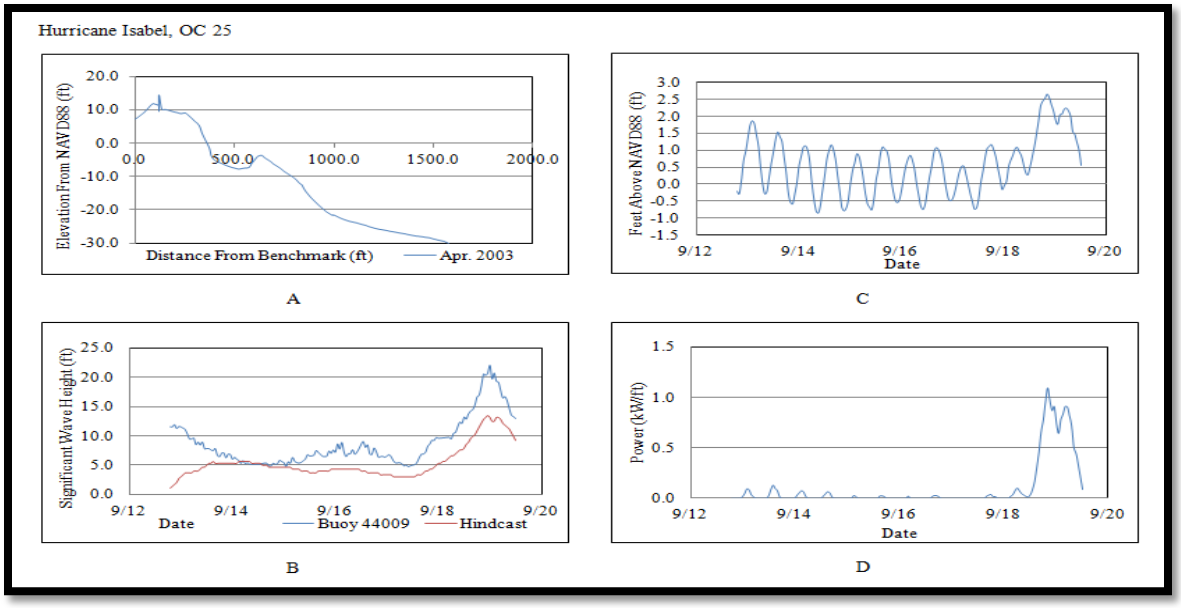

Figure B.81: OC 25 Conditions and Results during Hurricane Isabel. A) The pre-Hurricane Isabel profile. B) Hurricane Isabel wave heights. C) Water levels at OC 25. D) SSIM Results at OC 25 during Hurricane Isabel.

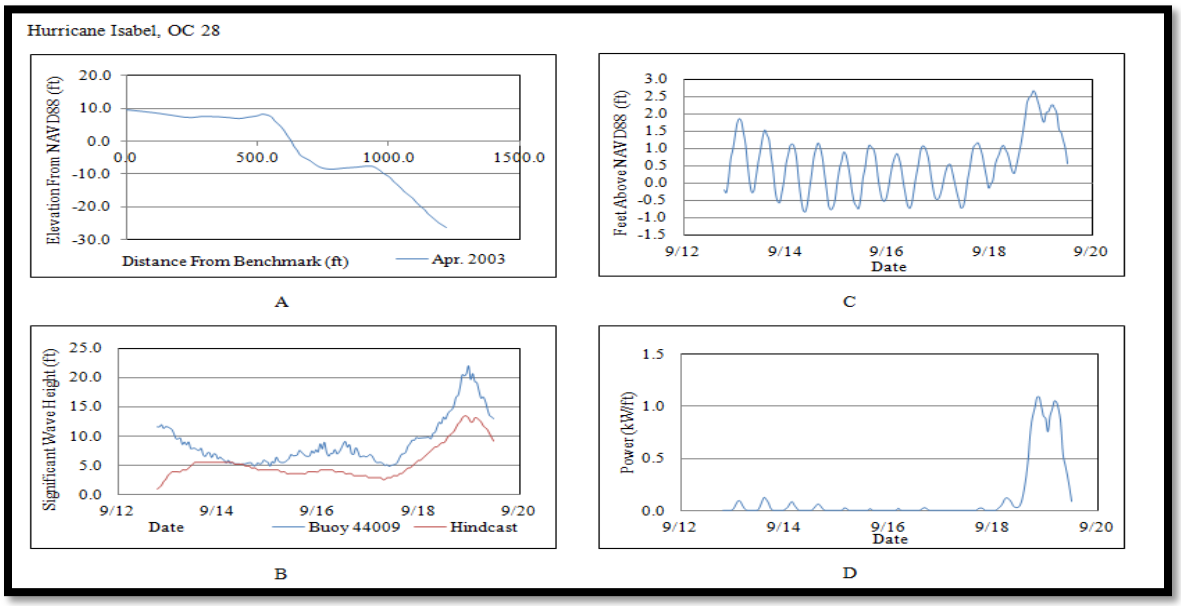

Figure B.82: OC 28 Conditions and Results during Hurricane Isabel. A) The pre-Hurricane Isabel profile. B) Hurricane Isabel wave heights. C) Water levels at OC 1. D) SSIM Results at OC 1 during Hurricane Isabel.

APPENDIX C: GULF OF MEXICO

This appendix contains the graphs of the water levels, wave heights, beach profiles, and energy fluxes above the normal mean high water lines for Hurricanes Georges, Ivan, Elena, and Opal, as well as for Tropical Storm Debby. The wave heights in the panhandle were taken from WIS Station 73354 while the wave heights for Clearwater are from WIS station 73362. The hindcast obtained from the WIS stations were then subjected to a version of the Steady State Spectral Wave program (STWAVE) that is modified to include bottom friction. Table C.1 has a summary of the storms that had an impact in the Gulf of Mexico in this Thesis.

Table C.1: Gulf of Mexico Storms Summary

Storm	Dates	# of Profiles	Profile Locations	Distance from Impact Point	Wave Data Source	Water Level Source
Hurricane Georges	9/26/1998 - 10/1/1998	2	West Ship Island, MS, Santa Rosa Island, FL	5 Miles West of MS, 100 Miles East of FL	WIS Stations 73349, MS, 73354 (FL)	NOAA 8726724, FL, NOAA 8747766, MS
Hurricane Ivan	9/15/2004 - 9/17/2004	8	Between Destin and St. George Island, FL	100 Miles West	WIS Station 73354	NOAA 8729210
Hurricane Elena	8/29/1985 -9/2/1985	2	Pinellas County, FL	80 Miles N.W.	WIS Station 73362	Florida Coastal Data Network Station, Clearwater
Hurricane Opal	10/4/1995 - 10/7/1995	3	Pinellas County, FL	300 Miles West	WIS Station 73362	NOAA 8726724
Tropical Storm Debby	6/3/2012- 6/7/2012	5	Pinellas County, FL	50 Miles North	WIS Station 73362	NOAA 8726724

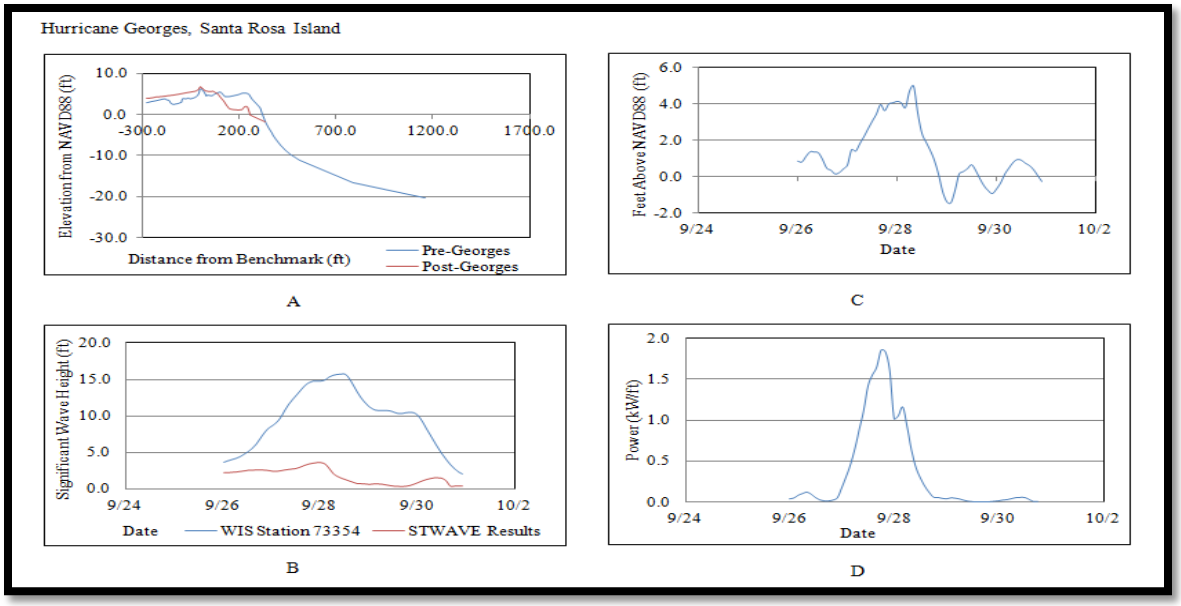

Figure C.1: Santa Rosa Island Conditions and Results during Hurricane Georges. A) The pre- and post-Hurricane Georges profile. B) Hurricane Georges wave heights. C) Water levels at Santa Rosa Island. D) SSIM Results at Santa Rosa Island during Hurricane Georges.

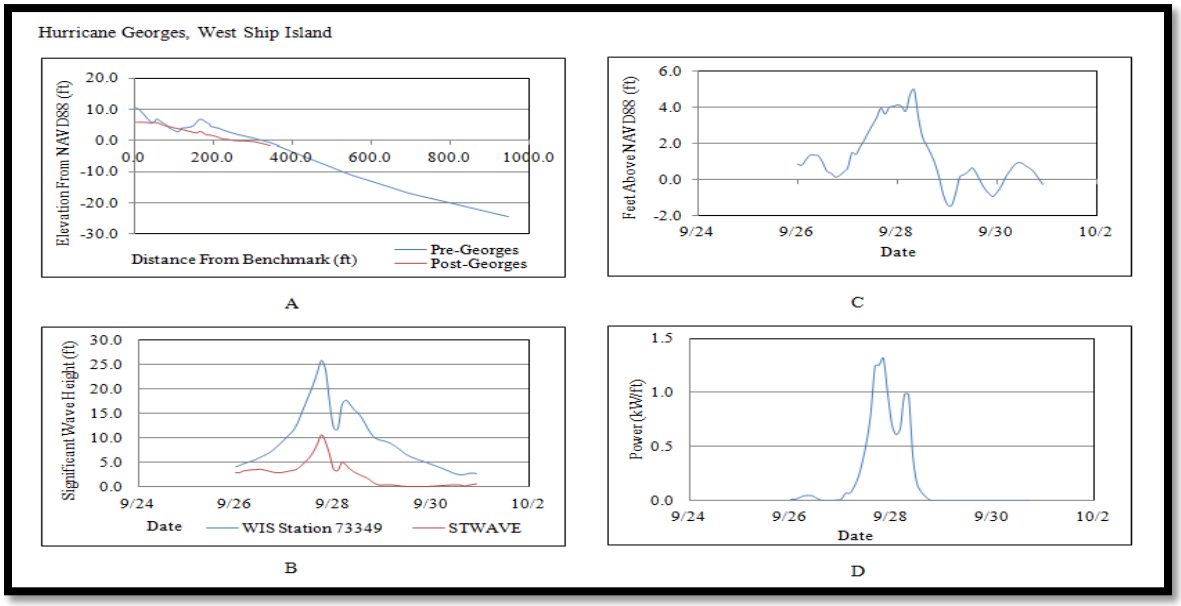

Figure C.2: West Ship Island Conditions and Results during Hurricane Georges. A) The pre- and post-Hurricane Georges profile. B) Hurricane Georges wave heights. C) Water levels at West Ship Island. D) SSIM Results at West Ship Island during Hurricane Georges.

.

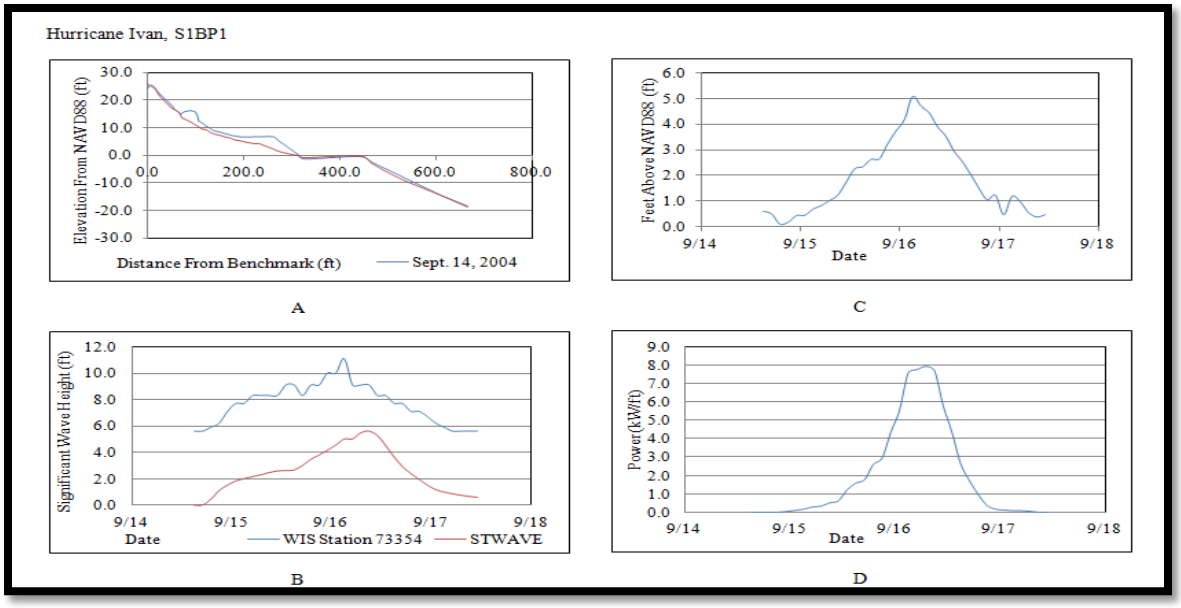

Figure C.3: S1BP1 Conditions and Results during Hurricane Ivan. A) The pre- and post-Hurricane Ivan profile. B) Hurricane Ivan wave heights. C) Water levels at S1BP1. D) SSIM Results at S1BP1 during Hurricane Ivan.

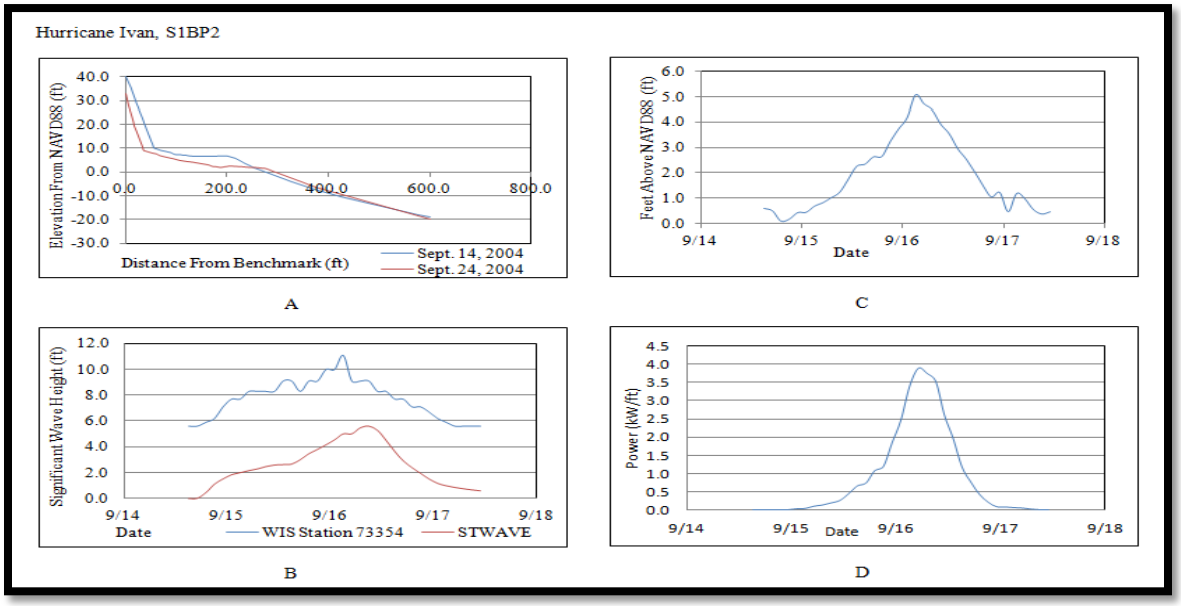

Figure C.4: S1BP2 Conditions and Results during Hurricane Ivan. A) The pre- and post-Hurricane Ivan profile. B) Hurricane Ivan wave heights. C) Water levels at S1BP2. D) SSIM Results at S1BP2 during Hurricane Ivan.

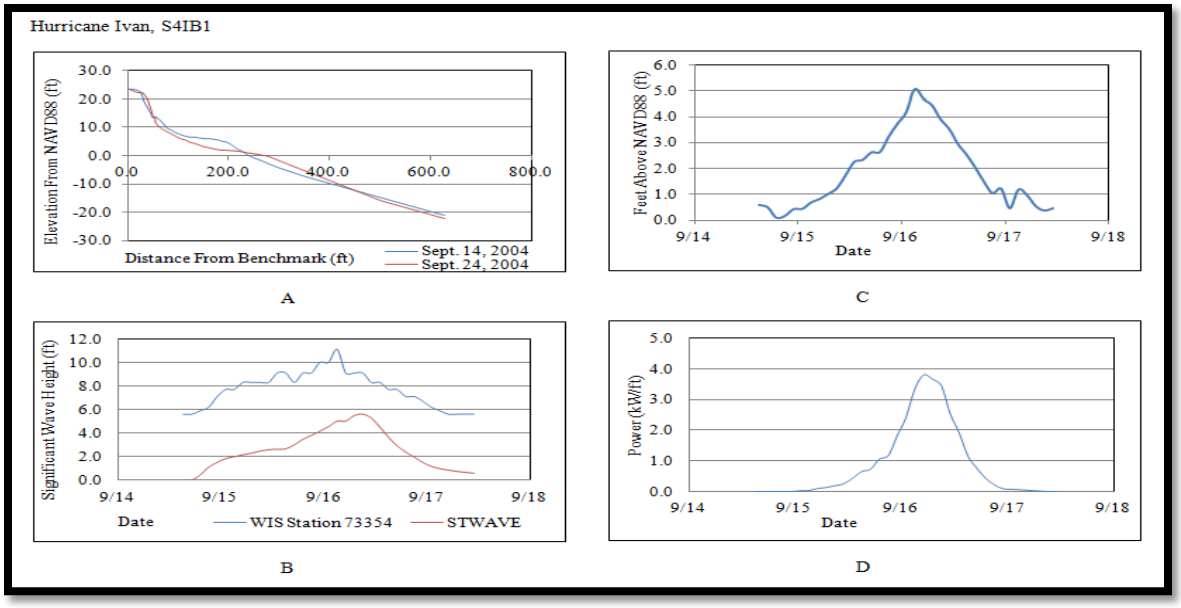

Figure C.5: S4IB1 Conditions and Results during Hurricane Ivan. A) The pre- and post-Hurricane Ivan profile. B) Hurricane Ivan wave heights. C) Water levels at S4IB1. D) SSIM Results at S4IB1 during Hurricane Ivan.

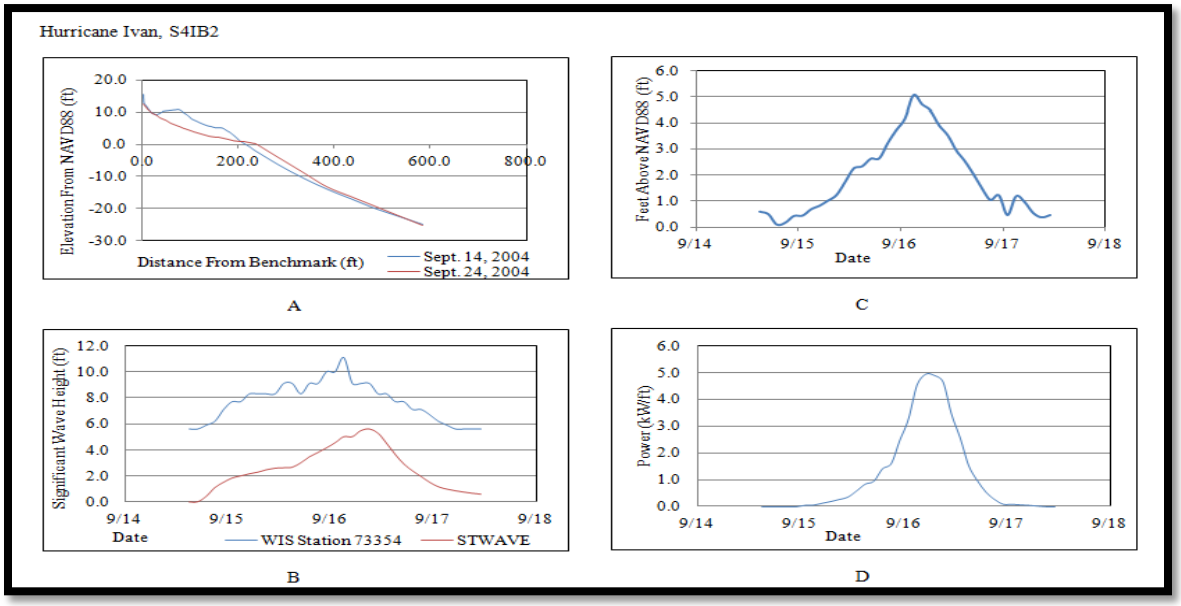

Figure C.6: S4IB2 Conditions and Results during Hurricane Ivan. A) The pre- and post-Hurricane Ivan profile. B) Hurricane Ivan wave heights. C) Water levels at S4IB2. D) SSIM Results at S4IB2 during Hurricane Ivan.

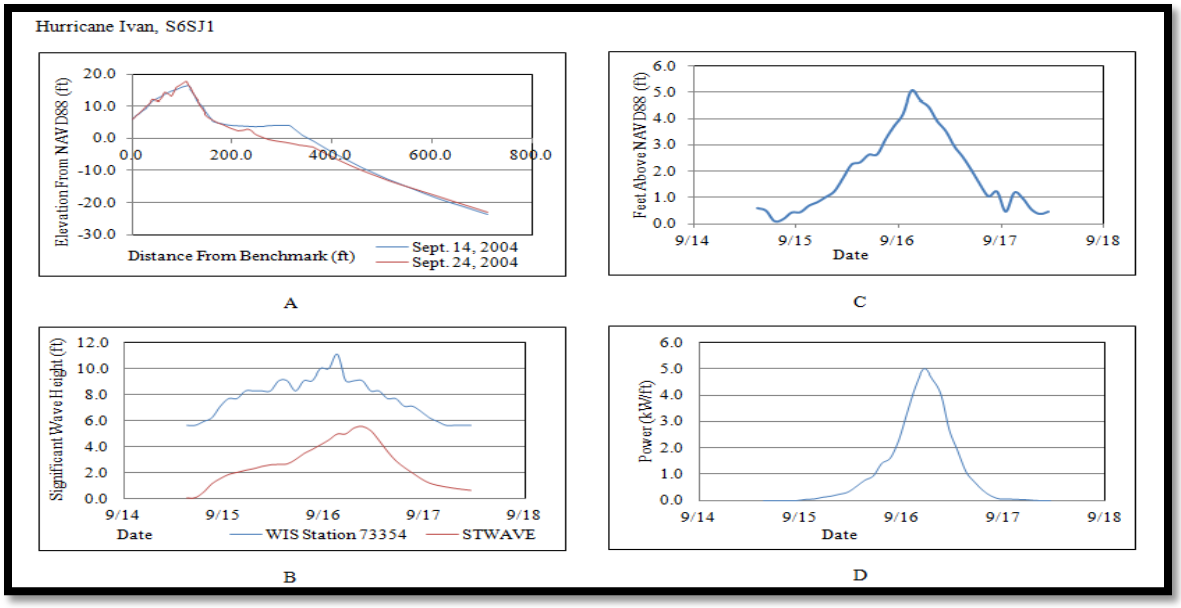

Figure C.7: S6SJ1 Conditions and Results during Hurricane Ivan. A) The pre- and post-Hurricane Ivan profile. B) Hurricane Ivan wave heights. C) Water levels at S6SJ1. D) SSIM Results at S6SJ1 during Hurricane Ivan.

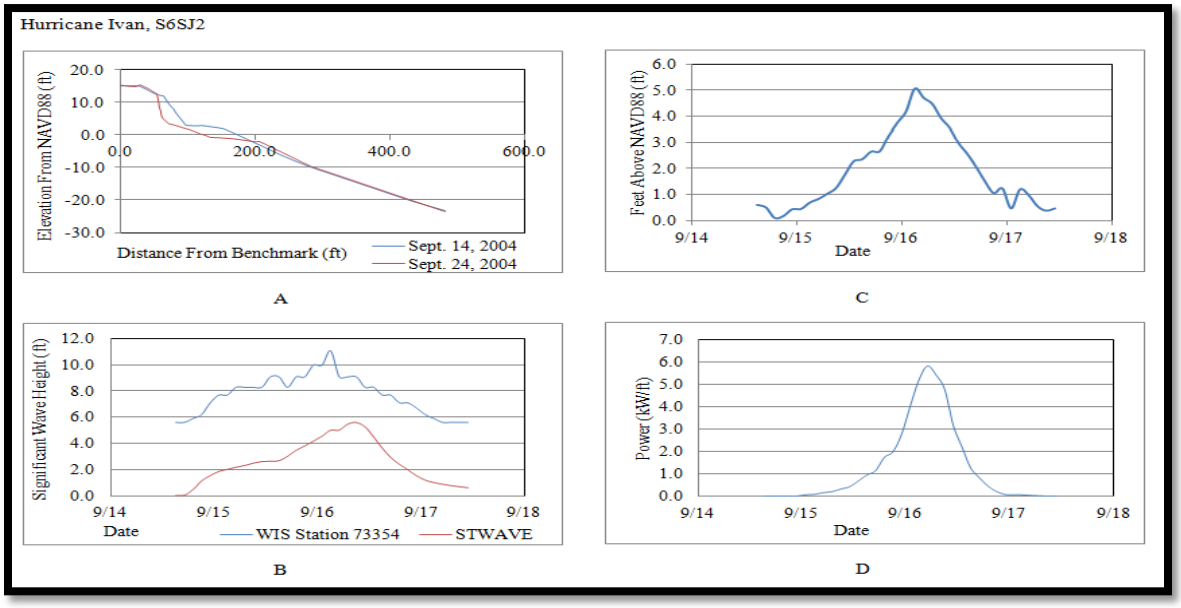

Figure C.8: S6SJ2 Conditions and Results during Hurricane Ivan. A) The pre- and post-Hurricane Ivan profile. B) Hurricane Ivan wave heights. C) Water levels at S6SJ2. D) SSIM Results at S6SJ2 during Hurricane Ivan.

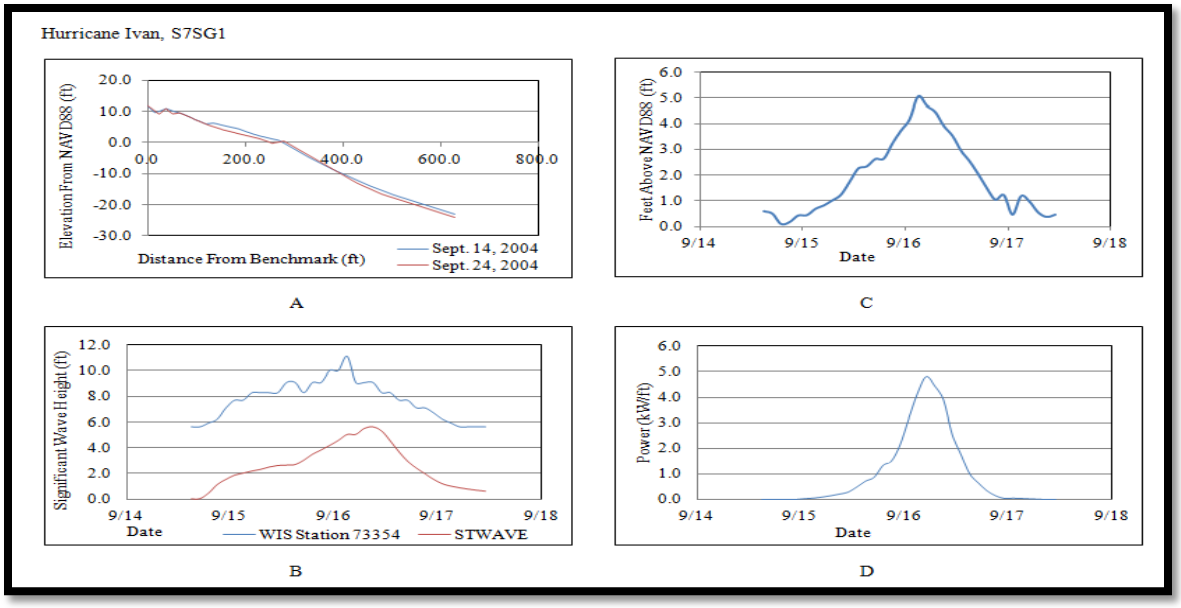

Figure C.9: S7SG1 Conditions and Results during Hurricane Ivan. A) The pre- and post-Hurricane Ivan profile. B) Hurricane Ivan wave heights. C) Water levels at S7SG1. D) SSIM Results at S7SG1 during Hurricane Ivan.

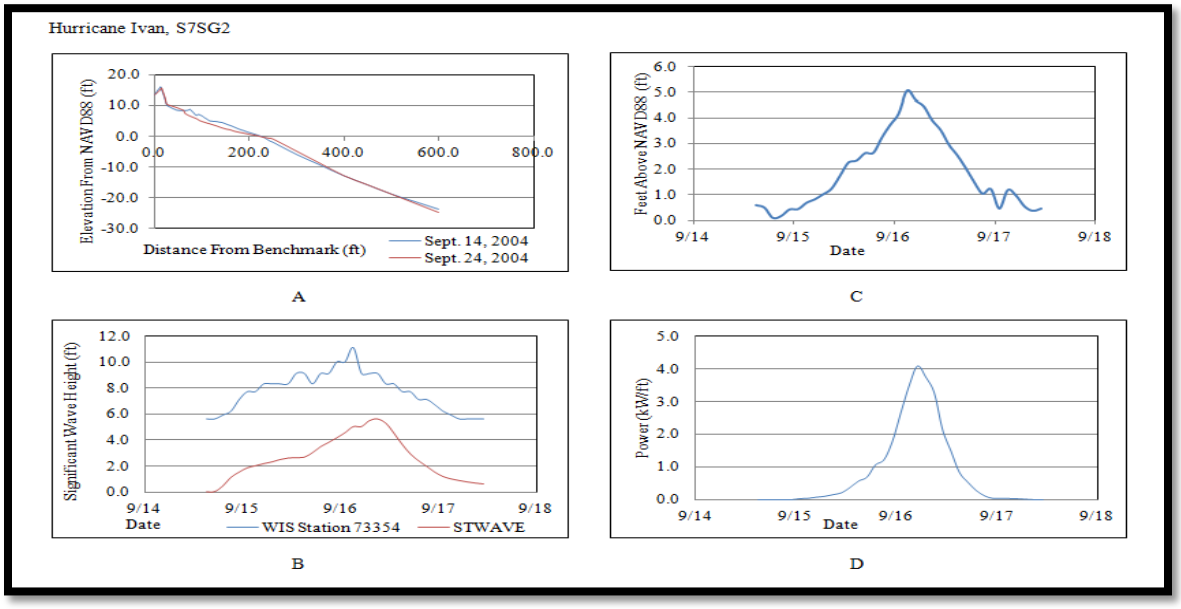

Figure C.10: S7SG2 Conditions and Results during Hurricane Ivan. A) The pre- and post-Hurricane Ivan profile. B) Hurricane Ivan wave heights. C) Water levels at S7SG2. D) SSIM Results at S7SG2 during Hurricane Ivan.

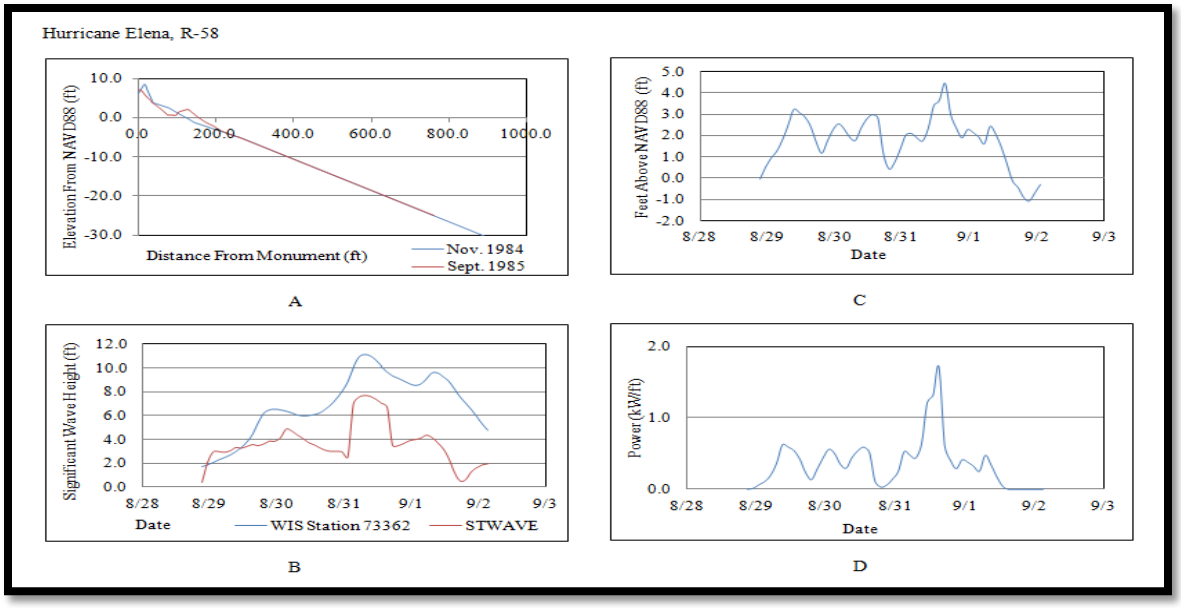

Figure C.11: R-58 Conditions and Results during Hurricane Elena. A) The pre- and post-Hurricane Elena profile. B) Hurricane Elena wave heights. C) Water levels at R-58. D) SSIM Results at R-58 during Hurricane Elena.

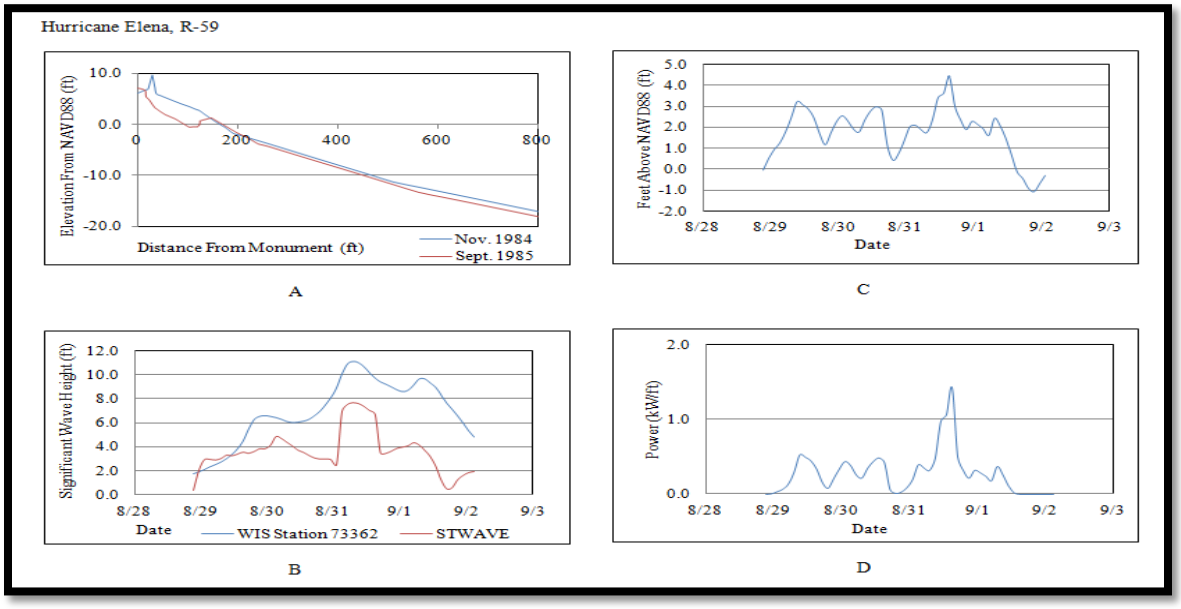

Figure C.12: R-59 Conditions and Results during Hurricane Elena. A) The pre- and post-Hurricane Elena profile. B) Hurricane Elena wave heights. C) Water levels at R-59. D) SSIM Results at R-59 during Hurricane Elena.

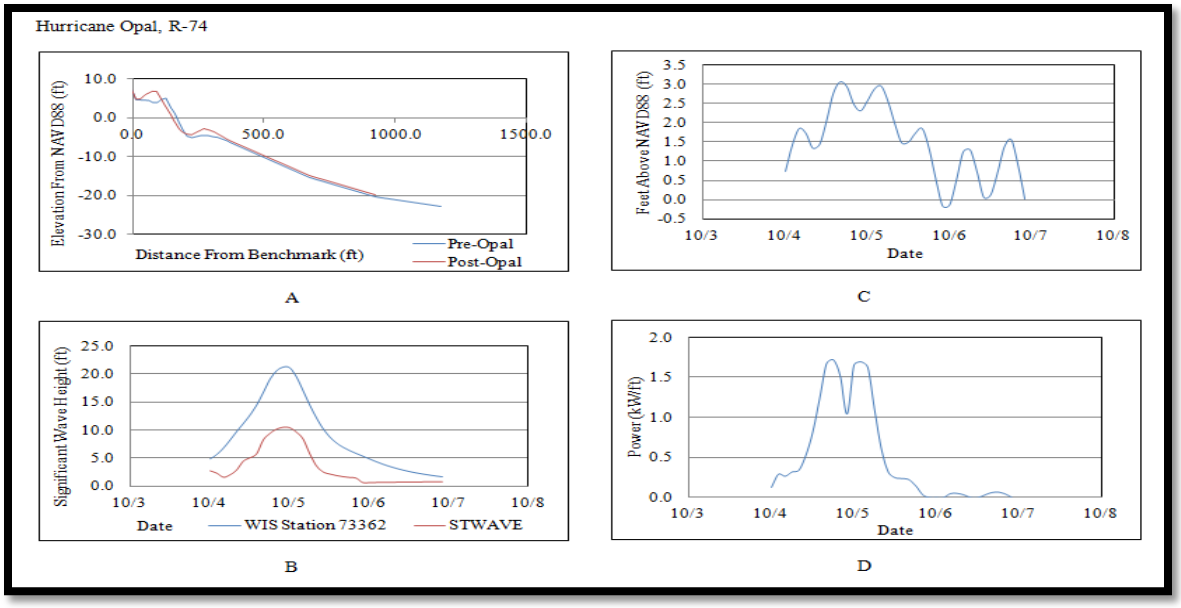

Figure C.13: R-74 Conditions and Results during Hurricane Opal. A) The pre- and post-Hurricane Opal profile. B) Hurricane Opal wave heights. C) Water levels at R-74. D) SSIM Results at R-74 during Hurricane Opal.

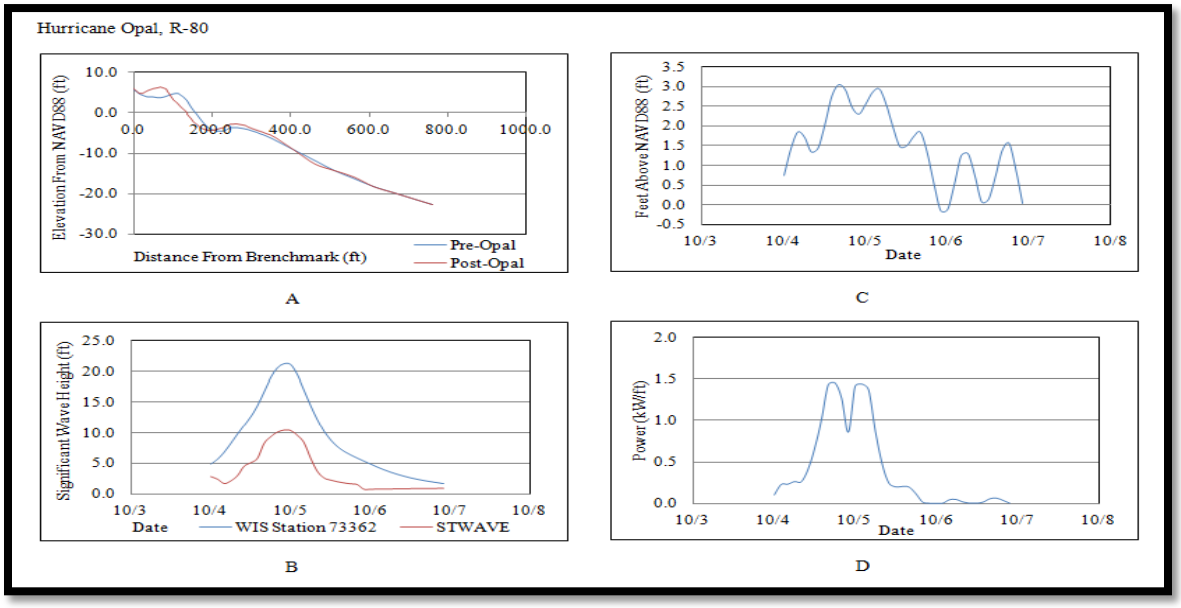

Figure C.14: R-80 Conditions and Results during Hurricane Opal. A) The pre- and post-Hurricane Opal profile. B) Hurricane Opal wave heights. C) Water levels at R-80. D) SSIM Results at R-80 during Hurricane Opal.

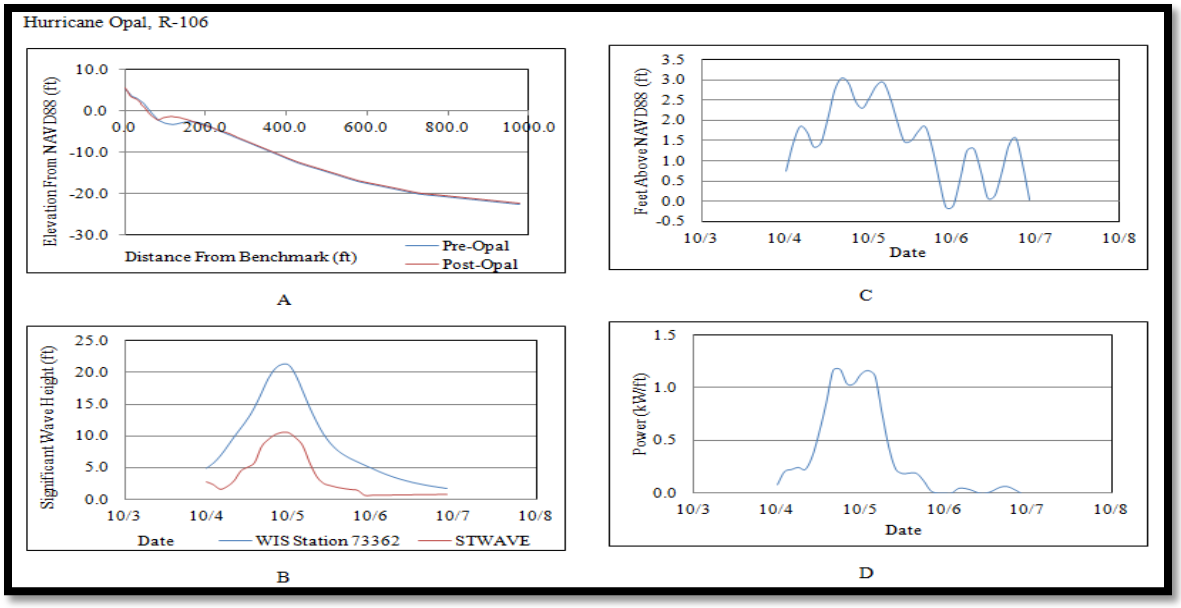

Figure C.15: R-106 Conditions and Results during Hurricane Opal. A) The pre- and post-Hurricane Opal profile. B) Hurricane Opal wave heights. C) Water levels at R-106. D) SSIM Results at R-106 during Hurricane Opal.

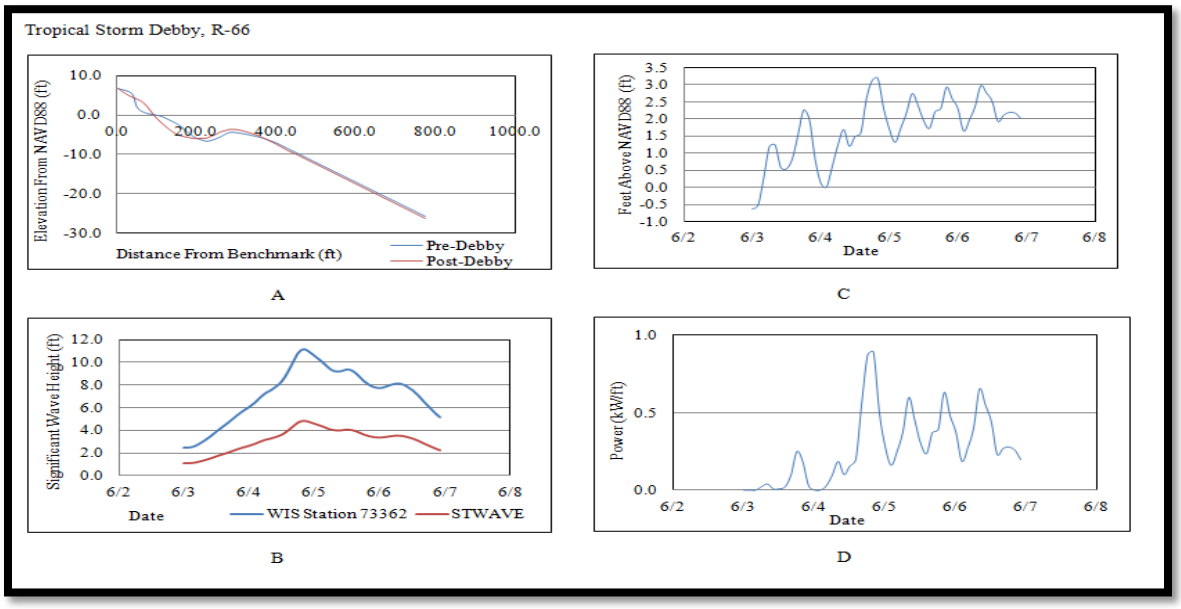

Figure C.16: R-66 Conditions and Results during Tropical Storm Debby. A) The pre- and post-Tropical Storm Debby profile. B) Tropical Storm Debby wave heights. C) Water levels at R-66. D) SSIM Results at R-66 during Tropical Storm Debby.

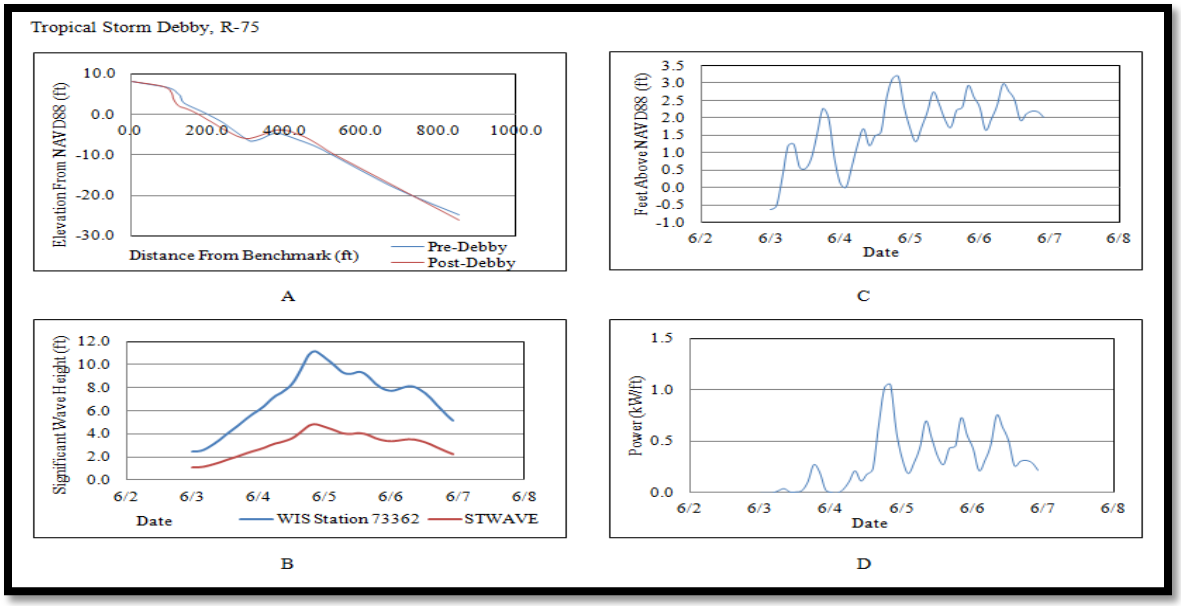

Figure C.17: R-75 Conditions and Results during Tropical Storm Debby. A) The pre- and post-Tropical Storm Debby profile. B) Tropical Storm Debby wave heights. C) Water levels at R-75. D) SSIM Results at R-75 during Tropical Storm Debby.

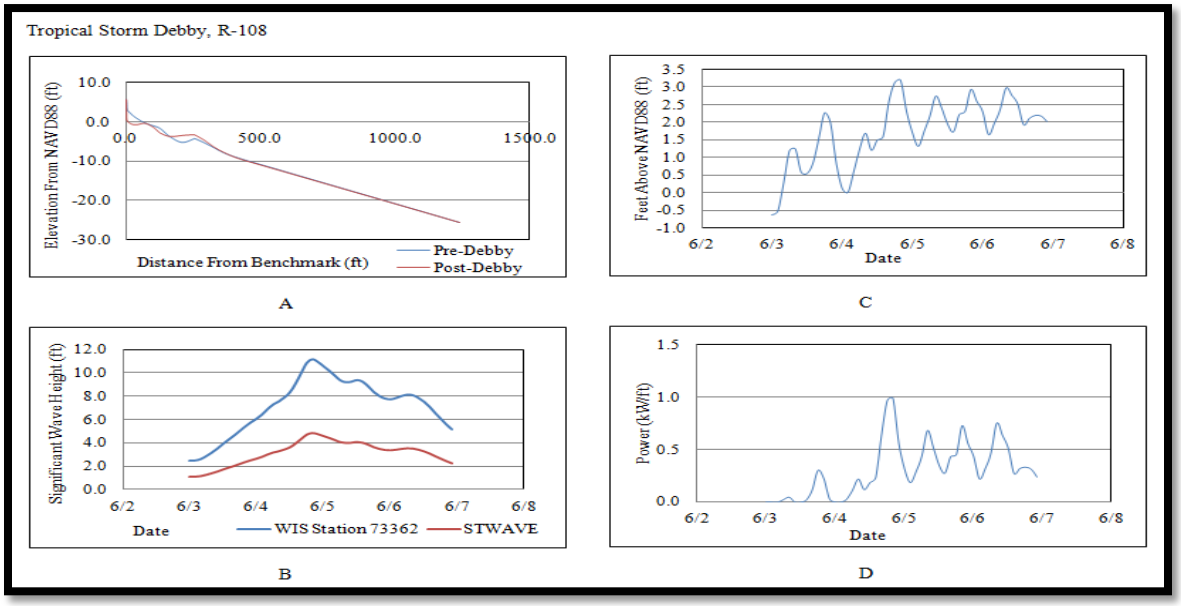

Figure C.18: R-108 Conditions and Results during Tropical Storm Debby. A) The pre- and post-Tropical Storm Debby profile. B) Tropical Storm Debby wave heights. C) Water levels at R-108. D) SSIM Results at R-108 during Tropical Storm Debby.

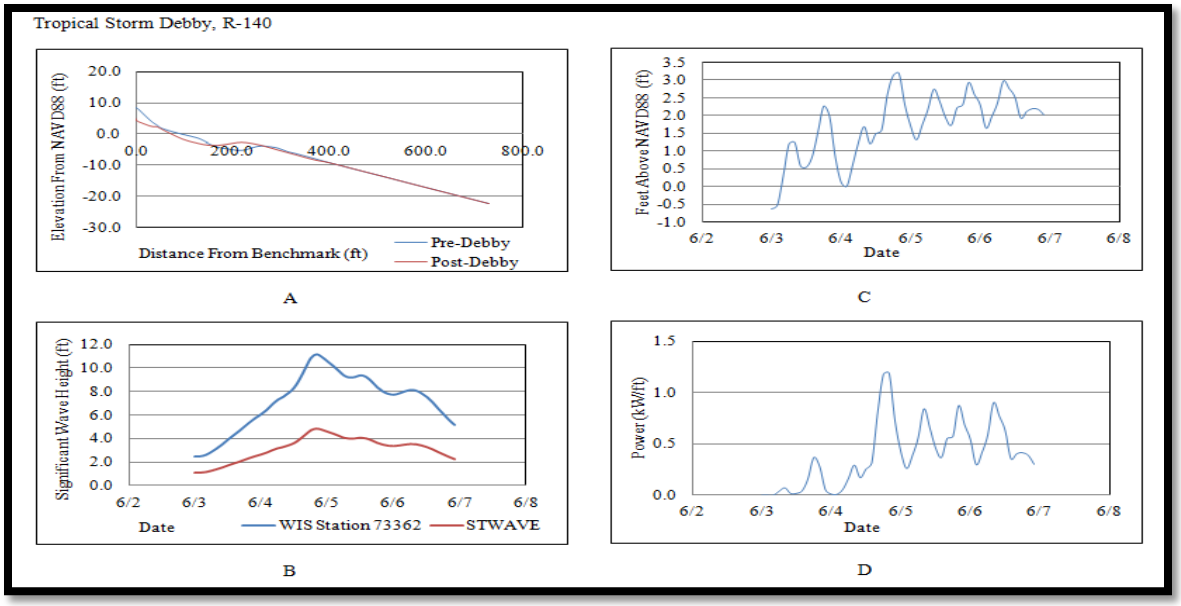

Figure C.19: R-140 Conditions and Results during Tropical Storm Debby. A) The pre- and post-Tropical Storm Debby profile. B) Tropical Storm Debby wave heights. C) Water levels at R-140. D) SSIM Results at R-140 during Tropical Storm Debby.

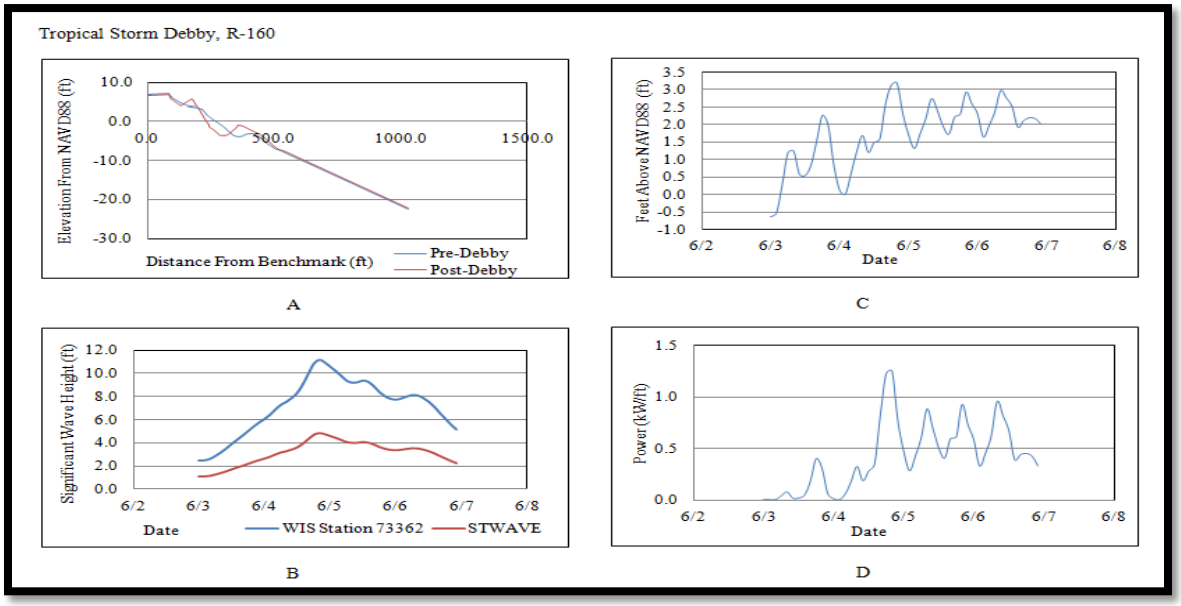

Figure C.20: R-160 Conditions and Results during Tropical Storm Debby. A) The pre- and post-Tropical Storm Debby profile. B) Tropical Storm Debby wave heights. C) Water levels at R-160. D) SSIM Results at R-160 during Tropical Storm Debby.

APPENDIX D: TWENTY-FOUR POINT SCALE RESULTS

Rank	Storm	Location	SSIM Index	Water Index	Category
1	Hurricane Sandy	NJBPN 167	6	10	16
2	Hurricane Sandy	NJBPN 153	6	10	16
3	El Nino Winter	OC 22	10	5	15
4	El Nino Winter	OC 16	8	6	14
5	El Nino Winter	OC 25	8	6	14
6	El Nino Winter	OC 7	9	3	12
7	Hurricane Sandy	NJBPN 173	8	4	12
8	Hurricane Sandy	NJBPN 183	7	5	12
9	Hurricane Sandy	NJBPN 177	7	5	12
10	Hurricane Sandy	NJBPN 248	5	7	12
11	January 1992 Nor'easter	OC 10	5	7	12
12	Hurricane Georges	Santa Rosa Island	5	7	12
13	Hurricane Sandy	NJBPN 171	8	3	11
14	El Nino Winter	OC 19	8	3	11
15	Hurricane Opal	R-106	3	8	11
16	January 1992 Nor'easter	OC 4	4	6	10
17	Hurricane Opal	R-74	4	6	10
18	Hurricane Ivan	S4IB2	7	3	10
19	Hurricane Sandy	NJBPN 150	9	0	9
20	El Nino Winter	OC 10	7	2	9
21	Hurricane Sandy	NJBPN 168	6	3	9
22	January 1992 Nor'easter	OC 13	5	4	9
23	Hurricane Sandy	NJBPN 163	4	5	9
24	North American Blizzard	OC 25	4	5	9
25	Hurricane Opal	R-80	3	6	9
26	Tropical Storm Josephine	OC 28	2	7	9
27	North American Blizzard	OC 28	2	6	8
28	El Nino Winter	OC 4	7	0	7
29	El Nino Winter	OC 13	7	0	7
30	North American Blizzard	OC 13	3	4	7

Rank	Storm	Location	SSIM Index	Water Index	Category
31	Hurricane Ivan	S6SJ2	7	0	7
32	Hurricane Sandy	NJBPN 138	6	0	6
33	Hurricane Sandy	NJBPN 145	5	1	6
34	Tropical Storm Helene	OC 16	4	2	6
35	Maryland Ice Storm	OC 22	4	2	6
36	Maryland Ice Storm	OC 1	2	4	6
37	Hurricane Floyd	OC 28	1	5	6
38	Hurricane Ivan	S1BP2	6	0	6
39	Hurricane Ivan	S4IB1	6	0	6
40	Hurricane Ivan	S6SJ1	6	0	6
41	Hurricane Ivan	S7SG1	6	0	6
42	Hurricane Sandy	NJBPN 141	5	0	5
43	Tropical Storm Josephine	OC 7	2	3	5
44	Tropical Storm Josephine	OC 4	2	3	5
45	Hurricane Ivan	S1BP1	5	0	5
46	Hurricane Ivan	S7SG2	5	0	5
47	Maryland Ice Storm	OC 13	4	0	4
48	Maryland Ice Storm	OC 10	4	0	4
49	Christmas 1994 Nor'easter	OC 10	2	2	4
50	Hurricane Isabel	OC 16	2	2	4
51	Hurricane Isabel	OC 7	1	3	4
52	Hurricane Georges	West Ship Island	4	0	4
53	Hurricane Sandy	NJBPN 133	3	0	3
54	Hurricane Sandy	NJBPN 109	3	0	3
55	Christmas 1994 Nor'easter	OC 4	3	0	3
56	Tropical Storm Helene	OC 22	3	0	3
57	North American Blizzard	OC 22	3	0	3
58	North American Blizzard	OC 16	3	0	3
59	North American Blizzard	OC 19	3	0	3
60	Tropical Storm Helene	OC 19	3	0	3

Rank	Storm	Location	SSIM Index	Water Index	Category
61	Tropical Storm Helene	OC 25	3	0	3
62	Hurricane Isabel	OC 28	2	1	3
63	Tropical Storm Josephine	OC 19	2	1	3
64	Tropical Storm Helene	OC 28	1	2	3
65	Hurricane Elena	R-58	3	0	3
66	Hurricane Elena	R-59	3	0	3
67	North American Blizzard	OC 1	2	0	2
68	North American Blizzard	OC 10	2	0	2
69	Unknown Storm	OC 28	2	0	2
70	Christmas 1994 Nor'easter	OC 13	2	0	2
71	Hurricane Isabel	OC 22	2	0	2
72	Hurricane Isabel	OC 25	2	0	2
73	Tropical Storm Josephine	OC 22	2	0	2
74	Unknown Storm	OC 19	2	0	2
75	Tropical Storm Josephine	OC 16	2	0	2
76	Tropical Storm Josephine	OC 13	2	0	2
77	Tropical Storm Helene	OC 10	2	0	2
78	Hurricane Isabel	OC 10	2	0	2
79	Tropical Storm Josephine	OC 10	2	0	2
80	Tropical Storm Josephine	OC 1	2	0	2
81	Unknown Storm	OC 13	2	0	2
82	Tropical Storm Helene	OC 13	2	0	2
83	Tropical Storm Helene	OC 1	2	0	2
84	Unknown Storm	OC 22	2	0	2
85	Maryland Ice Storm	OC 4	2	0	2
86	Unknown Storm	OC 7	2	0	2
87	Christmas 1994 Nor'easter	OC 22	2	0	2
88	Tropical Storm Josephine	OC 25	2	0	2
89	Unknown Storm	OC 10	2	0	2

Rank	Storm	Location	SSIM Index	Water Index	Category
90	Tropical Storm Helene	OC 4	1	0	1
91	Tropical Storm Helene	OC 7	1	0	1
92	Hurricane Isabel	OC 13	1	0	1
93	Hurricane Floyd	OC 16	1	0	1
94	Unknown Storm	OC 16	1	0	1
95	Hurricane Floyd	OC 10	1	0	1
96	Hurricane Isabel	OC 4	1	0	1
97	Hurricane Floyd	OC 25	1	0	1
98	Hurricane Floyd	OC 7	1	0	1
99	Unknown Storm	OC 25	1	0	1
100	Hurricane Floyd	OC 1	1	0	1
101	Hurricane Isabel	OC 1	1	0	1
102	Hurricane Floyd	OC 19	1	0	1
103	Hurricane Floyd	OC 22	1	0	1
104	Hurricane Floyd	OC 13	1	0	1
105	Hurricane Floyd	OC 4	1	0	1
106	Hurricane Bob	OC 13	1	0	1
107	Hurricane Bob	OC 10	1	0	1
108	Hurricane Bob	OC 4	1	0	1
109	Tropical Storm Debby	R-66	1	0	1
110	Tropical Storm Debby	R-75	1	0	1
111	Tropical Storm Debby	R-108	1	0	1
112	Tropical Storm Debby	R-140	1	0	1
113	Tropical Storm Debby	R-160	1	0	1

APPENDIX E: RUNNING THE STORM SEVERITY INDEX MODEL

The Storm Severity Index Model (SSIM) was written in FORTRAN77. The SSIM uses wave parameters (i.e. significant wave heights, peak periods, mean direction) or fully directional wave spectra, surveyed or idealized beach profiles, and measured water levels as input.

The SSIM functions using two input files. The program will commence by asking the user to enter the input file name. This file contains the wave information and it is saved in a .inp format. The layout of the wave file is organized in the following way:

The first line in the file contains the name of the second file that is required for the SSIM. This second file contains the beach profile information and is in a .dat format.

The second line in the wave file has three pieces of information. It contains the offshore slope of the profile, followed by the landward slope of the profile, and ending with the normal mean high water elevation. These three values need to be calculated from the available information and manually inputted into the file.

The third line of the file only contains the number of wave heights that are provided in the file. If the file contains 100 rows of wave data, then the value 100 is written to inform the program of the number of waves that it needs to work through.

The remaining lines in the file contain the wave information needed by the program. There are five columns for each wave. The first column contains the root mean squared wave heights in feet that have been translated into their nearshore components using STWAVE. The second column contains the mean wave period (TBAR). The third column contains the band

width parameter (XNU). The fourth column holds the mean wave direction in deep water (ABAR). The final column holds the still water levels including the astronomical tide and storm surge referenced to National Geodetic Vertical Datum (NGVD) or North American Vertical Datum of 1988 (NAVD88). An example of the wave input file can be found in Figure E.1, below.

```
OMAC.DAT
 0.040 0.000 1.09
168

0.02      2.00      0.6       187.30    -0.77
0.04      2.00      0.6       189.14    -1.44
0.11      2.00      0.6       195.48    -1.59
0.47      2.03      0.6       202.50    -0.81
0.70      2.56      0.6       196.53     0.19
```

Figure E.1: Example of Wave Input File.

```
BE-607
R-1          00     0.000     0.000  0.00 0.00
 5.4 FT 27JUL93 27AUG85 033  0100 25

 -13.7    12.80
   4.9    13.70
  23.5    15.80
  24.6    16.10
  32.7    18.60
  37.7    19.30
  41.3    19.70
  45.2    20.10
  51.1    19.40
  56.8    18.40
  63.5    16.10
  72.5    13.90
  72.6    13.90
  95.3     8.70
 106.3     8.60
 113.4     8.50
 136.7     9.80
 141.1     9.70
 170.5     5.50
 185.5     2.70
 205.3     1.00
 246.8    -1.00
```

Figure E.2: Example of Beach Profile Input File.

The second input file that is required contains the local beach profile. An example of the beach profile input file can be found in Figure E.2. The first line of the beach profile file contains the title of the file. The second line of the file is in Florida Department of Environmental Protection (FDEP) format and contains the monument I.D., the established date, optional 8 code, double zeros, monument N&E coordinates, azimuth, and monument elevation. The third line is written in the following format: upland data date, beach date, offshore date, total number of points, upland points, beach points, and offshore points. The remaining lines contain X and Y coordinates for the beach profile surveys.

The first part of the program focuses on editing the beach profile to make it suitable to use. The program first runs a subroutine that eliminates all of the redundant and erroneous points in the initial beach profile. This aids in preparing the dataset so that a cubic spline approximation can be constructed. A cubic spline is a numeric function that is made from piecewise third-order polynomials that pass through a set of controlled points (the points provided from beach profile surveys).

The program then finds the survey point that is closest to the normal mean high water level by comparing the normal mean high water level to each subsequent point in the profile. Once the point above the normal mean high water level is found, the program uses the split the difference method to find the approximate location of the NMHWL to within 0.01 ft.

The next part of the program begins to read the wave information off the input file. The momentum flux at the mean high water level is then set to be zero in order to establish a baseline for the normal amount of energy that the hits the beach.

The mean wave direction is then converted from degrees to radian and the maximum period is calculated as 2.5 times the average period (TBAR). Using Equation 20, the deepwater wavelength for the longest wave in the histogram is calculated.

$$L_o = g\frac{T^2}{2\pi} \tag{20}$$

The still water depth is set to the longest wave length, as computed above. After the depths are set, the initial joint histogram of the height, period, and direction is created. The cross-shore radiation stress and the energy flux are then calculated.

The next step is to establish the conditions at Station 2, which is located at the end of the beach profile. First, the depths are established. The still water depth is the elevation of the profile added to the water level. The estimated depth and total depth are assumed to be the same as the still water depth. The waves are now transformed from their deepwater conditions to Station 2. First, the SSIM determines whether the wave is breaking or shoaling. The breaking criterion is determined and if the height/depth ratio is less than the breaker criterion then the wave is still shoaling, otherwise the wave is now breaking. Next the input wave conditions are transformed due to whether it is shoaling or breaking. If it is shoaling then the waves are transformed using the Shuto model.

This process is repeated at Station 3 which is located 2 feet closer to the shore. The depths, radiation stress, and energy flux are calculated at this station in relation to the cubic spline estimation. In addition to these factors, there are a number of other variables that are found. These include the statistically representative wave, the irribarren number, the runup, and the wave setup.

The statistically representative wave is found by sorting all of the waves in the series and then taking the average of the highest 1/3 of the waves. The statistically representative wave is

then used to find the irribarren number which is a dimensionless parameter that is used to estimate the wave runup on beaches.

Once the wave information and beach profiles for a location are gathered, the model is utilized to find the energy flux above the normal mean high water line, the overwash volume, and the inundation volume. The energy flux (EC_g) and cross-shore radiation stress (S_{XX}) are calculated using Equations 21 and 22, respectively (Dean & Dalrymple, 1991).

$$EC_g = \frac{\rho g H^2}{8} nC \tag{21}$$

$$S_{XX} = E\left[n\left(\cos^2\theta + 1\right) - \frac{1}{2} \right] \tag{22}$$

where:

$$E = \frac{1}{8}\rho g H^2 L \tag{23}$$

$$C_g = nC \tag{24}$$

$$C = \frac{2\pi D}{Tk} \tag{25}$$

In which ρ is the density of water, g is the acceleration due to gravity, H is wave height, L is the wave length, C is the wave celerity, D is the water depth, T is the wave period, k is the wave number and n is given by:

$$n = \frac{1}{2}\left(1 + \frac{2kh}{\sinh(2kh)}\right) \tag{26}$$

The energy flux is dependent on the depth of the water at a given point. The water depth is referenced to the beach profile and the mean high water line, both of which are referenced to NAVD88. If the water depth is less than the mean high water line then the energy flux is

assumed to be zero. If the depth is greater than the mean high water line then the energy flux is the recorded and added to the output file.

The wave setup is estimated using an iterative solution developed by Dally (1995) in which the initial depth is assumed to be the still water depth and the difference in radiation stress between stations is the driving force for the change in water depth. The difference in new water depth and still water depth is taken to be the wave setup. Then the new water depth is inserted in place of the still water depth and the process is repeated. The process is repeated until the change of depth between iterations is less than 0.05 feet.

Once the wave setup at a station is determined, then the maximum wave setup and total water level are calculated. The maximum wave setup is estimated to be 20% of the significant wave height (Masselink, Hughes, & Knight, 2011). The total water level is the sum of the still water level, the 2% runup, and the maximum wave setup. The maximum wave setup is used as opposed to the setup at the station that was previously calculated because the SSIM is programmed to stop running when it reaches the mean high water line but if the water level is higher than the mean high water line, the setup at the last station will underestimate the actual setup value at the shoreline. The total water level is then used to check the overwash and inundation.

The SSIM then takes the next step by moving 2 feet closer to the shore. It determines whether the next station is at the mean high water line. If it is at the mean high water line, then the program ends. If it has not reached the line, then the process repeats itself for the next step until the line is finally reached. The SSIM records the energy flux at the normal mean high water line, the setup, the 2% runup, and the total water level.

APPENDIX F: EROSION

One of the goals of this thesis was to find a link between erosion and energy flux. In an attempt to determine this, the energy flux was plotted against the change in volume at each of the sites at which a pre- and post-storm survey was available. This can be seen in Figure F.1. The linear trend line only had an R^2 value of 0.20 which does not show much confidence in a correlation.

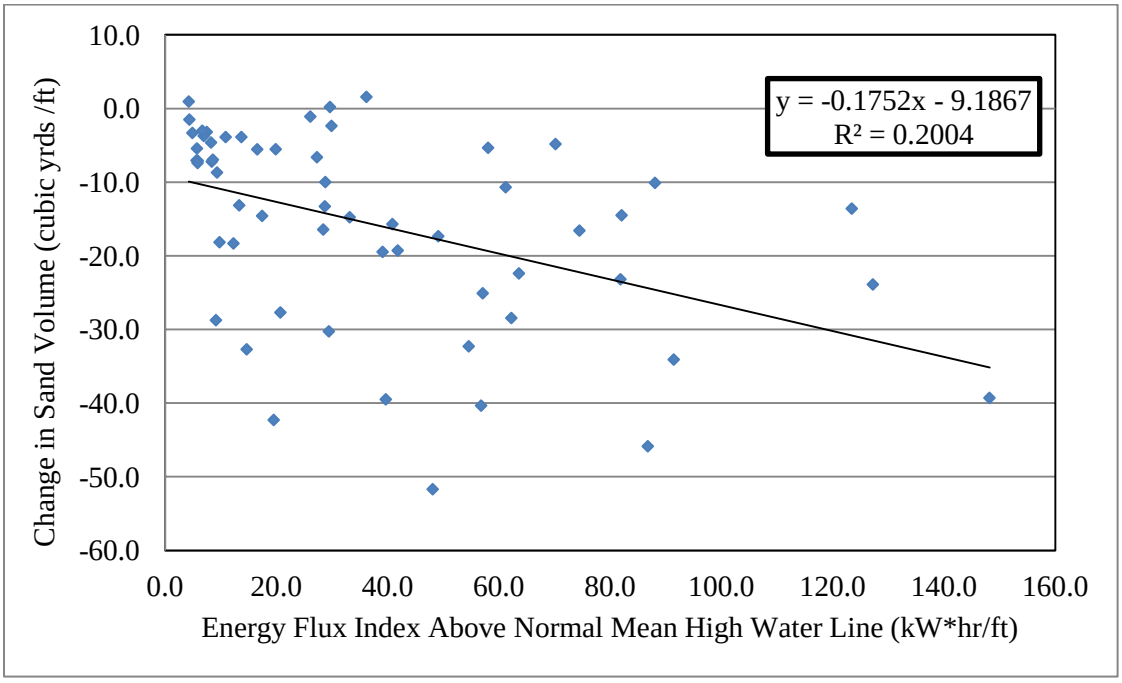

Figure F.1: Change in sand volume against Energy Flux Index.

However, at many of the locations, the beach profiles did not immediately bracket the passing of the storm. In some cases a month or two passed which can have impact on the amount

of sand change that occurred at a location because beach recovery begins very quickly after the passing of storms. In total there are 59 locations that with both a pre- and post-storm profile but at only 27 of those locations did the profiles occur within a week of the event. These 27 events were plotted in Figure F.2 in an attempt to see if the slope had an impact on energy flux levels. There was a stronger correlation here. The R^2 value in this case was 0.38.

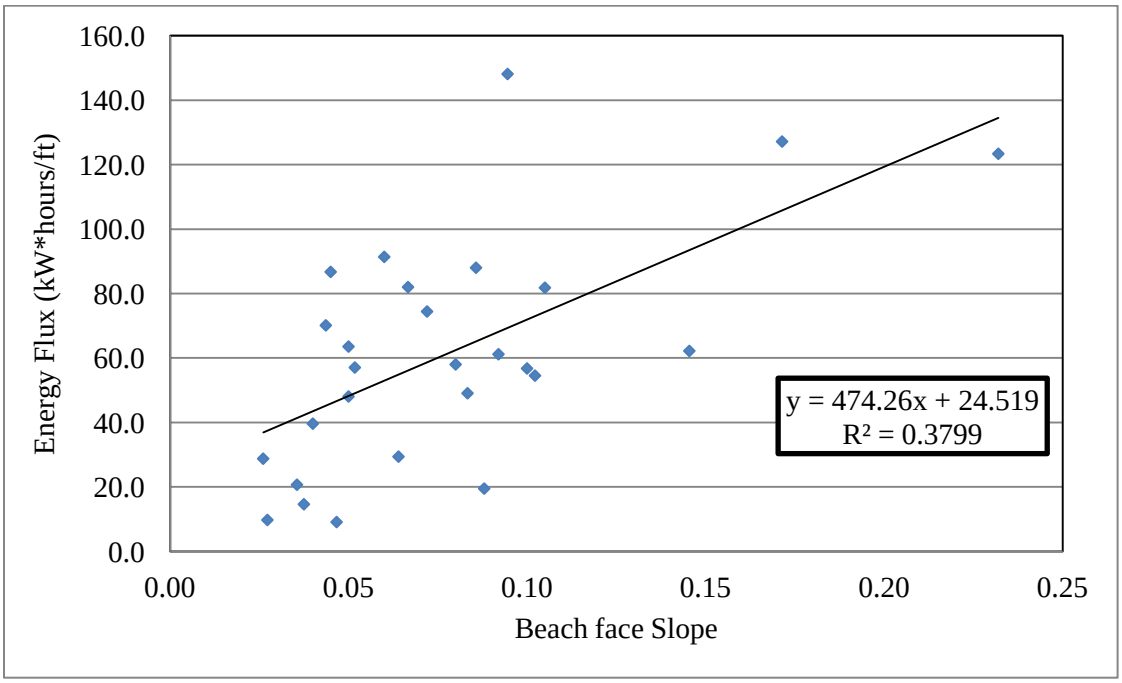

Figure F.2: Energy Flux Index versus beachface slope.

Because the beach face slope may have an impact on the energy flux values above the normal mean high water line, a new term was created. This term is called the slope-factored change in volume and it is simply the slope multiplied by change in sand volume at each location. This value was then plotted in Figure F.3, above. A linear trend line was plotted with an R^2 value of 0.40, which is double the original value. There is not enough evidence to claim a

strong linear correlation, but there appears to be a trend between the beach face slope, the amount of change in sand volume, and the energy flux above the normal mean high water line.

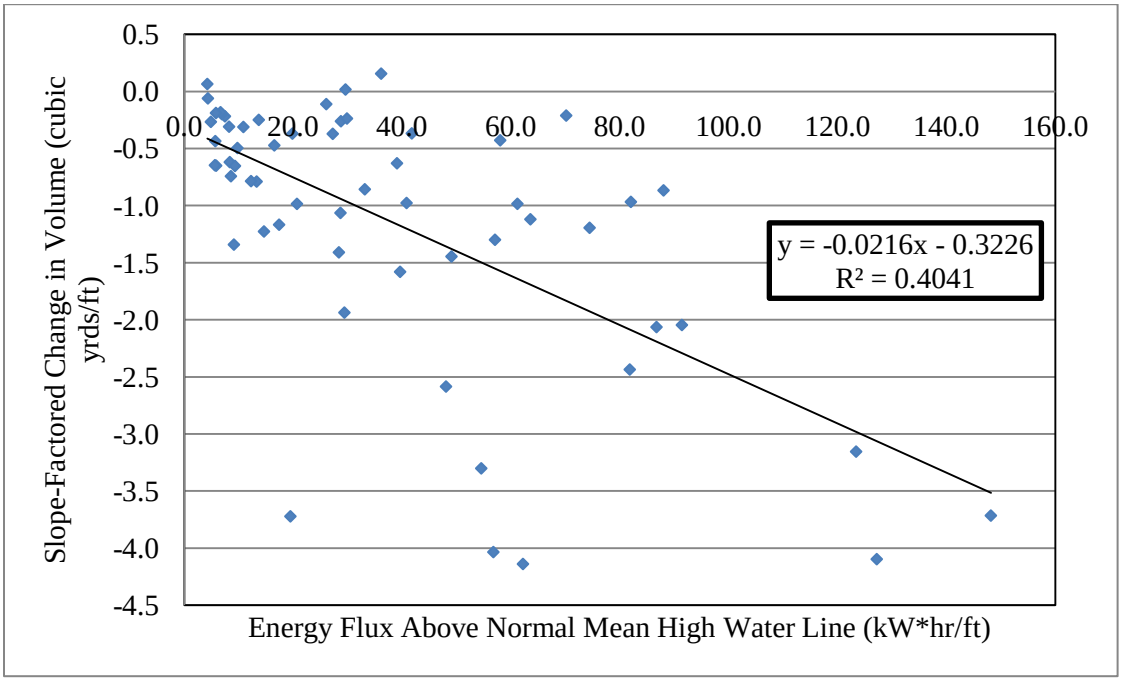

Figure F.3: Slope-Factored change in volume versus the Energy Flux Index.

REFERENCES

Ahrens, J. P. (1981). Irregular Wave Runup on Smooth Slopes. *Coastal Engineering technical Aid NO. 81-17*, 11-12.

Balica, S., Wright, N., & van der Meulen, F. (2012). A Flood Vulnerability Index for Coastal Cities and its Use in Assessing Climate Change Impacts. *Natural Hazards and Earth System Sciences*, 64,73-105.

Basco, D. R., & Mahmoudpour, N. (2012). The Modified Coastal Storm Impulse (COSI) Parameter and Quantification of Fragility Curves for Coastal Design. *ICCE.* Santander: ASCE, NY.

Basco, D. R., & Walker, R. A. (2010). Application of the Coastal Storm Impulse (COSI) Parameter to Predict Coastal Erosion. *ICCE.* Shanghai: ASCE, NY.

Blake, E., Kimberlain, T., Berg, R., Cangialosi, J., & Beven II, J. (2013). *Tropical Cyclone Report Hurricane Sandy.* National Hurricane Center.

Bodge, K., & Kriebel, D. (1985). *Storm Surge and Wave Damage Along Florida's Gulf Coast from Hurricane Elena.* Gainesville: University of Florida.

Bruun, P. (1962). Sea-Level Rise as a Cause of Shore Erosion. *Harbors Coastal Eng. Div. Am. Soc. Civ. Eng.*, 88,117-130.

CNN. (2014, august 22). *Hurricane Katrina Statistics Fast Facts*. Retrieved from CNN.com: http://www.cnn.com/2013/08/23/us/hurricane-katrina-statistics-fast-facts/

Dally, W. R. (1987). *Wave Transformation in the Surf Zone. Ph.D. Dissertation, Coastal and Oceanogr. Eng. Dep.* Gainesville, Florida: University of Florida.

Dally, W. R. (1992). *Random Breaking Waves: Field Verification of a Wave by Wave Algorithm for Engineering Application.* Amsterdam: Elsevier Science Publishers.

Dally, W. R., & Brown, C. A. (1995). Development of Governing Equations for Wave, Wind, and Tide-Driven Currents for Numerical Modeling of the Sebastian Inlet System. *Journal of Geophysical Research 100(C12), 24873–24883*, doi:10.1029/95JC02868.

Davis, R., & Wang, P. (1996). Hurricane Opal Induced Changes on Natural and Nourished Beaches, West-Central Florida. *25th International Conference on Coastal Engineering* (pp. 2982-2993). Orlando: Asce, NY.

Dean, R. G. (1973). Heuristic Models of Sand Transport in the Surf Zone. *Proc. Conf. Eng. Dynamics in the Surf Zone*, (pp. 208-214). Sydney.

Dean, R. G. (1991). Equilibrium Beach Profiles: Principles and Applications. *Journal of Coastal Research*, 7,1,53-84.

Dean, R. G., & Dalrymple, R. (1991). *Water Wave Mechanics For Engineers and Scientists.* Hackensack, NJ: World Scientific Publishing Co.

Dean, R. G., & Dalrymple, R. (2002). *Coastal Processes with Engineering Applications.* New York, NY: Cambridge University Press.

Dean, R., & Dalrymple, R. (2002). *Coastal Processes with Engineering Applications.*

Dolan, R., & Davis, R. (1992). An Intensity Scale for Atlantic Coast Northeast Storms. *Journal of Coastal Research*, 8, 352-364.

Google.inc. (2015, August 15). Google Earth V.7.1.5.1557. New Jersey.

Haylock, M. (2011). European Extra-Tropical Storm Damage Risk from a Multi-Model Ensemble of Dynamically-Downscaled Global Climate Models. *Natural Hazards and Earth System Sciences*, 11, 2847-2857.

Hebert, C., & Weinzapfel, R. (2010). Hurricane Severity Index: A New Way of Estimating a Tropical Cyclone's Destructive Potential. *Conference on Hurricanes and Tropical Meteorology.* Tucson, AZ: Impact Weather.

Impact Weather. (2008). *The Hurricane Severity Index – A New Method of Classifying the Destructive Potential of Tropical Cyclones.* Retrieved from Doctor Flood: http://doctorflood.rice.edu/SSPEED_2008/downloads/Day2/4A_Chambers.pdf

Irish, & Resio. (2010). A Hydrodynamics-Based Surge Scale for Hurricanes. *Ocean Engineering*, 69-81.

Kantha, L. (2008). Tropical Cyclone Destructive Potential by Integrated Kinetic Energy. *Bulletin of the American Meteorological Society*, 88, 219–221.

Kantha, L. (2010). Discussion of "A Hydrodynamics-Based Surge Scale for Hurricanes.". *Ocean Engineering*, 37, 1081-1084.

Kaye, K. (2006, June 5). *Florida Officials Worry about 'Hurricane Fatigue'*. Retrieved from The St. Augustine Record: http://staugustine.com/stories/060506/news_3878327.shtml#.VkzhqXarSt8

Larson, M., Wise, R., & Kraus, N. (2004). *Coastal Overwash: Part 2, Upgrade to SBEACH.* U.S. Army Corps of Engineers.

Mase. (1989). Random Wave Runup Height on Gentle Slope. *Journal of Waterway, Port, Coastal, and Ocean Engineering, vol. 115, no. 5*, 649–661.

Masselink, G., Hughes, M., & Knight, J. (2011). *Introduction to Coastal Processes and Geomorphology.* New York, NY: Hodder Education Publishers.

Miller, J., & Livermont, E. (2008). An Index for Predicting Storm Erosion Due to Increased Waves and Water Levels. *Solutions to Coastal Disaster Congress.* Oahu, Hawaii: Asce.

National Oceanic and Atmospheric Administration. (2015). Center for Operational Oceanographic Products and Services. United States.

National Science Foundation. (2007, September 21). *Saffir-Simpson Hurricane Scale*. Retrieved from https://serc.carleton.edu/details/images/10713.html

NOAA. (2010, February 7). *What Percentage of the American Population Lives Near the Coast?* Retrieved from National Ocean Service: http://oceanservice.noaa.gov/facts/population.html

Palma, J. (2015, March 24). *Coastal Engineering Introduction.* Retrieved from Slideshare: http://www.slideshare.net/jcpalma/coastal-engineering-introduction

Powell, M., & Reinhold, T. (2007). *Tropical Cyclone Destructive Potential by Integrated Kinetic Energy.* American Meteorological Society.

Rygel, L., O'sullivan, D., & Yarnal, B. (2006). A Method for Constructing a Social Vulnerability Index: An Application to Hurricane Storm Surges in a Developed Country. *Mitigation and Adaption Strategies for Global Change*, 741-764.

Saffir, H. S. (1973). Hurricane Wind and Storm Surge. *The Military Engineer, Vol. 423,* 4-5.

Simpson, R. H. (1974). The Hurricane Disaster Potential. *Weatherwise*, 27, 169–186.

Smith, J., Sherlock, A., & Resio, D. (1999). STWAVE: Steady-State Spectral Wave Model, Version 2.0. *Instructional Report CHL-99-1*.

Stone, G., Liu, B., Pepper, D., & Wang, P. (2004). The Importance of Extratropical and Tropical Cyclones on Short-Term Evolution of Barrier Islands Along the Northern Gulf of Mexico, USA. *Marine Geology*, 210, 63–78.

Streeter, V., & Wylie, B. (1979). *Fluid Mechanics Seventh Edition.* New York: McGraw Hill.

The Richard Stockton College of New Jersey. (2012). *An Assessment of Cape May County Beaches at the New Jersey Beach Profile Network (NJBPN) Sites After Hurricane Sandy Related to (DR-NJ 4086).* New Jersey.

The Weather Channel. (2015). Retrieved from Weather Underground: http://www.wunderground.com

U.S. Army Corps of Engineers. (2015). *Wave Information Studies*. Retrieved from Wave Information Studies: http://wis.usace.army.mil/wis.shtml

Wang, P., & Roberts, T. (2012). *Volume and Shoreline Changes along Pinellas County Beaches during Tropical Storm Debby.* Tampa Bay, FL: Coastal Research Laboratory Report, University of South Florida.

Wang, P., Kirby, J., Haber, J., Horwitz, M., Knorr, P., & Krock, J. (2006). Morphological and Sedimentological Impacts of Hurricane Ivan and Immediate Poststorm Beach Recovery along the Northwestern Florida Barrier-Island Coasts. *Journal of Coastal Research, 22 (6)*, 1382–1402.

Watts, M., & Bohle, H. (1993). The Space of Vulnerability: The Causal Structure of Hunger and Famine. *Progress in Human Geography*, 43-67.

Wehof, J., Miller, J., & Engle, J. (2014). Application of the Storm Erosion Index (SEI) to Three Unique Storms. *Coastal Engineering Proceedings*.

Wu, S.-Y., Yarnal, B., & Fisher, A. (2002). Vulnerability of Coastal Communities to Sea-Level Rise: A Case Study of Cape May County, New Jersey, USA. *Climate Research*, 255-270.

You, Z.-J., & Lord, D. (2008). Influence of the El Nino-Southern Oscilliation on NSW Coastal Storm Severity. *Journal of Coastal Research*, 203-207.

VITA

Gabriel Todaro was born to Ronald and Chantal Todaro. He is the oldest of three sons.

Gabriel then accepted a scholarship to the University of North Florida to study engineering. He completed his Bachelor of Science degree in Civil Engineering in 2013. Gabriel remained at the University of North Florida and accepted a graduate assistantship at the Taylor Engineering Research Institute School of Coastal Engineering. There, he studied with Dr. William Dally and wrote his thesis (The Development of a Hydrodynamics-Based Storm Severity Index), which he hopes to publish. He graduated in December of 2015 with his Masters of Science degree in Coastal Engineering.